Research and Development of an Integral Separator

Final Report
For Contract DE-FG02-03ER83847

to

The U. S. Department of Energy
National Energy Technology Laboratory

by

Lance Hays
Ron Franz

Energent Corporation
Santa Ana

February 26, 2007

Table of Contents

Appendices

EXECUTIVE SUMMARY

Research and development of a new dewpoint control and separation device (Integral Separator) was conducted. The functions of the Integral Separator are to expand a wet gas mixture to low temperature, separate the resulting condensed liquid phase, and compress the dry gas. The Integral Separator is a compact device suitable for remote gas production facilities. Injection of a liquid seed is used to initiate the formation of condensate in the expansion process on large droplets to facilitate separation.

Test units and a prototype unit were designed with the aid of computational fluid dynamics (CFD). Tests were conducted with air and water mixtures, with nitrogen and water mixtures and with high pressure natural gas and injected heavy hydrocarbons.

The air-water tests showed complete separation and dry gas compression with a compact device with a stationary separation surface. Pressure recovery was close to CFD predictions.

High pressure nitrogen-water tests also showed complete separation and compression with a prototype unit. Pressure recovery was less than predicted due to internal slots and secondary liquid recovery holes.

Operation of the prototype unit with high pressure natural gas was accomplished. Separation and pressure recovery were less effective than with air-water and nitrogen water tests. Contributing factors were determined to be the solution of the injected seed by the high pressure methane and flow reversal from the liquid capture passage induced by a recirculation zone.

An integral separator with an improved flow field design and baffles to prevent flow reversal was designed to eliminate the above problems.

The results of the market study conducted on the program showed a potential market for over 2,000 integral separators for offshore, subsea and land based remote gas production. In addition a market was identified for wet gas metering for distributed gas well fields.

A supplemental plan was designed to complete demonstration of a commercial Integral Separator and is presented.

1. Introduction

The integral separator is a concept whose purpose is to dehydrate and lower the dewpoint of high pressure natural gas streams. The device can have a rotating or static separation surface[1] and is compact to enable its use for offshore and remote applications. The initial geometry considered with a stationary separation surface is illustrated in figure 1.

The theoretical basis of operation involves the following processes:

1) Temperature of a wet gas stream is lowered by a near isentropic expansion in a nozzle. Injection of a seed liquid at the inlet of the nozzle provides nucleation sites for condensing water and heavy hydrocarbons.

2) The two-phase stream from the nozzle or nozzles is directed tangentially to a cylindrical chamber (hereafter referred to as the vortex chamber) creating a swirling flow. The wall can either rotate or be stationary. The initial geometry had a stationary wall.

3) The centrifugal forces in the flow cause the liquid droplets to separate from the gas vortex.

4) The liquid is ducted to a collection vessel for transport or re-injection.

5) The swirl of the dry gas stream is recovered as pressure in a diffuser, lowering the dewpoint of the gas to a value suitable for pipeline transport and processing.

The objective of this project was to develop and test a commercially viable integral separator. The prototype unit was demonstrated in an operating high pressure gas test facility at the Colorado Experimental Engineering Test Station with the support of Chevron Texaco.

The critical technical issues to be resolved were:

1) Efficacy of seed injection to establish equilibrium condensation in the expanding hydrocarbon flow

   Expansion of a saturated gas typically is super-cooled until the reversion point is reached (Wilson line in steam). At this point when sufficient super-cooling is reached, spontaneous condensation occurs resulting in sudden formation of very small droplets, <.1 to .2 μm in diameter. Injection of a seed liquid in the form of larger size droplets, >10 μm, is predicted to produce equilibrium condensation

[1] Brown, R., *Liquid Extraction and Separation Method for Treating Fluids Utilizing Flow Swirl*, US Patent 6,592,654 B2, July 15, 2003

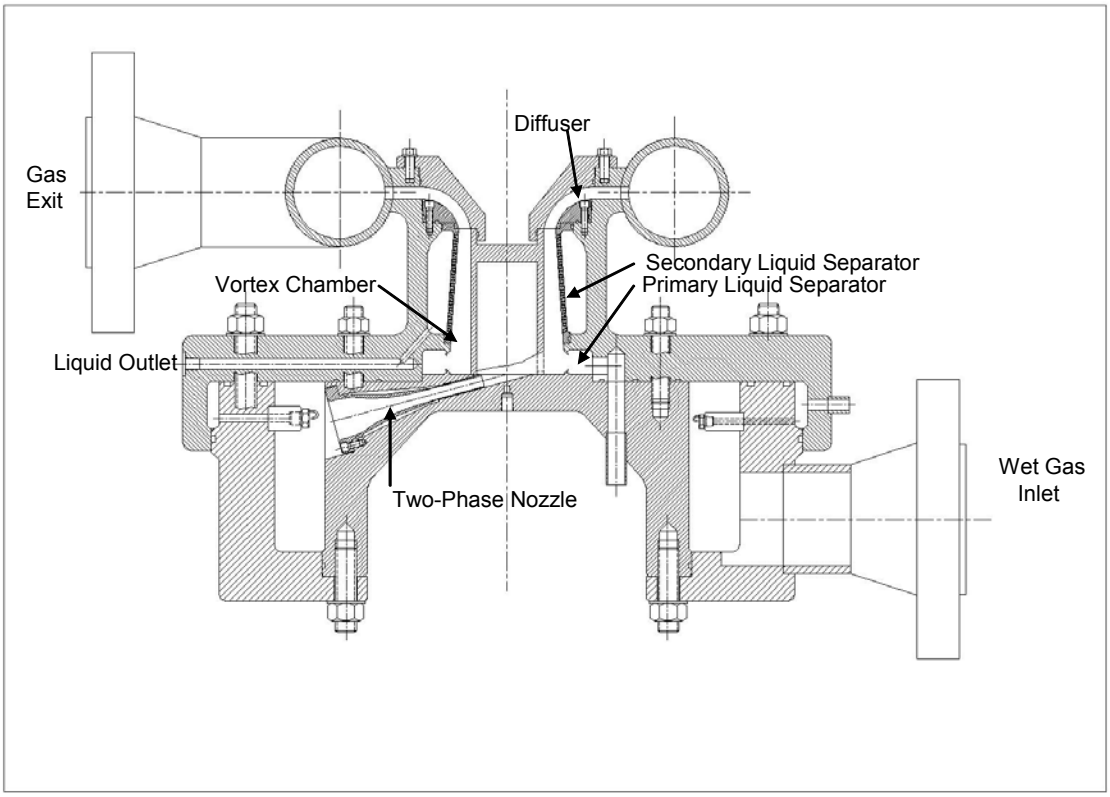

Figure 1 Cross Section of Integral Separator

during the expansion. The resulting larger droplets should enable greatly improved separation of the condensate.

2) Separation efficiency of the vortex chamber

The large centrifugal forces produced by the swirl will drive the droplets to the outer periphery of the vortex chamber. The residence time must be sufficient to remove all of the droplets from the gas flow. The liquid impact surfaces must be designed to prevent secondary entrainment and carryover of the liquid by the gas stream.

3) Energy losses in vortex chamber

Energy losses in the vortex chamber result in heating of the gas and separated liquid which will result in re-evaporation of the liquid, increasing the dewpoint of the gas. It is desirable to minimize the friction of the separated high velocity liquid stream and to recover the kinetic energy as pressure. A rotating wall accomplishes this by keeping the velocity of the separated liquid stream and gas stream at the free stream value. A stationary wall will result in a higher temperature due to recovery in the boundary layer. Friction losses in the gas stream once the separated liquid is removed will not increase the dewpoint by evaporation of the liquid but instead will increase it due to a decrease in the kinetic energy available for re-compression of the gas stream in the diffuser.

4) Pressure field in vortex chamber.

In a free vortex the tangential velocity is proportional to r^{-1}, where r is the radius and the pressure is proportional to r^{-2}. The lower pressure at the core can be utilized for recirculation of a portion of the flow to separate any secondary liquid entrainment. In the real flow field separation and wall friction occur limiting the pressure difference available for recirculation.

5) Efficiency of gas diffuser.

The gas dewpoint will depend on the expansion temperature at which the liquid is condensed and separated and the pressure to which the dry gas is compressed by the diffuser. The efficiency of the radial diffuser shown in figure 1 will depend upon the stability of the vortex flow and recirculation induced by turning the flow. The efficiency of an axial diffuser being investigated in the first gas test unit (cf. below) will depend upon the entering swirl and entering boundary layer of the flow from the vortex chamber.

2. Project Overview

Task1 Experimental Determination of Optimum Primary Separation Configuration

The first task was to design and test an Integral Separator with variable geometry. Geometric and flow parameters with air and water test fluids were varied to determine the most efficient method to separate the liquid from the gas in the two-phase nozzle stream. Pressure recovery in the diffuser was determined for the variations made in the primary separation zone. The results were be used to guide the design of the field test unit.

Task 2 Experimental Confirmation of the CFD Liquid Path and Gas Path Analyses and One Dimensional Analysis.

CFD analysis of the final test unit geometry was conducted. Predicted performance was determined for the flow conditions tested. Measurement of the axial and radial pressure profile in the separated gas vortex, the pressure increase in the liquid diffuser and the pressure increase in the radial gas diffuser was performed. The results were compared to the CFD predictions. The CFD model was validated.

A one-dimensional (hereafter referred to as "1-D") design code was formulated and compared to the CFD results and experimental results. The 1-D code was utilized to design the field test unit and the rotating Integral Separator.

Task 3 Design and Fabricate Commercial Prototype Integral Separator

Analysis and evaluation of remote gas production applications was completed. ChevronTexaco and other major and independent producers were contacted for requirements. In consultation with ChevronTexaco, process range and size were selected for the first prototype Integral Separator. A multiple nozzle commercial prototype Integral Separator and the demonstration skid were designed.

Task 4 High Pressure Laboratory Tests

The multiple nozzle prototype unit was tested with high pressure nitrogen and water mixtures to determine the separation and pressure recovery performance.

A single two-phase nozzle with temperature and pressure taps along the axis was designed and built. Tests were conducted with saturated natural gas with and without seed injection to determine the effect on the expansion process and on separation.

Task 5 Testing with High Pressure Wet Natural Gas

The prototype Integral Separator was tested with water saturated natural gas.

This unit was operated at a maximum natural gas flowrate of 15 MMscfd and a maximum pressure of 1100 psig.

Methanol and hydrocarbons were injected as the seed liquid. The pressure ratio across the nozzles and the seed flowrate were varied to test a range of operation for dewpoint control and separation efficiency.

Task 6 Field Demonstration

Demonstration of the prototype unit was conducted for ChevronTexaco at the Colorado Engineering Test Station. It was determined that the production unit, as configured was not ready to be operated in a production setting.

3. Analytical Results

Dehydration/Dewpoint Improvement

The lowering of the dewpoint is proportional to the expansion and liquid collection efficiency. Turboexpanders have a maximum isentropic expansion efficiency in the 85-90% range. However, expansion in the nozzles of the Integral Separator results in an isentropic nozzle efficiency above 98%.

The frictional heating during the expansion is:

$$\Delta Q = \int T ds$$

Where: ΔQ = frictional heat; T = temperature of mixture; s = entropy of mixture

The higher the expansion efficiency, the lower is the change in entropy. An entropy change of zero (expansion efficiency = 100%) means there is no frictional heating, hence the maximum cooling and liquid production.

In order to achieve high expansion efficiency the saturated gas was mixed with a seed liquid and expanded in a two-phase nozzle with an optimum pressure profile to the desired temperature. The seed liquid was provided to produce equilibrium expansion and droplets of the condensed liquid which were large enough for separation utilizing the centrifugal forces resulting from the flow swirl. The analysis of spontaneous condensation gave predicted droplet sizes in the .05 to .1 micron range. Introduction of seed droplets with a diameter of 762 microns (.030") resulted in a predicted rapid breakup of the seed droplets to provide a large surface area for equilibrium condensation of the water and gas liquids. A droplet diameter of about 5 microns at the nozzle exit was calculated by the code.

Two gas production applications of interest were provided by ChevronTexaco under a confidentiality agreement. Stream 1 is a subsea gas field. Stream 2 is an offshore gas field. The process conditions have previously been reported[2].

An innovative feature of the Integral Separator is to provide a hydrate inhibitor as the seed liquid. The amounts to be utilized in Stream 1 and Stream 2 are acceptable to ChevronTexaco and are equal to the amounts required anyhow for the separated liquids at the dewpoint temperatures sought (when other applications are addressed where hydrate suppression is not a requirement a small fraction of the cooled, separated liquids would be re-circulated to the nozzle inlet).

A HYSYS simulation was modeled for the complete process from the wellhead through the two-phase nozzle and Integral Separator. Per ChevronTexaco, the wellhead pressure

[2] Hays,L., and Franz, R., *Research and Development of an Integral Separator*, Semi-Annual Report, Contract DE-FG02-03ER83847, Energent Corporation, Santa Ana, California, February, 2004

was throttled to the two-phase nozzle inlet pressure and a heat exchanger module and free liquid separation module were provided to produce saturated gas at the desired inlet conditions. The complete HYSYS simulation output is provided in Appendix A.

The two-phase nozzle equations were re-programmed into a spreadsheet formulation with a dynamic link with the HYSYS properties code. Sample cases were run and the results were compared with the previous two-phase nozzle code (which produced excellent agreement between predicted and measured expansion efficiency[3]). Agreement within 0.1% was demonstrated between the two codes.

The inlet pressure to the nozzles was set at 1200 psia to achieve the required dewpoint (< 40F) while providing dry gas at a pressure of at least 1,000 psia. Higher gas transport pressures at the same dewpoint can be obtained by increasing the inlet pressure while keeping the same nozzle expansion ratio. The inlet temperature was set at 80 F per ChevronTexaco.

The expansion pressure for each resource was varied until the target expansion temperature was achieved. In the case of Stream 1 the value was 39 F, in the case of Stream 2 the value was 35 F. Lower values could be attained by increasing the pressure ratio across the nozzle. For the case where a hydrate inhibitor such as methanol or glycol is used as the liquid seed, the expansion temperature can be below the freezing point for water. This is an important feature for deepwater subsea resources where very cold ambient temperatures occur.

The outputs of the two-phase nozzle code are provided in reference 3. The specified expansion temperatures were attained with 6 in long nozzles. The isentropic expansion efficiency is greater than 98% in both cases.

Tables 1 and 2 summarize the results for the subsea case and offshore case.

[3] Elliot, D.G. and Weinberg, E., *Acceleration of Liquids in Two-phase Nozzles*, TR32-987, Jet Propulsion Laboratory, Pasadena, July 1968.

Table 1 Process Summary for Subsea Case

Inlet Pressure	1200 psia
Inlet Temperature	80 F
Inlet Flowrate	50 MMscfd
Separation Pressure	860 psia
Separation Temperature	38.7 F
Methanol Rate	1.7 Bbl/d
Liquid Outlet Pressure	1109 psia
Dry Gas Outlet Pressure	1053 psia
Dry Gas Outlet Temperature	74 F
Dry Gas Dewpoint	40.7 F
Effective Compression Power	422 kW
Weight	1140 lb
Volume	5.5 ft^3

Table 2 Process Summary for Offshore Case

Inlet Pressure	1200 psia
Inlet Temperature	80 F
Inlet Flowrate	50 MMscfd
Separation Pressure	835 psia
Separation Temperature	35 F
Methanol Rate	6.6 Bbl/d
Liquid Outlet Pressure	1084 psia
Dry Gas Outlet Pressure	1036 psia
Dry Gas Outlet Temperature	74 F
Dry Gas Dew Point	37 F
Effective Compression Power	565 kW
Weight	1140 lb
Volume	5.5 ft^3

Separation Improvement

The use of a seed liquid in the two-phase nozzle design resulted in a high velocity two-phase jet with properties similar to those for which excellent separation efficiency was demonstrated. This innovation was found to be a key to good separation performance for condensing flows.

A two-phase separator having a moving wall is shown in figure 2. The two-phase jet leaving the nozzle impinges tangentially on the moving liquid surface. As can be seen 100% of the liquid is separated, forming a clear film that is removed by the open scoop. In this case, the droplets are sufficiently large that the separation occurs in a very short axial distance. Allowing the separating liquid surface to move with the gas eliminates secondary entrainment, minimizes gas friction losses, and controls the liquid inventory.

A recently tested innovation is to utilize a stationary wall with a deep liquid layer to provide the moving liquid surface instead of a rotating solid surface having moving parts.

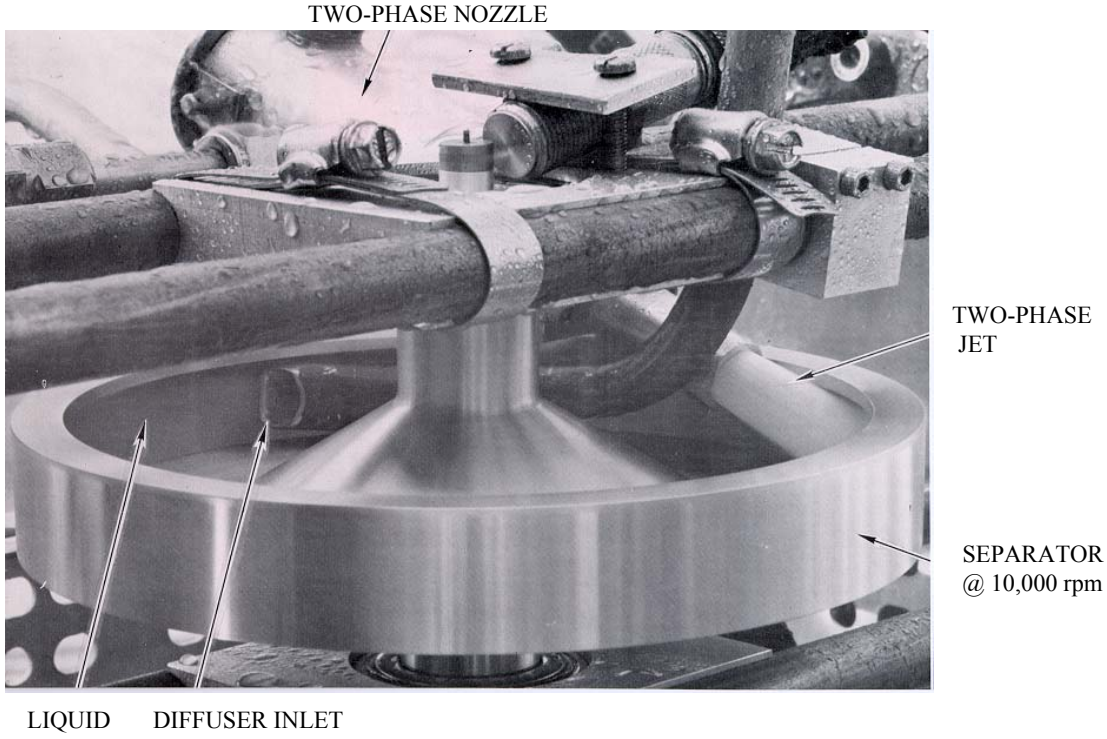

Figure 2 Separator with Moving Wall

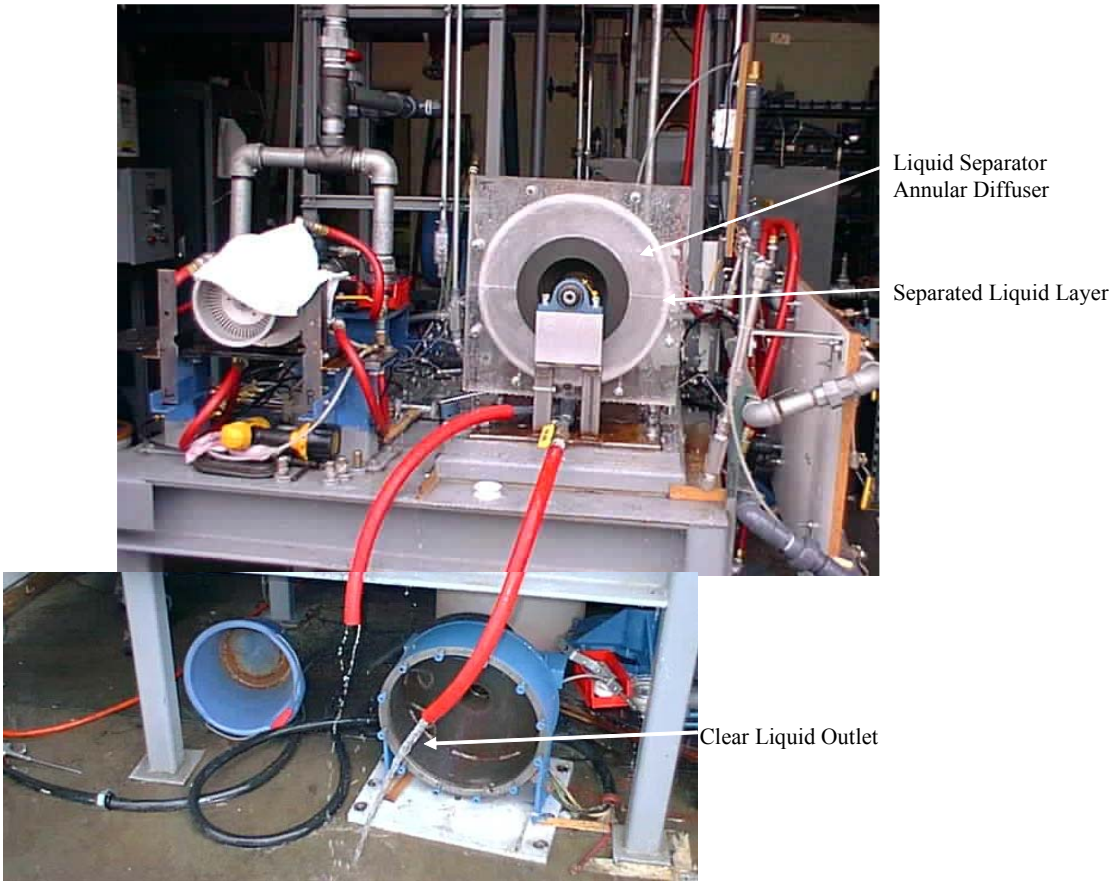

Figure 3 Separator with Free Liquid Surface and Stationary Wall

This is illustrated in figure 3. The high G centrifugal force maintains the liquid layer and results in a "stiff" liquid surface[4]. The deep liquid layer minimizes the friction loss of the separated liquid enabling a high tangential liquid velocity at the interface. The centrifugal forces of the swirling liquid produce a pressure rise as the liquid spirals radially outward. Friction losses occur on the sidewalls. However, for the cases analyzed (c.f. below) the increase in pressure results in sub-cooled liquid at the outlet. This part of the Integral Separator is referred to as the "liquid separator annular diffuser".

The main advantage for the liquid separator annular diffuser is to enable complete separation of the produced liquids and water from the cold gas with no moving structures. This feature is a major advantage for subsea and other remote applications.

[4] Engel, O., E., *Crater Depth in Liquid Impacts*, Journal of Applied Physics, Volume 37, Number 4, March 1966

To evaluate the separation an analysis was performed.

The length required for the Integral Separator is inversely proportional to the diameter of the droplets formed. The forces acting on a droplet in a swirling flow are:

$$F_n = F_c - F_p - F_d$$

Where: F_n = net force towards the separation surface
F_c = centrifugal force
F_p = pressure force
F_d = drag force

The force relations as given by Plat[5] are:

$$F_n = (4\pi r_s^3 \rho_l / 3g_c) \, d^2r/dt^2$$

$$F_c = [\pi (2r_s)^3 (\rho_l - \rho_g) \omega^2 / 6g_c] \, r$$

$$F_d = (6\pi\mu r_s) \, dr/dt$$

$$F_p = (\pi\rho_g\omega^2 r_s^3 / 2g_c) \, r$$

Where: r_s = droplet radius
r = radial distance
ω = rotational speed
t = time
μ = viscosity
ρ = density (l = liquid, g = gas)
g_c = gravitational constant

The force balance was programmed using these equations, the gas and liquid properties, droplet size and swirl (assuming solid body rotation). The flow and geometric parameters for applications above were examined. The calculations were performed for an inner radius of 1.5 inches and an outer radius of 2.35 inches (the actual Integral Separator geometry for the preliminary design) and a tangential two-phase velocity of 799 ft/s (the two-phase nozzle exit velocity for Stream 1). The design provides an effective "G" force of 93,000 times gravity at the inner radius and 56,500 at the separation radius.

Figure 4 provides the results of the analysis. The flow path separation length required is only 2.5 in. A flow path length of greater than 600 ft is required for the droplet size produced by spontaneous condensation, ~.05 microns. For the nozzle entry angle of the

[5] Plat, R., *Gravitational and Centrifugal Oil-Water Separators with Plate Pack* Internals, Delft University press, Delft, May, 1994

Phase 1 design, 15 degrees, the axial distance for complete separation calculated to be only .64 inches.

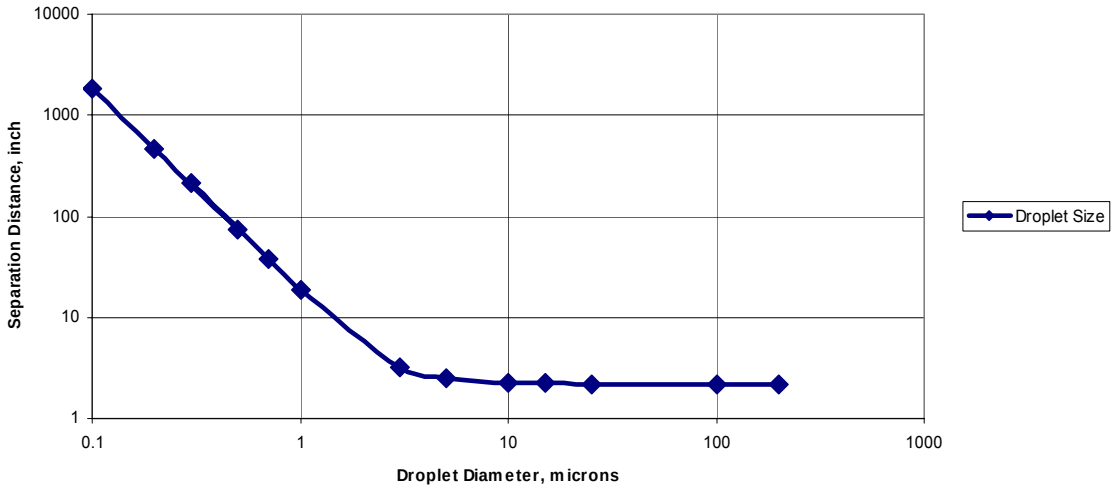

Figure 4 Required Separation Distance in Integral Separator Versus Droplet Size For Gorgon Flow Conditions

Separation of smaller droplets in the spectrum and/or mist or splash can be achieved if required by providing a porous outer wall. The high centrifugal forces in the gas vortex provide continuing separation. The pressure difference between the outer wall and the inner core of the gas vortex is quite large, c.f. below. This enables recirculation and separation of any secondary separation stream if needed.

Liquid Pressure Recovery

A liquid annular diffuser enables the recovery of pressure in the separated liquid to maintain a subcooled state.

Computational fluid dynamic (CFD) analysis was carried out for the liquid flow in the liquid annular diffuser of the Integral Separator. At the inner boundary, the separated liquid has a velocity equal to the tangential velocity of the impinging two-phase jet. As the liquid annulus swirls outward the pressure increases. However, frictional losses and heating occur due to the sidewall friction. The design goal is to increase the pressure as the temperature increases such that the liquid remains in a subcooled state. If vapor were formed it could flow counter to the liquid flow and remix with the separated gas, increasing the dewpoint slightly.

For the geometry analyzed a pressure rise of over 200 psi was calculated. This corresponds to a pumping efficiency of 20% based on the incoming kinetic energy. The results were input to the HYSYS model, Appendix A. A pumping efficiency of 16% was used for conservatism. Zero vapor flow was calculated by the HYSYS model for these conditions.

Dry Gas Pressure Recovery

A key result of Phase 1 was the efficient conversion of the flow swirl into compression of the dry gas. A "compressor" efficiency of greater than 60% was determined for a stationary wall Integral Separator. This result enabled a unit with no moving parts to be designed for the applications considered. For the subsea case the avoided compressor power was 422 kW.

CFD analysis of the separated dry gas was performed using Numeca software. Both moving and stationary walls were analyzed. Over twenty (20) variations in geometry were made to determine the best configuration. A geometry with a stationary wall was found which produced sufficiently high compression efficiency (>60%) to provide the gas pressure required for pipeline transmission (~1000 psia) for the applications provided by ChevronTexaco.

A view of the gas path geometry and liquid geometry is provided in figure 5. Gas enters the inlet at an angle of 15 degrees to the inlet plane. Transition to the vortex flow occurs in the transition region. The vortex flow proceeds and the flow enters the radial diffuser swirling outward until entering an exit manifold, outlet. This geometry was analyzed for rotating wall sections as indicated and a stationary wall. We will report on the stationary wall results.

Figure 5 shows the variation of pressure from the inlet, 860 psia to the outlet, 1049 psia. The pressure rise from the inner wall to the outer wall is seen to be 100 psi. This provides a substantial pressure difference to re-circulate any secondary separated liquid flow from the outer wall. The pressure coefficient – static pressure rise divided by inlet kinetic energy – was calculated to be 61% for the geometry shown.

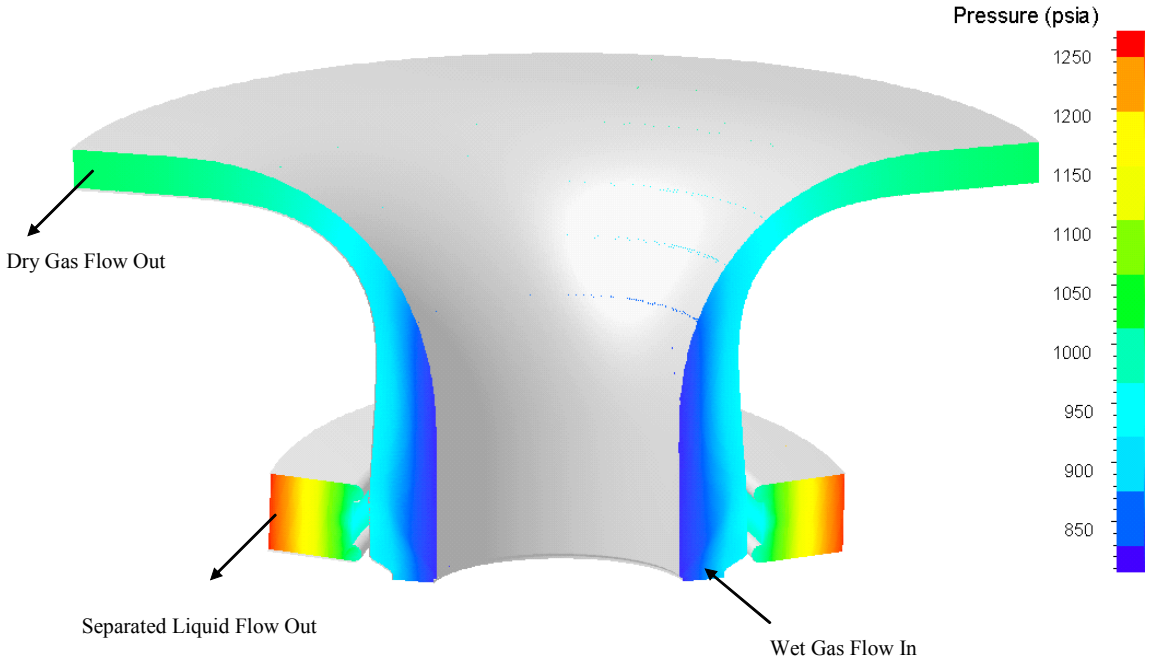

Figure 5 Integral Separator Geometry Analyzed by CFD

Figure 6 is a plot of tangential velocity from the inlet value, about 700 ft/s to the outlet, 162 ft/s. As the gas flows outward the velocity head is converted to pressure.

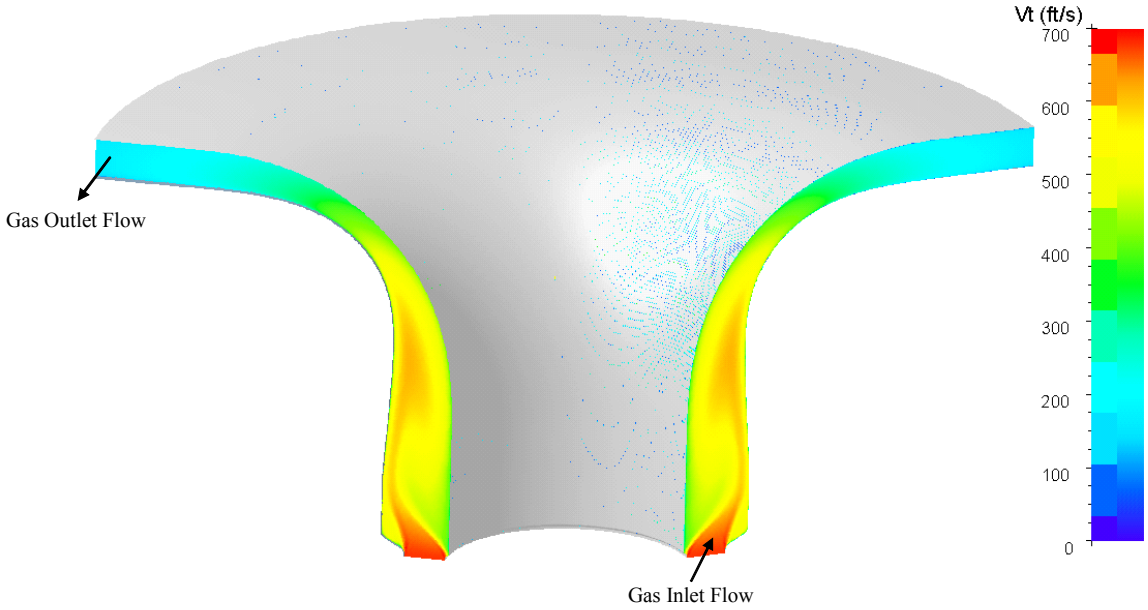

Figure 6 Tangential Velocity Field in Integral Separator

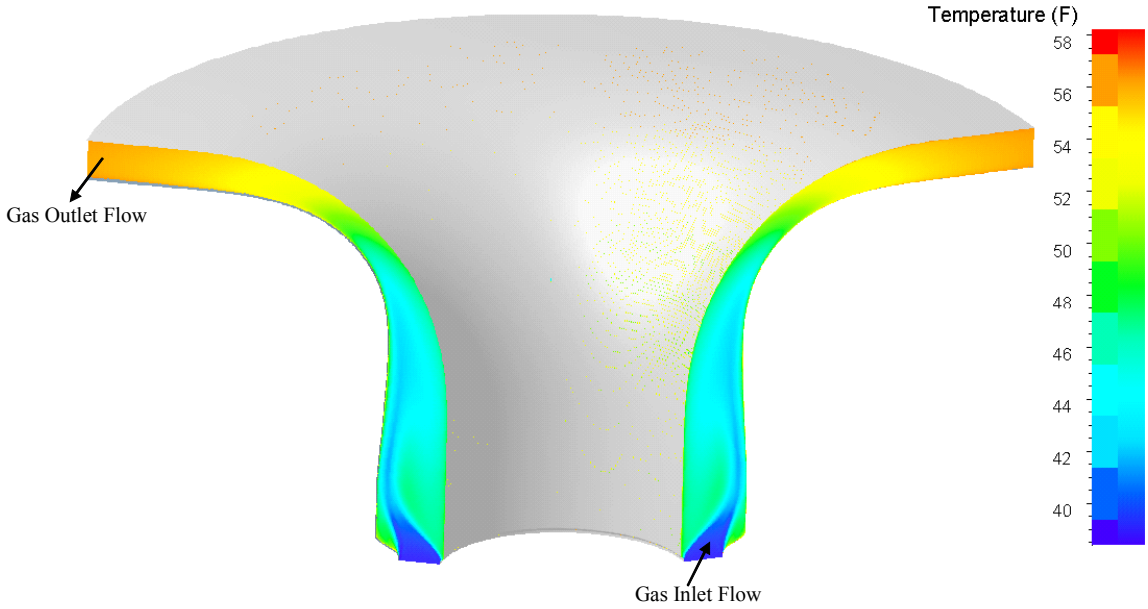

Figure 7 Temperature Field in Integral Separator

The gas static temperature is shown in figure 7. It slowly increases from the inlet and separation region to the exit of the diffuser. The inlet value of 39 F increases to 56 F as a consequence of the compression. The final diffuser geometry is vaneless which should enable good off-design operation.

The CFD analysis of the flow in the integral separator described above utilized a uniform end wall entry flow as a boundary condition. This results in an axisymmetric flow model.

The test model and the field unit will have a discrete circular nozzle penetrating the end wall at an angle. The nozzle opening is an ellipse on the end wall surrounded by a flat end wall surface. To enable a more realistic comparison of the experimental results the discrete nozzle case was modeled. Figure 8 shows the part of the nozzle included in the computation.

For a more exact CFD calculation, the flow through the Integral Separator was assumed to be periodic with the number of nozzles, eight. The intersection of the nozzles with the axial wall of the vortex chamber is an ellipse. Because these ellipses are closely spaced, the periodic boundary of the grid of one nozzle sector was chosen to be the midplane of the nozzle that contains the minor (radial) axis of the ellipse. This kept the computation of the flow in the region just inside the chamber between the nozzle streams within the grid domain. The expected nicer looking flow at the nozzle mid-span would cross the periodic grid boundary.

A butterfly mesh topology was used within the nozzle to have a nice grid near the walls. A butterfly mesh was also used in the inlet region of the vortex chamber to provide a transition from the elliptic cross section with the grid clustered near the intersection boundary to a cylindrical mesh in the main body of the chamber. Figure 9 shows selected cross-sections of the grid.

The design drawing of the Integral Separator, which the grid modeled, had the nozzles inserted into holes at the inlet of the vortex chamber. From the inner diameter of the nozzle to that of the hole (bore) was a sudden expansion. To avoid needing additional grid points to describe this step, the change in cross section was smoothed. The contoured nozzle was placed an additional distance of one quarter of the radius of the hole upstream to accommodate this smoothing.

The inlet of the computational grid was placed just inside the exit of the nozzle. The linearized Jet Propulsion Laboratory nozzle code, reference 3, provided the target boundary conditions for the CFD computation.

To simplify the computation for the present study of the gas flow within the vortex chamber, the fluid was regarded as a perfect gas, with the specific heat at constant pressure, c_p, and the ratio of the specific heats at constant pressure and volume, γ, chosen to match the properties predicted at the nozzle exit.

The focus of this calculation was the mixing of the nozzle streams inside the vortex chamber, consequently the diffuser was not included.

This case with the discrete nozzles, labeled "3-D" is compared to an axisymmetric equivalent, labeled, "axisym." For the axisym geometry, the total area of intersection of the eight nozzles with the front of the vortex chamber was represented as an annulus of the same area. This annulus was extended slightly upstream to accommodate the development of the boundary layer from the inlet conditions.

The nozzles are placed at a large angle to the axis of the vortex chamber to introduce swirl. A parameter, similar to nozzle efficiency, is introduced.

$$\eta_\theta = (V_{\theta 2})^2 / 2 / (h_{o1} - h_{2s})$$

where the quantities are mass flow averaged over a cross section.
h_{o1} = total enthalpy at station 1
h_{2s} = static enthalpy at station 2, through an isentropic process from station 1

A parameter expressing the efficacy of the vortex chamber in conserving the flow energy is the ratio of the total pressure at the exit of the vortex chamber to the value at the inlet to the chamber. Since the pressure actually increases and hence is available for pressure recovery in the diffuser, this parameter reflects the actual efficiency of the process.

Table 3 compares the results of the calculation at different station points within the vortex region. The labeled station points are indicated in Figure 15.

Table 3 Swirl Production Efficiency Parameters

		η_θ		P_{t2}/P_{t1}	
Cross section: 1 – 2		3-D	Axisym	3-D	Axisym
Inlet	Lrd_2	0.810	0.899	0.962	0.989
Inlet	Cylp	0.746	0.847	0.952	0.981
Inlet	Outlet	0.668	0.779	0.936	0.969
Ellp	Lrd_2	0.861	0.902	0.981	0.990
Ellp	Cylp	0.791	0.850	0.971	0.981
Ellp	Outlet	0.708	0.782	0.955	0.969

Note that ‘inlet’ refers to the inlet of the computational domain, and not to the same cross-section.

The axisymmetric calculation has higher kinetic energy efficiency and higher pressure recovery efficiency, as expected. The details of the nozzle jets merging in the chamber and the attendant mixing losses are not included in the axisymmetric calculation.

The nozzles are contoured to condense droplets out of the flow stream along the nozzle path. Between the exit of the contoured nozzle and the elliptic cross-section, there is an expansion through the remainder of the bore in which the nozzle is inserted. As discussed above, for the calculation this change in cross section was smoothed. There was a noticeable increase in entropy across this expansion, associated with the flow behind the “step.”

The computational results confirm the loss in the expansion from the nozzle internal diameter to the diameter of the bore. In the 3-D case the kinetic energy loss from the nozzle internal diameter to the outlet of the bore is nearly 5 percentage points. This result agrees with the loss observed during the air-water testing and indicates the nozzles should terminate flush to the end wall.

The difference in pressure recovery efficiency from “Ellp” to “Outlet” between the 3-D case and the axisymmetric case is only 1½ percentage points. The results indicate a modest advantage may be obtained with a full admission nozzle or with a single nozzle discharging into a curved passage.

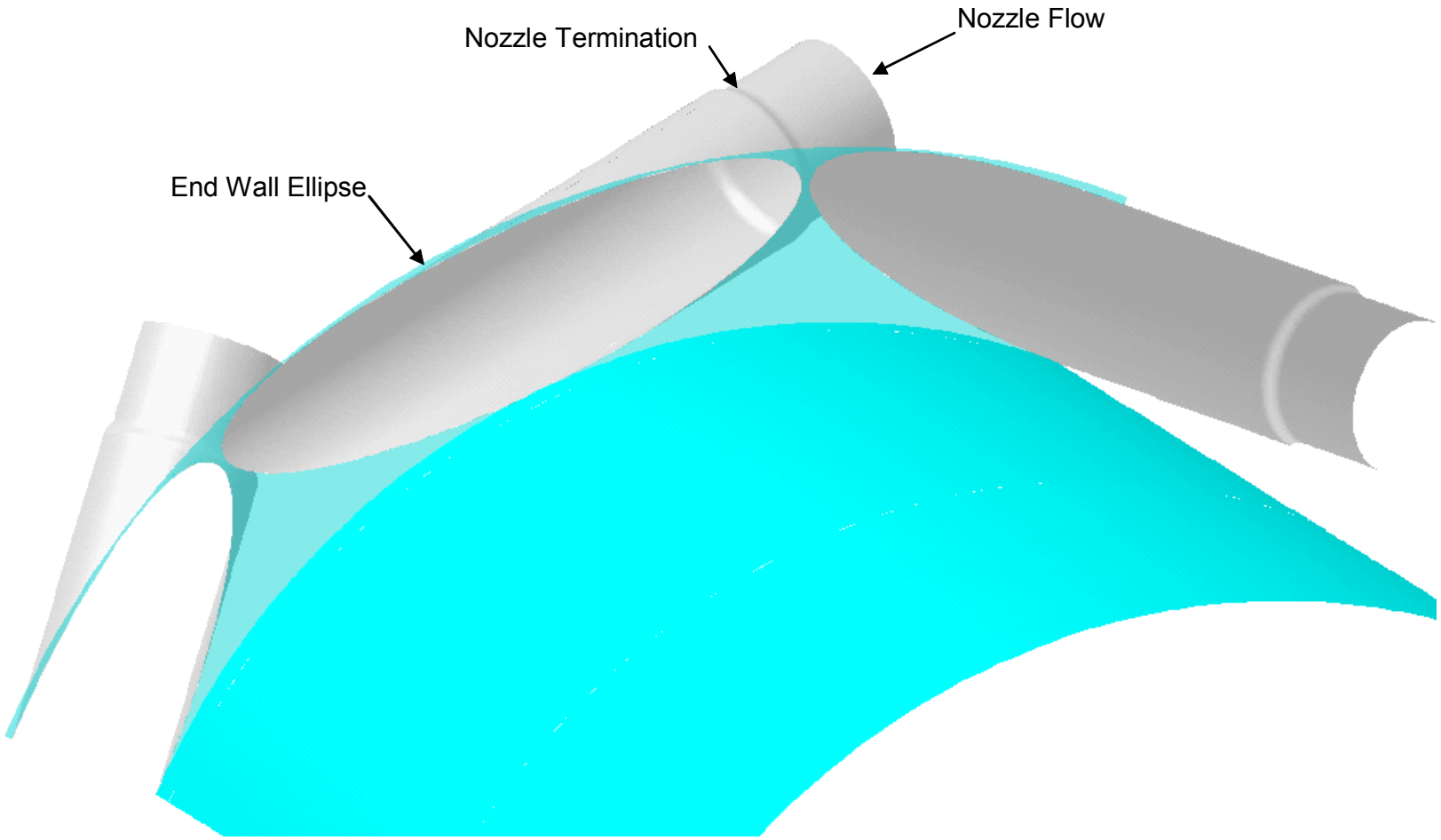

Figure 8 Geometry Analyzed in 3 Dimensional CFD Calculation

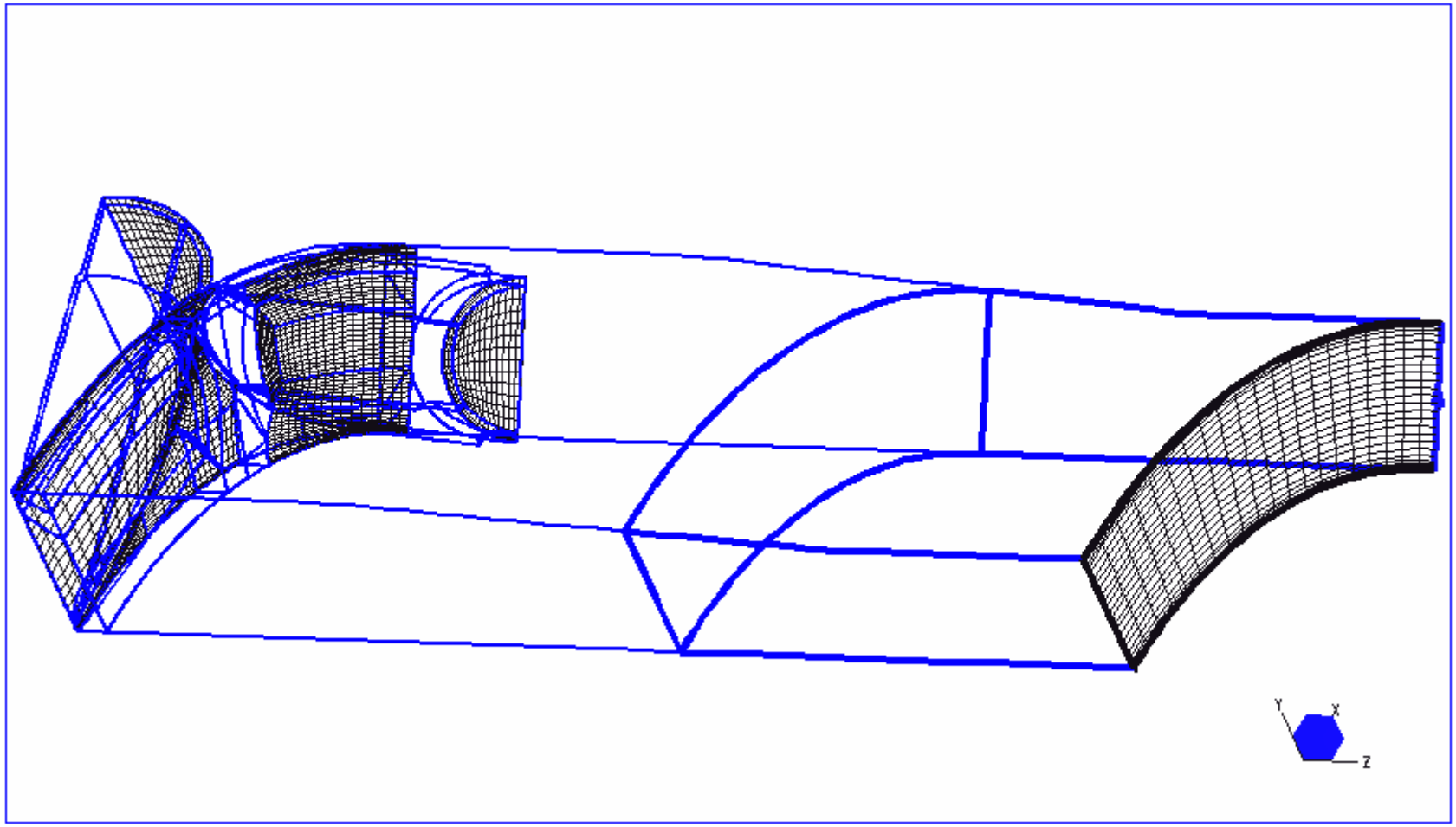

Figure 9 Mesh for 3 Dimensional CFD Calculation

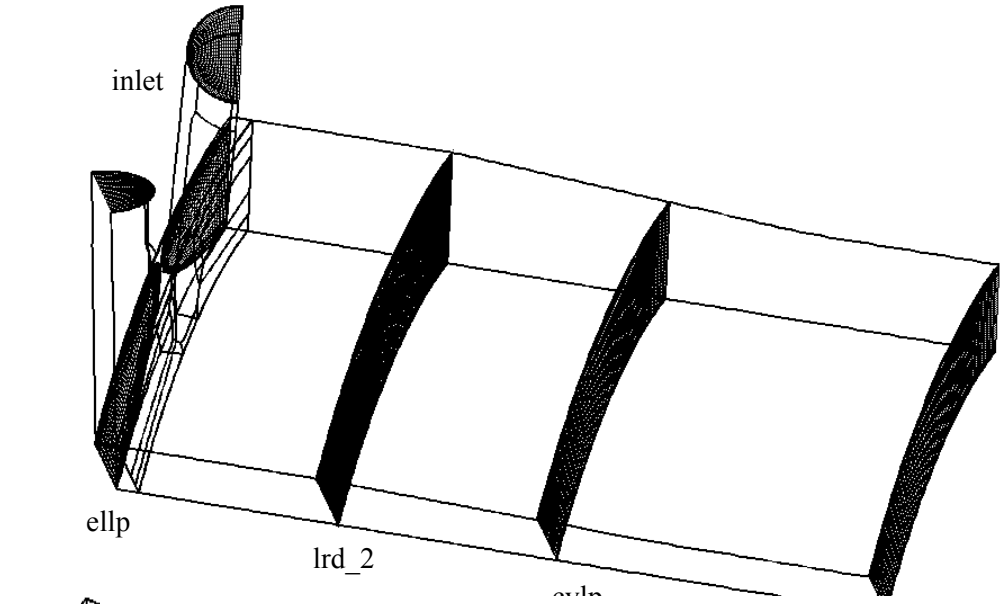

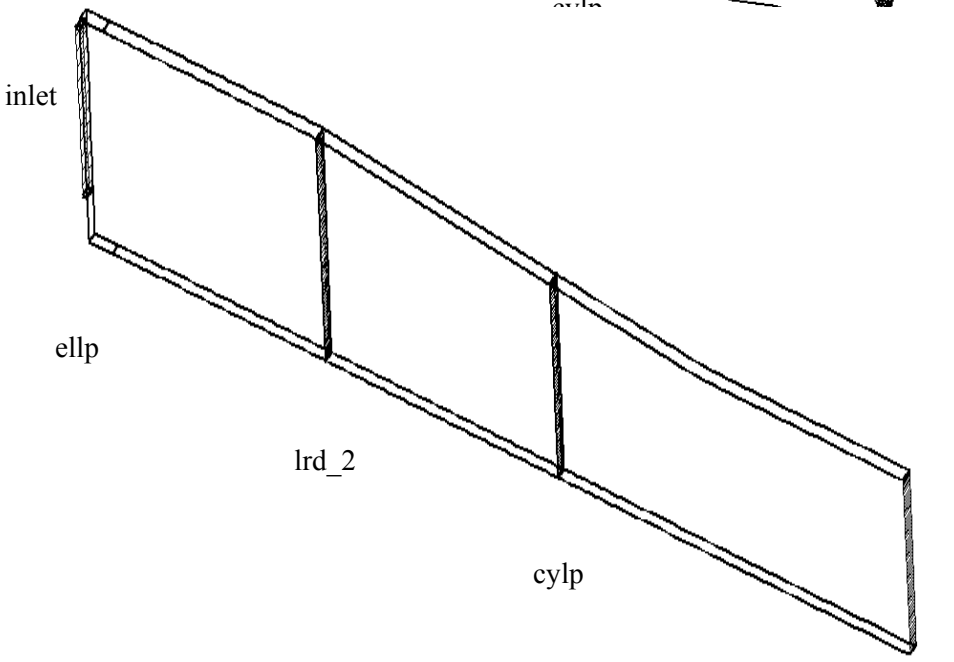

Figure 10 Flow Stations for CFD Calculations

One Dimensional Model

The CFD model continues to provide the best tool to analyze the Integral Separator flow field and losses. However, the large number of data points for the test unit and the various tradeoffs in design require an analytical tool that is less time consuming to use. A one dimensional analytical model with loss coefficients was developed for this purpose. The one dimensional (hereafter referred to as "1-D") model was then applied to the subsea case and the results compared to those predicted by the axisymmetric case.

The input to the 1-D model is the output from the two-phase nozzle code. The code is a linearized treatment of the JPL code and was tested against the JPL code. Several cases were run with an agreement of the predicted two-phase velocity to within 1%. The linearized version was programmed into an Excel spreadsheet which calls fluid properties for every step from HYSYS properties code.

The nozzle exit outputs from the code which are inputs for the 1-D model are:

Pressure, p_e
Momentum Averaged Two-Phase Velocity, V_b
Nozzle Exit Diameter, d_n
Liquid Droplet Radius, r_d
Liquid Flow, m_l
Gas Flow, m_g
Liquid Density, ρ_l
Liquid Viscosity, μ_l
Gas Density, ρ_g
Gas Viscosity, μ_g

Additional parameters which are specified for the design are:

Nozzle Inlet Angle with End Wall, θ_n
Vortex Chamber Radius, r_o
Vortex Chamber Length, l_c
Diffuser Pressure Coefficient, η_d
Extension of Liquid Separation Surface Past Geometric Impingement, l_s/l_i

The successful separation with a solid impingement surface led to consideration of this approach for the initial separation, similar to the JPL impingement separators[6] problems encountered with operation of multiple nozzles with free liquid in the entering gas, led to construction of a 1-D model that could consider single or multiple nozzle operation. Figure 11 is a cross section of the geometry considered.

[6] Elliott, D.G., Cerini, D.J., and Hays, L.G., *Liquid MHD Power Conversion*, Space programs Summary 37-45, Volume IV, Jet Propulsion Laboratory, Pasadena, California, June 1967.

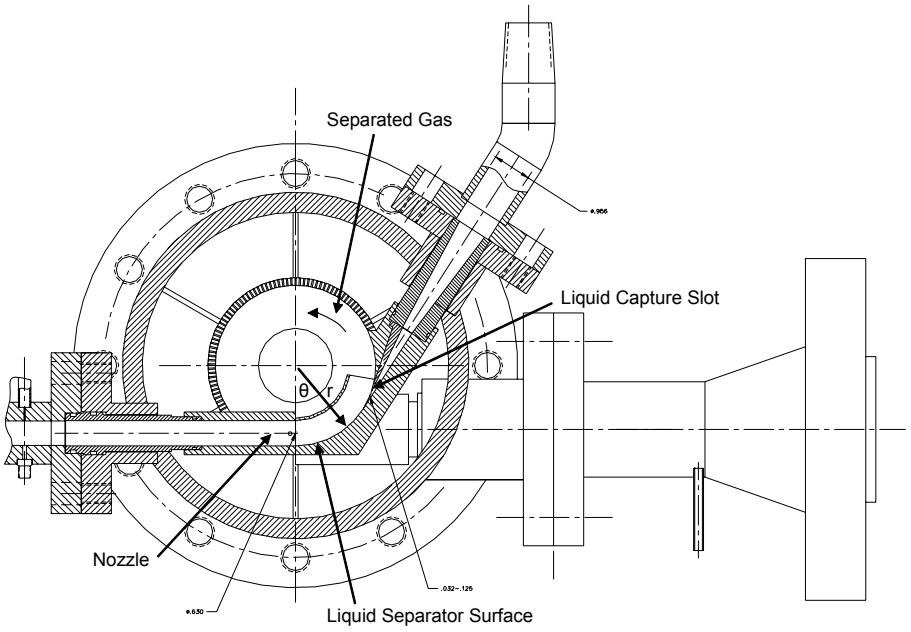

Fig 11 Cross Section of single Nozzle Separator

For the single nozzle case, flow from the nozzle impinges on a curved plate. The centrifugal forces cause separation of the liquid, which forms a high velocity liquid layer. The liquid is captured by a slot. The separated gas swirls in the vortex chamber, centrifuging remaining liquid to a porous wall. The dry gas subsequently enters a diffuser, either radial or axial, where the swirl is recovered as pressure.

The liquid velocity variation on the separation surface was determined by considering the momentum flux entering a control volume at the nozzle velocity and the retarding force due to wall friction. The Blasius equation[7], reference 4 was applied to an element at an angle θ with the separation surface having a radius of curvature, r, equal to the radius of the vortex chamber.

$$f = .316 / (Re^{-.25})$$

$$\tau_w = f \rho_l V_l^2 / 8$$

$$F_d = \tau_w d_n r_o d\theta$$

[7] Eckert, E.R.G., and Drake, R.M., *Heat and Mass Transfer*, McGraw-Hill, New York, 1959.

The incoming momentum flux is:

$$dMom = dm_l \, V_b$$

$$dMom = m_l \, V_b \, r_o \, d\theta / \sin\theta \, d_n$$

Collecting terms gives an expression for the change in velocity of the liquid along the separator surface:

$$dV = (V_b \cos\theta / \theta - V/\theta - C_1 \, V^2 / \theta \sin\theta) \, d\theta$$

$$\text{where } C_1 = .316 \, \mu_l^{.25} \, d_n^{.25} \, \rho_l / \, m_l^{1.25}$$

A numerical integration over the separation surface was programmed into the code.

The pressure recovery from the separated liquid was calculated assuming a hydraulic jump at the capture slot entrance.

$$\Delta p_l = (m_l / d_n \, \Delta h \,) \, (V_e - m_l / \rho_l \, d_n \, \Delta h)$$

The gas vortex friction loss was estimated using a flat plate relation, ibid:

$$f_{pm} = .074/Re^{.2} - 1700/Re$$

and:

$$\tau_{fp} = f_{pm} \, \rho_g \, V_b^2 \, /8$$

The momentum loss was determined from the force on the vortex chamber wall:

$$m_g \, (V_b - V_e) = \tau_{fp} \, 2\pi \, r_o \, l_c$$

The pressure recovery in the gas diffuser was calculated using the pressure recovery coefficient C_2 as an input parameter:

$$\Delta p_g = C_2 \, \rho_g \, V_e^2 \, / \, 2$$

The distance required to separate droplets in the two-phase nozzle flow is given by the balance of centrifugal, pressure and drag forces:

$$F_n = F_c \; - \; F_p \; - \; F_d$$

Where: F_n = net force towards the separation surface
F_c = centrifugal force
F_p = pressure force
F_d = drag force

The force relations as given by Plat, ibid, are:

$$F_n = (4\pi r_d^3 \rho_l / 3g_c) \, d^2r/dt^2$$

$$F_c = [\pi (2r_d)^3 (\rho_l - \rho_g) \omega^2 / 6g_c] \, r$$

$$F_d = (6\pi\mu r_d) \, dr/dt$$

$$F_p = (\pi\rho g_c \omega 2r_d^3 / 2g_c) \, r$$

Where: r_d = droplet radius
r = radial distance
ω = rotational speed
t = time
μ = viscosity
ρ = density (l = liquid, g = gas)
g_c = gravitational constant

The force balance was programmed using these equations, the gas and liquid properties, droplet size and swirl (assuming solid body rotation).

The resulting 1-D code was programmed in Excel and used to predict gas pressure recovery with multiple nozzles for the subsea application. The results give a calculated outlet pressure of 1047 psia for a diffuser coefficient of .85 in close agreement with the CFD prediction of 1049 psia.

Process Performance with Integral Separator

A process simulation for the ChevronTexaco applications showed the Integral Separator with the performance calculated met the process requirements for both subsea and offshore operation.

A process simulation was prepared using HYSYS to determine the results of application of the Integral Separator to the two applications provided by ChevronTexaco. Figure 12 is the complete process flow diagram for the simulation.

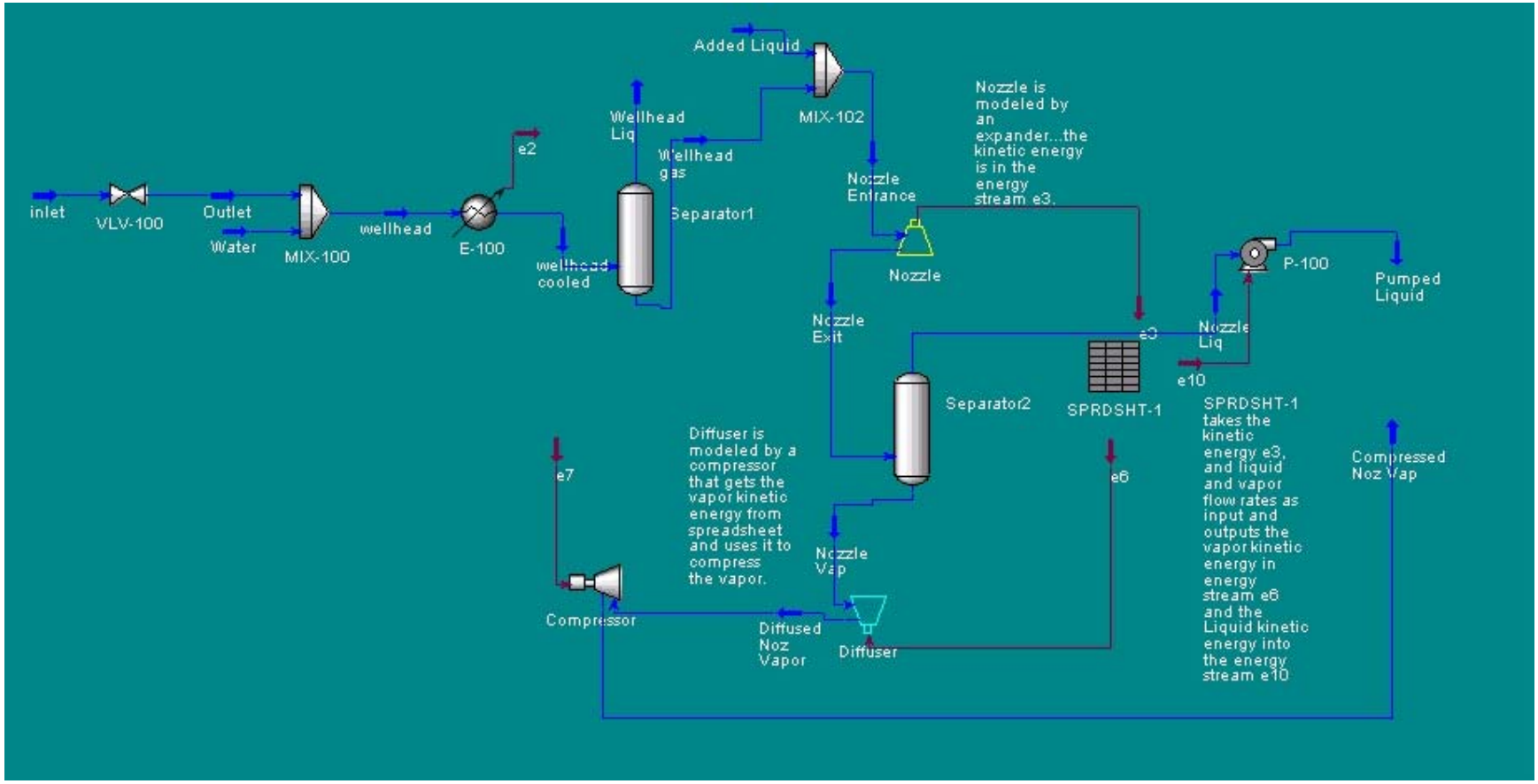

Figure 12 HYSYS Model of Integral Separator System

The process begins with the well flow, “inlet”. The flow is throttled to the desired inlet pressure through valve “VLV-100”. Water is mixed, “MIX-100”, to ensure that the gas is saturated with water vapor. The flow is cooled or heated by an exchanger, “E-100”, to set the required inlet temperature. The free liquids are separated at the higher inlet temperature in “Separator 1” to minimize the amount of hydrate inhibitor that must be injected to prevent hydrate formation at the lower expansion temperature (this separator can be another compact Integral Separator operating at a lower expansion ratio).

The saturated gas stream flows to the Integral Separator mixer, “MIX-102”, where the seed liquid, “Added Liquid”, is injected. The mixture is expanded in the two-phase nozzle, “Nozzle”. The nozzle is modeled with an expander module in HYSYS where the input efficiency is the value calculated with the nozzle code.

The flow from the two-phase nozzle is separated, “Separator 2”. The separated liquid flows to a splitter, “Splitter 1” which can be varied to produce any value of liquid carryover from the separator into the separated gas stream. The separated liquid flows to a pump module, “P-100”. The input energy for the pump is the liquid kinetic energy produced by the nozzle expansion. The pump efficiency is the efficiency calculated for the liquid annular diffuser. The resulting flow goes to a separator module, “V-100”. If gas evolves in the annular diffuser due to low efficiency it is separated and re-mixed with the liquid carryover into the primary separated gas stream, MIX-101.

The gas stream is diffused to a higher pressure, “Diffuser”. The diffuser is modeled with a HYSYS compressor module. The energy input for that module is the gas kinetic energy calculated by the two-phase nozzle code. The efficiency input for the module is the value calculated by the CFD analysis of the gas path.

The high pressure gas flow is split, “Splitter 2”. The sidestream is cooled, “E-101” until the first liquid appears. The dewpoint, “Dewpoint” is output for the process.

The process simulation outputs for Streams 1 and 2 are given in Appendix B. The dewpoint calculated for Stream 1 was 40.7 F. For Stream 2 it was 37.9 F. In each case the dewpoint could be decreased by increasing the nozzle expansion pressure ratio.

The output of the gas diffuser was 1049 psia for Stream 1 and 1036 psia for Stream 2. Each had a substantial margin for the stated 1000 psia requirement. In view of the high wellhead pressures, 5,000 psia and 5,900 psia, respectively, an ample margin exists to provide higher gas pipeline pressures if required.

4. Integral Separator Design

Three basic geometries were designed and manufactured on the program instead of the two originally planned. The additional geometry was designed to determine the feasibility of a single nozzle unit to reduce the size. The single nozzle was also used to acquire basic information on the nozzle pressure and temperature profiles and on the effect of seed injection. Additional geometric variations were made during testing of each.

Multiple Nozzle Test Unit

An integral separator was designed to model the geometry of the preliminary design for the subsea application, figure 1. The test unit design is shown in figures 13 and 14. Eight (8) two-phase nozzles were provided. The nozzles are fed by a plenum into which compressed air and water are supplied. Injectors are also fed by another plenum into which pressurized water is supplied.

After expanding in the nozzles the two-phase flow is directed onto the separation surface. The separation surfaces tested were a free liquid layer and a cylindrical solid surface with the separated liquid leaving tangentially into the free liquid surface.

The separated air forms a vortex, spiraling upwards towards the diffuser. Two outer walls were tested – a solid wall and a porous wall with 1/32" dia. holes. The purpose of the porous wall was to remove any liquid not separated by the initial separation surface.

The air stream enters a radial diffuser feeding a plenum and flows to a secondary separation tank to measure any carryover of liquid.

A removable inner wall was provided in the vortex chamber. Tests were conducted with and without an inner wall.

Figure 15 shows a view of the nozzle holder. Figure 16 shows the nozzle inserts installed. Figure 17 provides a view of the liquid separation annulus with the outer wall of the vortex chamber installed. The assembled test unit is shown in figure 18.

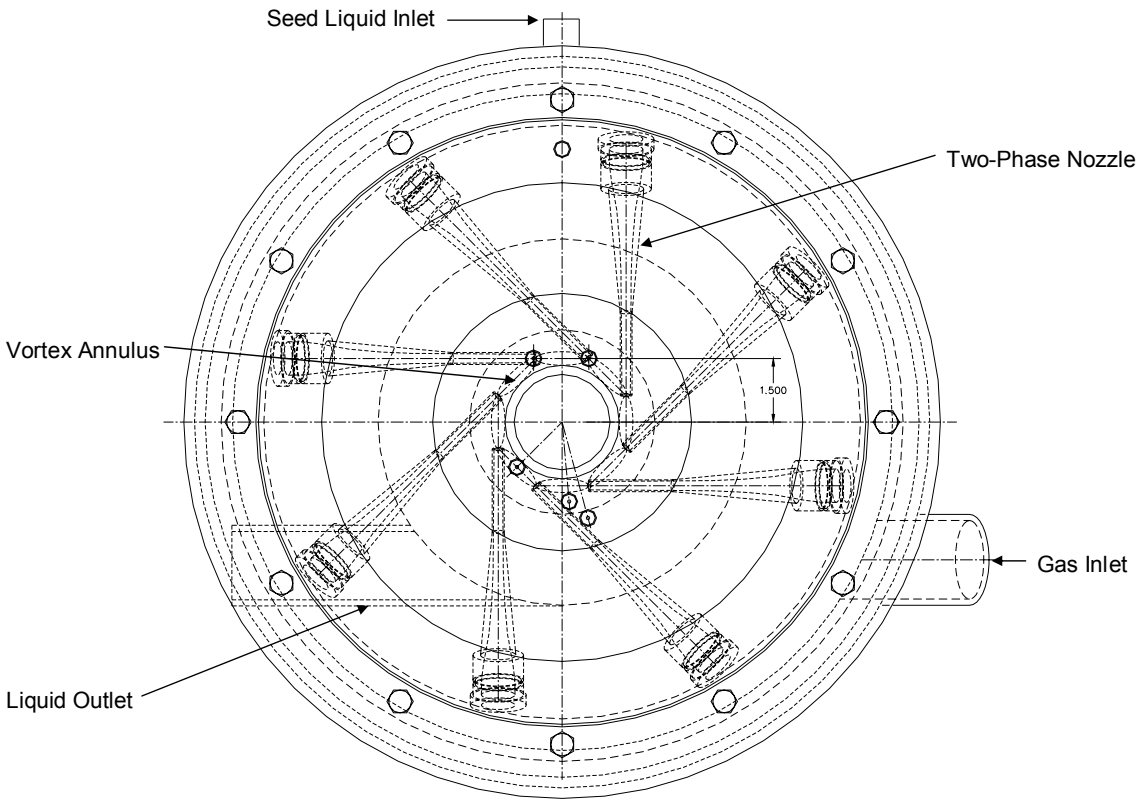

Figure 13 End View of Test Section

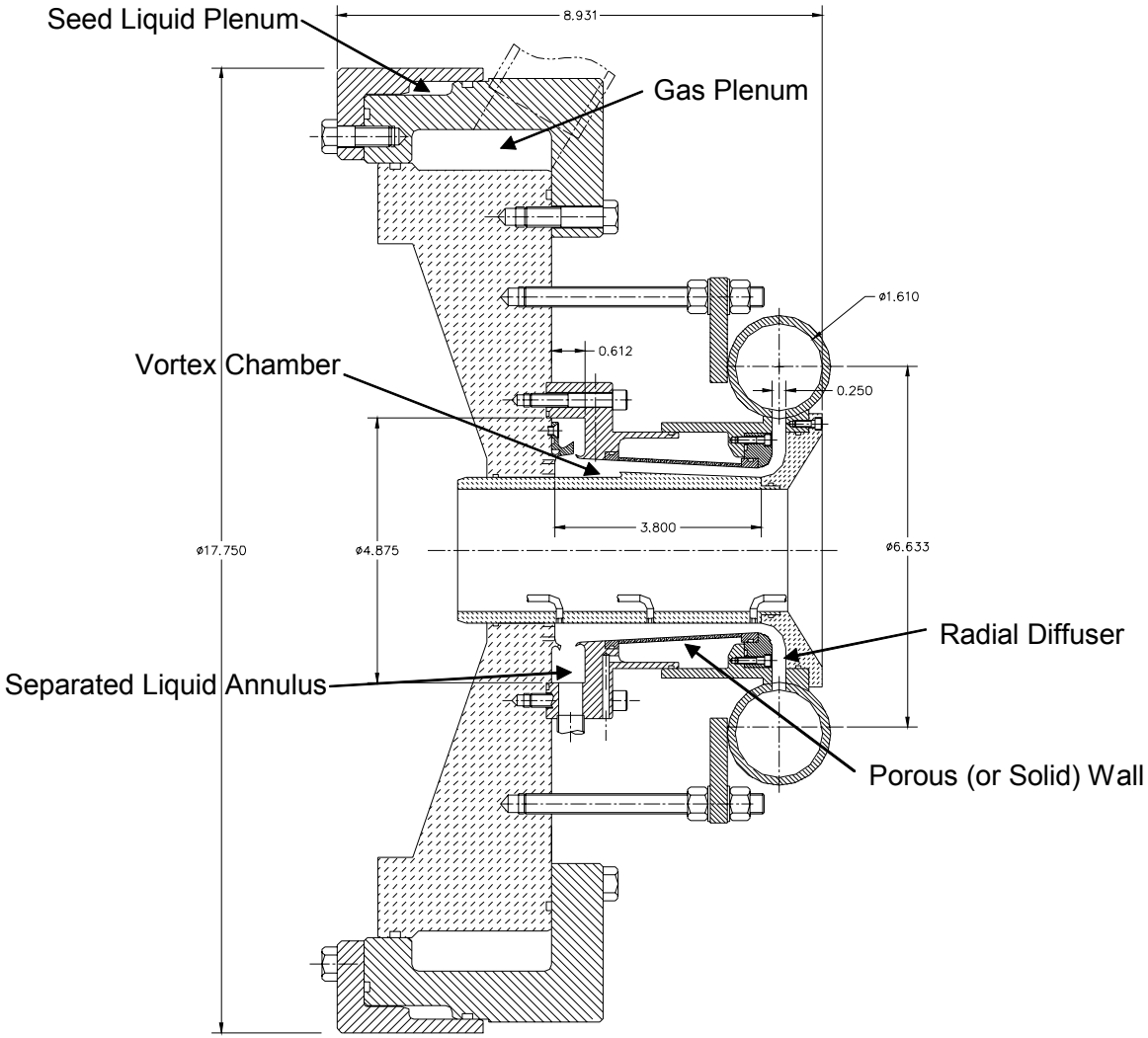

Figure 14 Cross Section of Air-Water Test Unit

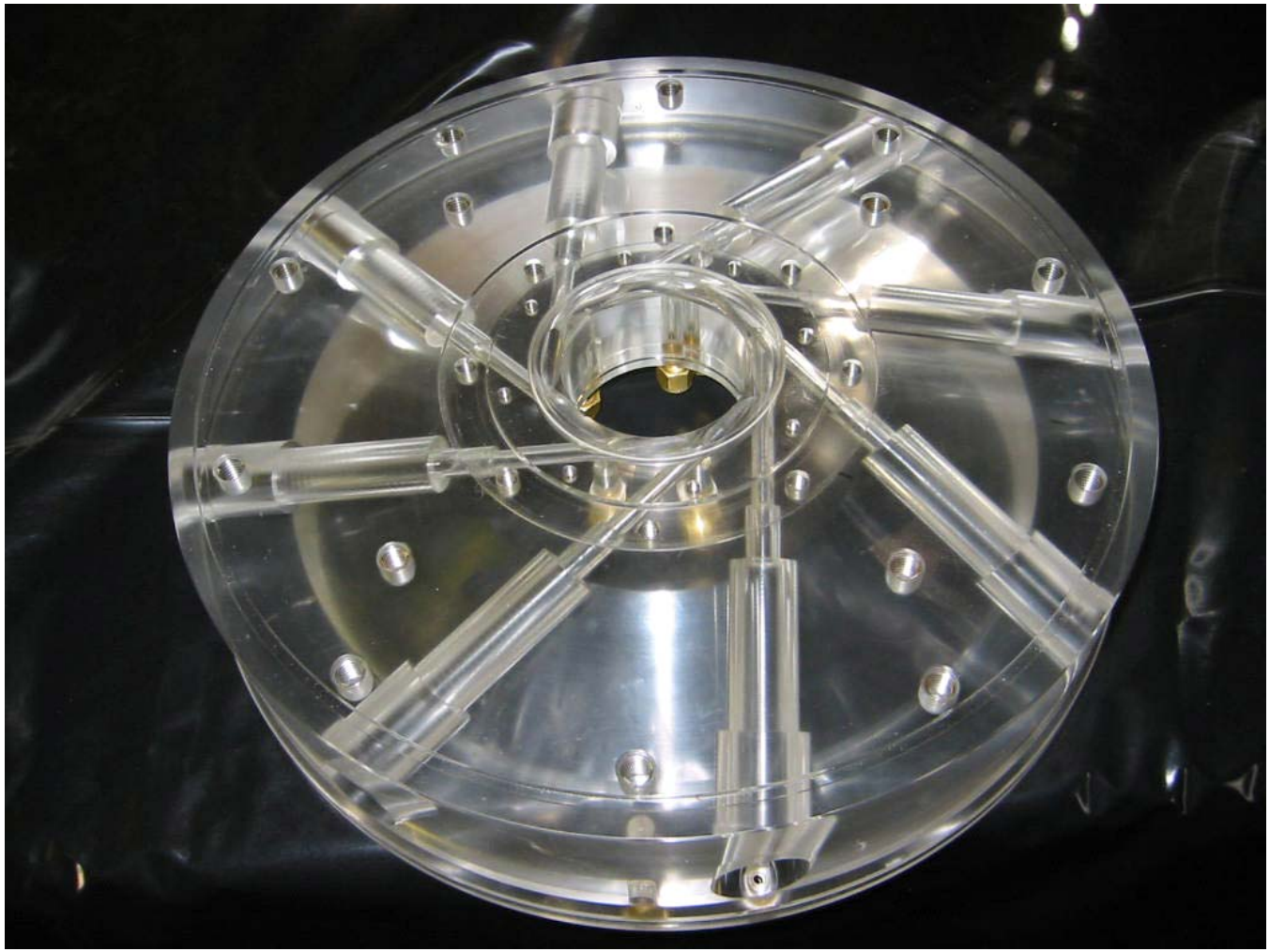

Figure 15 Nozzle Holder

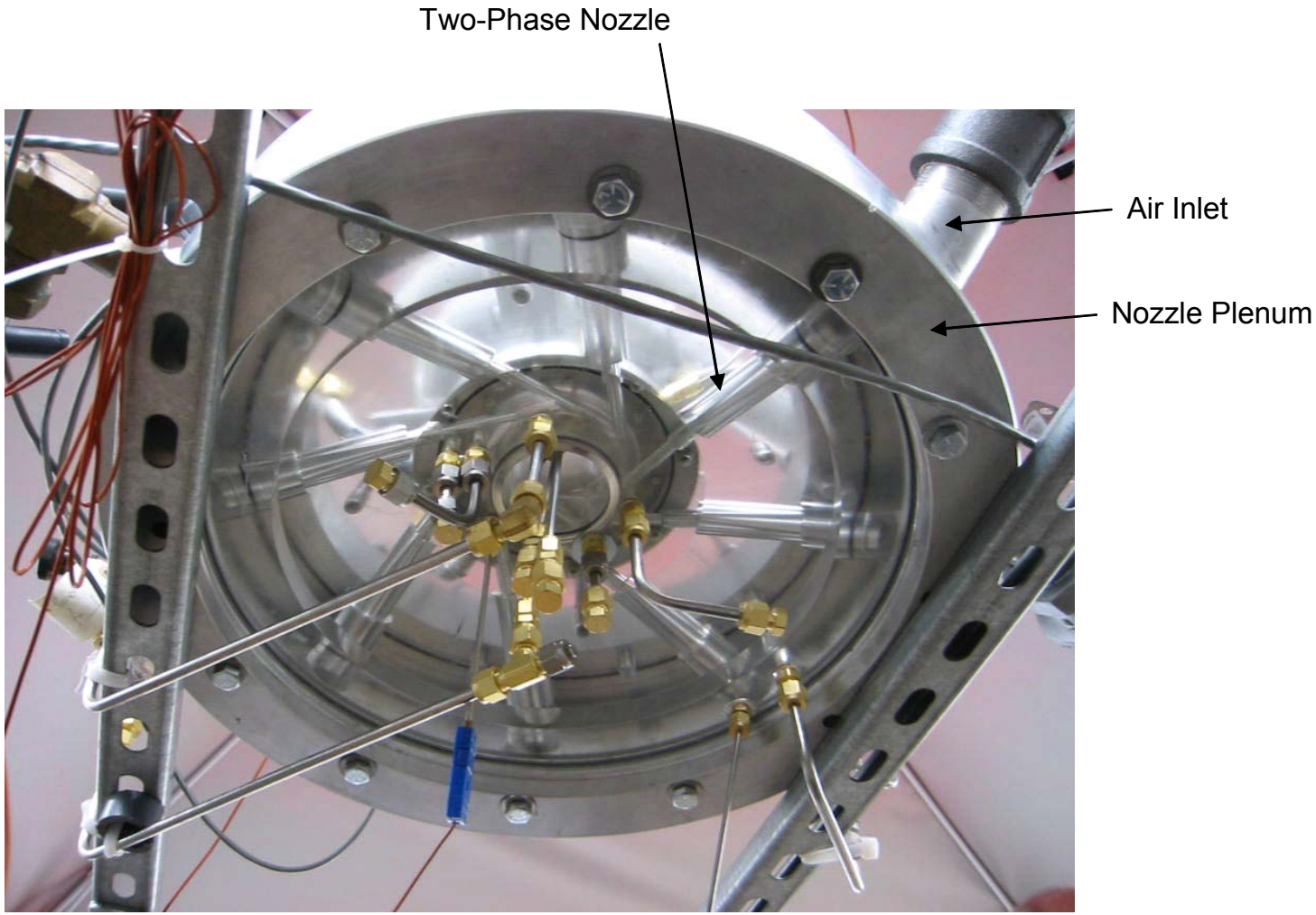

Figure 16 Bottom View of Air-Water Test Separator

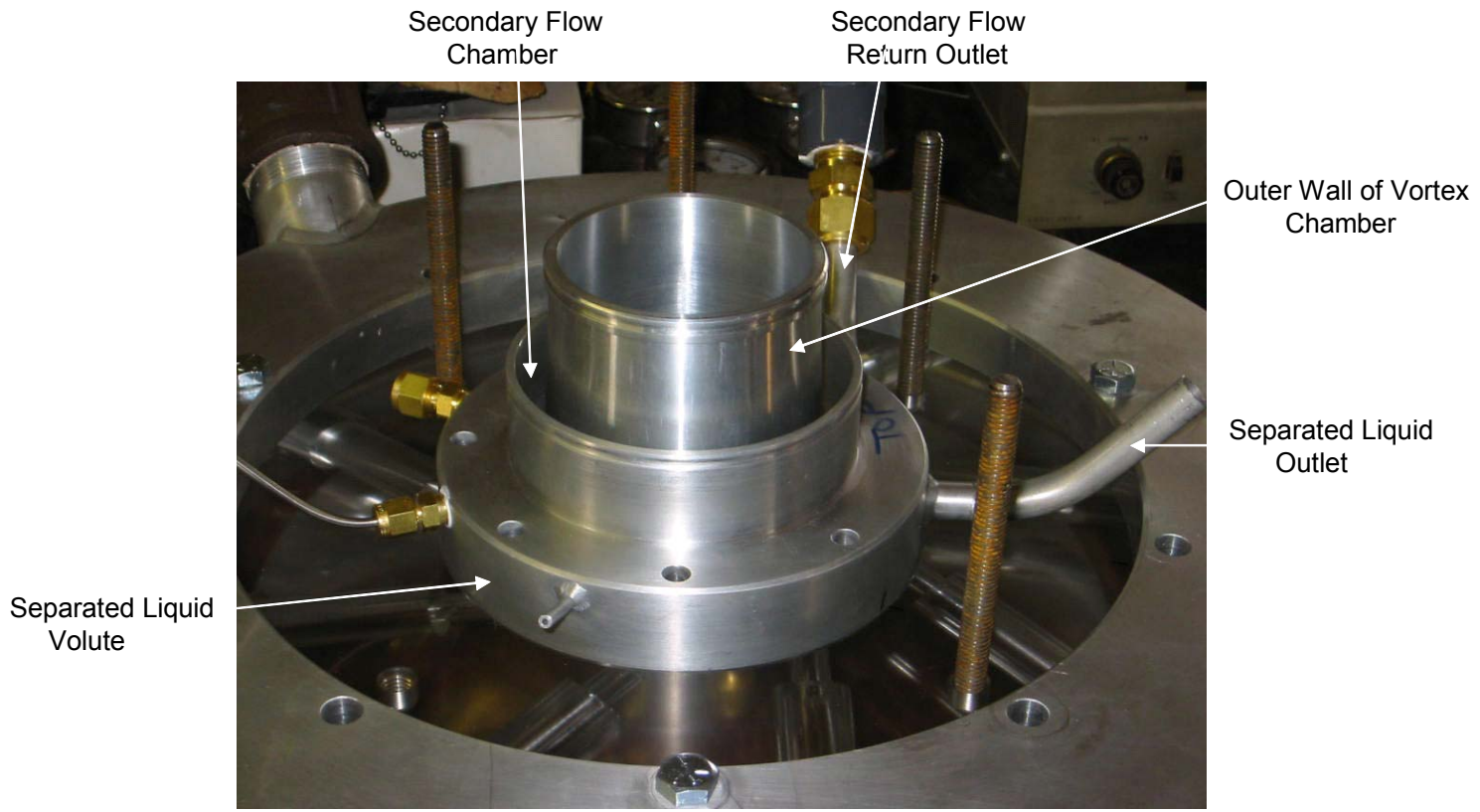

Figure 17 Separated Liquid Volute with Solid Outer Wall

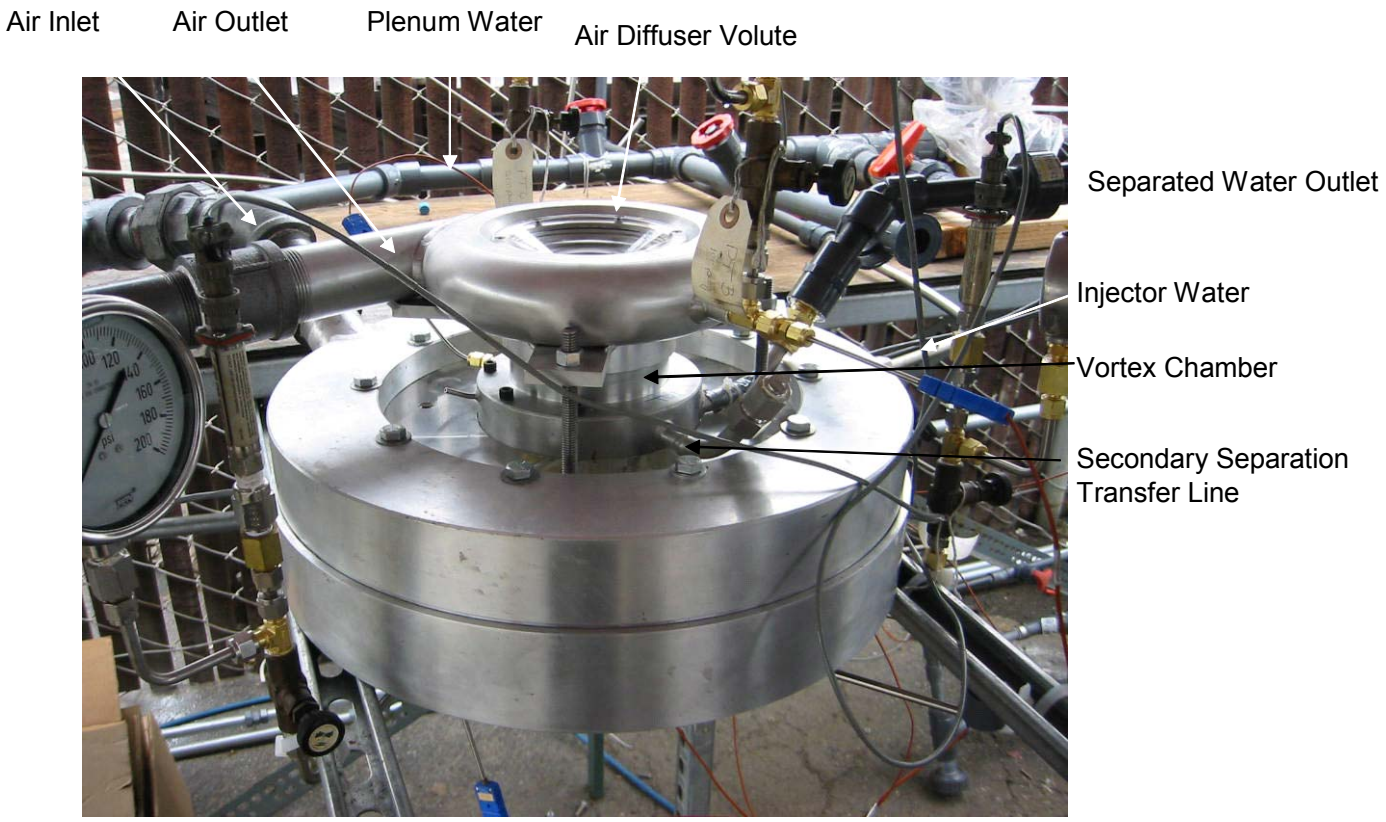

Figure 18 Air-Water Test Assembly

Single Nozzle Test Unit

A prototype Integral Separator was designed based on the successful laboratory testing with solid surface impingement and porous wall recirculation. The use of a solid surface separator enables the use of a single nozzle rather than multiple nozzles. The prototype was therefore designed with a single nozzle. In addition to simplifying the design and operation, the single nozzle will enable basic information to be obtained on hydrocarbon vapor expansion.

Consultation with ChevronTexaco concerning the availability of field test sites and consultation with the Colorado Engineering Experimental Test Station concerning the test system capabilities led to the selection of 1100 psia and 10 MMscfd as the nominal operating conditions. The unit was designed to operate with this flow and condense and separate heavy hydrocarbon constituents during initial tests. Later tests with hydrates will require modification of the initial prototype. The unit was designed to easily accommodate modifications to the geometry.

The three primary test streams were natural gas with pentane, natural gas with butane and natural gas with free decane liquid.

In the first two tests the natural gas was saturated with the heavy hydrocarbons up to the vapor limit. Tests were conducted expanding the gas to measure the reversion point and separation with no seed injection. This was followed by tests with injection of decane seed to determine the efficacy in establishing an equilibrium expansion with larger droplets and better separation.

The tests with natural gas and free liquid were conducted to determine the separation effectiveness and pressure recovery over a range of gas-liquid ratios and pressure.

Figures 19, 20 and 21 are views of the prototype Integral Separator. The flow enters the nozzle and is expanded from the inlet pressure to the expansion pressure, cooling the stream. A seed liquid can be injected into the nozzle through an upstream injector. In each case the flow leaving the nozzle will be in the two-phase region.

The two-phase flow traverses a transition section and impinges directly on an inclined plane, of the type utilized at the Jet Propulsion Laboratory. The liquid separates from the gas due to the high inertia and centrifugal forces. The liquid film is slowed by friction on the separator surface but retains sufficient velocity head to recover pressure in a capture slot. The unit designed has stellite coating on all high velocity liquid surfaces.

The separated high velocity gas enters a vortex chamber tangentially, producing swirl. Secondary droplets are centrifuged to the porous wall of the vortex chamber where they are collected and flow to the liquid collection tank. The vortex flow leaves through an axial diffuser, which increases the pressure of the dry gas. An axial diffuser was used

for the first unit to enable expedited testing with natural gas. Later units may use an annular diffuser.

The initial test unit was analyzed using the nozzle code and the 1-D code to determine its performance for the CEESI tests. For the case of natural gas plus butane expansion from 1100 psia to 900 psia in the nozzle results in a predicted spouting velocity of 597 ft/s and equilibrium condensation of about 9% by weight.

The pressure and temperature profiles were plotted for the equilibrium case and calculated and plotted for frozen flow. For the frozen flow case the inlet gas composition was assumed to be fixed during the expansion and the temperature and area dependency on pressure was calculated for a 99% velocity coefficient.

The results are shown in figure 22, a plot of temperature versus pressure for the frozen (super cooled) expansion and an equilibrium expansion of the natural gas butane mixture. A significant temperature difference exists. The test nozzle is instrumented along its length to determine the pressure profile. We expect to measure a difference between the expansion without seed injection, which should be super cooled for a significant fraction of the nozzle length and the expansion with seed injection (which should induce an equilibrium expansion). In addition for the super cooled expansion we hope to determine the point of reversion to an equilibrium expansion by measuring the temperature profile.

Pressure versus area is shown in figure 23. The values are much closer for the two different expansion characteristics than those for temperature. However, the colder temperature and higher density would require a greater flow to produce the pressure area variation in the case of a super cooled expansion.

The 1-D code output for the natural gas – butane mixture for a gas diffuser efficiency of .85, combined with the estimated gas friction loss would result in a dry gas outlet pressure of 1012 psia, a net recovery of 55%.of the expansion pressure difference.

Fabrication was completed. Figure 24 shows the seed injector and expansion nozzle which after completion. The prototype single nozzle separator was tested at CEESI. In figure 25, the nozzle inlet and liquid exit are shown installed in the outer vortex wall which is porous to allow secondary liquid separation. Inserts were used to vary the opening of the liquid capture slot.

The curved primary separation passage is shown in figure 26. The purpose of the walls was to constrain the separated gas to flow in a generally tangential direction to the vortex chamber wall. The gas outlet is shown at the near side of the assembly. A wall slot is expanded in a diffuser to convert the kinetic energy of the separated gas to pressure.

The completed unit, prior to shipping is shown in figure 27. Pressure taps and thermocouples are placed every 1’ to determine the profiles during expansion with and without liquid injection.

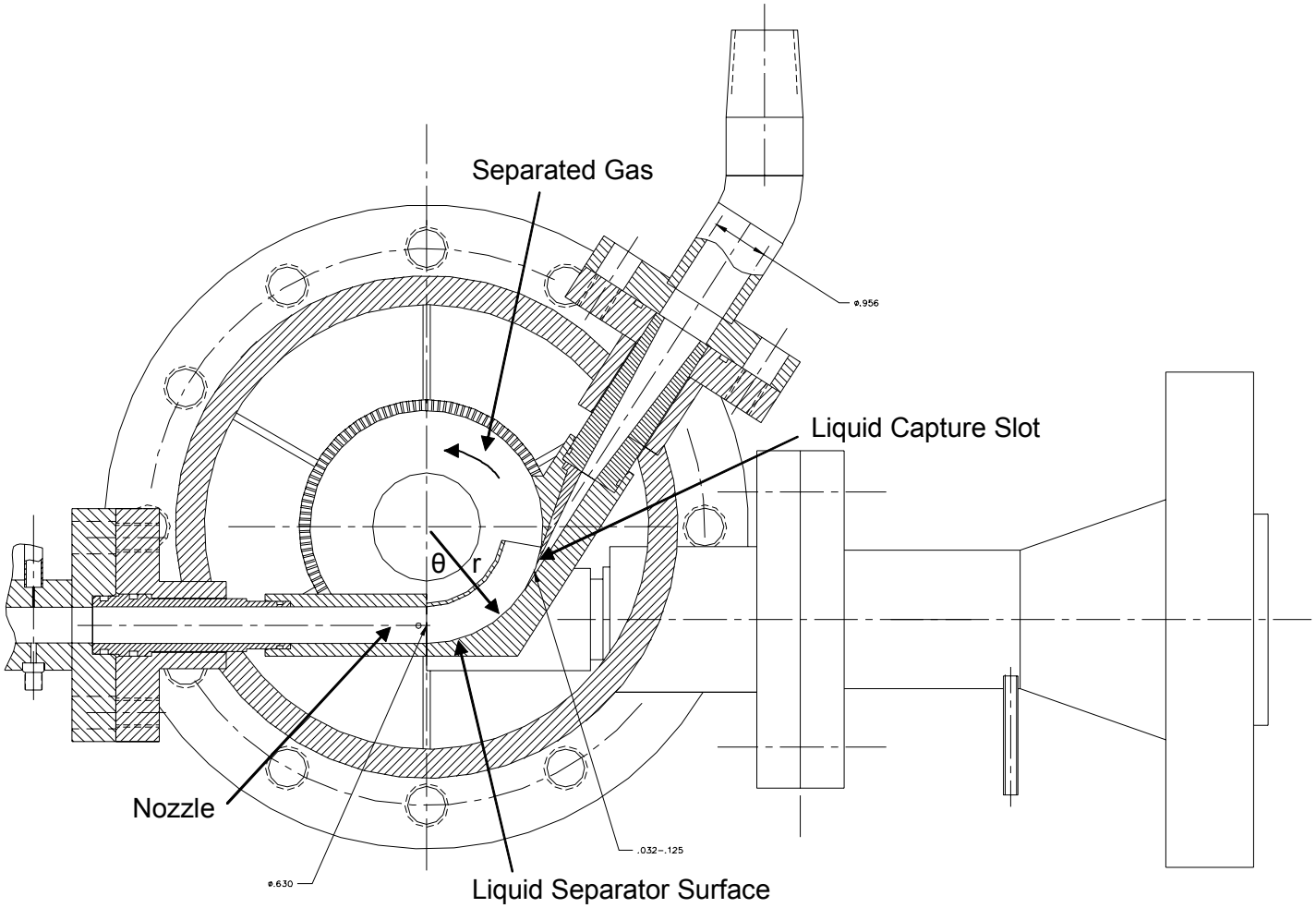

Figure 19 Prototype Single Nozzle Separator and Liquid Outlet

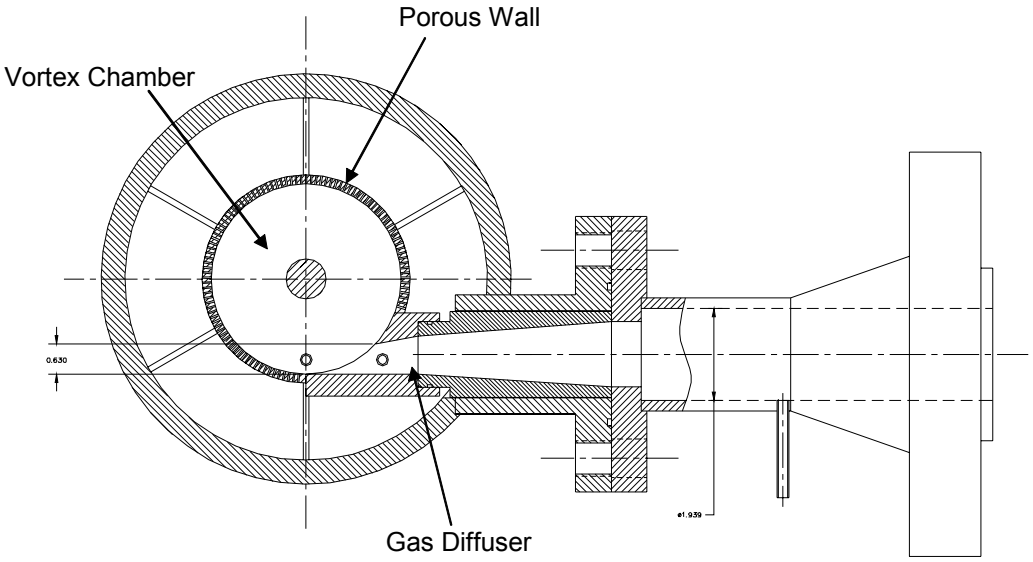

Figure 20 Top View of Gas Outlet

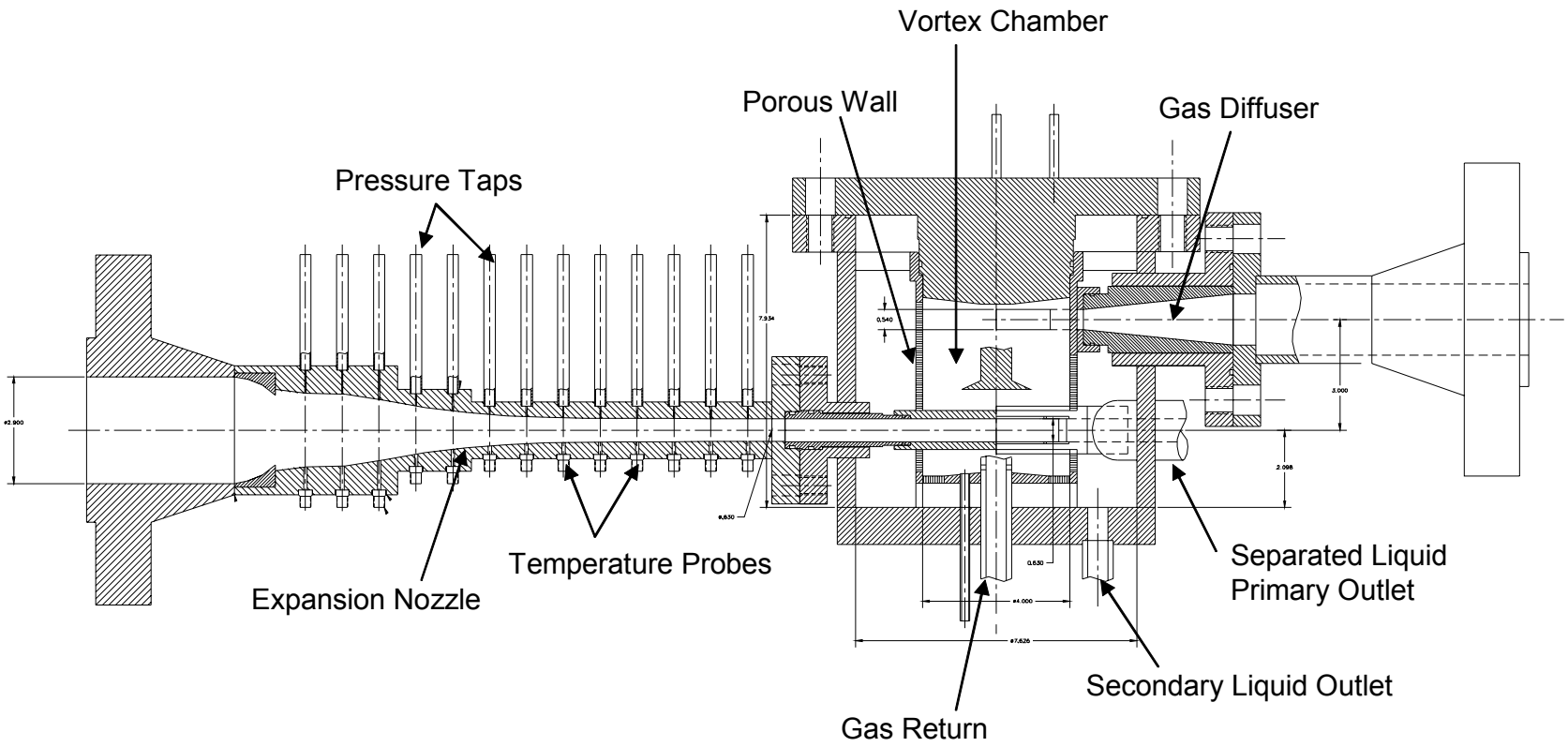

Figure 21 Prototype Single Nozzle Separator Assembly

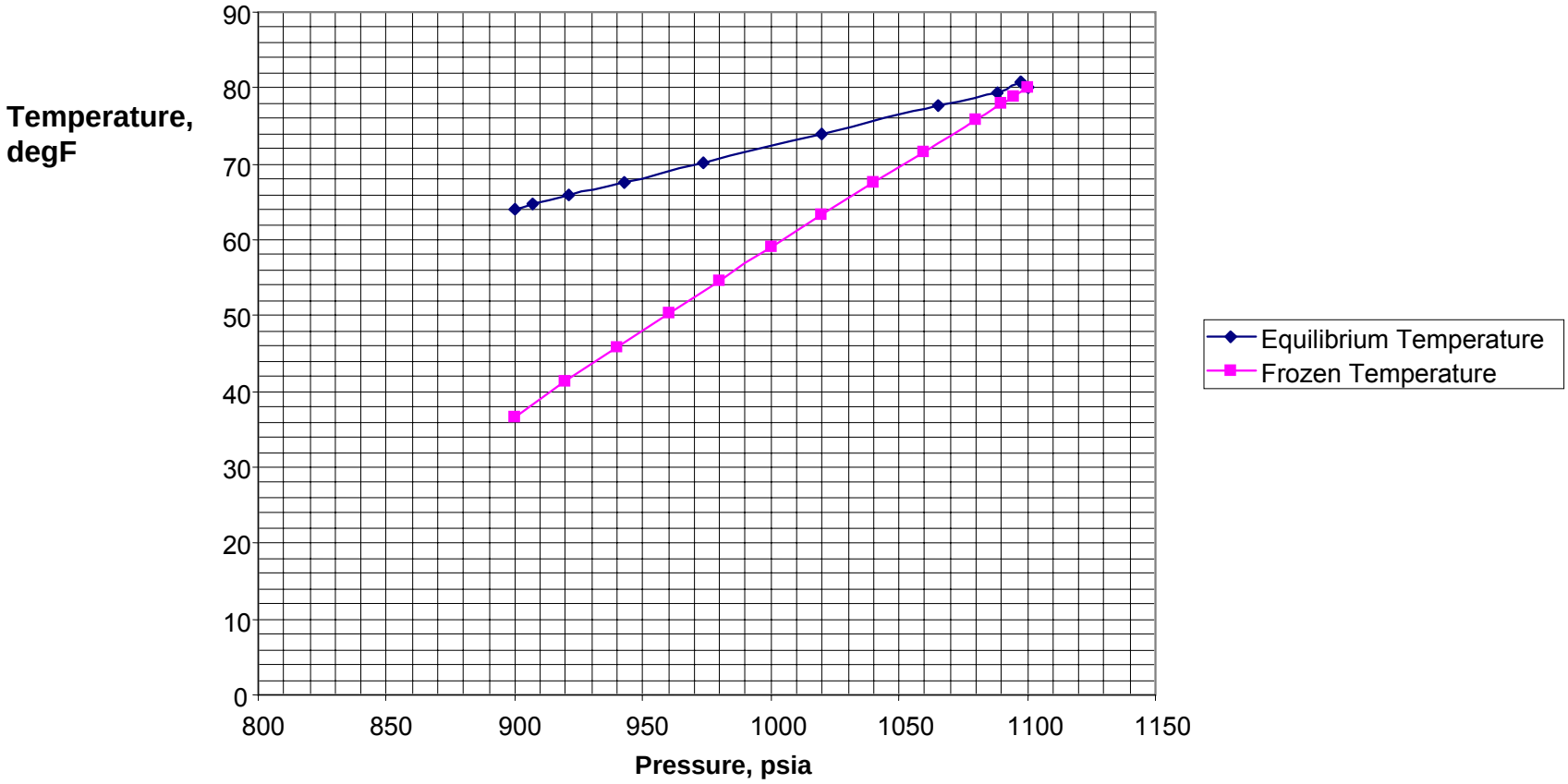

Figure 22 Comparison of temperature vs Pressure for Equilibrium Expansion and Supercooled Expansion of Natural Gas- Butane

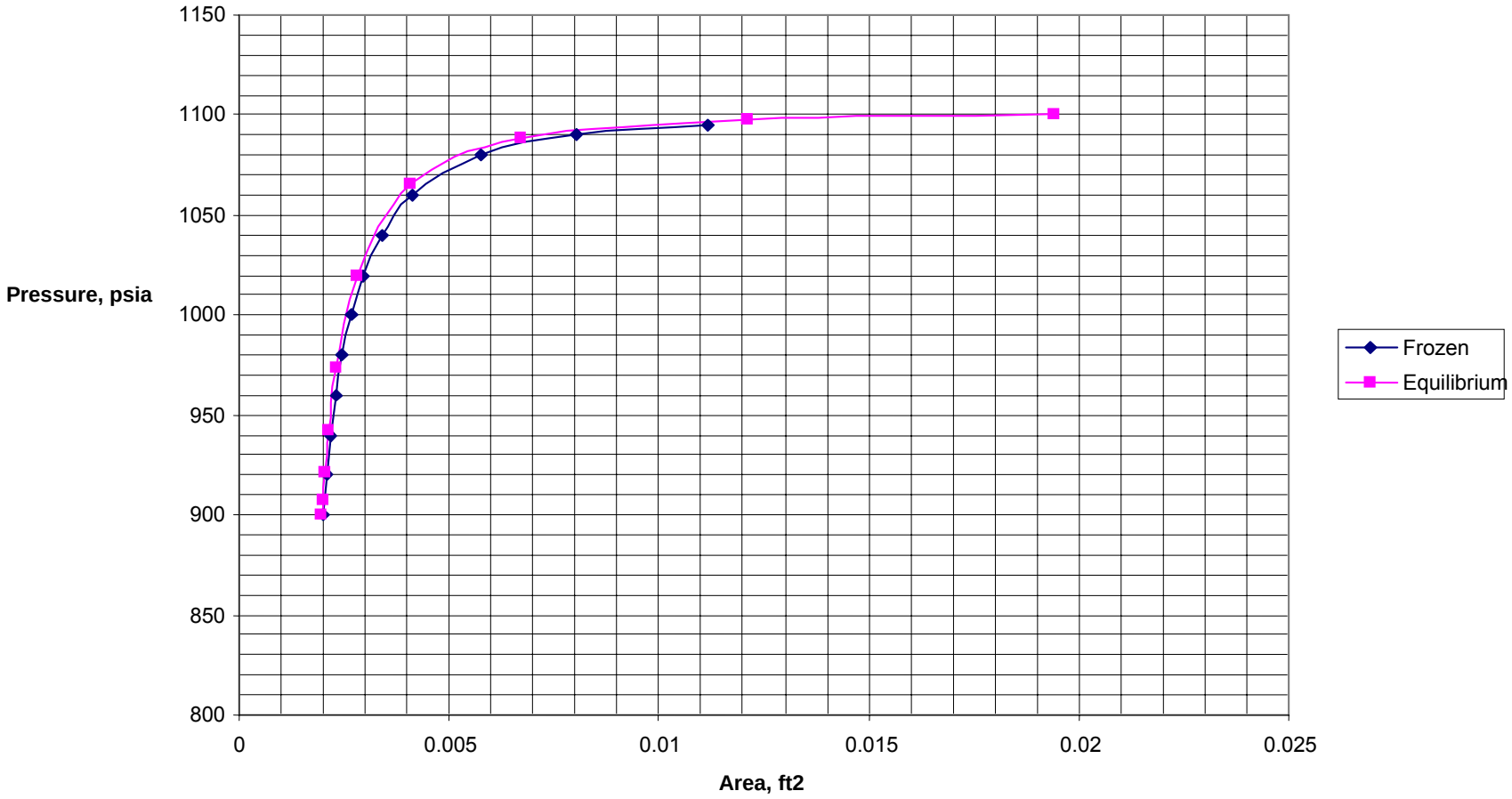

Figure 23 Pressure vs Area for Equilibrium and Supercooled Expansion of Natural Gas Butane Mixture

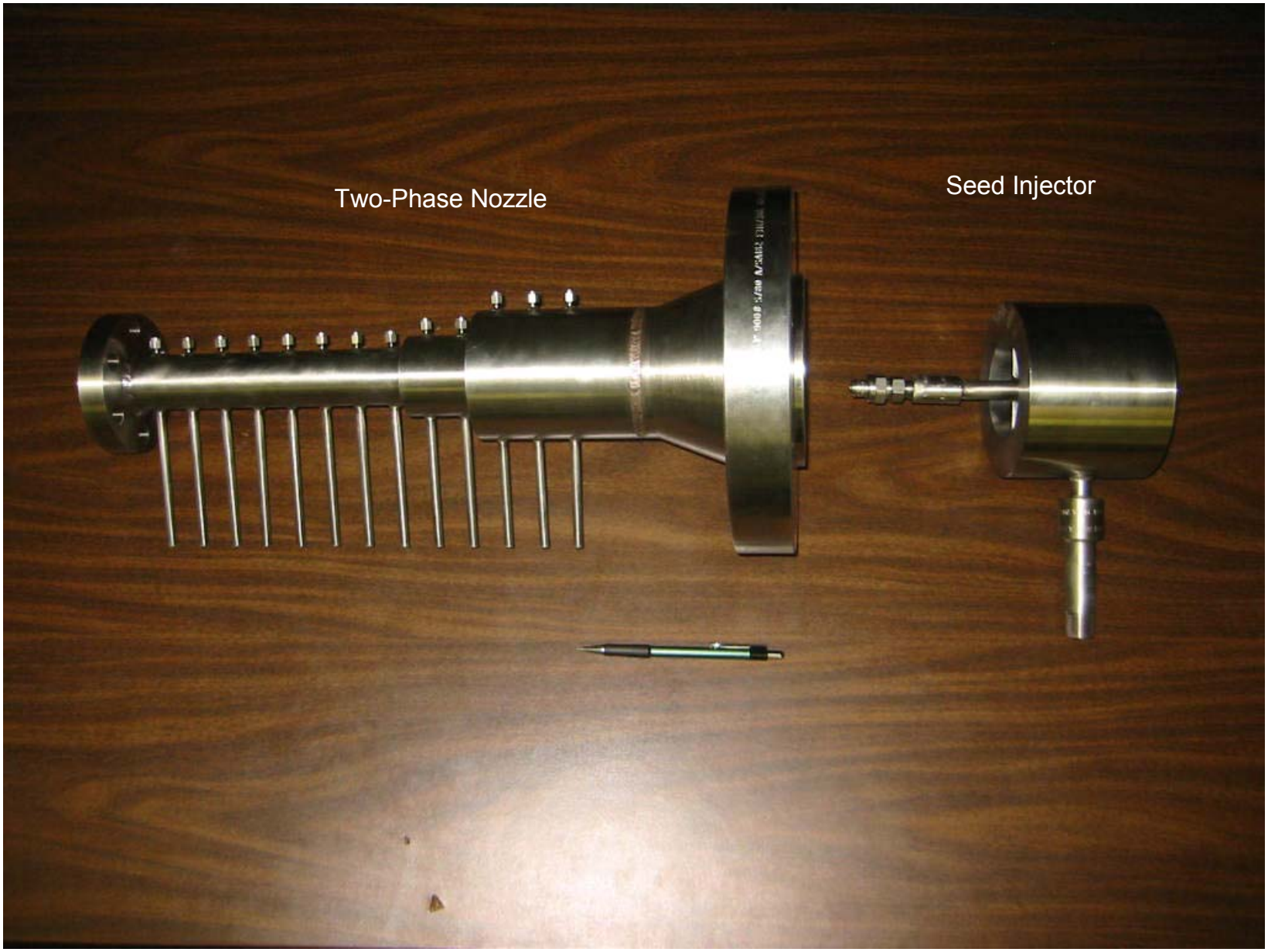

Figure 24 Completed Nozzle and Seed Injector

Figure 25 Vortex Chamber

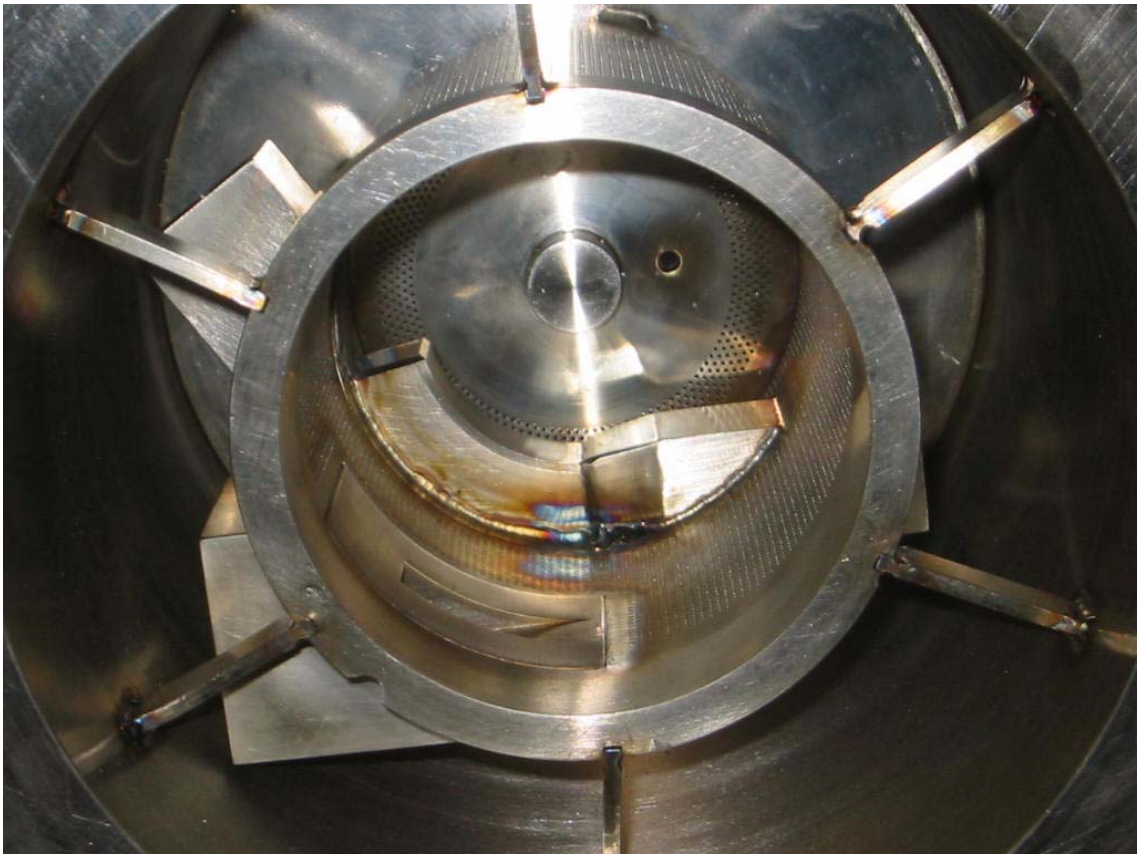

Figure 26 Vortex Chamber and Nozzle Extension

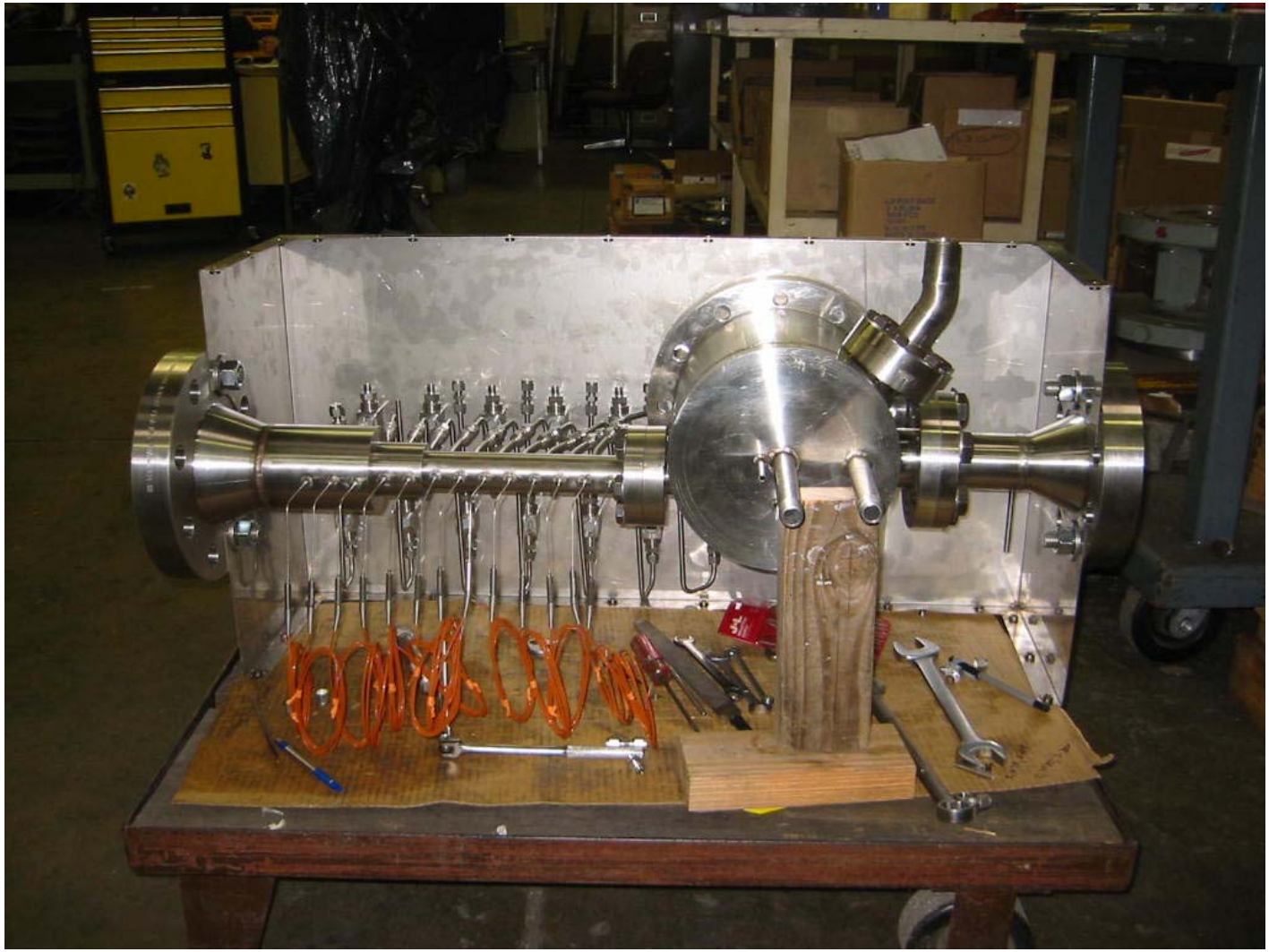

Figure 27 Nozzle and Separator Prepared for Shipping

Multiple Nozzle Prototype Unit

The final prototype unit was designed and manufactured based upon the results of testing the first two geometries and the analytical results

Commercial prototype was designed for a gas flowrate range of 5-20 MMscfd and a pressure range of 500 – 1200 psig. Flowrate and pressure variances will be accommodated by blanking off nozzles. At the upper end of flowrate and lower pressures larger nozzle inserts can be used.

Figure 28 is a cross section of the final multiple nozzle geometry Eight (8) nozzles are positioned tangentially at the bottom of the unit. The nozzles are feed by a single 3" pipe with a splitter and 8 individual channels to feed two-phase flow uniformly to each nozzle. The nozzles each have an outside adjustment to block the flow if desired.

The nozzles are also fed individually from a manifold carrying the seed liquid. Orifices at each nozzle entrance feed the seed liquid to the inlet. The unit is designed to also evaluate injection of the seed at a single upstream point. With a fine enough mist the droplets may remain through the manifold without deposition.

The nozzles enter the vortex chamber from the end wall and impinge tangentially on the primary separation surface. The separated liquid flows into the liquid volute through the capture slot.

The vortex chamber is designed with diverging walls, shown by CFD analysis to provide a gradual pressure increase. The pressure increase will provide a driving force for secondary separated liquid and associated gas to circulate towards the entrance and liquid volute. Porous zones are provided on the outer wall of the vortex chamber and on the inner wall to capture secondary separated liquid. The inner wall secondary liquid is recirculated back to the entrance region where the ejector action of the high velocity two-phase jets re-entrain the liquid and separate it.

The separated gas flows radially outward in the annular region, being re-compressed, lowering the dewpoint.

The arrangement of the inlet nozzle inserts is illustrated in figure 29, a solid model of the prototype integral separator. Figure 30 provides a closeup of the vortex chamber and radial diffuser. Figure 31 shows the assembly.

The final manufactured separator is shown in the next series of photographs. Figure 32 is an interior view of the vortex chamber and outer wall of the diffuser. The outer wall of the diffuser has perforations to capture secondary liquid not captured by the primary separator.

The splitter at the inlet to the nozzles is shown in figure 33. The splitter acts to divide the gas and injected liquid into 8 relatively equal streams for the eight nozzles.

Separated liquid on the walls is re-introduced into the gas by wall shedders at each nozzle inlet.

Figure 34 is a view of the completed assembly from the nozzle inlet side while figure 35 shows the unit from the perspective of the diffuser exit.

The side view of the Integral Separator assembly on the test stand is provided by figure 36.

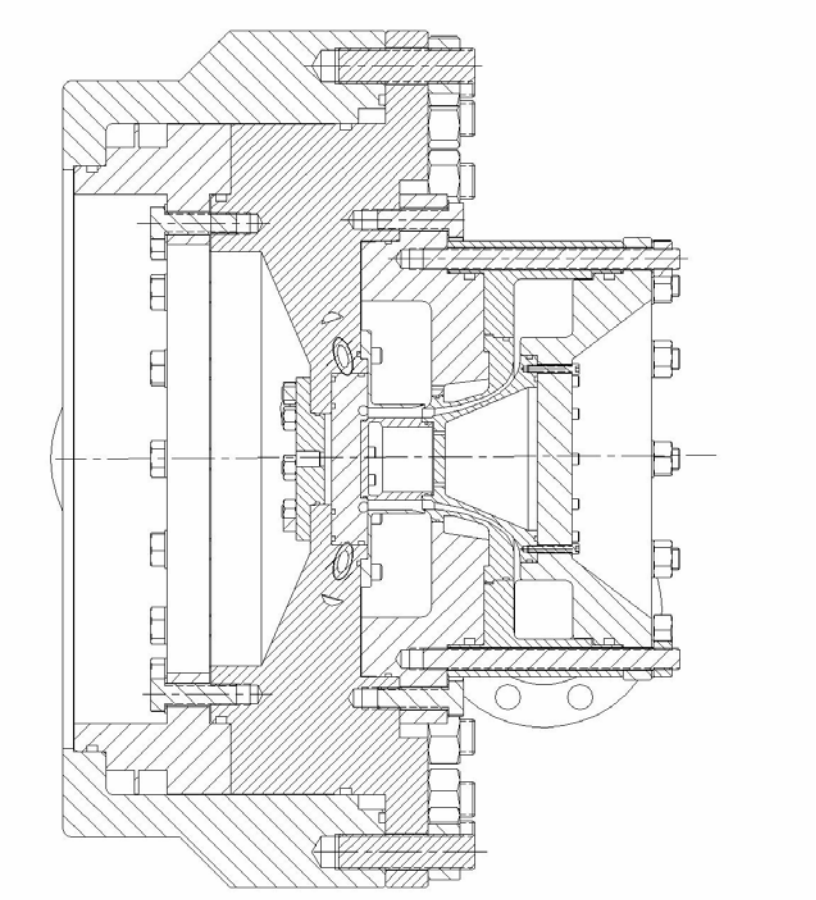

Figure 28 Cross Section of Multiple Nozzle Prototype Integral Separator

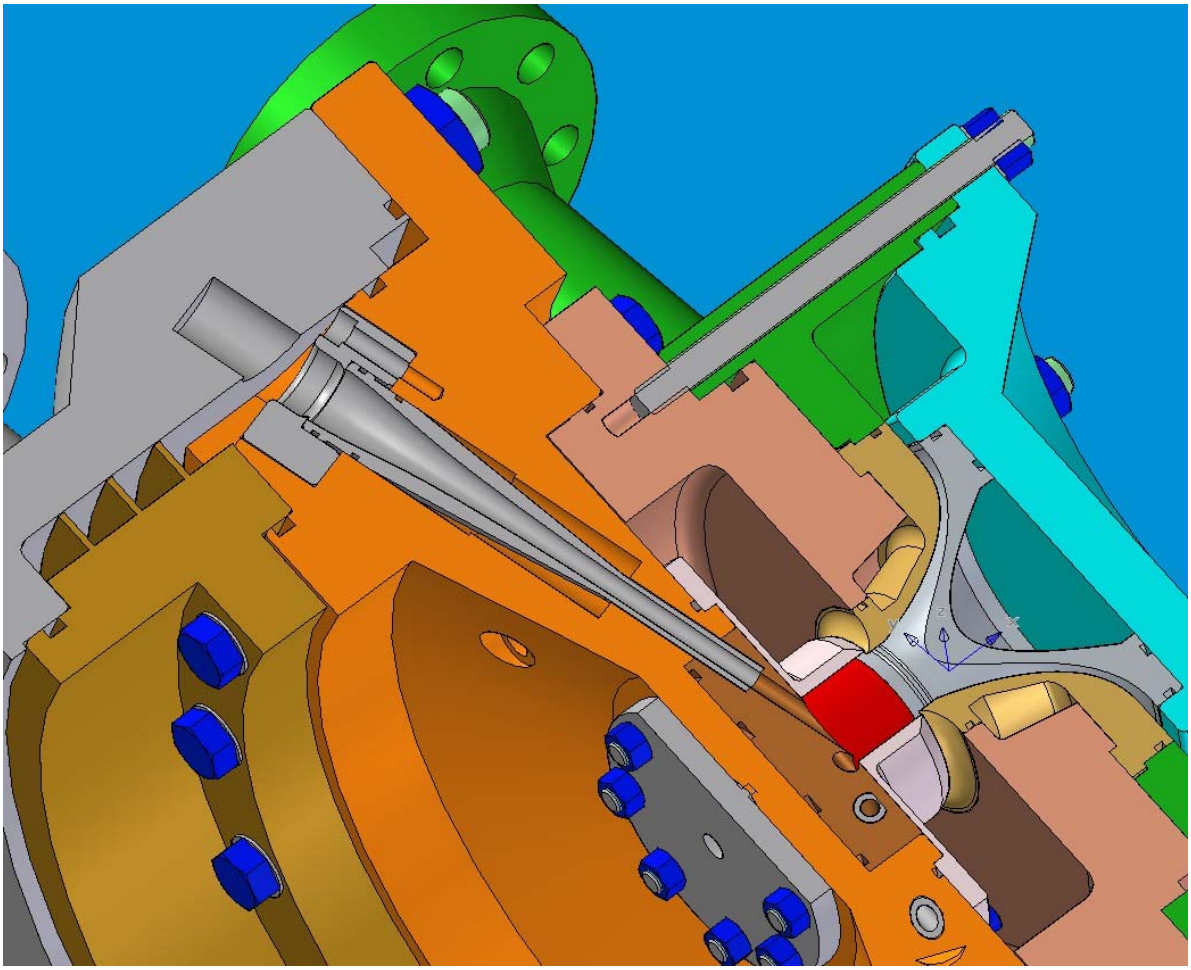

Figure 29 Solid Model Showing Nozzle and Vortex Chamber Geometry

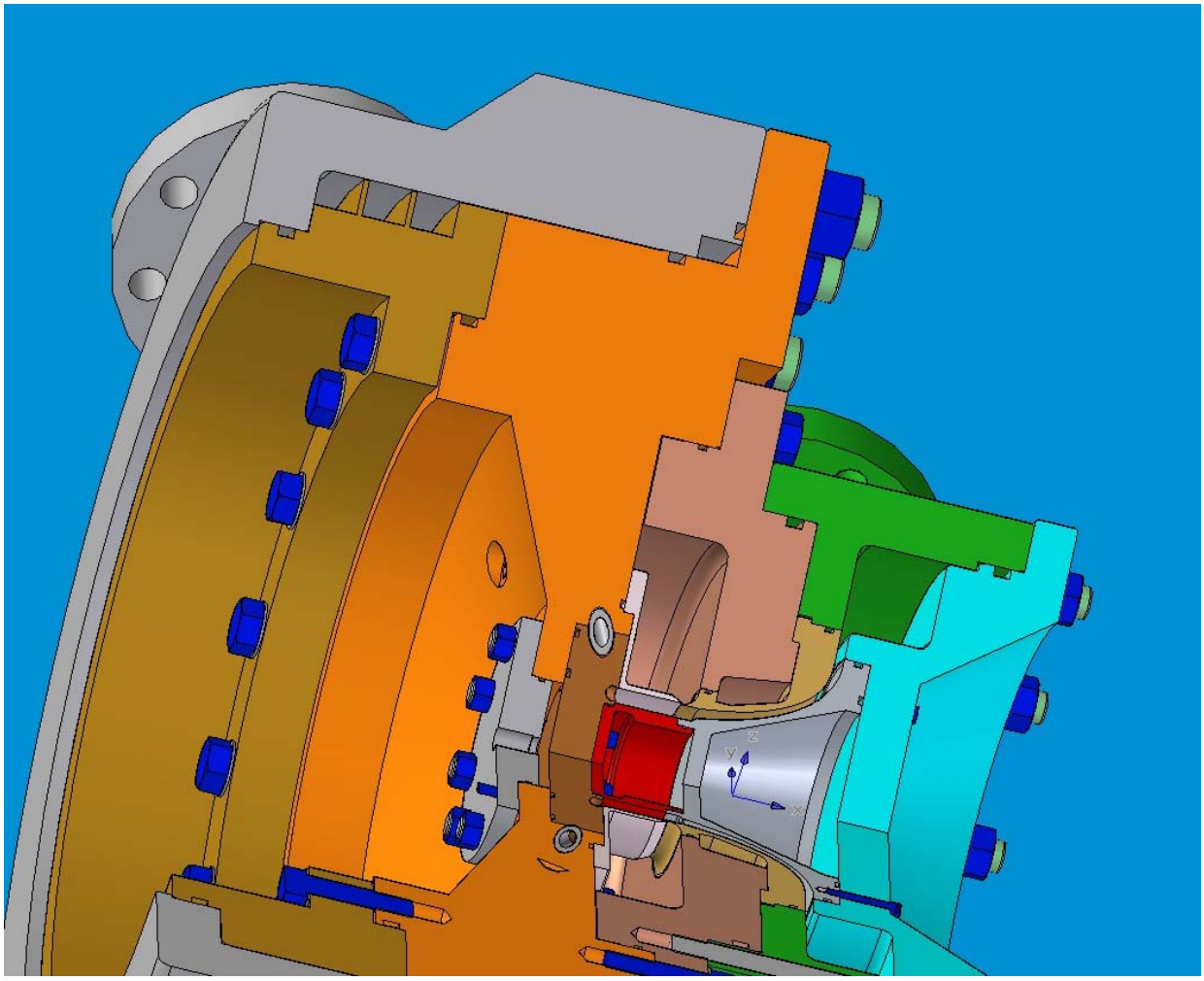

Figure 30 Solid Model Showing Vortex Chamber Diffuser and Liquid Chamber

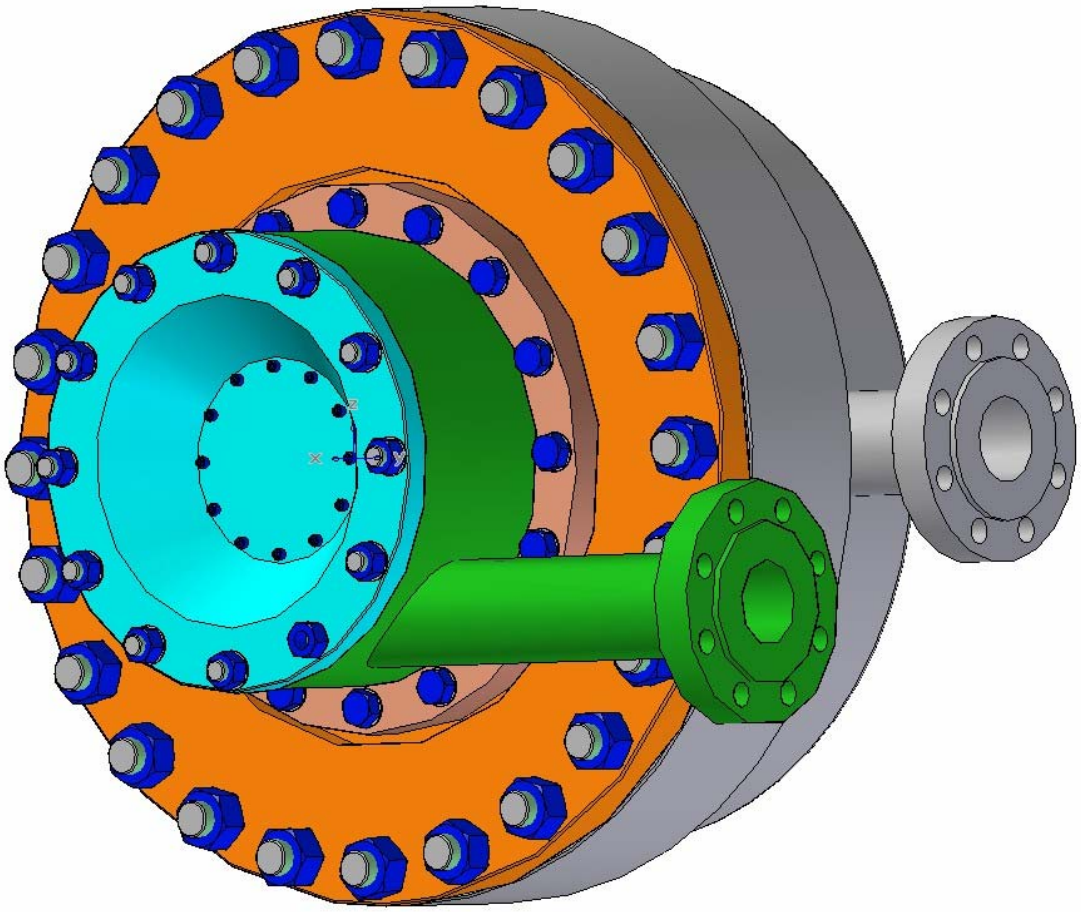

Figure 31 Solid Model Showing Completed Integral Separator Assembly

Figure 32 Interior of Vortex Chamber and Diffuser Outer Wall

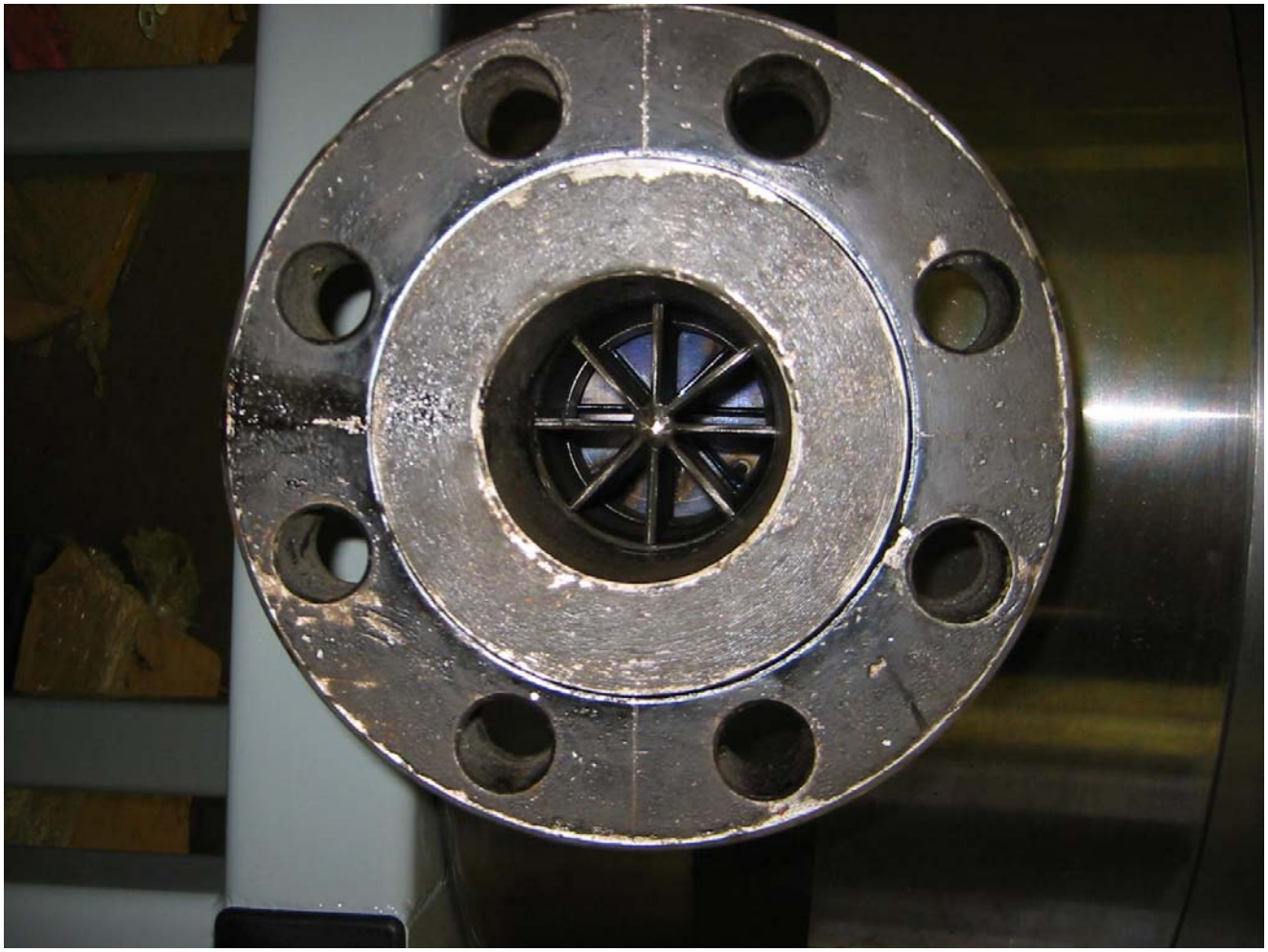

Figure 33 Inlet Flow Splitter

Figure 34 Integral Separator Assembly Showing Nozzle Inlet

Figure 35 Integral Separator Assembly Diffuser Exit

Figure 36 Integral Separator on Test Stand

5. Test Systems

Air-Water Lab System

The air- water test loop utilized for flow visualization and performance determination of the model integral separator was completed and commissioned. Figure 37 is a process diagram for the air-water test system. A photograph of the test system is shown in Figure 38.

Air is compressed by a helical screw compressor and flows through a control valve to the test unit. Water is pressurized by a centrifugal pump and flows through another control valve to the test unit. The two-streams are mixed at the inlets of the nozzles and expanded to the pressure of the separator section. The separated air flows into a vessel with a mist eliminator to remove any water not separated.

As shown in figure 37 the water flow from the pump can be mixed upstream of the nozzles with the compressed air to simulate gas flow with free liquid. Separate injectors were also provided to enable dry air to be feed to the nozzles with liquid injection at each, such as would be done for seed injection.

The separated water flows through a flow meter to a reservoir, from which the water is returned to the pump. Separated water was measured both by weighing and by volumetric determination in a catch vessel.

Entrained water leaving with the gas was measured volumetrically after separation in a mesh pad separator.

In most cases the entrained moisture was very low or zero. Estimation was made by touching the leaving gas stream. Typically the flow was dry and heated above ambient by the diffuser giving a “dry skin” feeling rather than a “moist skin” feeling.

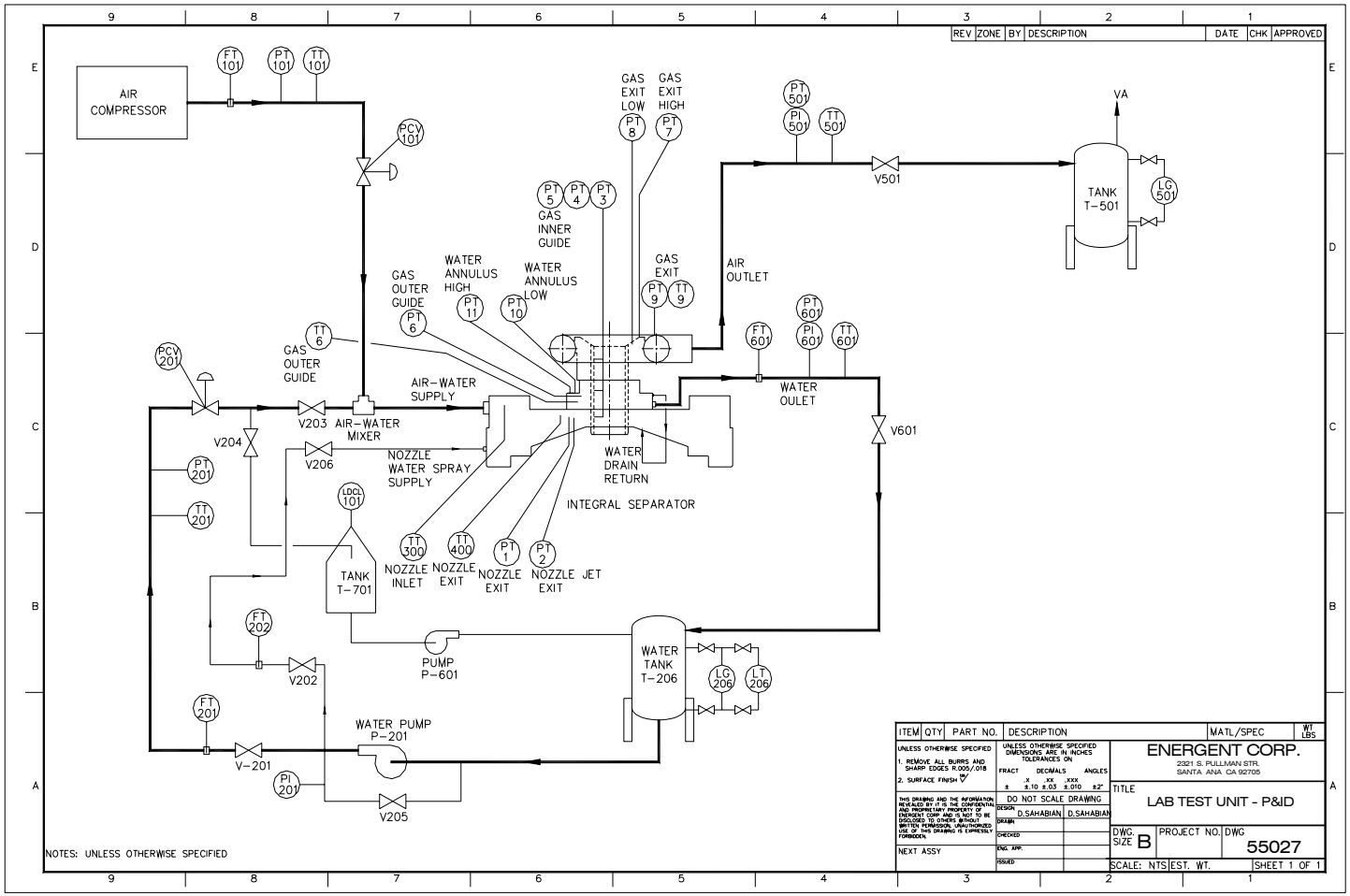

Figure 37 Schematic of Laboratory Air-Water Test System

Figure 38 Air - Water Lab Test System

Nitrogen-Water Lab System

A higher pressure nitrogen-water system was utilized to test the prototype Integral Separator before high pressure gas testing at CEESI. A schematic of the test setup is shown in figure 39 and a photograph in figure 40.

Nitrogen is pumped from a cryogenic storage tank to natural draft vaporizers. The gaseous nitrogen is then mixed with water from a high pressure vessel. The mixture is introduced to the separator. Separated water is collected in another vessel and weighed. Visual estimates of entrained water were made based upon the air-water test results.

The separator is shown mounted on the test stand in figure 41. Separated gas exits through a pressurized viewport. Figure 42 is a close up of the viewport. Liquid carry over had to be estimated at the high separation pressures since expansion of the gas to ambient temperature results in cooling and fog generation rendering liquid measurements ineffective.

Additional views of the test installation are provided in figures 43 and 44.

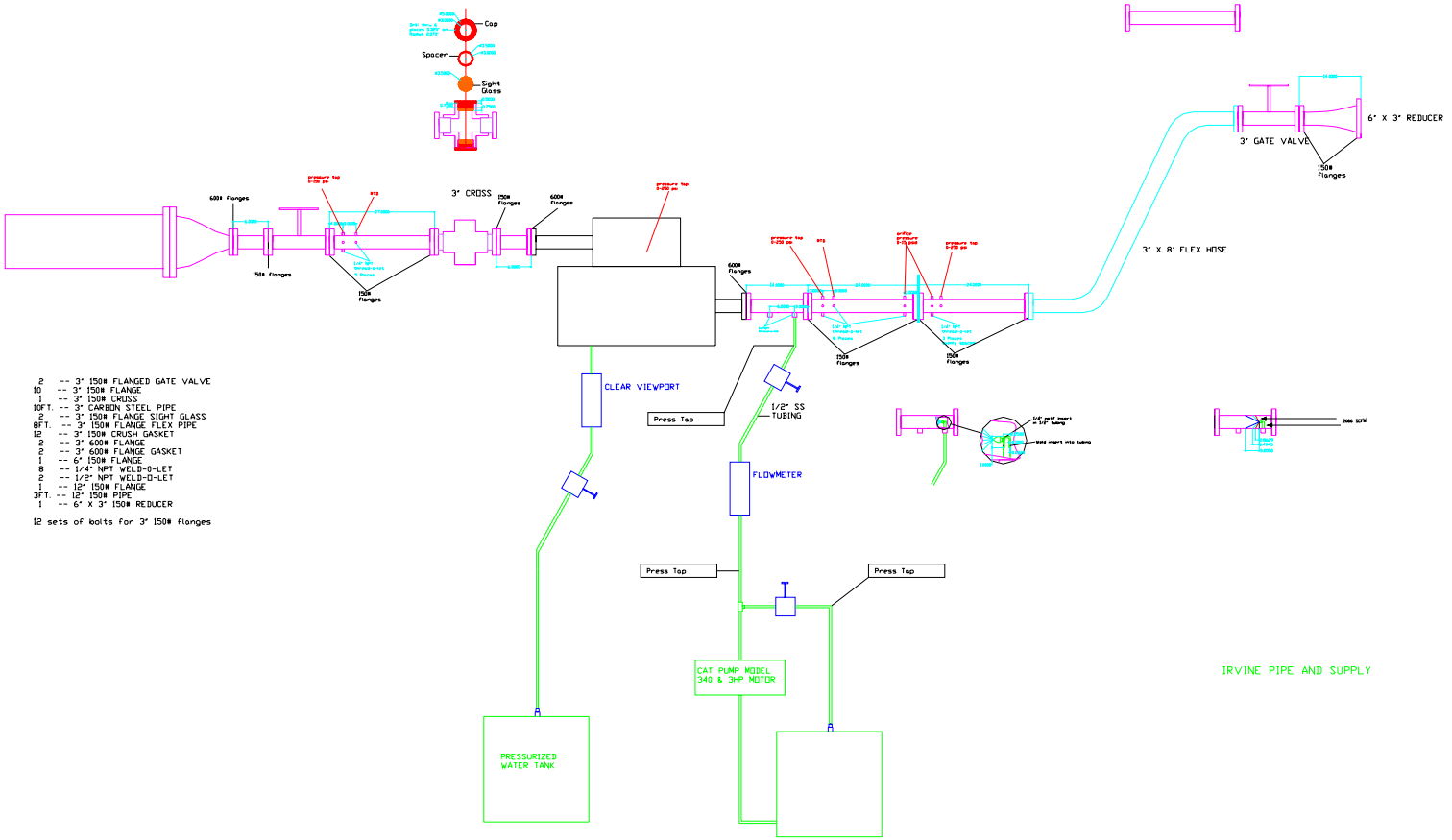

Figure 39 Schematic of Nitrogen Water Test System

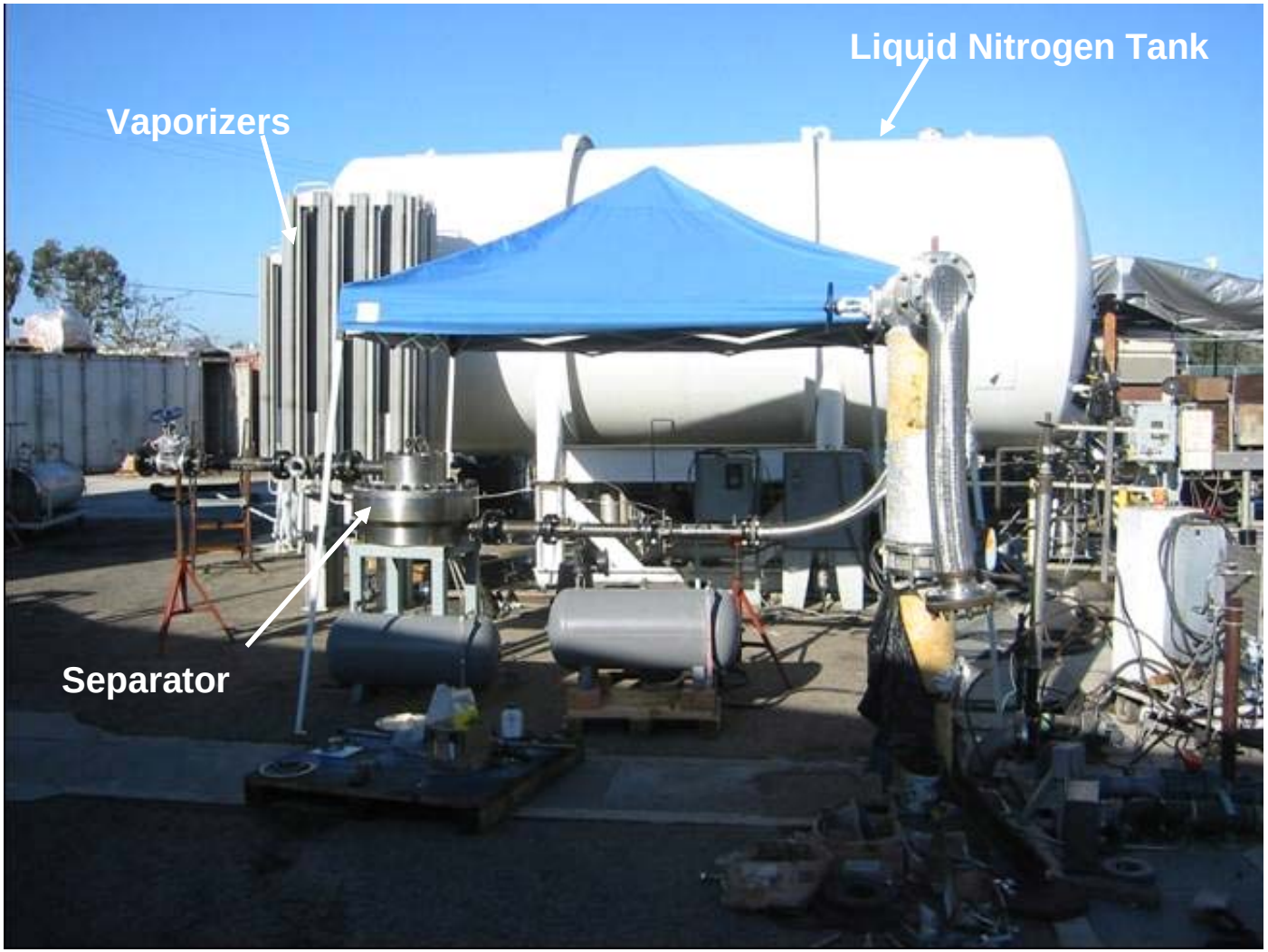

Figure 40 Nitrogen Water Lab Test System

Figure 41 Separator on Test Stand in Nitrogen-Water Test System

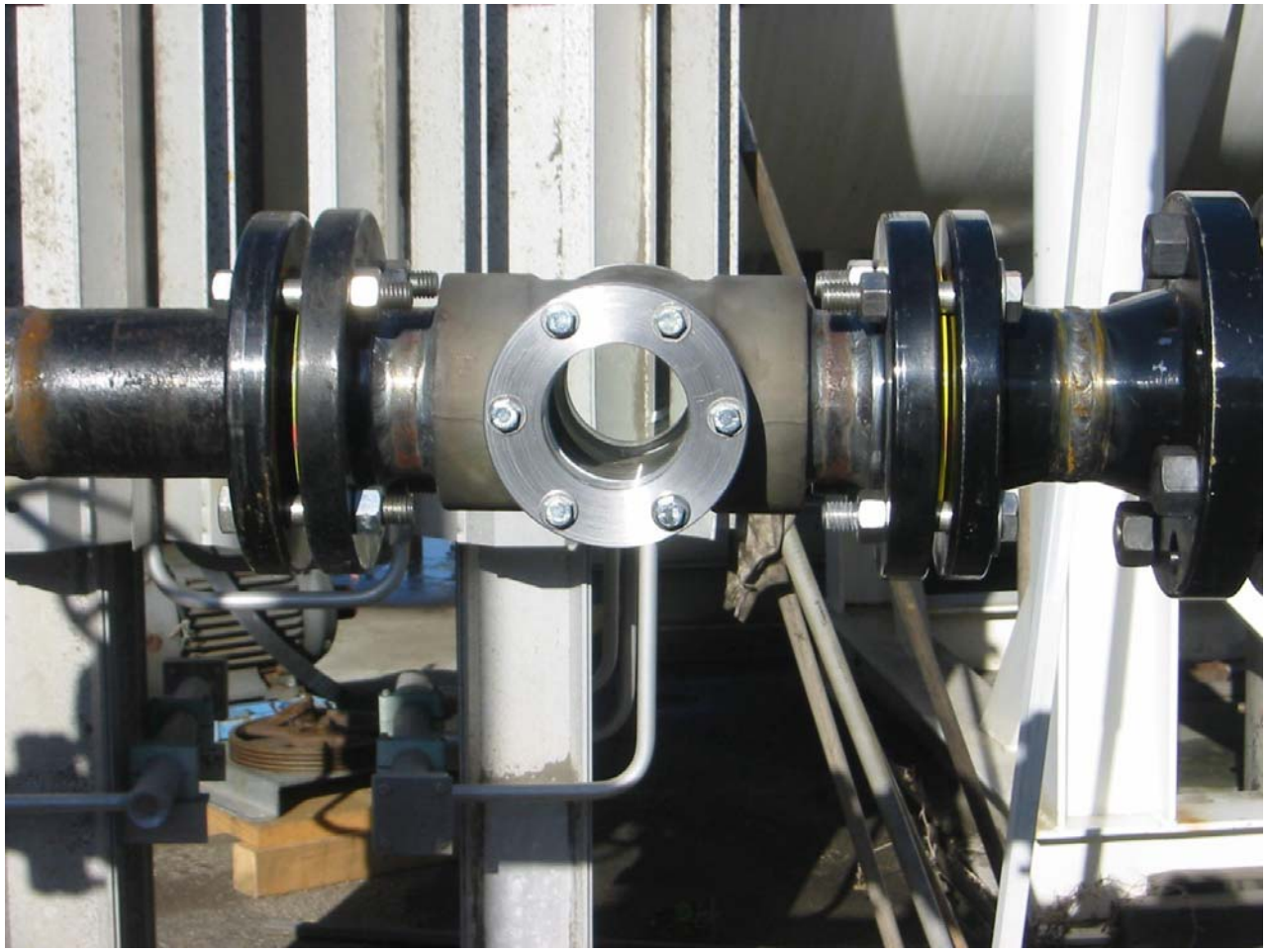

Figure 42 High Pressure Nitrogen Viewport

Figure 43 Integral Separator During Testing

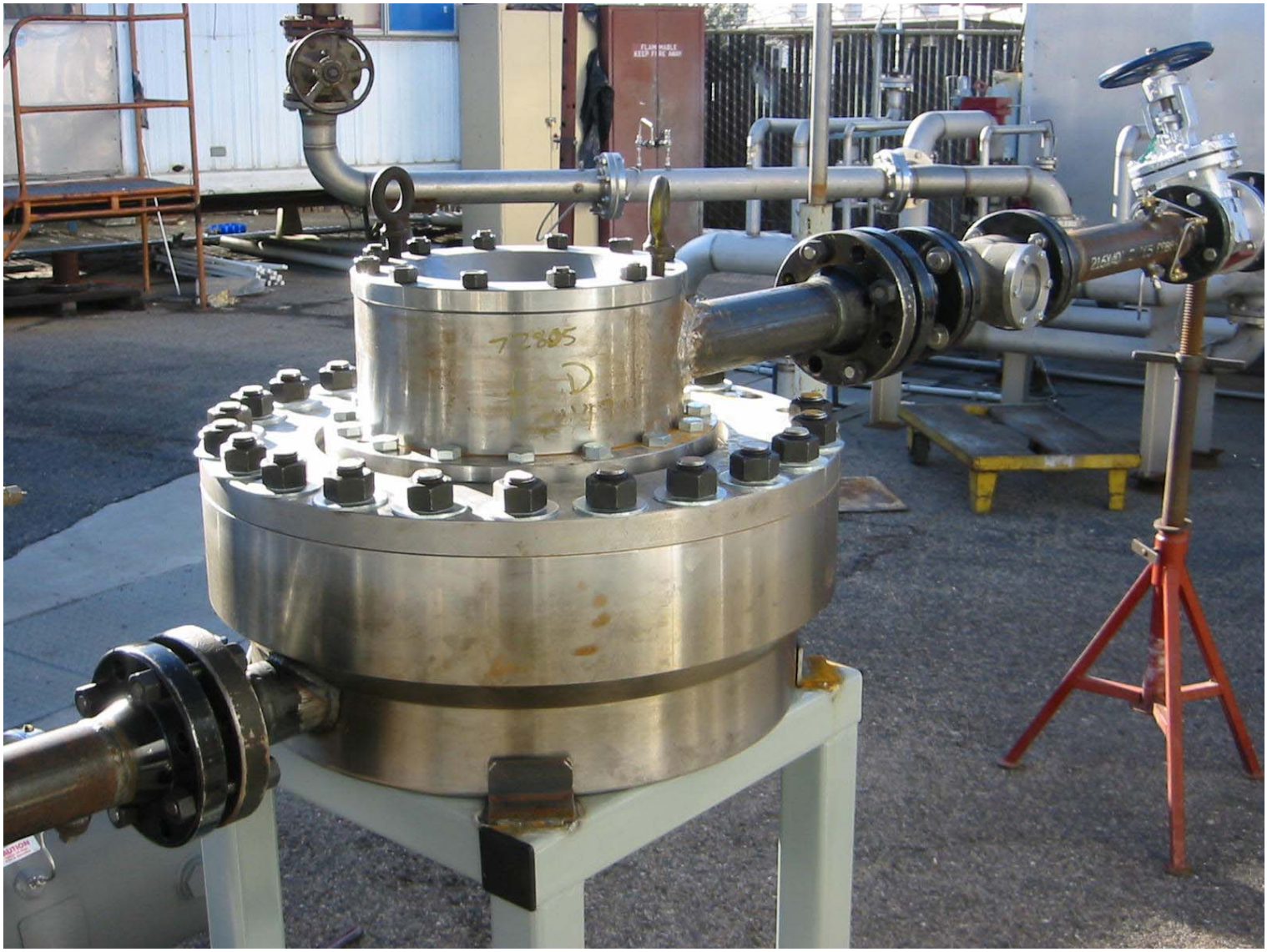

Figure 44 Integral Separator During Testing

High Pressure Natural Gas Test Facility

The prototype single nozzle separator and the prototype multiple nozzle separator were both tested at a high pressure test facility at the Colorado Engineering Experiment Station, Inc (CEESI). Natural gas from a pipeline is compressed to high pressure by an engine driven compressor and stored in a closed loop test system.

The system, shown in figure 45, allows circulation of the gas at high pressure. As shown the system has provision for injection of liquids at high pressure to evaluate separation devices, such as the integral separator. Two test loop separators are used to separate and measure liquids remaining in the gas to evaluate separation devices. When discussing test results these will be referred to as test loop separator 1 and test loop separator 2. Additionally, the gas can be saturated with water in a separate circuit and re-introduced to the main test loop to evaluate hydrate formation. During testing of the integral separator the gas was saturated with water to evaluate the dehydration provided.

A schematic of the test setup is shown in figure 46. Gas flows through an orifice flowmeter to a point where seed liquid is injected through a vortex flowmeter. The flow enters the test unit and is expanded to a low pressure in the nozzles. Separated liquid is collected from one or both of the liquid separation chambers and enters a calibrated sight glass. Collection time for a given volume is measured to determine the flowrate of separated liquid.

The gas flows through a sight glass to a secondary, cyclone separator to measure any liquid carryover. A third, larger separator is provided downstream of the secondary separator. During normal testing of separation devices the secondary separator catches any carryover. In this case however, at high pressures and flowrates a significant amount of liquid missed the primary and secondary separators and was collected only by the third, larger separator.

Pressure transmitters were provided to measure the inlet pressure, nozzle expansion pressure, outlet pressure and pressures of the liquid collection chambers. Temperature measurements using RTD's were also made at these locations.

In addition to the multiple nozzle integral separator, a single nozzle was tested to determine the effects of seed injection on the flow and to evaluate a cylindrical separator. The nozzle was instrumented with pressure transmitters and RTD's every inch to determine the pressure and temperature profiles. Figure 47 shows the single nozzle test installed at CEESI.

Figures 48 and 49 show the installation of the multiple nozzle integrated separator in the CEESI test system.

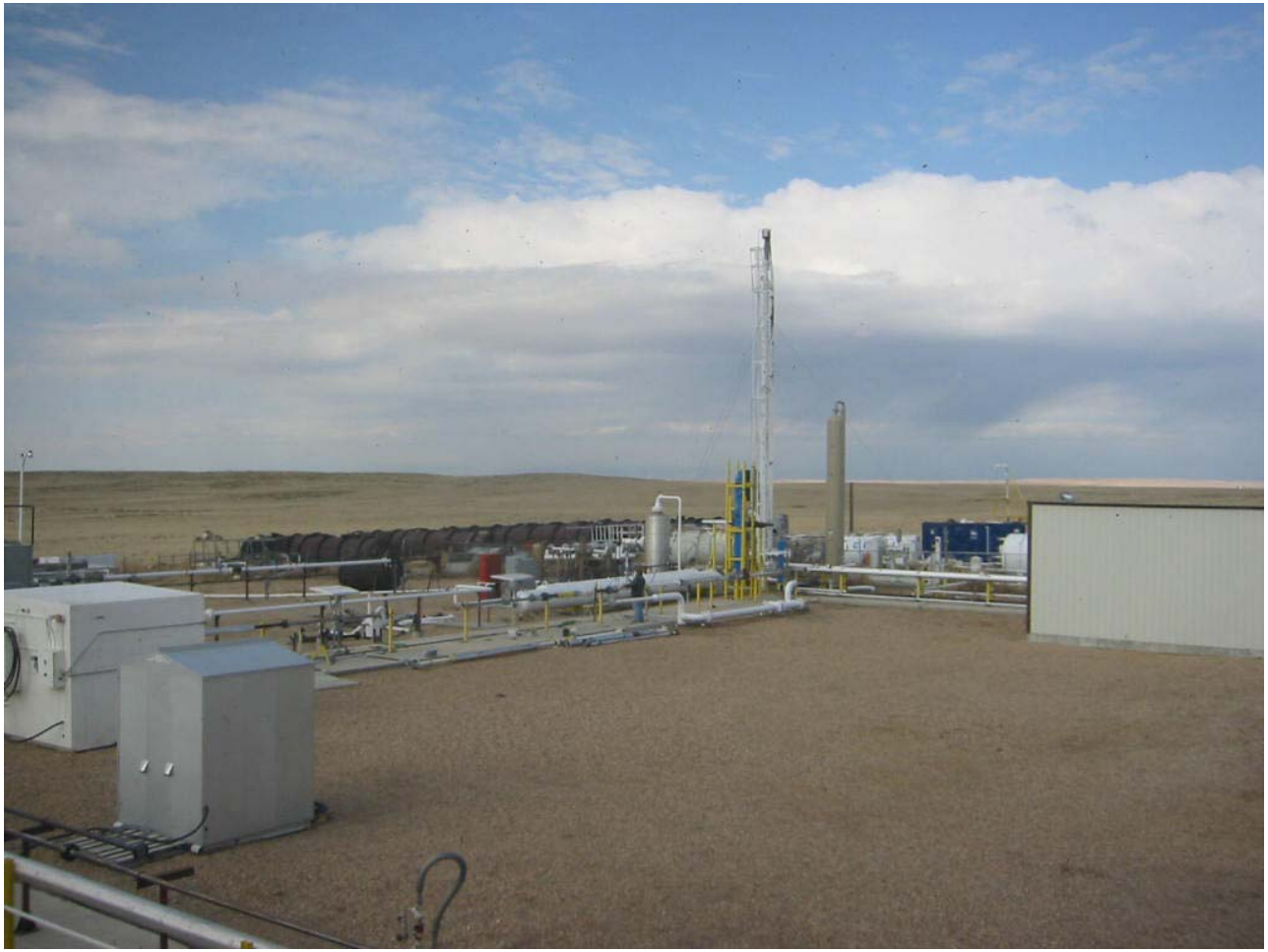

Figure 45 CEESI High Pressure Gas Test Facility

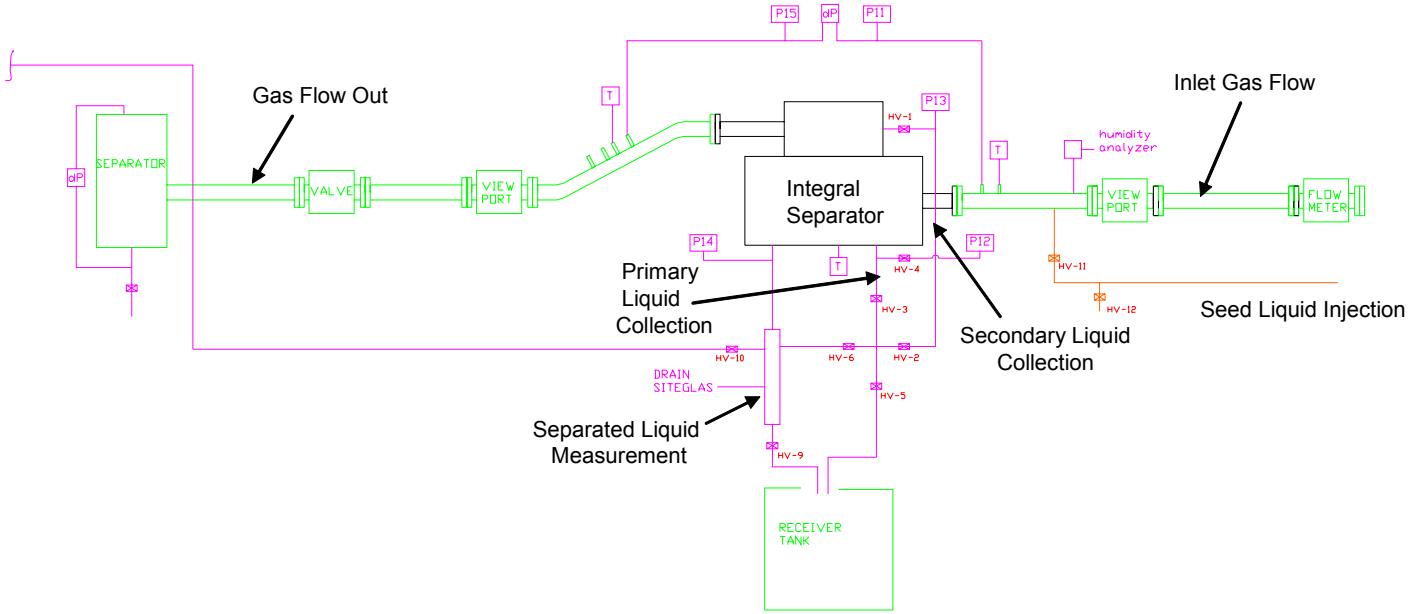

Figure 46 Schematic of Integral Separator Test at CEESI

Figure 47 Single Nozzle Test Installed at CEESI

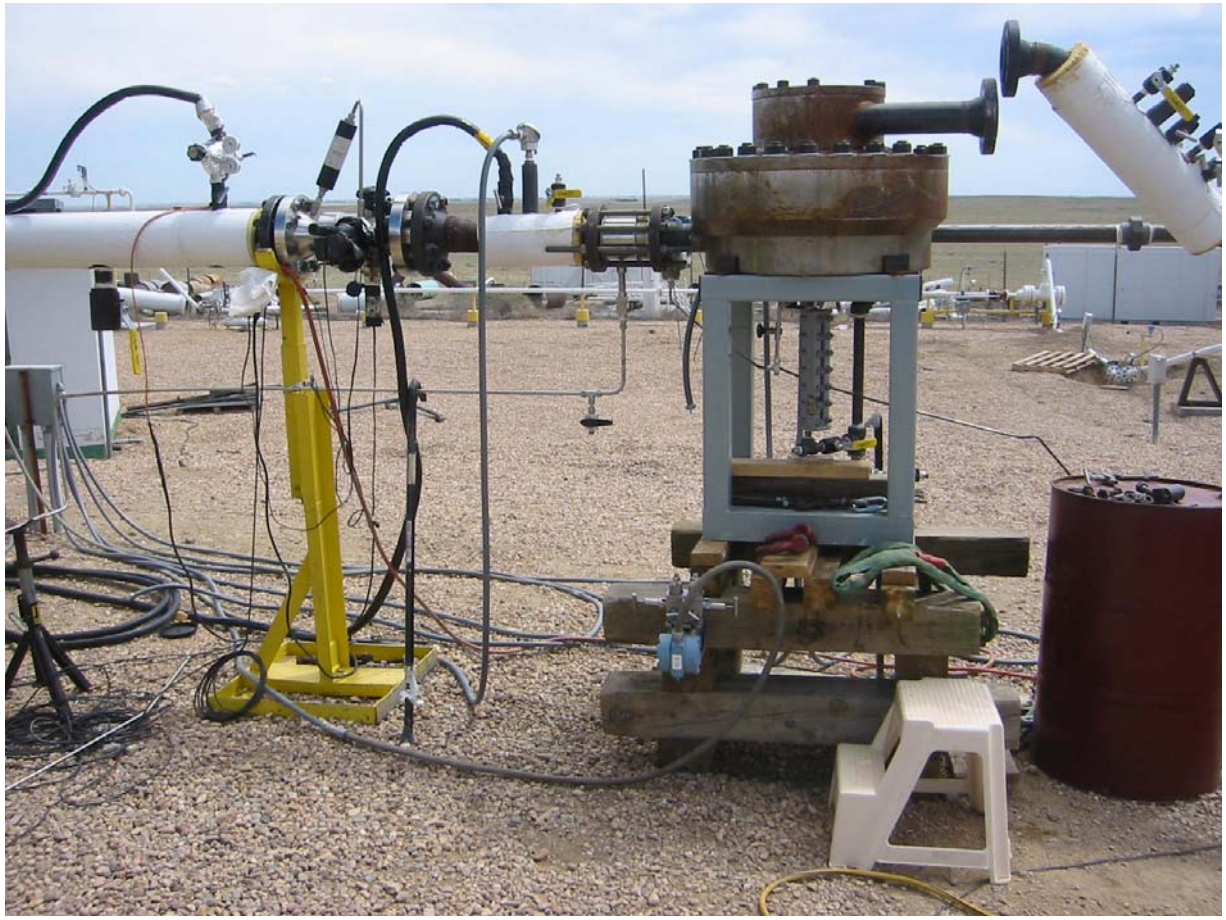

Figure 48 Multiple Nozzle Integral Separator and Upstream Piping Installed for Testing

Figure 49 Downstream Piping from Integral Separator

6. Test Results

Multiple Nozzle Test Unit

Separation

Initial tests were conducted with 4 nozzles, a free liquid separation surface, a solid outer wall and an inner wall. Water and air were premixed and fed to the nozzle plenum. A great deal of water carryover was observed. The transparent inner wall was completely obscured by the two-phase flow. Liquid was observed at the top of the inner wall. Figure 50 is a view of the top during operation. Water streaks can be seen at the top which is the entry to the air diffuser.

Visual observation was made of liquid being trapped and shed from the 4 nozzles that were not flowing. The unit was subsequently tested with all eight nozzles active. The same result occurred, namely excessive liquid carryover.

The unit was operated without the diffuser or outer wall to visually observe determine the cause of the liquid spray and carryover. The spray obscured visual observation but it appeared that the free liquid surface was disturbed by the high velocity jets resulting in liquid ejection from the liquid annulus.

The solid portion of the liquid separation surface was extended so that all of the two-phase jet was intercepted by the solid surface. A marginal improvement was seen, but excessive liquid carryover with the air still occurred.

Another series of observations without the air diffuser or outer wall was made. It was found that using the porous wall enabled the unit to operate without excessive spray at the top such that improved visual observation could be made. The main cause of the liquid carryover was found to be a severe mal-distribution of the flow into the nozzles from the inlet plenum. Figure 51 is a photograph of the unit operating showing that all of the liquid was coming from one nozzle. The high velocity air from the other nozzles deflected the jet and entrained liquid which was carried to the outlet.

The flow mal-distribution probably resulted from separation of the water from the air in the inlet plenum and preferential entry of the water layer into one nozzle. In order to eliminate the problem new injectors were made to enable higher, and controlled, liquid flowrates to be injected into each nozzle.

The unit was retested with the porous wall and no center wall. A test series with eight nozzles had no measurable liquid carryover. Figure 52 shows the unit operating. Separated water was collected in an open container to visually determine if there was any significant carry under of gas in the liquid. None was observed.

Water and air from the porous wall chamber was re-circulated into the center of the vortex. Figure 53 shows the re-injection tube and arrangement. The pressure difference

between the porous wall chamber and the center was sufficient to return the flow under all conditions.

No water carry over in the gas was measurable by the secondary separator for perfect or over-expansion conditions for the nozzle. The exit from the diffuser was opened to determine if there was any mist. As shown in figure 54 the exit air stream was perfectly clear with no mist or liquid carryover of any amount. Operation with the nozzle in a highly under-expanded condition resulted in a very light visually observable haze.

Test series with 4 nozzles and with 2 nozzles were also run. With 4 nozzles some operating conditions resulted in trace amounts of liquid carryover. With 2 nozzles all test conditions had large amounts of liquid carryover.

While good separation was achieved the pressure readings at the diffuser outlet and downstream of the nozzle did not indicate compression of the dry gas. An investigation showed that the nozzle exit pressure tap was downstream of the nozzle in the nozzle bore, which had a larger diameter than the nozzle inside diameter (0.3" versus .196"). The sudden expansion caused a higher reading than the actual nozzle exit pressure. The measurement point was moved to be immediately at the nozzle exit. This resulted in reading the true pressure difference. Figure 55 shows the pressure recovery efficiency versus nozzle exit velocity for air. The corrected values are those data for which the dynamic head loss due to the sudden expansion was subtracted from the nozzle exit dynamic head. A substantial increase was measured when the solid wall was tested instead of the porous wall. A further increase was measured when the inner wall was used. The maximum value measured, .56, is close to the predicted value for the subset application.

A comparison of the dry gas compression with no water and with mass ratios of water to air of .18 and .26 is given in figure 56. The addition of water reduces the nozzle exit velocity and the recirculation of secondary carryover further reduces the available head.

The following conclusions were reached as a result of the tests:

1) Complete separation of the liquid from the gas is achievable with a solid impingement surface and a porous wall.

2) Re-circulation of the porous wall chamber gas and liquid into the vortex without affecting separation performance is achievable.

3) An annular vortex chamber is more effective in recovery of the gas pressure than a cylindrical vortex chamber.

4) The liquid volute is effective in producing separated liquid with no gas carry under in significant quantities.

5) Use of multiple nozzles will require changes to the inlet plenum to function correctly with inlet gas flows having free liquid.

Additional tests were conducted with air and water to optimize the separation and pressure recovery. The following variations were made:

Length of primary separation surface

Orientation of Integral Separator

Design and Spacing of primary liquid capture slot

Axial location of secondary separation region

Figure 57 illustrates the separation as a function of the nozzle exit pressure. At a back pressure greater than 15 psig, complete separation was attained for all liquid flowrates tested.

Although complete separation was demonstrated for the IS a portion was carried over from the primary separation region and separated in the vortex chamber, captured by the porous walls. A goal of the tests was to maximize the portion captured by the primary region to reduce frictional losses in the vortex region, enabling a higher pressure recovery. The length was varied from .5" to 4", resulting in a variation in the ratio of the primary separator length to theoretical geometric impingement length (Impingement Length Ratio) of 1 to 8.

Figure 58 is a summary of the separation results for the variation in impingement length. Complete separation was obtained at the design conditions for the lengths varied. However, the percentage of liquid captured by the primary separator increased from 35% to 65% for the variation of length. The optimum impingement length was found to be 2". This value was used in the design of the commercial prototype.

Figure 59 shows the primary separation as a function of separator length and gap for Geometry 1. The liquid capture percentage increases with both length and gap. However, as the gap size was increased gas ingestion in the primary liquid chamber was increased.

An inner wall in the vortex chamber produced the best pressure recovery because of the reduction of flow recirculation. However, flow visualization showed liquid crawling along this wall under some flow conditions. In addition the converging shape of the vortex chamber produced a pressure decrease in the direction of flow which resulted in gas flow from the secondary separation chamber with entrained liquid in the downstream regions of the vortex chamber. These results caused a change in the design of the vortex chamber. Gradually diverging walls will be provided to produce a gradual pressure increase in the axial direction. Any secondary gas flow will occur at the entrance to this section rather than the inlet. A porous section will be provided at the

downstream region of the inner wall of the vortex chamber. The higher pressure in this region will result in liquid capture and recirculation to the inlet of the vortex region. These changes will be discussed later.

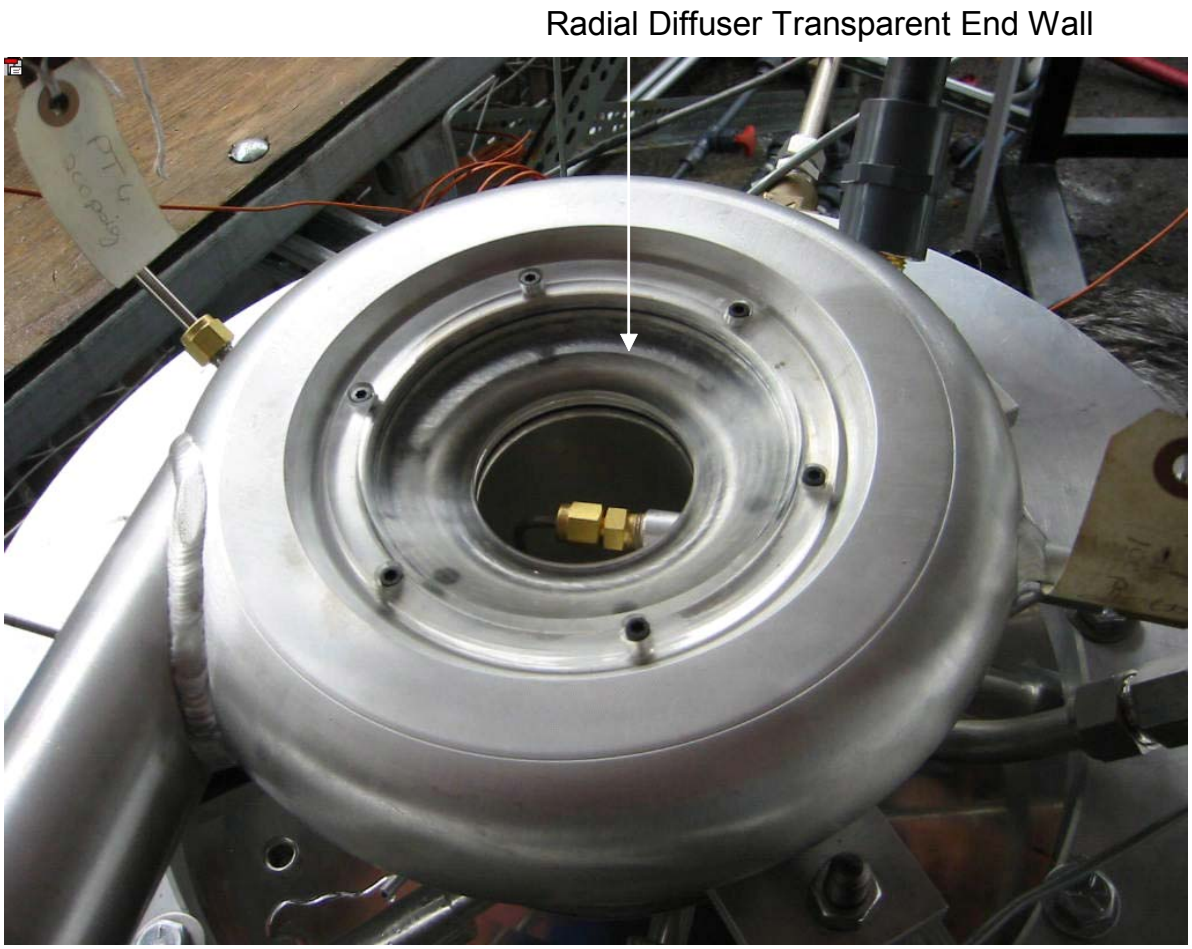

Figure 50 Operation of Air-Water Integral Separator with Liquid Carry Over

Figure 51 Operation with Mal-Distribution of Liquid, Top Removed

Figure 52 Operation of Integral Separator Showing Collection of Separated Liquid

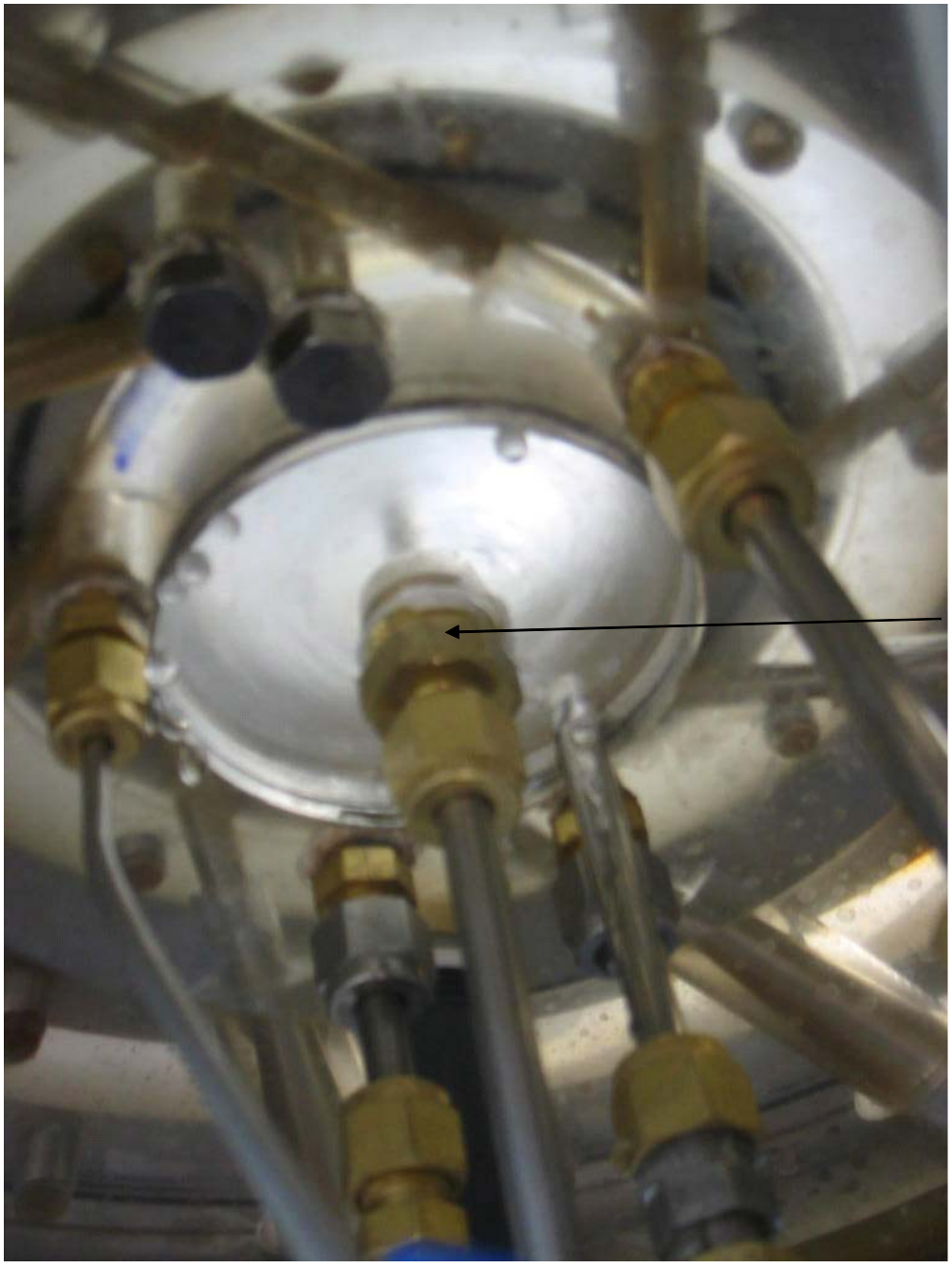

Figure 53 Operation with Complete Separation with Return
of Secondary Separated Liquid

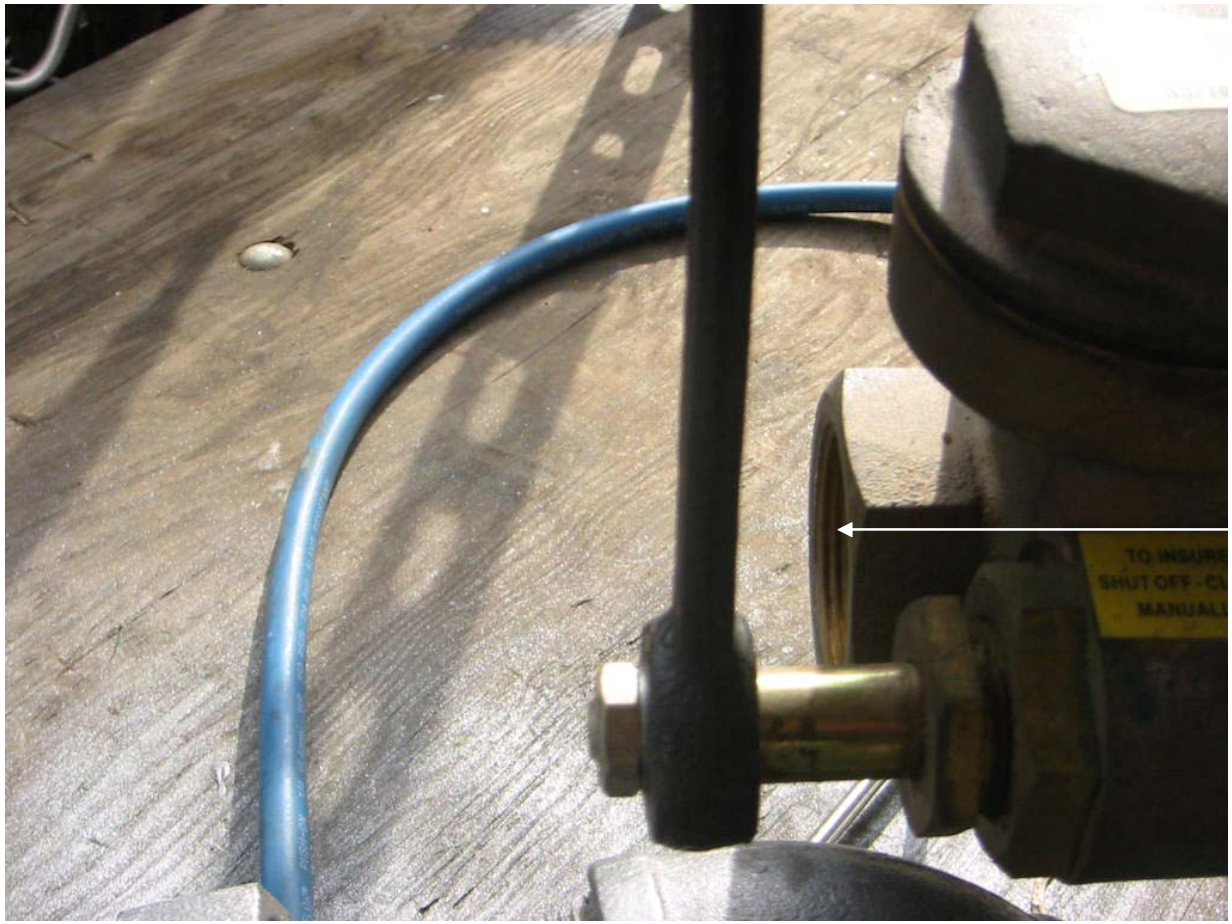

Figure 54 Operation with Dry Gas Outlet, No Liquid Carryover

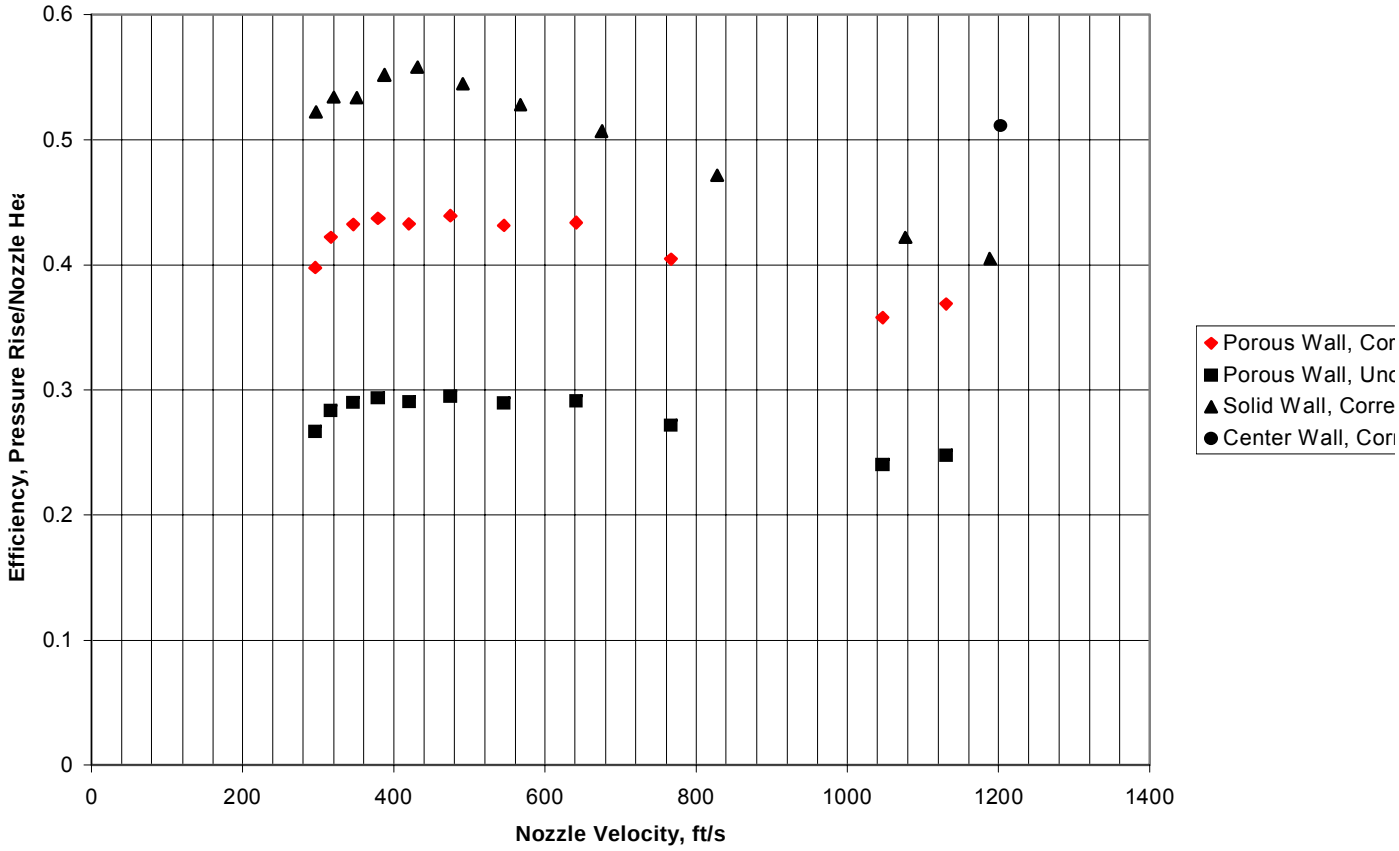

Figure 55 Pressure Recovery Efficiency of Integral Separator

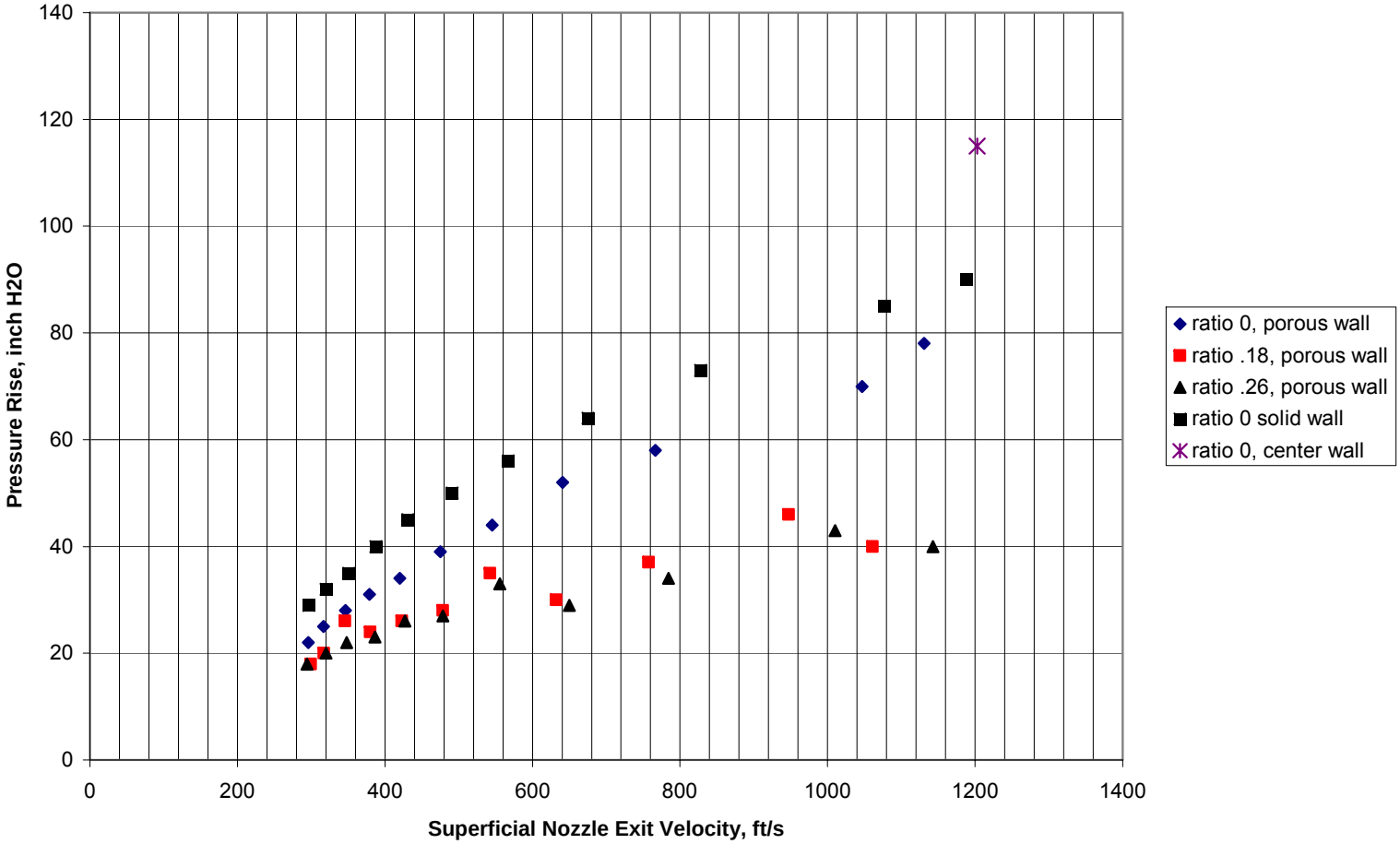

Figure 56 Dry Gas Compression for Integral Separator

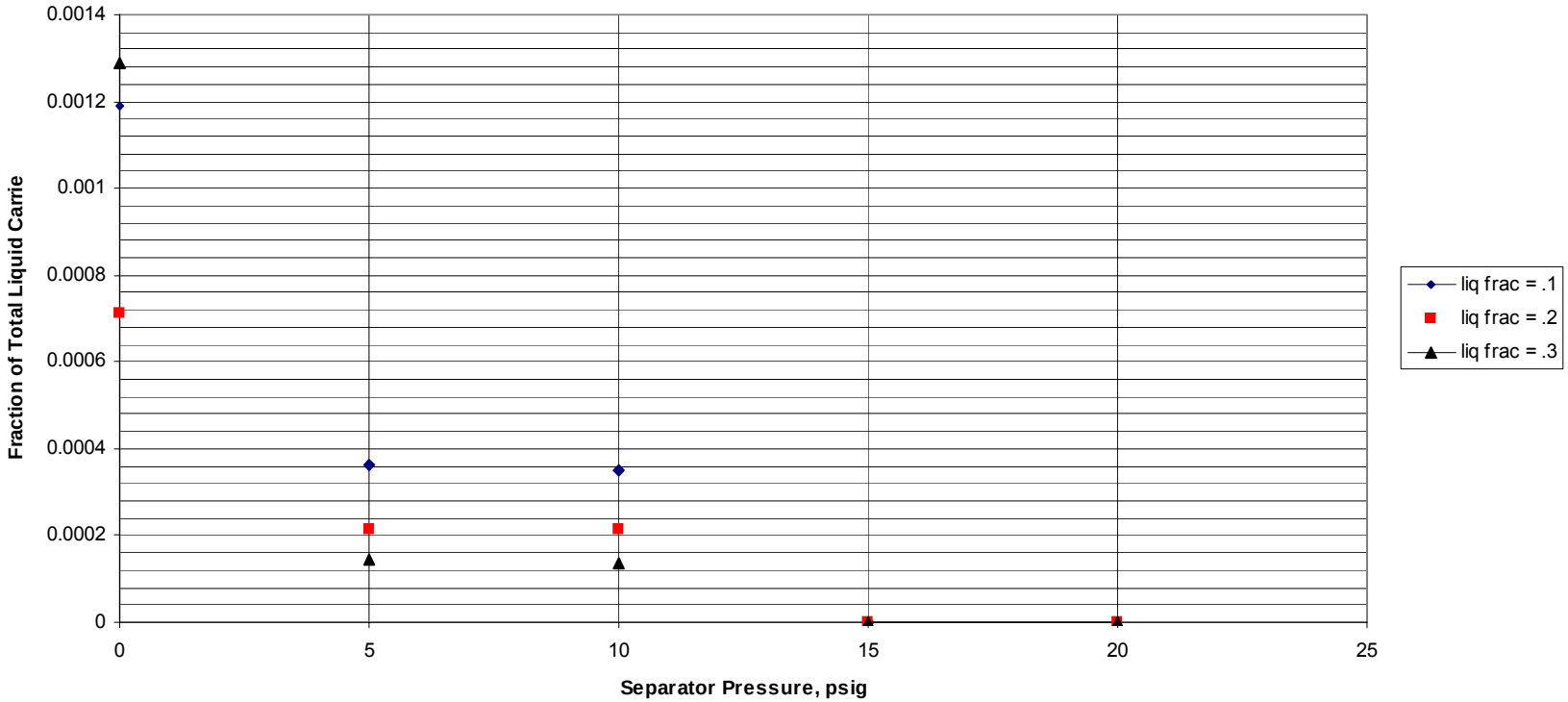

Figure 57 Liquid Carryover versus Separator Pressure

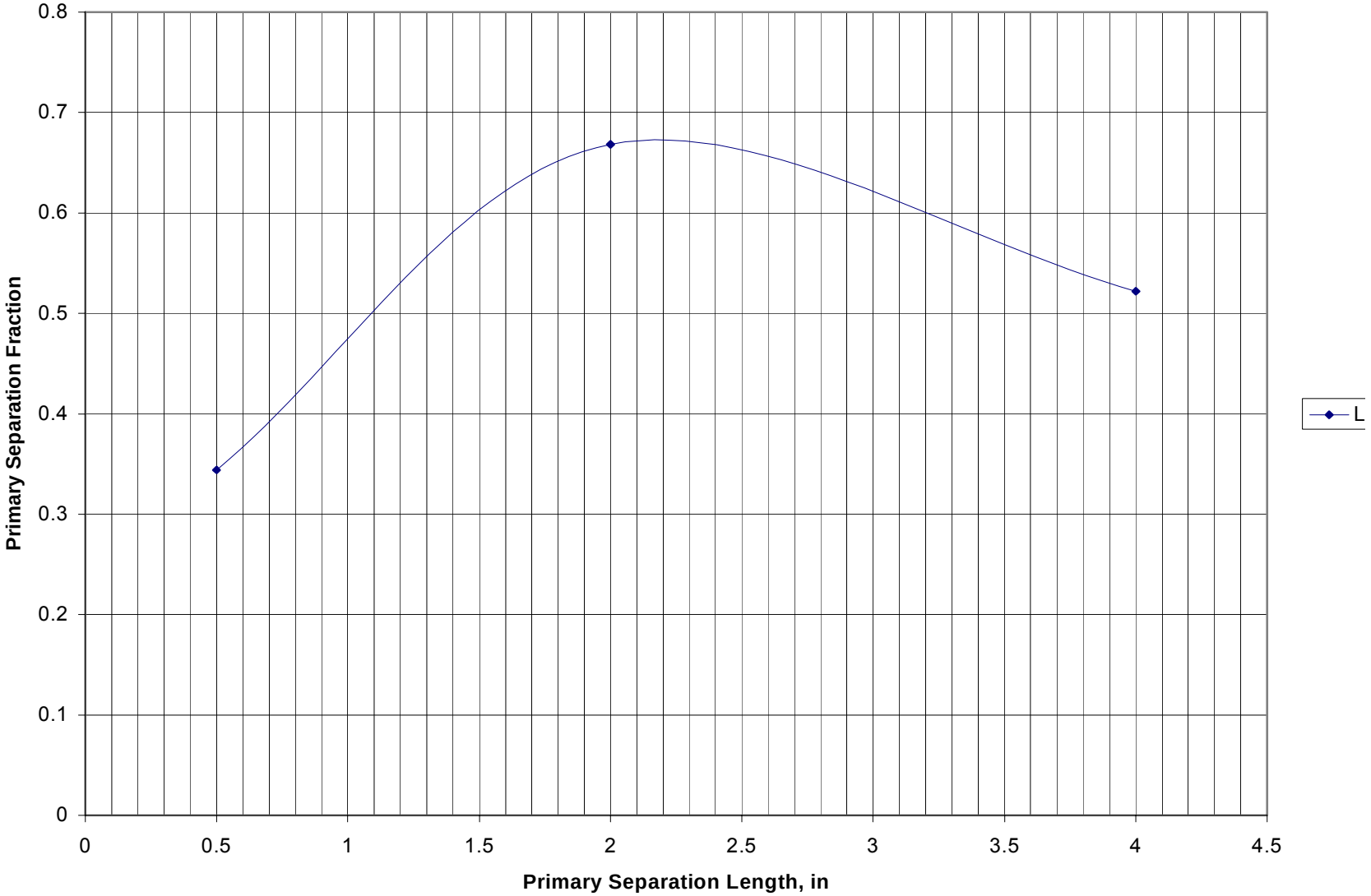

Figure 58 Fraction of Separation in Primary Separator versus Primary Separator Length

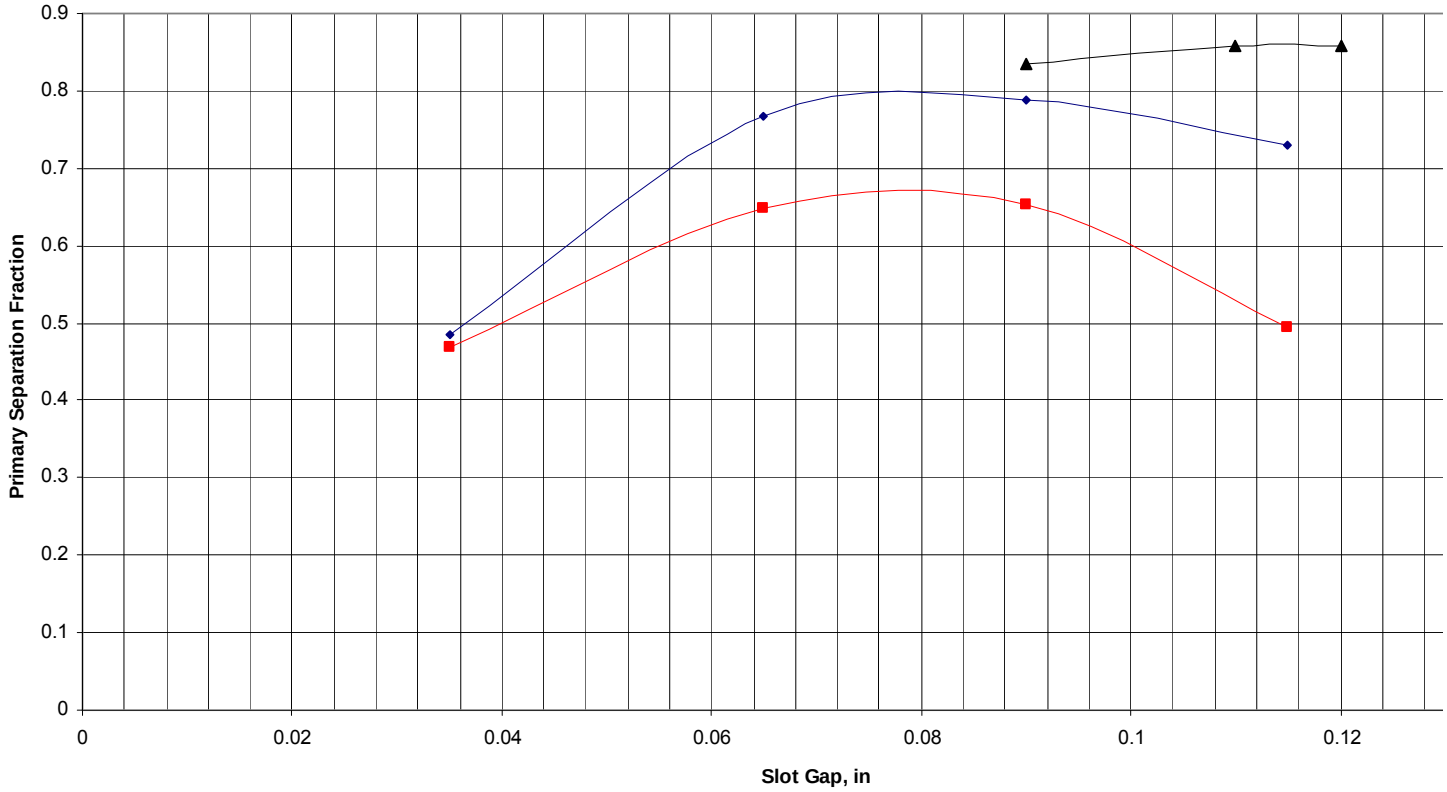

Figure 59 Primary separator Fraction versus Capture Slot Gap

Experimental Confirmation of CFD Analysis

Analysis of the geometry tested was conducted with the Fluent CFD code. The predicted results show general agreement with the measured trends.

Figure 60 is the result of analyzing geometry 1 for a gas flow of 100 scfm. Parameters of the analysis which correspond to the test conditions are provided in Appendix A. The pressure is predicted to rise from 29.865 psia at the inlet to 30.0 psia at the outlet, a pressure rise of 3.3" (H_20). The pressure rise from the region immediately downstream of the primary separation region (lrd_2) to the outlet is predicted by the CFD code to be 6.9". Test runs are summarized in Appendix B. A flowrate of 97.0 scfm at a nozzle exit pressure of 29.0 psia gave a measured pressure rise of 5.14" somewhat greater than the CFD prediction for the inlet but below the pressure rise after the primary separation region. This result suggests that the CFD code is overestimating the losses due to the sudden expansion in the primary separation region. The predicted loss in this region also suggests a smaller capture slot would reduce this loss.

The velocity field calculated by the CFD code is shown in figure 61. The results also support a modification to the design to reduce losses in the primary separation region. The tangential component of the inlet velocity, 518 ft/s, decreases to 360 ft/s after the primary separation region. As the flow traverses the vortex chamber a further loss to 183 ft/s is encountered. Finally the velocity is decreased in the diffuser to 84 ft/s.

The pressure variation and velocity decrease led to design and testing of a modified primary separator as discussed above. The separation wall capture slot was moved closer to the primary separation surface and streamlined. The capture slot was reduced to .030'. The results indicate an improved performance in energy recovery.

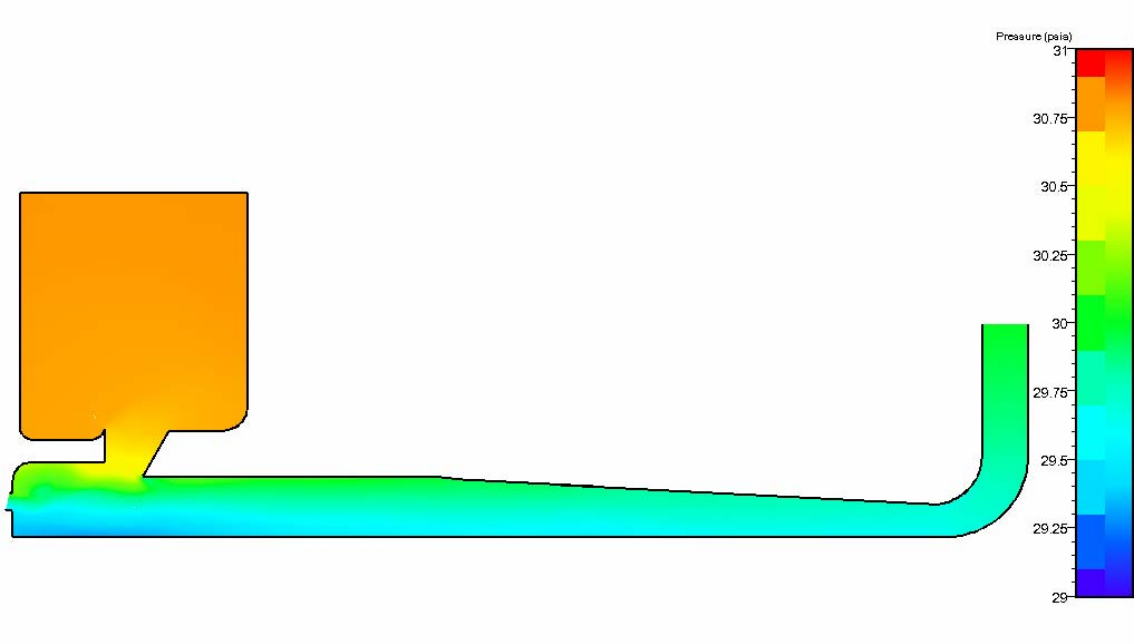

Figure 60 CFD Prediction of Pressure Field for Air-Water Test Case

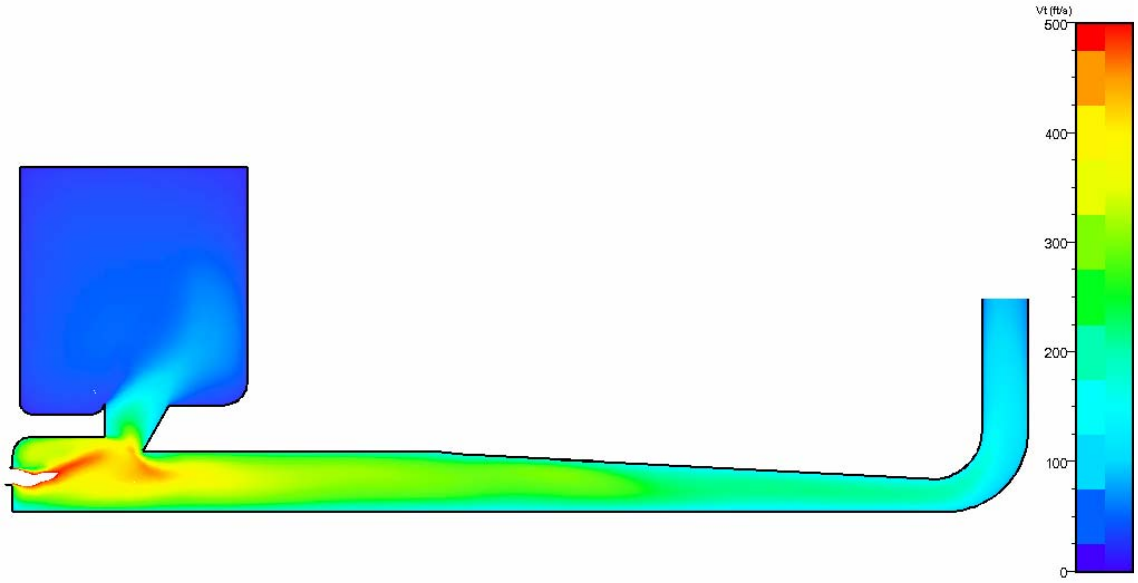

Figure 61 CFD Prediction of Velocity Field for Air-Water Test Case

High Pressure Gas Tests

Single Nozzle Separator

The single nozzle unit was installed in the Colorado Engineering Experiment Station (CEESI).

Initial tests were run with gas alone and with decane injection. The expansion through the nozzle agreed with the pressure profile predicted by the two-phase nozzle code using the gas composition and HYSYS property calculations in the upstream region. In the downstream region however, the profile flattened, possibly in response to a downstream obstruction (to be discussed later). Figure 62 shows the measured and calculated pressure profiles for two cases: an inlet pressure of 1120 psia and an inlet pressure of 934 psia. The gas flowrate was about 14,000 lb/h and the liquid flow was about 500 lb/h.

The temperature profile measured for the same cases showed a highly irregular behavior. Figure 63 is a plot of temperature versus length. The measured temperature was significantly above the calculated temperature due to the temperature recovery factor for the cylindrical thermocouples used. However, an abrupt slowing of the temperature decrease at about 9 inches was followed by an abrupt drop. Replacement of the thermocouples and variation of insertion depth were tried but the same behavior was noted.

The predicted static temperature was corrected by a recovery factor of .599 ($Pr^{1/2}$ for methane) to determine the validity of the prediction. Figure 64 shows a reasonable agreement of predicted measured temperature with actual measured temperature except for the noted region. It is hypothesized that the temperature variation is a result of two-phase pressure increases occurring to adjust the nozzle internal flow (which is subsonic) to the exit conditions of the separator induced by a barrier to the flow (discussed later).

A composite of all the test runs is shown in figure 65. The same temperature characteristic is found in all the runs. Application of the estimated recovery factor of .599 to run number 2 provides agreement between the predicted measured temperature and the actual measured temperature. Calculation of the nozzle exit temperature using the HYSYS process code with the calculated nozzle efficiency of 98% gives close agreement with the nozzle code static temperature.

The liquid carryover with the gas and secondary liquid flowrates were measured. The liquid carryover was very large. Furthermore a pressure drop was experienced from the nozzle exit to the gas exit, rather than a pressure rise.

Post test examination revealed that the Stellite coating on the separation surface had parted, blocking the liquid exit. The loose pieces were removed, the adjustable knife edge replaced and the testing resumed. A large carryover was again experienced. A post

test inspection revealed that the adjustable knife edge to change the gap of the liquid capture slot had come loose, protruding into the flow passage. Figure 66 is a photograph showing the blockage resulting from the protruding knife edge. The obstruction blocked the liquid passage and also was a barrier over the entire surface of the separated high velocity liquid, undoubtedly producing a non-directed spray which exited through the gas exit, producing the liquid carryover and pressure drop.

The knife edge piece was removed completely and testing resumed. The liquid carryover was reduced but the wide gap resulting from the knife edge removal provided additional flow interference.

The decision was made to continue air water testing of the single nozzle version while proceeding with a multiple nozzle design for the field test unit. In the event a favorable single nozzle geometry is found, that unit will be re-tested and a decision as to the final unit made at that time.

The instrumented nozzle was left at CEESI to conduct additional testing to determine the effect of seed liquid on droplet formation. Figure 67 shows the nozzle during testing.

Tests were conducted with natural gas doped with butane to about 4.5% mole fraction. Calculations were made with HYSYS for operation without and with seed injection. Condensation of the butane is not predicted for the conditions of the test. However, with the injection of decane the solubility of the gaseous components results in a predicted increase in liquid flow from the injected 492 lb/h to 862 lb/h.

Figure 68 is a photograph which shows the view downstream of the nozzle. The faint fog indicates some condensation is occurring with very small particle sizes. At the right hand side of the window the outline of the nozzle is visible.

Injection of the decane seed resulted in larger liquid droplets which produced liquid films separating and recirculating in the window region. The nozzle exit was completely obscured, as shown in figure 69.

The measured temperature profile and the differential temperature profile from the inlet are plotted in figures 70 and 71. The differential temperature is much less with the decane injection indicating condensation and solution is occurring during that part of the test.

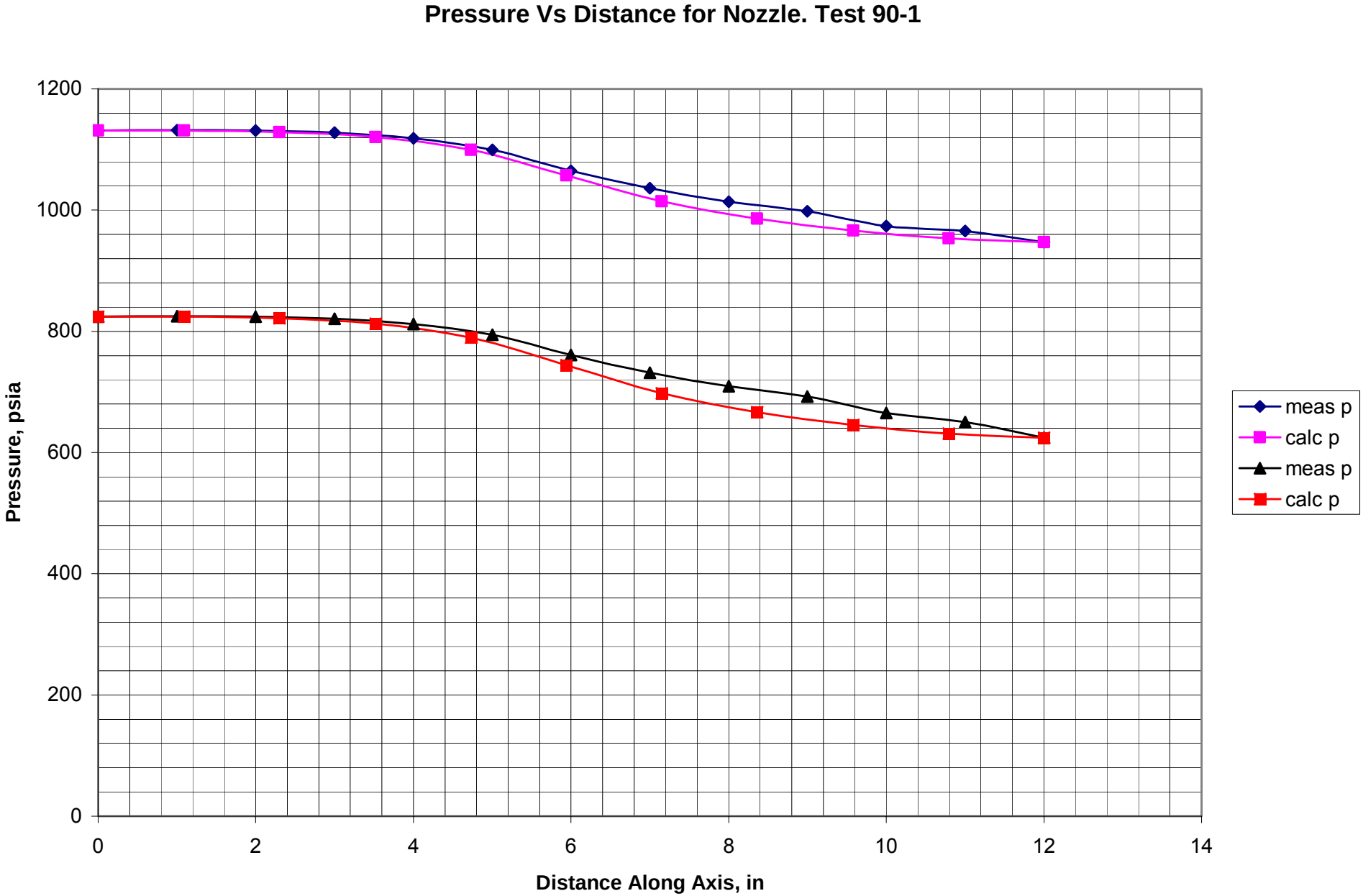

Figure 62 Pressure Profile of Nozzle with Decane Injection

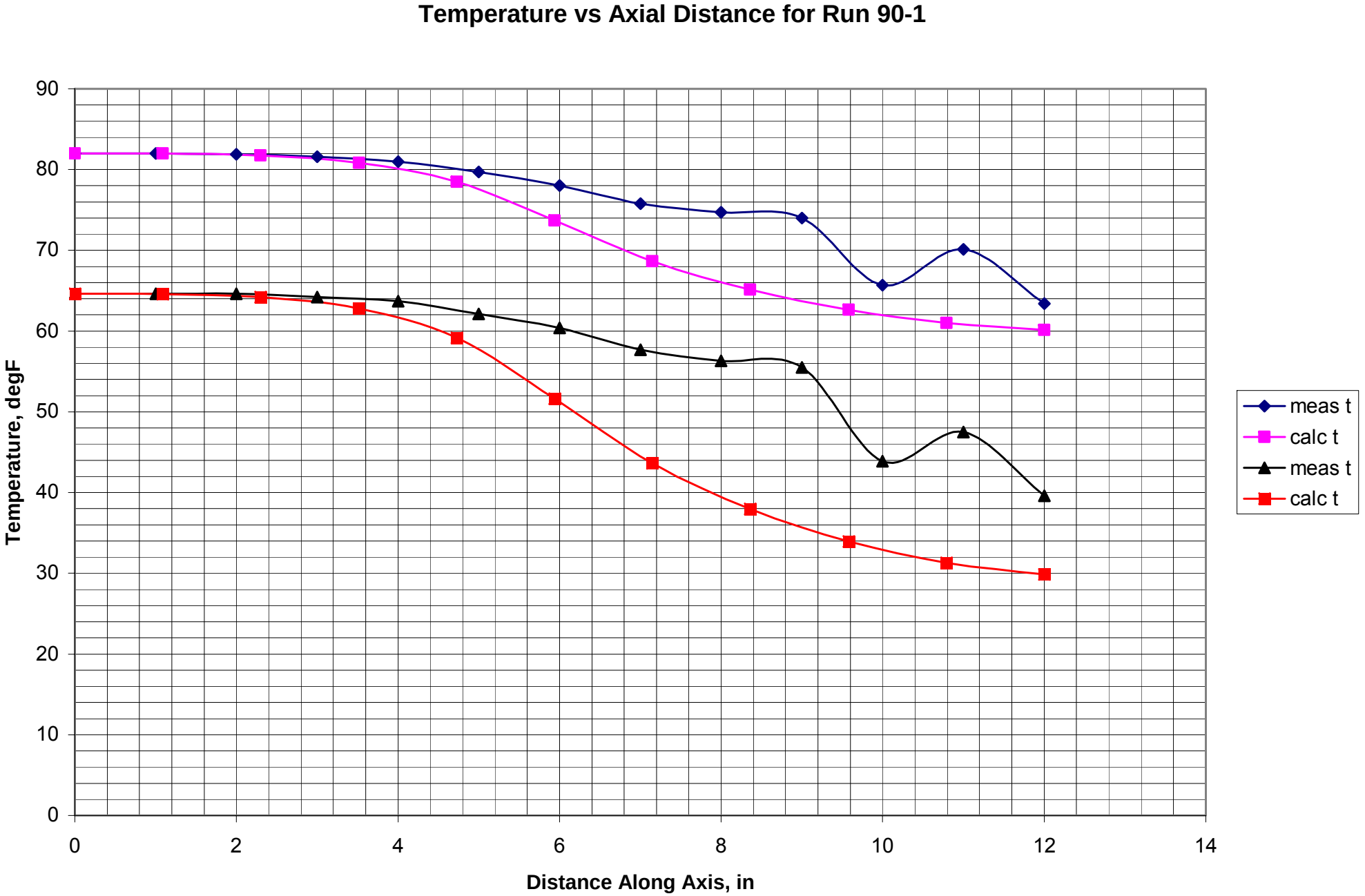

Figure 63 Temperature Versus Axial Distance for Nozzle with Decane Injection

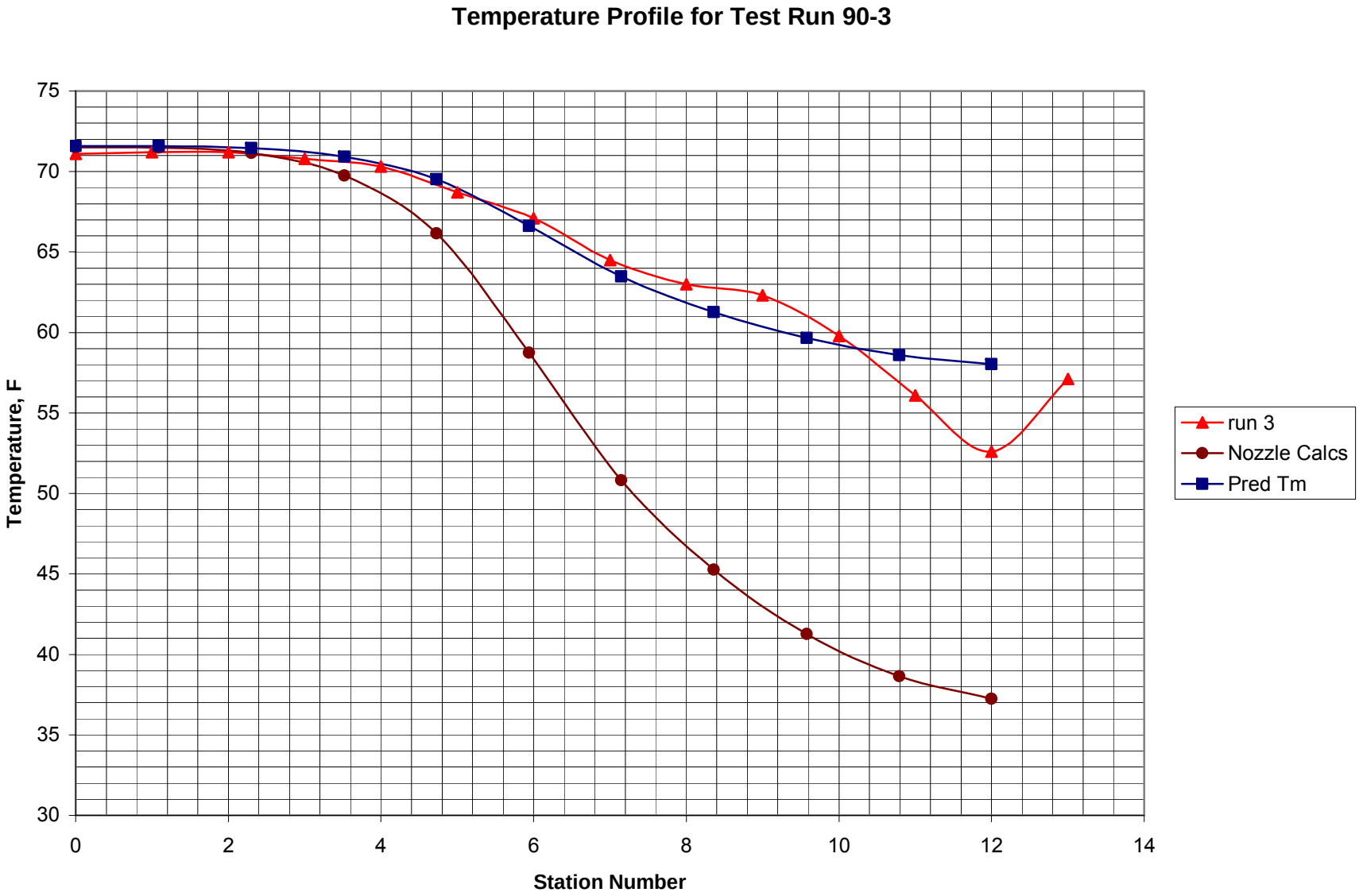

Figure 64 Comparison of Measured and Calculated Wall Temperature for Two-Phase Nozzle with Decane Injection. Calculated Static Temperature Shown for Reference

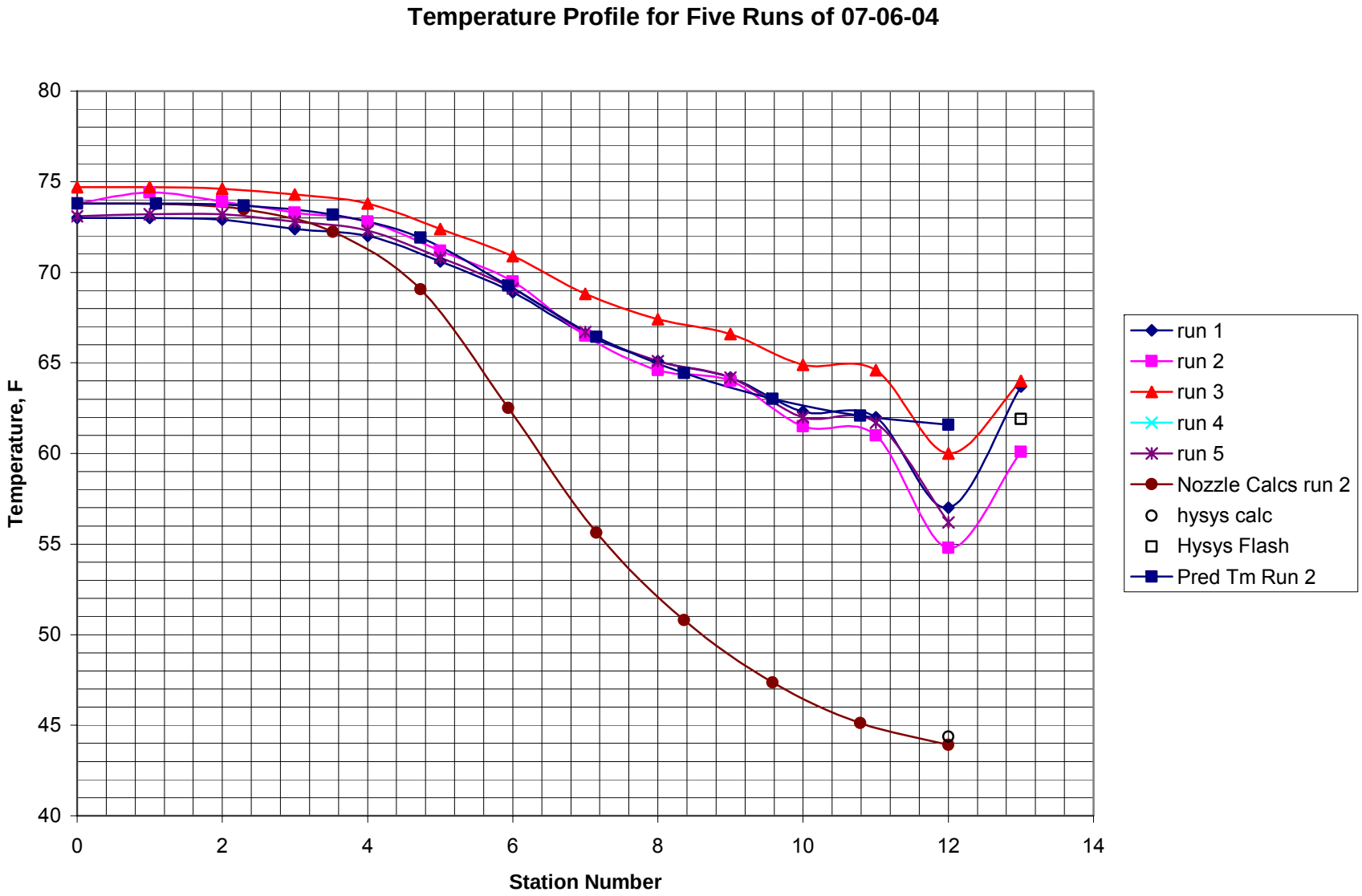

Figure 65 Comparison of Temperature Profiles for Five Test Runs

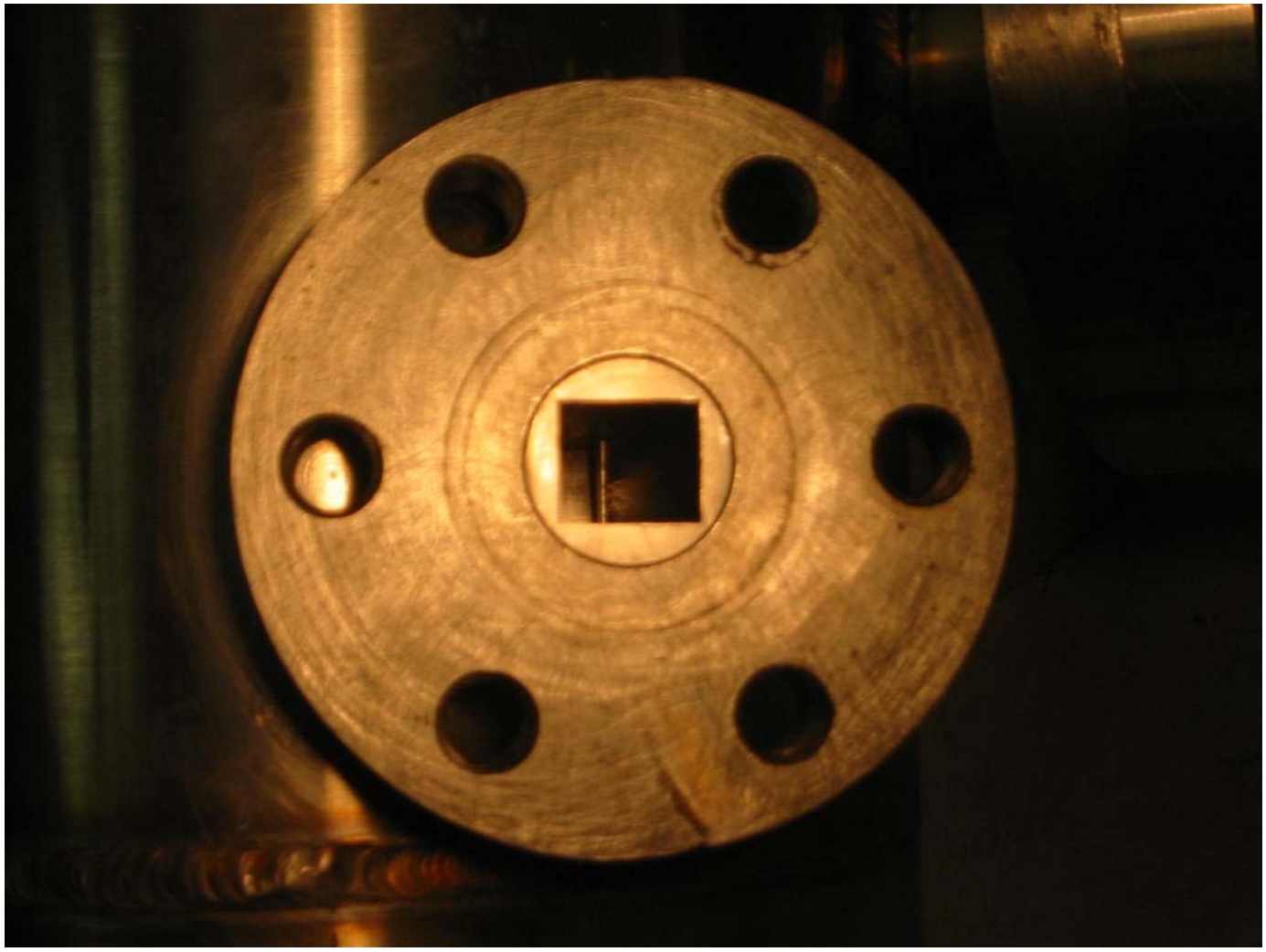

Figure 66 Photograph of Separation Passage Showing Blockage By Knife Edge Gap Adjuster

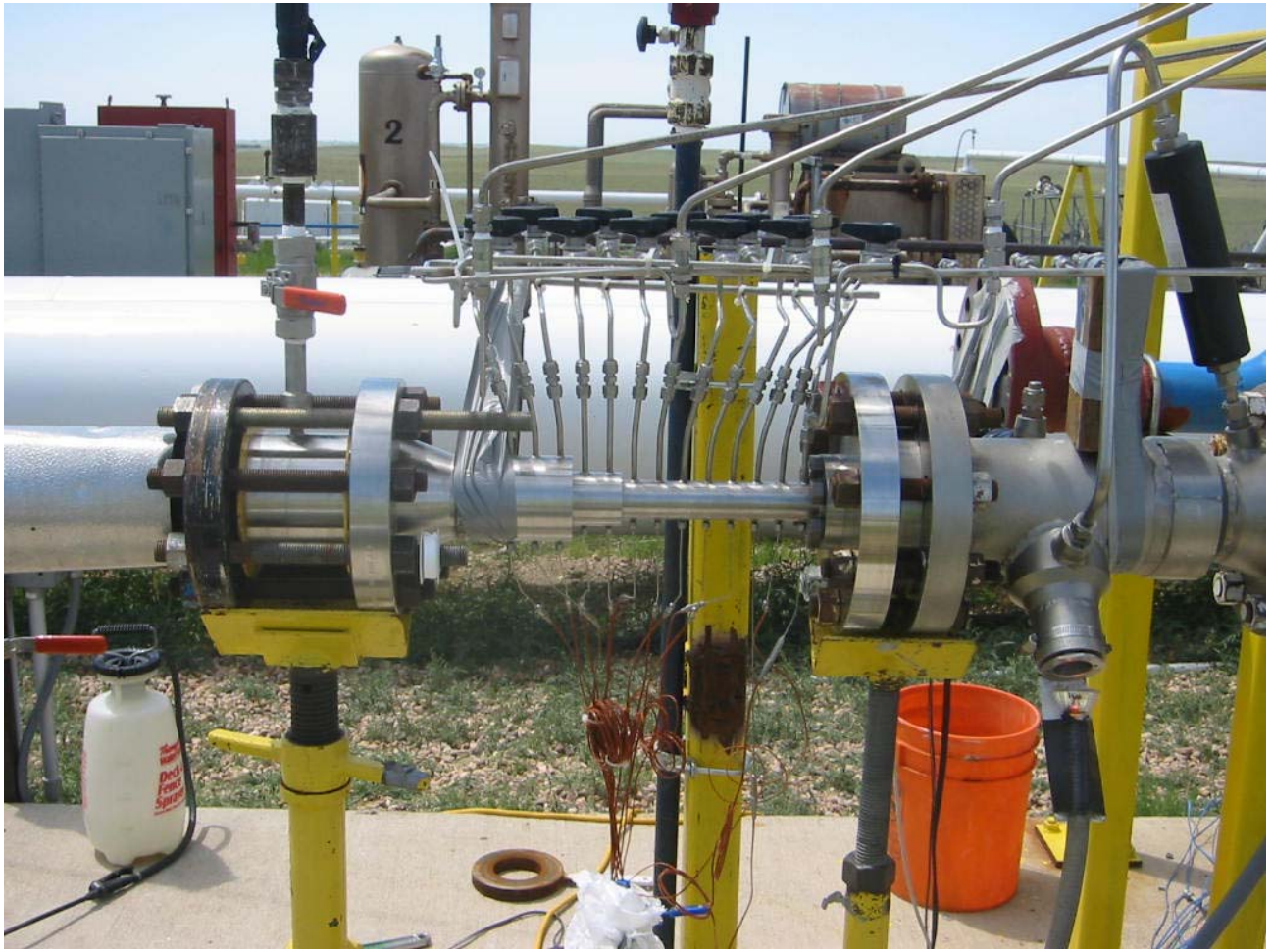

Figure 67 Two-Phase Nozzle During Seed Injection Tests, Viewport at Right

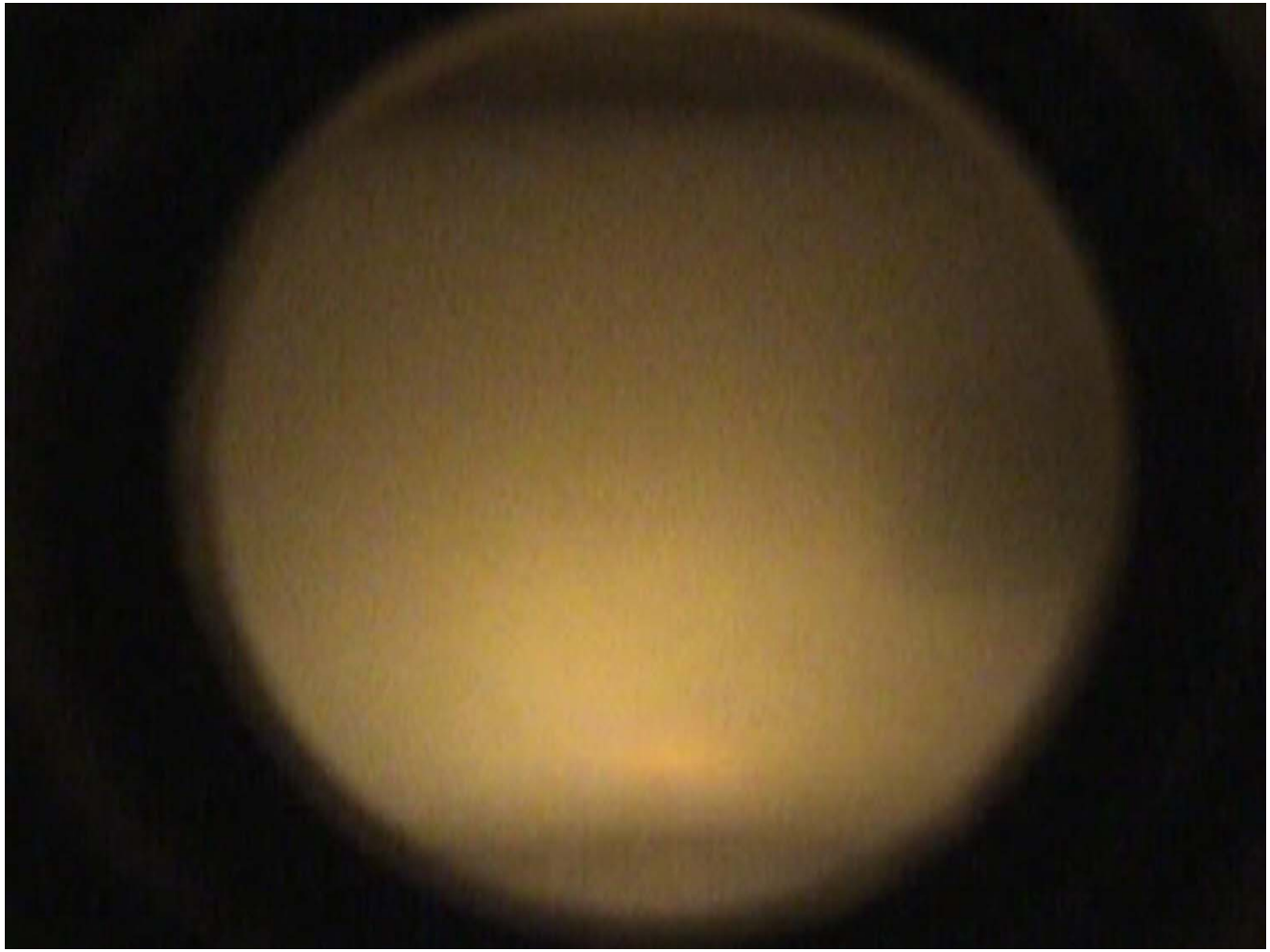

Figure 68 Condensate Fog Before Decane Seed Injection

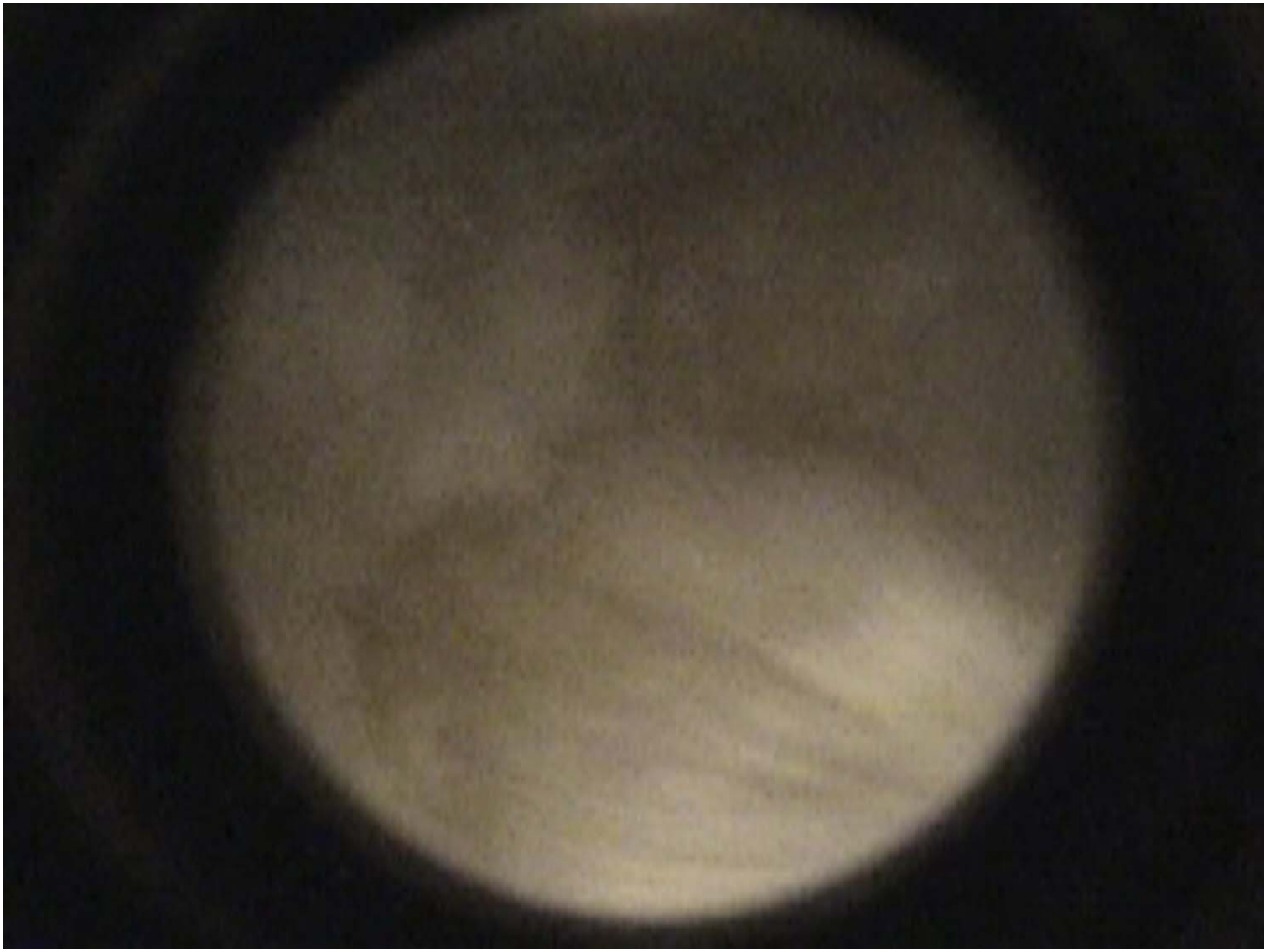

Figure 69 Liquid Film at Nozzle Exit After Decane Seed Injection

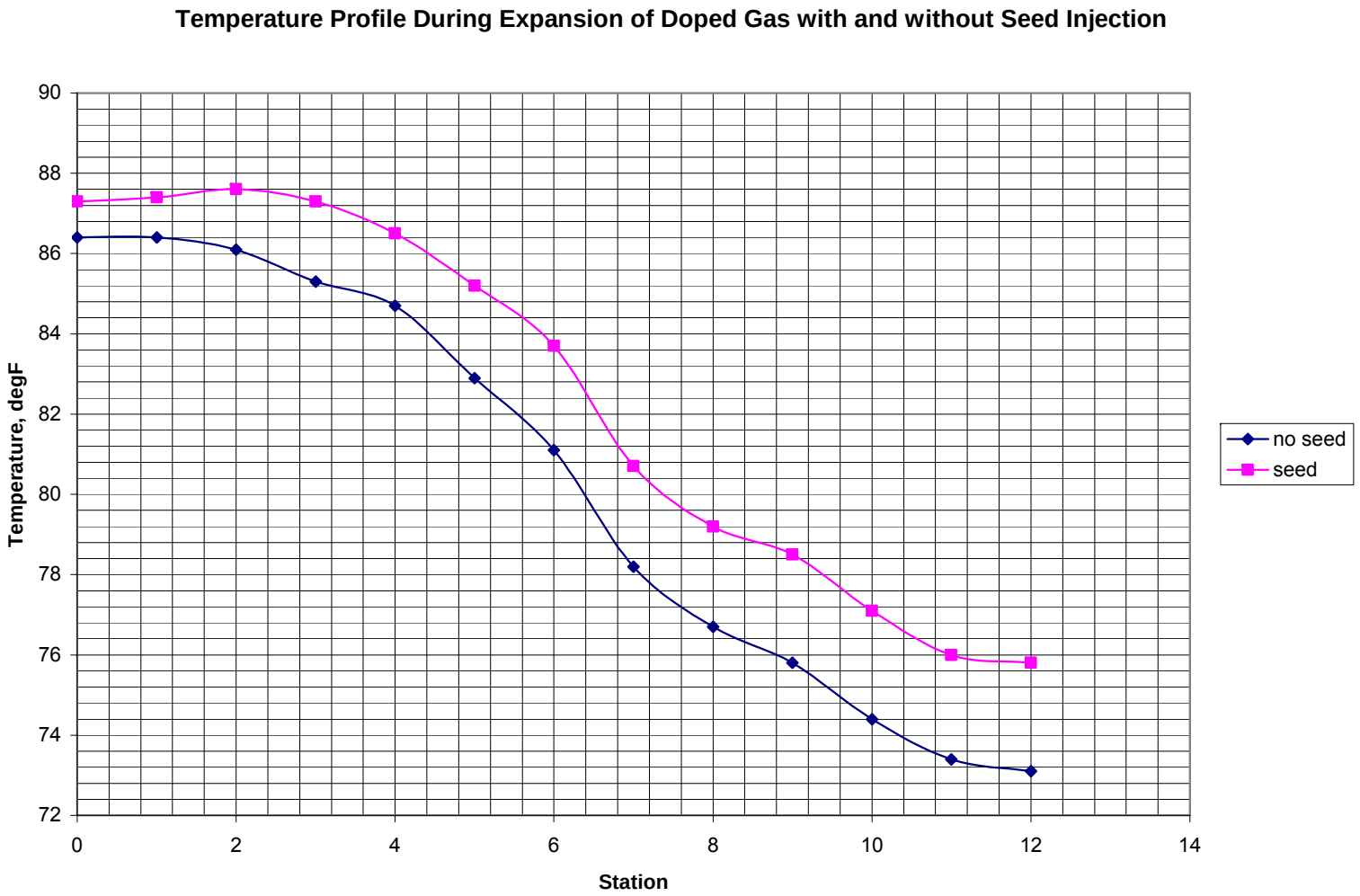

Figure 70 Temperatutre Profile of Doped Gas Expansion With and Without Decane Seed Injection

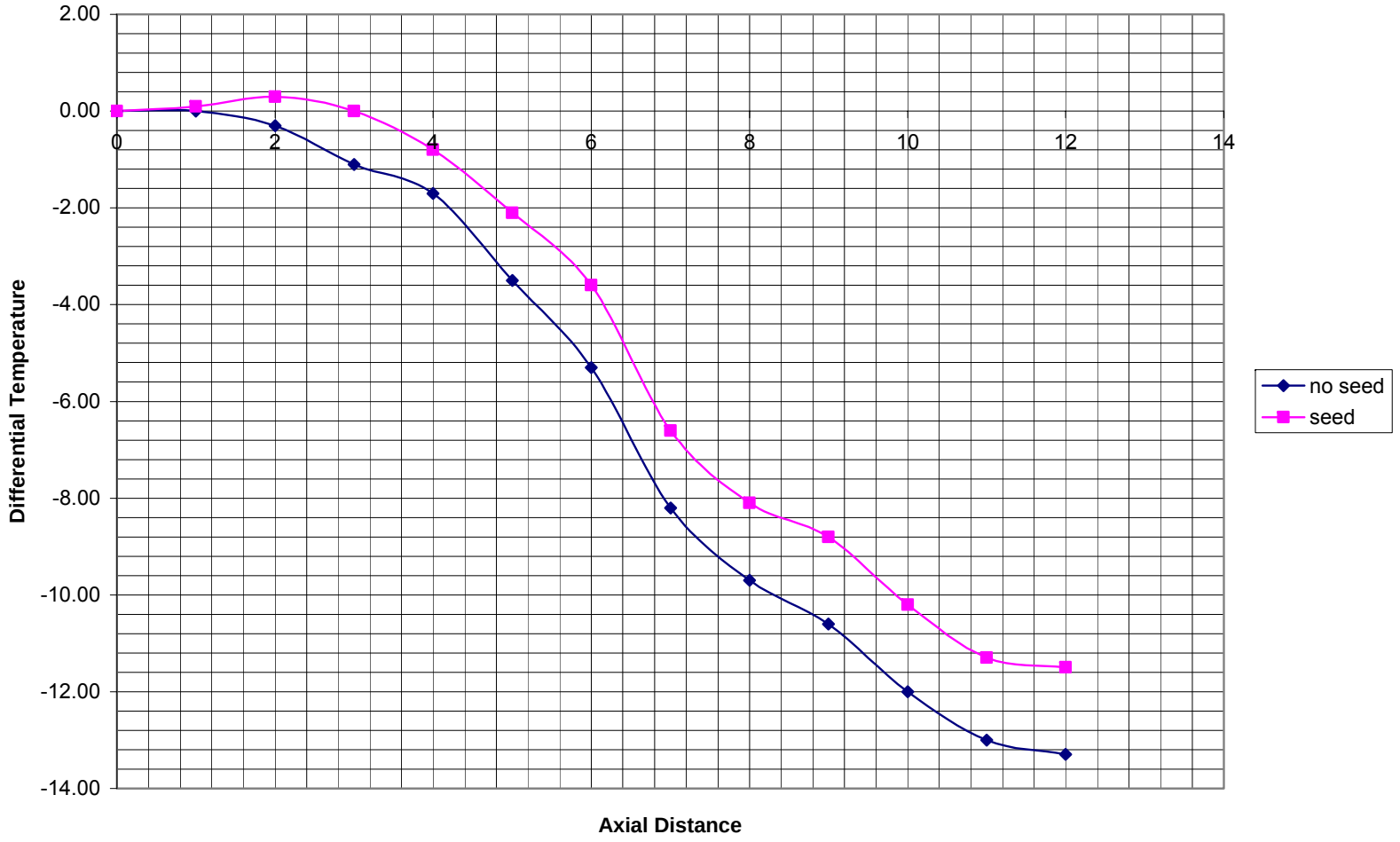

Figure 71 Differential Expansion Temperature of Doped Gas Expansion With and Without Decane Seed Injection

Multiple Nozzle High Pressure Gas Test Results

The prototype multiple nozzle integrated separator was tested at CEESI with high pressure natural gas which was saturated with water. A methanol-water mixture and "Stodard solvent" were injected as seed liquids for the condensation process. The composition of the gas is provided in Table 4. The composition of the Stodard solvent is provided in Table 5. Appendix D provides the reduced data and Appendix E provides data recorded by CEESI for three tests as well as the single nozzle tests.

Table 4 Gas Composition for CEESI Tests

Component	Mole Percent
methane	85.88
ethane	9.672
propane	1.297
i-butane	0.0583
n-butane	0.0686
i-pentane	0.0055
n-pentane	0.0032
c6's	0.0005
c7's	0.0002
c8's	0.0001
c9+	0.0217
nitrogen	0.6003
carbon dioxide	2.3921

Table 5 Solvent Composition for CEESI Tests

Component	Mass Fraction
C3	0.089
C4	0.064
C5	0.171
C6	0.193
C7	0.337
C8	0.862
C9	2.51
C10	27.77
C11	55.72
C12	10.30
C13	1.98

Tests were conducted with both 2" and 8" long separation surfaces. Methanol and the Stodard solvent were used as seed liquids.

Figure 72 shows the overall collection efficiency as a function of the gas flowrate for both methanol and solvent. The collection efficiency is the ratio of the liquid collected by the integral separator and the downstream cyclone separator to the liquid injection flow, as measured by a vortex flowmeter.

The result is surprising in that a significant fraction of the injected liquid is not collected at higher flowrates - even by the downstream cyclone separator, the collection efficiency is a strong function of the gas flowrate. As shown the efficiency ranges from 110% to 20% as the gas flow is increased from 1 lb/s to 9 lb/s.

For these data the gas pressure is simultaneously increasing with gas flow from about 200 to 900 psi. The gas velocity is nearly constant. As a consequence the shear force on the injected liquid is approximately proportional to the gas mass flowrate producing smaller droplets as the gas flow is increased. Smaller droplets, c.f. section 3, are more difficult to separate in a vortex field.

Another result of higher gas pressures would reduce the separation is the higher gas density. The separation driving force is the density difference between the liquid phase and gas phase. Increasing the gas pressure increases gas density, reducing this potential.

A third effect which could worsen separation as the gas pressure is increased is the absorption of the injected liquid by gas. XXXXX et al have measured absorption of heavy hydrocarbons in methane over a range of pressures. Extrapolation of their results to the test conditions predict complete absorption of the injected solvent at the higher test pressures. The result is contradictory to HYSYS predictions and remains to be verified.

Figure 73 also shows the collection efficiency for methanol to be lower than the solvent in spite of the fact that the density is higher. HYSYS predicts a partial absorption of the methanol by the gas at the test conditions.

The collection efficiency of the integral separator and the cyclone separator as a function of liquid injection flowrate and gas pressure are shown in figure 74. The collection efficiency peaks at a liquid flowrate of about 0.04 lb/s.

To examine the effect of mass flow ratio the collection efficiency was plotted versus liquid to gas ratio for the data taken at 250 psi and 500 psi. As shown in figure 75 the flow ratio varies from .0037 to .045, a range of about 10:1. (Data from higher pressures was too scattered to show a trend).

The results show a trend of increasing collection efficiency for both the integral separator and cyclone separator as the liquid to gas ratio is increased. The integral separator increases the collection efficiency from about 40% to 70% as the mass ratio is

increased from .0037 to .045. The total collection is increased from 60% to 110% over the same range.

Pressure recovery measured is given in figure 76. The pressure recovery coefficient is defined as the exit pressure minus the expansion pressure divided by the inlet pressure minus the expansion pressure. For the shorter 2 inch separator the pressure rise above the separation pressure ranged from 1 to 33 psi, while for the longer 8 inch separator the range was about 1 to 7 psi.

As shown the recovery efficiency was relatively flat ranging from .12 to .1 over a gas flowrate range of 2 to 9 lb/s. The longer separator had a lower coefficient, about .06. Testing without liquid produced a coefficient of about .18.

CFD Analysis of Integral Separator Tests

A CFD analysis was performed of a CEESI test point to determine the agreement with prediction and to ascertain if any insight into the low separation efficiency.

Figure 77 shows the predicted pressure field for an inlet pressure of 715 psia and a flowrate of 8.8 lb/s. A radial gradient is established upon entering the vortex region. From that point the pressure remains constant until the flow enters the radial diffuser. The pressure slowly increases to the predicted outlet pressure of 790 psia, a pressure increase of 75 psi. In the test case the outlet pressure increase was 30 psi. Contributing factors to the shortfall include the finite nozzle entrances, which result in sudden expansion losses; the secondary separator porous wall, which produces additional wall friction; and flow separation.

Figure 78 plots the velocity field, both in magnitude and direction. As can be seen separation and flow reversal occur the radial diffuser passage producing uncertainties in the flow field and pressure recovery.

The radial pressure gradient in the vortex region is shown in figure 79. The pressure ranges from 710 psia at the inner wall to 760 psia at the outer, separation wall.

The temperature distribution is shown in figure 80. The lowest temperature of 34 F occurs in the initial separation region. The temperature is shown to gradually increase to 46 F as the flow is diffused to higher pressure at the outlet.

An important factor in the separation performance was identified by the CFD analysis. Figure 81 is a close up of the velocity field in the region of the capture slot. The arrow heads show the direction and magnitude of the local velocity. The recirculating flow field in the liquid collection chamber can be seen to produce a strong velocity field and flow reversal beginning at the lip where the separated liquid attempts to flow into the collection chamber. Since the liquid is released from the separation surface in a purely tangential direction the flow reversal could easily cause the liquid to re-enter the main flow stream.

The flow field can be modified by the installation of baffles to eliminate the re-circulation.

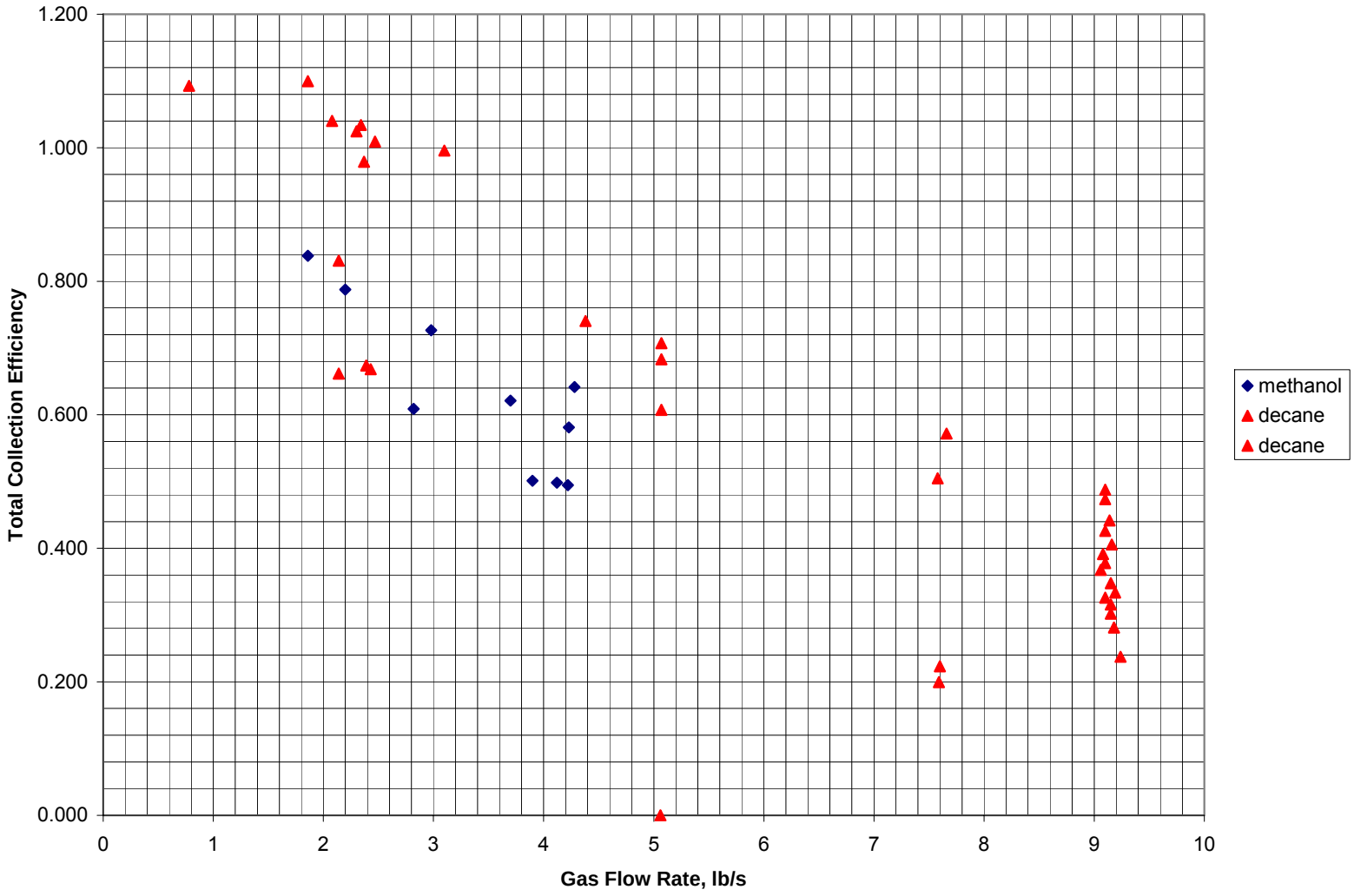

Figure 72 Liquid Collection Efficiency versus Gas Flowrate for All CEESI Test Data

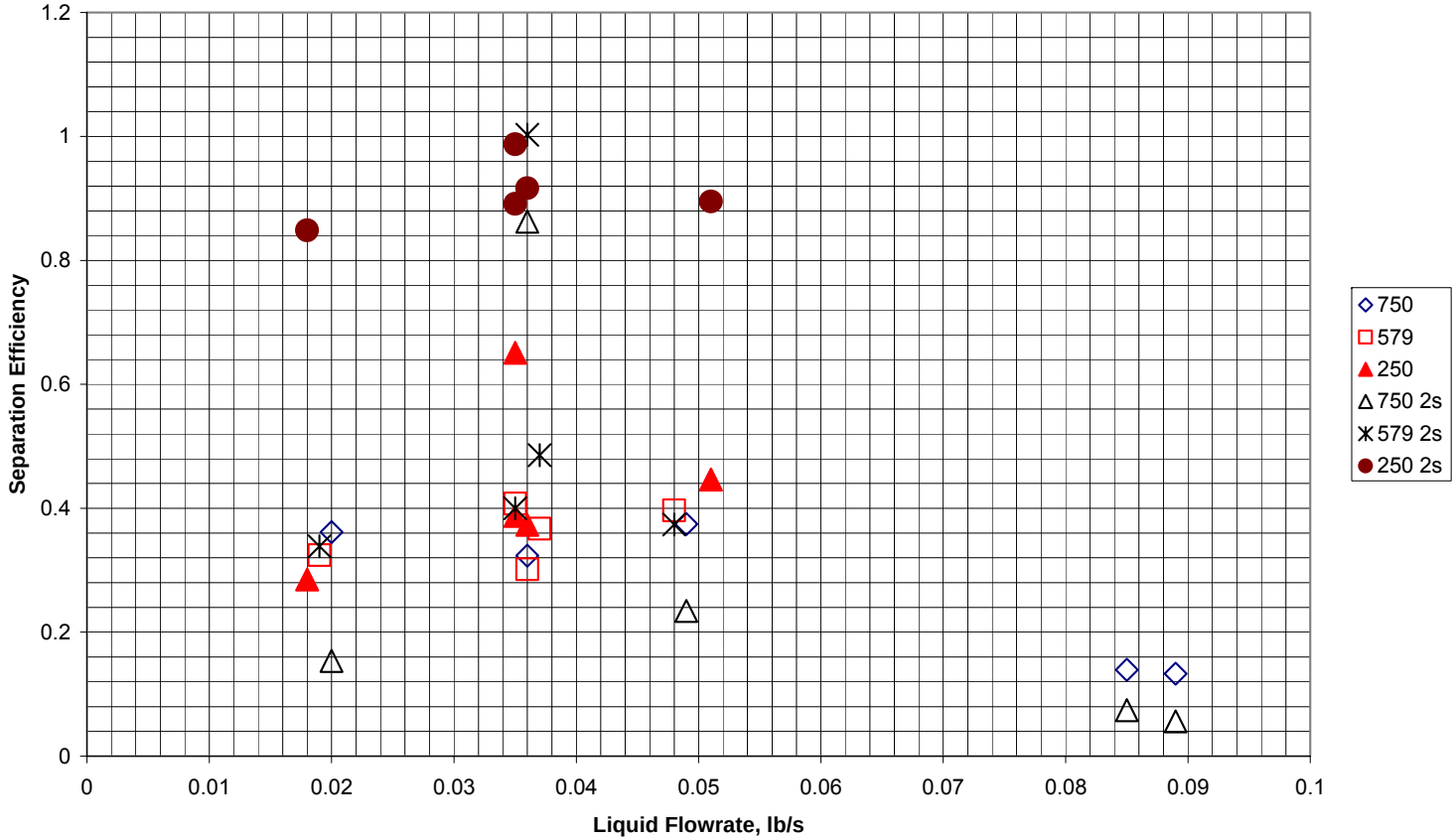

Figure 73 Separation Efficiency Versus Liquid Injection Flow for Integral Separator and for Cyclone Separator

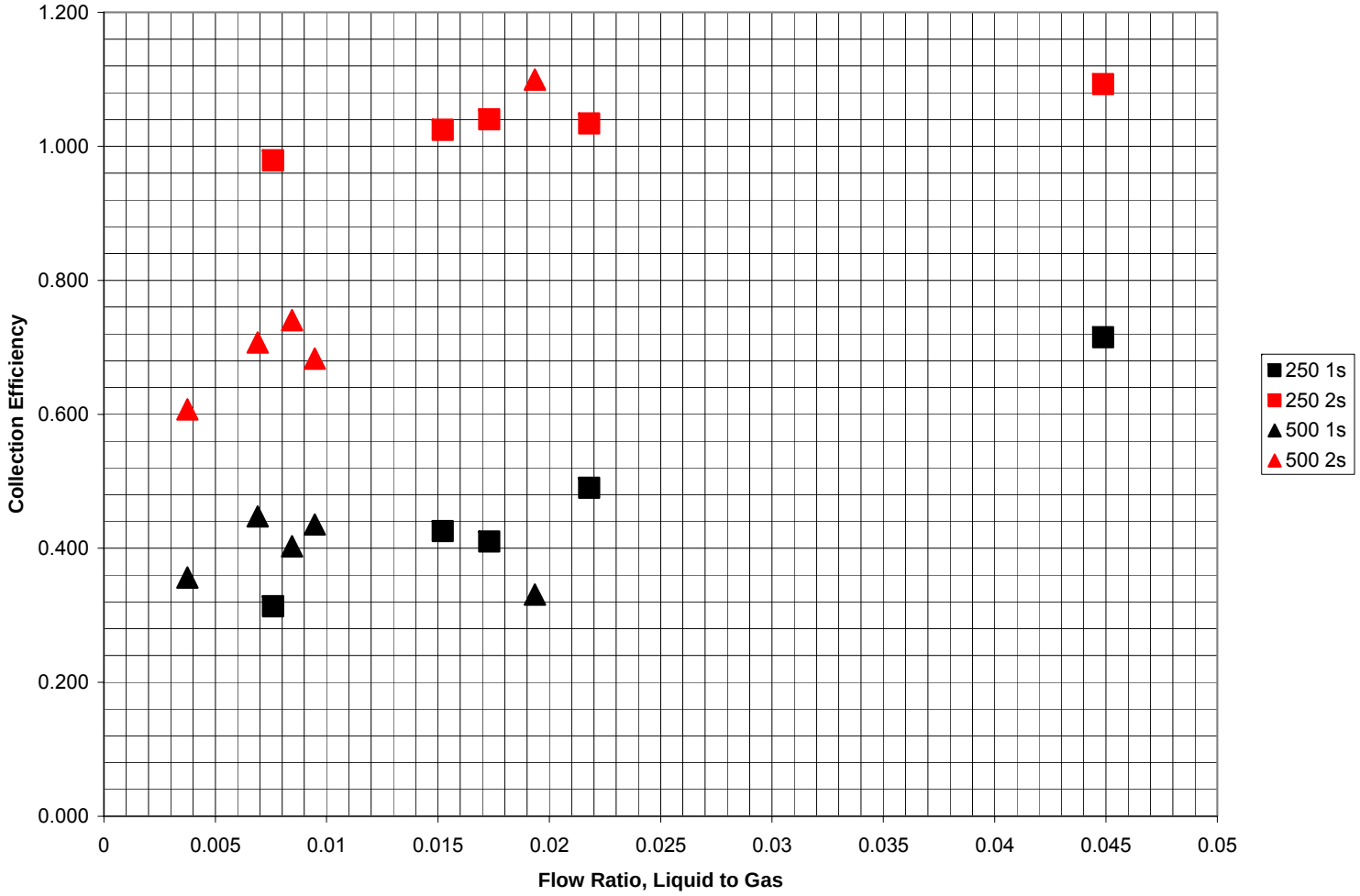

Figure 74 Separation Efficiency Versus Liquid to Gas Mass Flow Ratio for 250 psia and 500 psia Gas Pressure

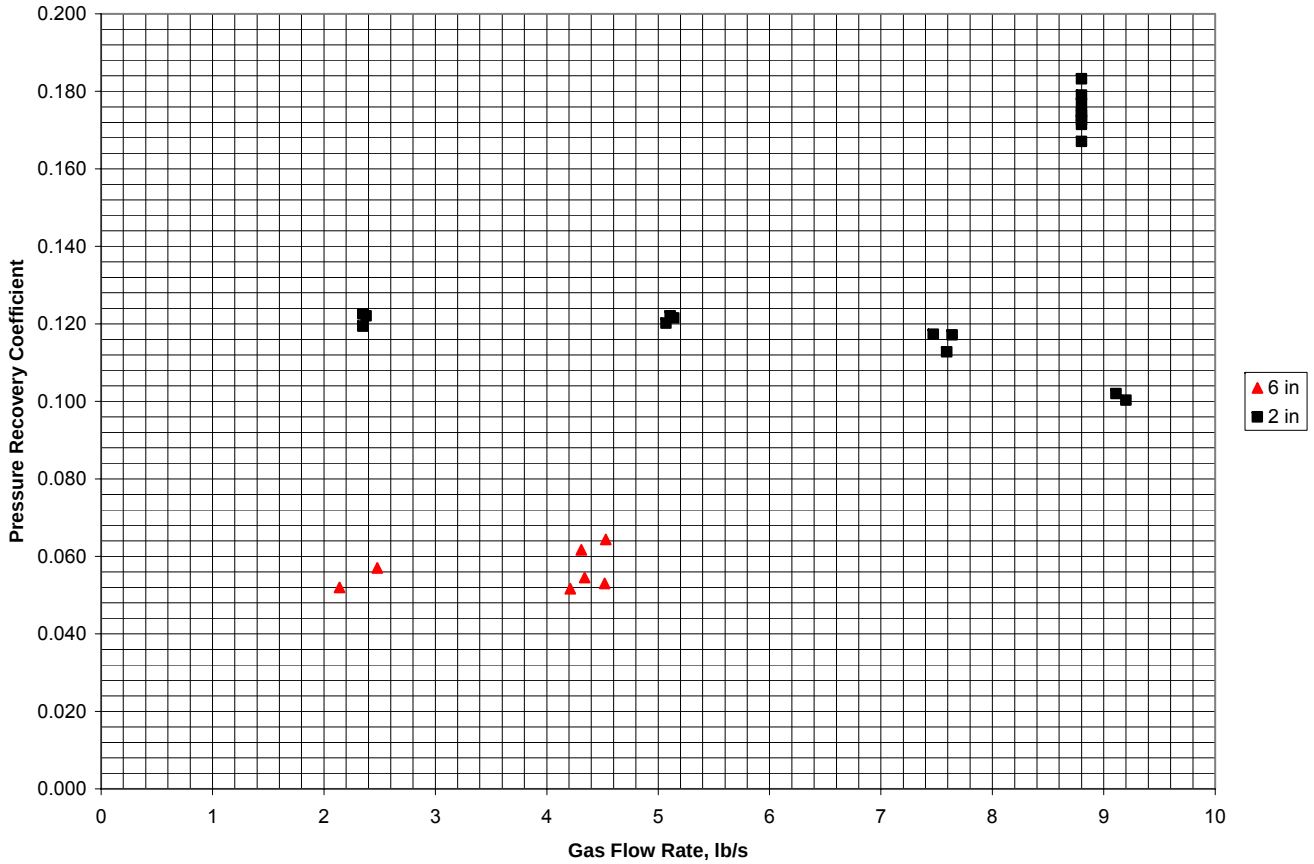

Figure 75 Pressure Recovery Coefficient Versus Gas Flowrate for Two Separator Lengths

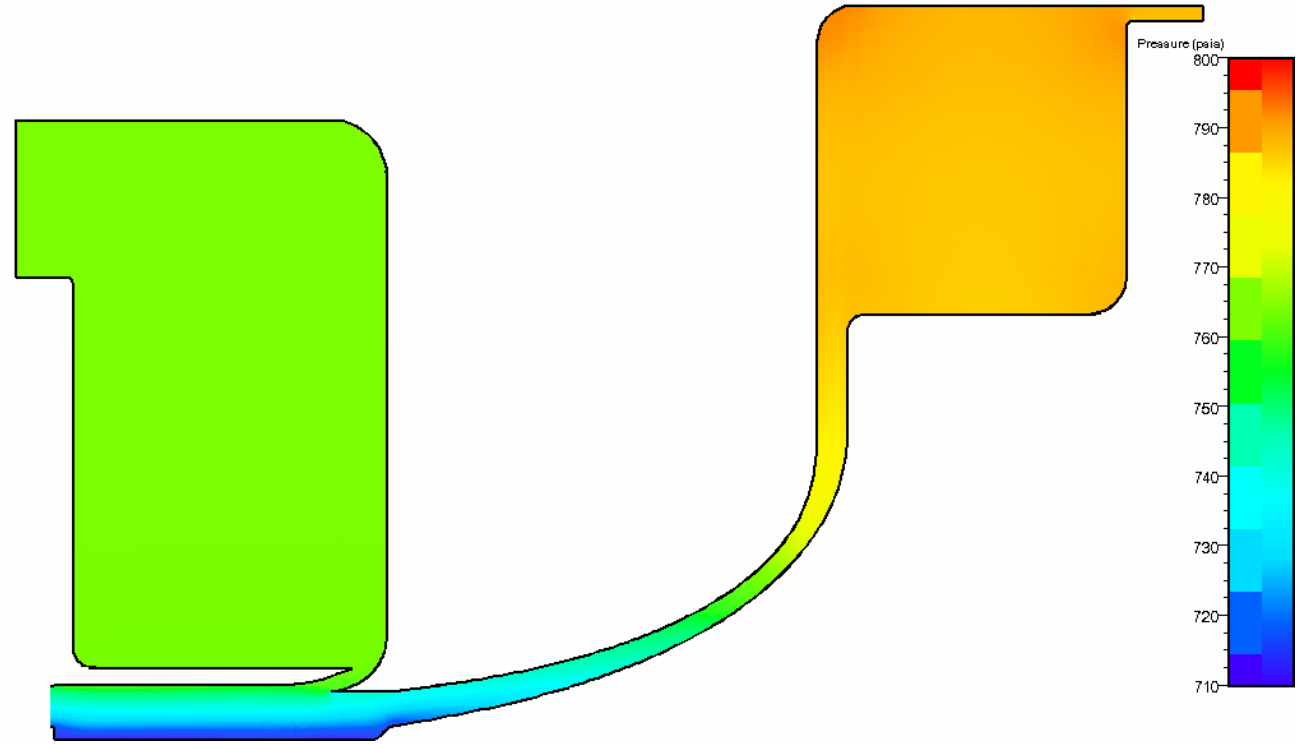

Figure 76 Calculated Pressure Field in Integral Separator for CEESI Test Conditions

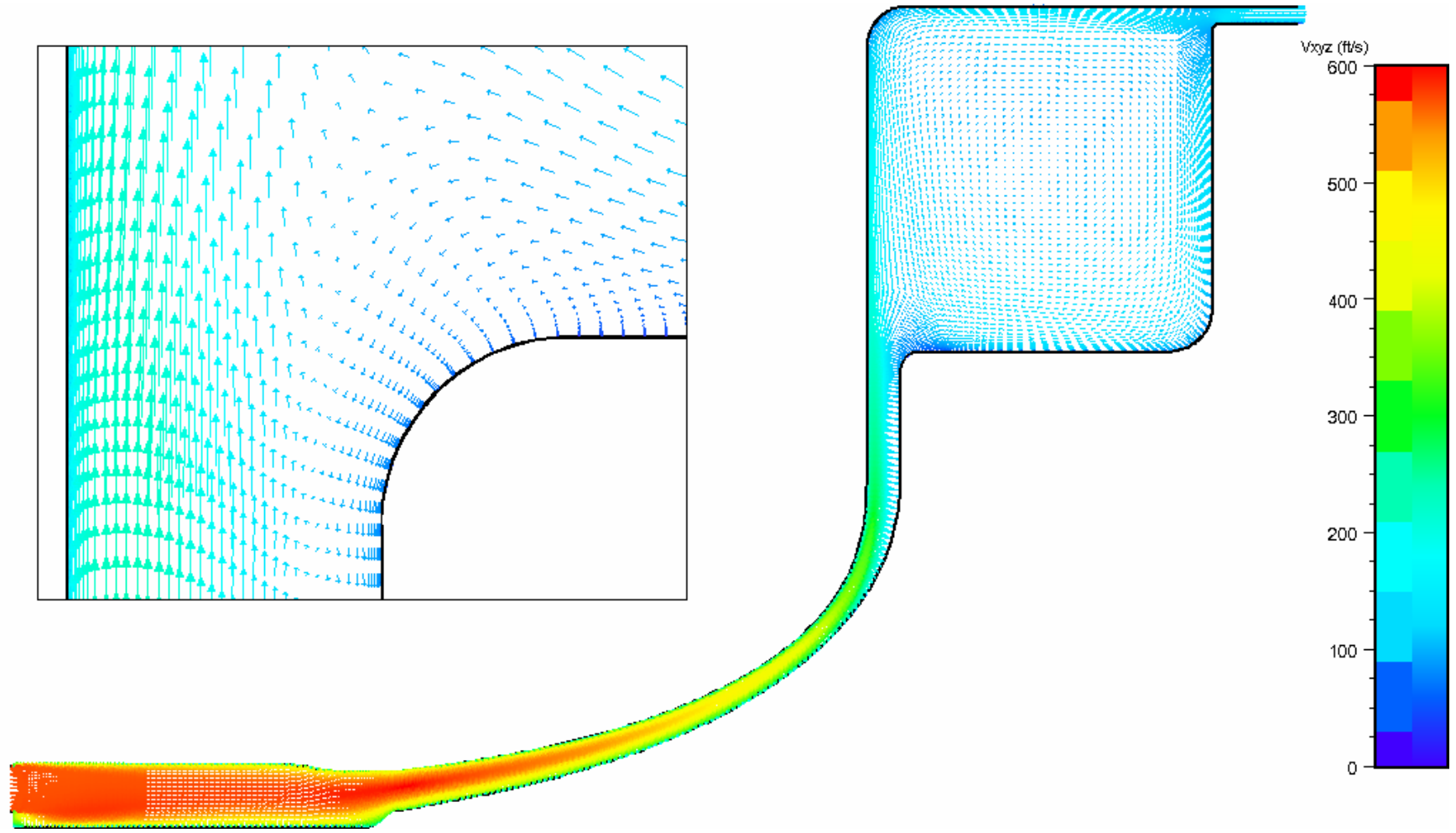

Figure 77 Calculated Meridonal Velocity Profile for CEESI Test Conditions

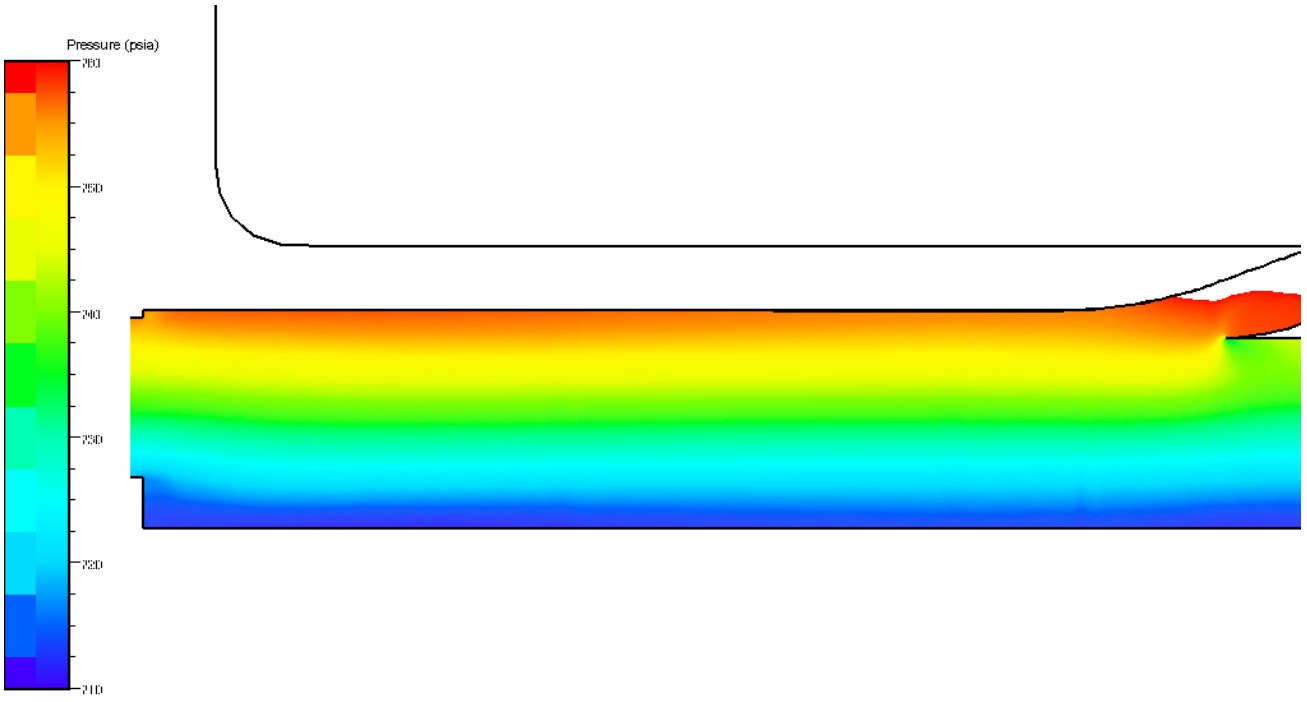

Figure 78 Calculated Radial Pressure Profile in Vortex Chamber for CEESI Test Conditions

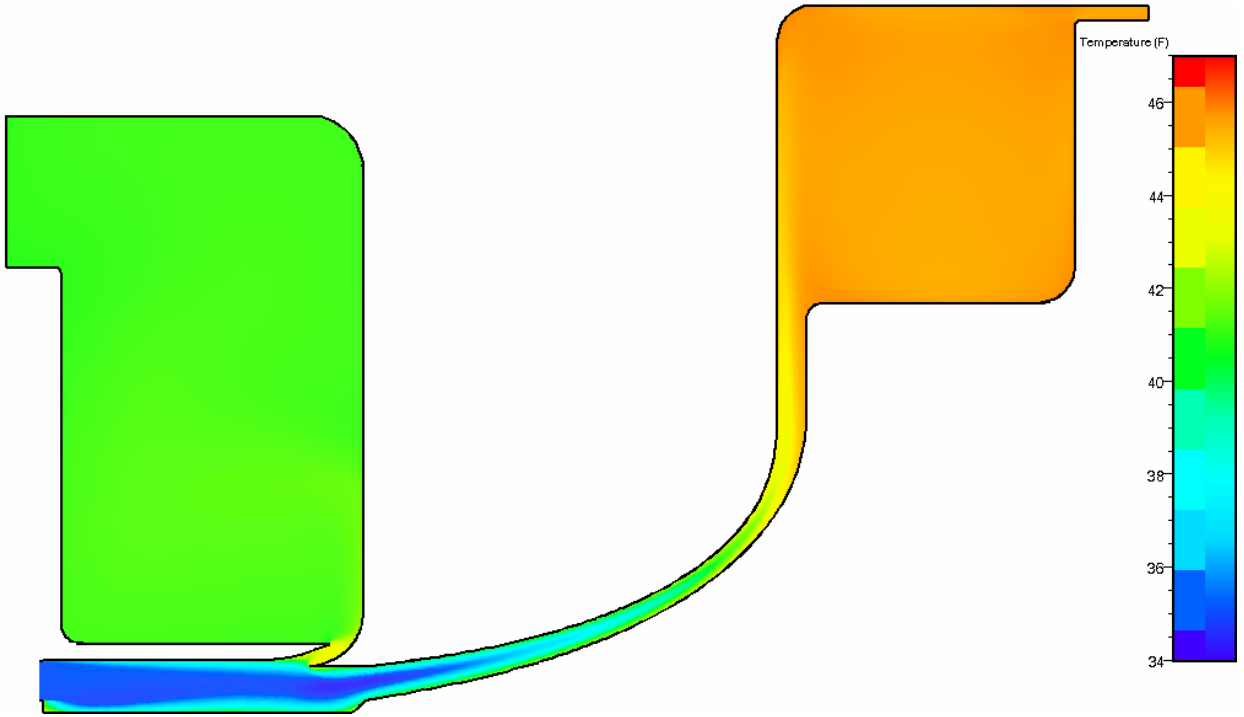

Figure 79 Calculated Temperature Field for CEESI Test Conditions

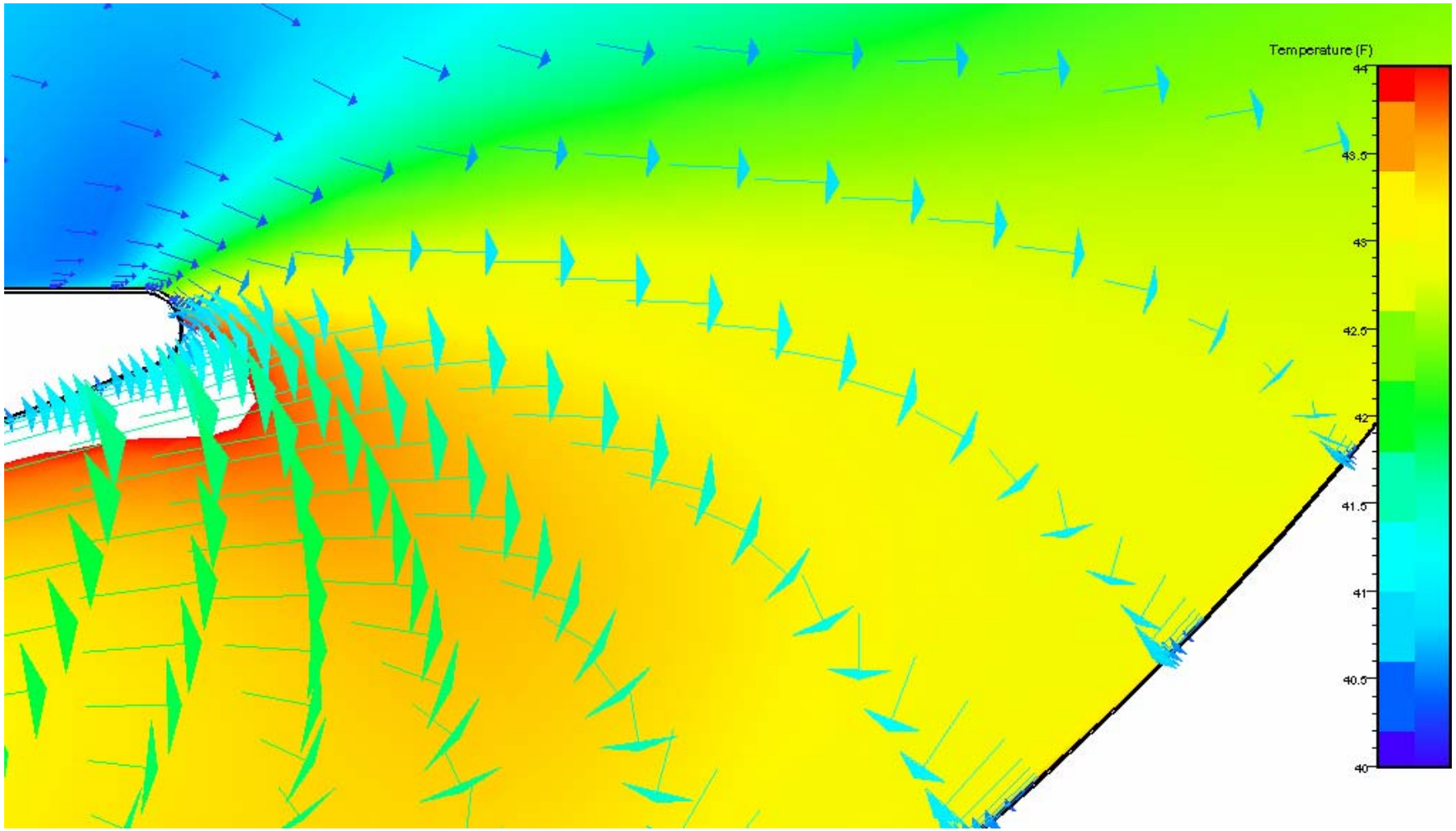

Figure 80 Calculated Local Velocity and Temperature Field in Region of Liquid Capture Slot

7. Market Study

A market study for the integral separator was carried out for Energent by Dawnbreaker Incorporated. The results show an extremely large market for major subsea resources with over 2,000 new subsea wells planned in the next several years. The intended application for remote and marginal production ties in well with petroleum industry needs. A summary of the study and findings is provided in Appendix C.

8. Conclusions and Recommendations

The results of integral separator air-water tests clearly demonstrated the viability of the integral separator concept and design approach. Complete separation and dewpoint reduction with a pressure increase in the dry gas was measured. Results agreed with CFD predictions within the error introduced by geometric simplification for the analysis.

Tests with high pressure gas were less successful. Liquid carryover from the integral separator as well as two facility separators at CEESI was observed at high gas pressure and flowrates. Analysis revealed secondary flow patterns and reverse velocities from the liquid capture passage which is a probable source of part of the liquid leaving the device. The higher gas dynamic forces and smaller gas-liquid density difference would aggravate any such effects compared to lower pressures.

Another probable source is the solubility of the solvent and the methanol used as seed liquids in the methane. References measuring solubility were found which predicted up to 100% absorption by the methane at the injection pressure. This would have been followed by dissolution at the lower expansion pressures, but with smaller, delayed spontaneous condensation droplets. The resulting small droplets would have been more difficult for the integral separator to separate as well as the facility separators. Results showed higher separation efficiency as more seed liquid was injected, possibly providing nucleation sites for even the absorbed liquid.

Improvement of the separation can be accomplished by baffles placed to interrupt the secondary flow pattern and prevent the ejection of separated liquid from the collection passage into the gas stream. One such baffle design is shown in figure 81. The baffle structure is placed to deflect the high velocity separated liquid back into the collection chamber where it can be drained to the collection vessel. This design also redirects the secondary gas flow.

Condensation of absorbed liquid seed as well as that of heavy components and water onto the liquid seed can be promoted by longer nozzles having greater flow residence time. A compact configuration can be maintained by using coaxial multiple nozzles which are curved at their exit to produce a tangential impingement. This design has been successfully applied to a rotating gas separator[8]. A preliminary design of this concept is provided in figure 82. Packaging multiple flow passages over the bulk of the expansion length avoids erosion problems that can result from turning vanes.

In order to implement and test these improvements a supplemental program is required.

[8] *Design Report for Inline Rotary Separator*, Douglas Energy Company, Placentia, California, Dec 1999

The program proposed is:

1. Design a multiple coaxial nozzle assembly to add to the existing multiple nozzle prototype integral separator. Test with air and water to establish exit flow pattern.

2. Design baffle assembly for liquid collection passage to be added to existing integral separator.

3. Assemble new components into existing integral separator. Add flow visualization and additional local instrumentation to assembly.

4. Test modified integral separator with high pressure gas. Employ methanol, glycol and recycled heavy hydrocarbons for seed gases. Test a wide range of liquid seed flowrate. Test three different nozzle lengths. Validate design relations.

5. Utilize design relations to select a beta site with Chevron. Establish commercial demonstration program and commercialization plan.

The estimated time required for this program is 8 months using existing equipment and test system built on phase II. Estimated cost is $250,000.

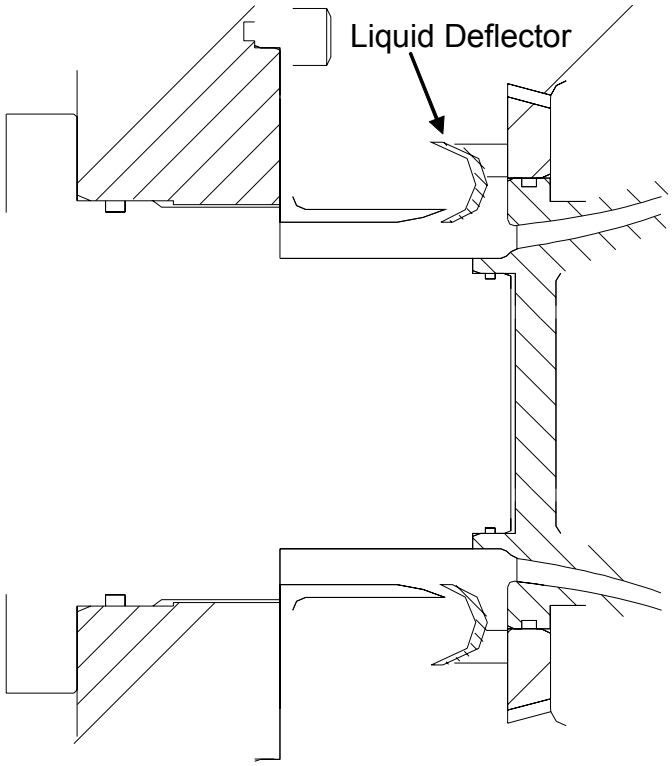

Figure 81 Schematic of Baffle to Direct Separated Liquid into Collection Chamber

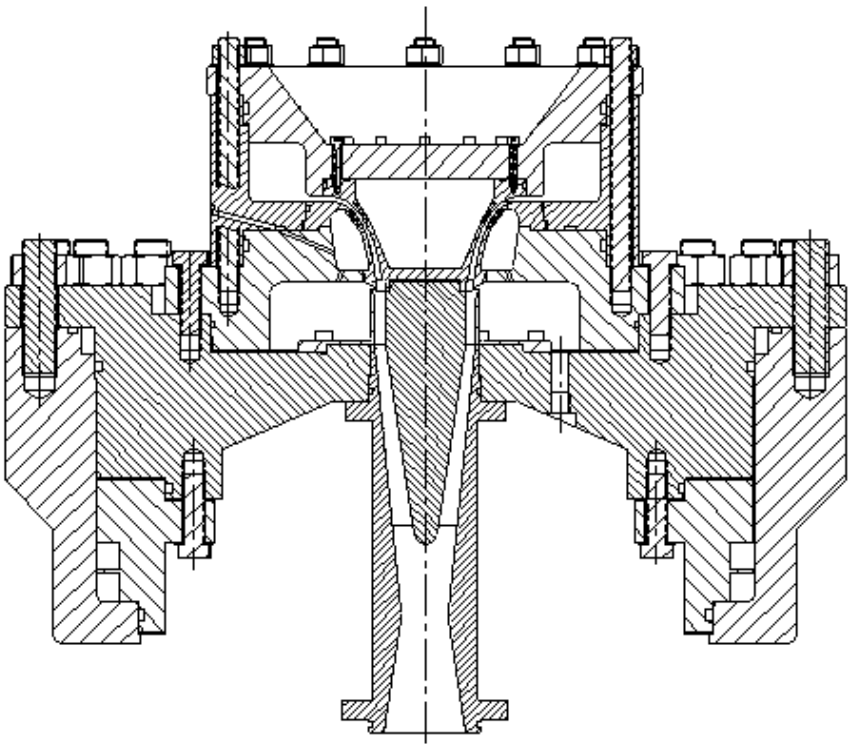

Figure 82 Schematic of Multiple Coaxial Nozzle Modification to Integral Separator

Appendix A
HYSYS Simulation of Subsea Dewpoint Control Application

Comp	inlet	Outlet	Water	wellhead	wellhead	Wellhead	Wellhead	Added	Nozzle	Nozzle	Nozzle
Mole Frac					cooled	Liq	gas	Liquid	Entrance	Exit	Liq
H2O	0	0	1	0.123262	0.123262	0.959106	7.08E-04	0	6.63E-04	6.63E-04	8.63E-03
CO2	0.133972	0.133972	0	0.117458	0.117458	6.98E-03	0.133657	0	0.125088	0.125088	7.14E-02
Nitrogen	3.17E-02	3.17E-02	0	2.78E-02	2.78E-02	2.09E-04	3.18E-02	0	2.98E-02	2.98E-02	1.09E-03
Methane	0.773407	0.773407	0	0.678075	0.678075	1.03E-02	0.775989	0	0.726239	0.726239	6.31E-02
Ethane	3.75E-02	3.75E-02	0	3.29E-02	3.29E-02	1.71E-03	3.75E-02	0	3.51E-02	3.51E-02	1.02E-02
Propane	1.19E-02	1.19E-02	0	1.04E-02	1.04E-02	1.32E-03	1.18E-02	0	1.10E-02	1.10E-02	6.37E-03
i-Butane	1.81E-03	1.81E-03	0	1.59E-03	1.59E-03	3.76E-04	1.76E-03	0	1.65E-03	1.65E-03	1.37E-03
n-Butane	2.69E-03	2.69E-03	0	2.36E-03	2.36E-03	7.18E-04	2.60E-03	0	2.43E-03	2.43E-03	2.96E-03
i-Pentane	9.90E-04	9.90E-04	0	8.68E-04	8.68E-04	4.81E-04	9.25E-04	0	8.65E-04	8.65E-04	1.78E-03
n-Pentane	7.80E-04	7.80E-04	0	6.84E-04	6.84E-04	4.63E-04	7.16E-04	0	6.70E-04	6.70E-04	1.80E-03
n-Hexane	6.80E-04	6.80E-04	0	5.96E-04	5.96E-04	8.24E-04	5.63E-04	0	5.27E-04	5.27E-04	2.73E-03
n-Heptane	9.10E-04	9.10E-04	0	7.98E-04	7.98E-04	1.99E-03	6.22E-04	0	5.83E-04	5.83E-04	4.47E-03
n-Octane	1.25E-03	1.25E-03	0	1.10E-03	1.10E-03	4.32E-03	6.22E-04	0	5.82E-04	5.82E-04	5.93E-03
n-Nonane	2.40E-03	2.40E-03	0	2.10E-03	2.10E-03	1.12E-02	7.69E-04	0	7.20E-04	7.20E-04	8.73E-03
Methanol	0	0	0	0	0	0	0	1	6.41E-02	6.41E-02	0.809397

Comp Mole Frac	Nozzle Vap	Diffused Noz Vapor	Pump Liquid	Rcycled Liquid	Pumped Liquid	Noz Vap + Liq	Compressor Inlet	Compressed Noz Vap	Dew Point Vapor	Dew Point
H2O	1.76E-06	1.76E-06	1.76E-06	8.63E-03	8.63E-03	8.63E-03	1.76E-06	1.76E-06	1.76E-06	1.76E-06
CO2	0.129542	0.129542	0.129542	7.14E-02	7.14E-02	7.14E-02	0.129542	0.129542	0.129542	0.129542
Nitrogen	3.22E-02	3.22E-02	3.22E-02	1.09E-03	1.09E-03	1.09E-03	3.22E-02	3.22E-02	3.22E-02	3.22E-02
Methane	0.781301	0.781301	0.781301	6.31E-02	6.31E-02	6.31E-02	0.781301	0.781301	0.781301	0.781301
Ethane	3.71E-02	3.71E-02	3.71E-02	1.02E-02	1.02E-02	1.02E-02	3.71E-02	3.71E-02	3.71E-02	3.71E-02
Propane	1.14E-02	1.14E-02	1.14E-02	6.37E-03	6.37E-03	6.37E-03	1.14E-02	1.14E-02	1.14E-02	1.14E-02
i-Butane	1.67E-03	1.67E-03	1.67E-03	1.37E-03	1.37E-03	1.37E-03	1.67E-03	1.67E-03	1.67E-03	1.67E-03
n-Butane	2.39E-03	2.39E-03	2.39E-03	2.96E-03	2.96E-03	2.96E-03	2.39E-03	2.39E-03	2.39E-03	2.39E-03
i-Pentane	7.90E-04	7.90E-04	7.90E-04	1.78E-03	1.78E-03	1.78E-03	7.90E-04	7.90E-04	7.90E-04	7.90E-04

n-Pentane	5.77E-04	5.77E-04	5.77E-04	1.80E-03	1.80E-03	1.80E-03	5.77E-04	5.77E-04	5.77E-04	5.77E-04
n-Hexane	3.44E-04	3.44E-04	3.44E-04	2.73E-03	2.73E-03	2.73E-03	3.44E-04	3.44E-04	3.44E-04	3.44E-04
n-Heptane	2.60E-04	2.60E-04	2.60E-04	4.47E-03	4.47E-03	4.47E-03	2.60E-04	2.60E-04	2.60E-04	2.60E-04
n-Octane	1.38E-04	1.38E-04	1.38E-04	5.93E-03	5.93E-03	5.93E-03	1.38E-04	1.38E-04	1.38E-04	1.38E-04
n-Nonane	5.52E-05	5.52E-05	5.52E-05	8.73E-03	8.73E-03	8.73E-03	5.52E-05	5.52E-05	5.52E-05	5.52E-05
Methanol	2.23E-03	2.23E-03	2.23E-03	0.809397	0.809397	0.809397	2.23E-03	2.23E-03	2.23E-03	2.23E-03

Compositions are above this line.

Material Streams are below this line

Name	inlet	Outlet	Water	wellhead	wellhead cooled	Wellhead Liq	Wellhead gas	Added Liquid	Nozzle Entrance	Nozzle Exit	Nozzle Liq
Vapor Fraction	1	1	0	0.894939	0.872126	0	1	0	0.929152	0.923334	0
Temp, Deg F	300	236.6805	300	224.4211	80	79.99963	79.9996327	75	75.24007	36.51694	36.51694
Pressure, psi	5000	1200	1200	1200	1200	1200	1200	1200	1200	800	800
Molar Flow, lbmole/hr	4.58E-02	4.58E-02	6.44E-03	5.22E-02	5.22E-02	6.68E-03	4.56E-02	3.12E-03	4.87E-02	4.87E-02	3.73E-03
Mass Flow, lb/hr	1	1	0.116	1.116	1.116	0.134938	0.98106214	0.1	1.081062	1.081062	0.126347
Liquid Volume Flow, bbl/day	0.173756	0.173756	7.96E-03	0.181714	0.181714	9.98E-03	0.1717354	8.61E-03	0.180341	0.180341	1.17E-02
Heat Flow, BTU/hr	-2256.69	-2256.69	-762.682	-3019.38	-3132.33	-811.229	-2321.1041	-324.321548	-2645.43	-2659.82	-388.838
Mass Entropy, BTU/lb-F	1.626417	1.748528	1.073067	1.680716	1.515286	0.679204	1.63028221	0.116048711	1.492085	1.493499	0.221395
Mass Enthalpy, BTU/lb	-2256.67	-2256.67	-6574.78	-2705.51	-2806.72	-6011.81	-2365.8856	-3243.18285	-2447.04	-2460.35	-3077.51
Vap. Fraction, Mass Basis	1	1	0	0.911227	0.879087	0	1	0	0.896723	0.883127	0
Vap. Fraction, Vol Basis	1	1	0	0.962565	0.945083	0	1	0	0.942191	0.935151	0
Vap. Fraction, Mole Basis	1	1	0	0.894939	0.872126	0	1	0	0.929152	0.923334	0
Molar Vol, ft^3/lbmole	1.648118	5.780348	0.317273	5.06628	3.421941	0.344405	3.87317125	0.647546393	3.555571	5.036729	0.692721

Actual Vol, bbl/day	0.322662	1.131653	8.73E-03	1.131302	0.764121	9.83E-03	0.75428538	8.64E-03	0.739868	1.048077	1.11E-02
Mol. Weight	21.83425	21.83425	18.0151	21.36349	21.36349	20.20048	21.5340166	32.04190063	22.20769	22.20769	33.85422
Surface Tension, dynes/cm	<empty>	<empty>	48.9117	<empty>	<empty>	<empty>	<empty>	29.7692296	<empty>	<empty>	<empty>

Name	Nozzle Vap	Diffused Noz Vapor	Pump Liquid	Rcycled Liquid	Pumped Liquid	Noz Vap + Liq	Compressor Inlet	Compressed Noz Vap	Dew Point Vapor	Dew Point
Vapor Fraction	1	1	0	0	0	1	1	1	1	1
Temp, Deg F	36.51694	76.99792	36.51694	36.51694	51.27674	36.51694	76.9979232	98.24541262	76.99792	29.7625
Pressure, psi	800	1051.011	800	800	1327.529	800	1051.0113	1200	1051.011	1051.011
Molar Flow, lbmole/hr	4.49E-02	4.49E-02	3.73E-03	0	3.73E-03	4.49E-02	4.49E-02	4.49E-02	4.49E-06	4.49E-06
Mass Flow, lb/hr	0.954715	0.954715	0.126347	0	0.126347	0.954715	0.95461956	0.954619557	9.55E-05	9.55E-05
Liquid Volume Flow, bbl/day	0.168646	0.168646	1.17E-02	0	1.17E-02	0.168646	0.16862886	0.168628858	1.69E-05	1.69E-05
Heat Flow, BTU/hr	-2270.98	-2258.27	-388.838	0	-387.155	-2270.98	-2258.0444	-2250.960476	-0.22583	-0.22848
Mass Entropy, BTU/lb-F	1.661849	1.666834	0.221395	0.221395	0.243041	1.661849	1.66683388	1.670168811	1.666834	1.612566
Mass Enthalpy, BTU/lb	-2378.68	-2365.36	-3077.51	-3077.51	-3064.19	-2378.68	-2365.3629	-2357.942294	-2365.36	-2393.16
Vap. Fraction, Mass Basis	1	1	0	0	0	1	1	1	1	1
Vap. Fraction, Vol Basis	1	1	0	0	0	1	1	1	1	1
Vap. Fraction, Mole Basis	1	1	0	0	0	1	1	1	1	1
Molar Vol, ft^3/lbmole	5.397421	4.499101	0.692721	0.692721	0.69754	5.397421	4.49910056	4.136456397	4.499101	3.724347
Actual Vol, bbl/day	1.037026	0.864429	1.11E-02	0	1.11E-02	1.037026	0.8643421	0.794672927	8.64E-05	7.16E-05
Mol. Weight	21.24065	21.24065	33.85422	33.85422	33.85422	21.24065	21.2406535	21.24065349	21.24065	21.24065
Surface Tension, dynes/cm	<empty>	<empty>	<empty>	<empty>	<empty>	<empty>	<empty>	<empty>	<empty>	<empty>

Material Streams are above this line

Energy Streams are below this line

Name	e2	e3	e6	e7	e10	e100
Heat Flow, BTU/hr	112.9562	14.39607	12.71355	7.083933	1.682513	2.65E-03

Energy Streams are above this line

Schematic is below this Line

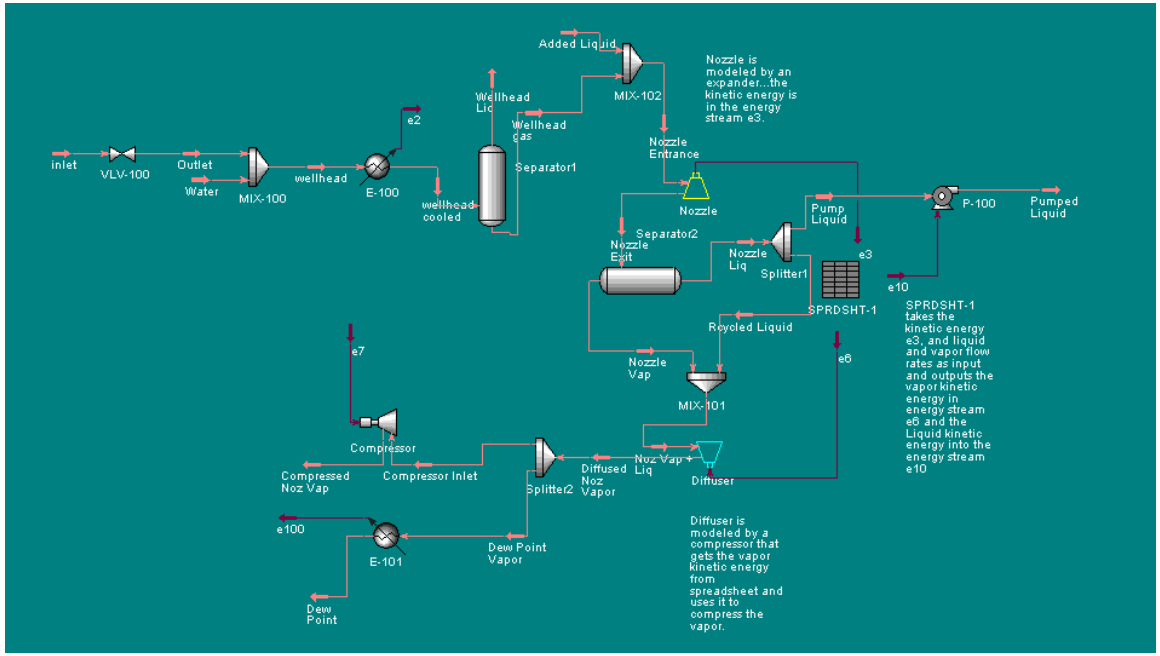

Schematic is above this line.

Appendix B
CFD Output Data for Air-Water Test Geometry

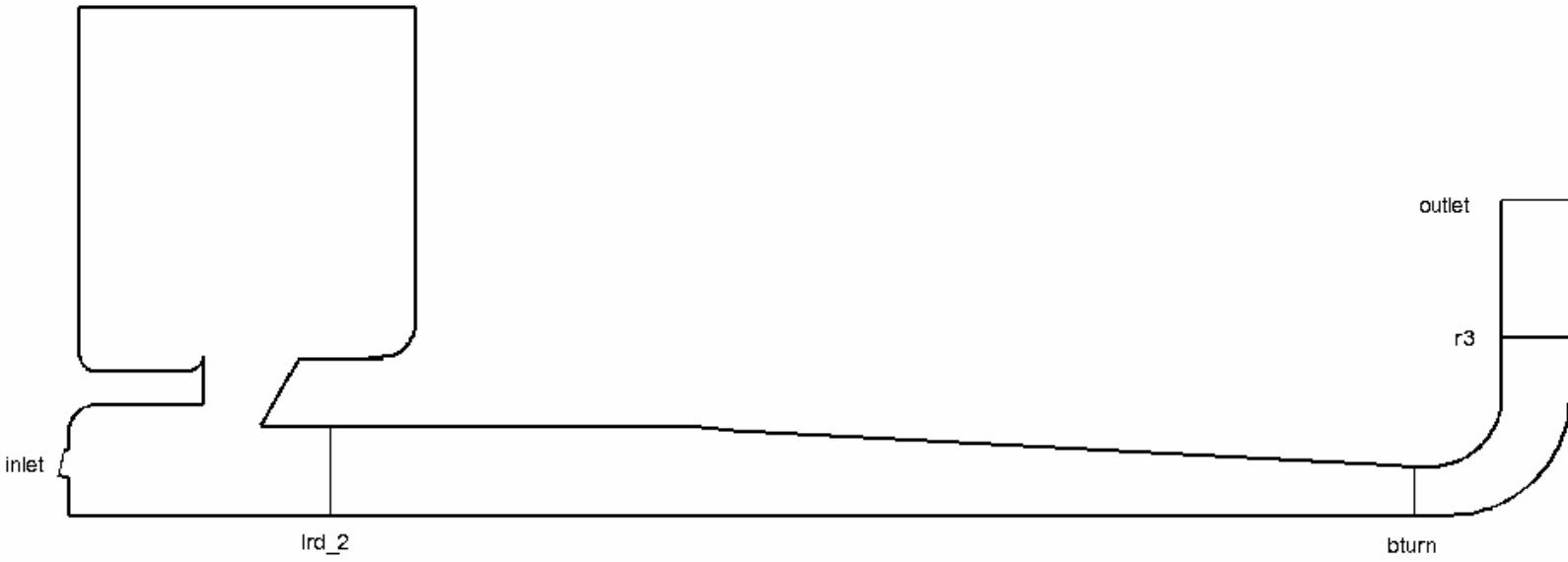

Project: F:/air_water_61/fmrd_gut_bend_a_614/fmrd_gut_bend_a_614_mt_ys_clen_cyl/
fmrd_gut_bend_a_614_mt_ys_clen_cyl.run
01/13/05 15:27:10

perfect gas
Specific_heat (cp) 0.2404 [Btu/(lbm F)]
Specific_heat_ratio 1.4000

block	name	imax	jmax	kmax	num_node	nperiod	RPM
1	fadm_inlet	25	33	2	1650	360	0
2	fadm_gg	25	81	2	4050	360	0
3	chbr_gg	41	73	2	5986	360	0
4	chbr_iarc_a	25	13	2	650	360	0
5	chbr_iarc_w	33	13	2	858	360	0
6	gut_inlet	45	81	2	7290	360	0
7	gut_marc_c	65	13	2	1690	360	0
8	gut_marc_h	25	17	2	850	360	0
9	gut_parc_c	37	13	2	962	360	0
10	gut_parc_h	25	13	2	650	360	0
11	gut_chbr	77	49	2	7546	360	0
12	chbr_ctw	25	57	2	2850	360	0
13	chbr_cylp	73	49	2	7154	360	0
14	chbr_bend	57	57	2	6498	360	0

total number of nodes: 48684

velocity components on surface (ft/sec)

surface	mfVr	mfVz	mfVm	mfVt	mfWt	mfV_
inlet	0.000	138.763	138.763	517.851	517.851	536.120
lrd_2	6.253	80.530	76.120	359.543	359.543	367.922
bturn	0.256	73.849	73.862	182.701	182.701	197.176
r3	43.121	2.858	43.234	117.385	117.385	125.474
outlet	32.271	-0.128	32.271	84.216	84.216	90.329

velocity angles (deg)

surface	mfAtan(Vt/Vr)	alpha_tr	mfAtan(Vt/Vz)	alpha_tz	mfAtan(Vt/Vm)	alpha_tc
inlet		74.999	74.999			
lrd_2		97.141	77.375			
bturn		67.914	67.991			
r3	70.297	69.829				
outlet	69.381	69.034				

Mach number

surface	V_Mach	VrMach	VzMach	VmMach	VtMach
inlet	0.4662	0.0000	0.1207	0.1207	0.4503
lrd_2	0.2794	0.0033	0.0319	0.0395	0.2756
bturn	0.1639	0.0002	0.0611	0.0611	0.1520
r3	0.1006	0.0310	0.0020	0.0310	0.0952
outlet	0.0731	0.0247	-0.0001	0.0247	0.0686

static variables

surface	tarea	tMassFlow	Pressure	mfTemp	Density	del mfEntropy
	in2	lbm/sec	psia	F	lbm/ft3	mBtu/(lbm F) (e-3)
inlet	0.906	-0.1249	29.865	90.00	0.1465	0.0000

lrd_2	3.120	-0.1160	29.720	96.05	0.1435	2.4684
bturn	1.615	-0.1131	29.676	106.10	0.1414	7.3718
r3	3.142	0.1121	29.912	108.49	0.1419	7.8508
outlet	3.927	-0.1120	30.000	109.24	0.1421	7.9657

total variables

surface mfTotalPress mfTotalTemp vfTotalPressDyn mfKineticEnergy mfKineticEnergy_t

	psia	F	psia	ft2/s2	ft2/s2
inlet	34.662	113.88	34.408	143712.148	134084.572
lrd_2	32.125	107.37	32.074	68092.195	65085.845
bturn	30.291	109.40	30.286	19847.658	17060.551
r3	30.156	109.81	30.155	7955.441	6936.364
outlet	30.127	109.93	30.127	4137.671	3585.786

massflowParameter inlet -0.1038 frac -0.69268

integral separator efficiency

inlet lrd_2 kinetic_t 0.48541

inlet bturn kinetic_t 0.12724

diffuser coefficients

		pressure	efficiency_h	enthalpy_isentropic	enthalpy
inlet	r3	0.00972	0.01325	0.01026	0.77396
bturn	r3	0.38286	0.53636	0.38757	0.72259
inlet	outlet	0.02817	0.03687	0.02970	0.80551
bturn	outlet	0.52681	0.56018	0.53274	0.95101

backflow_radial_parameter r3 0.00005

backflow_radial_parameter outlet 0.00004

Project: F:/air_water_61/fmrd_gut_bend_a_614/fmrd_gut_bend_a_614_mt_ys_clen_cyl/
fmrd_gut_bend_a_614_mt_ys_clen_cyl.run
01/13/05 15:27:10

perfect gas

Specific_heat (cp) 0.2404 [Btu/(lbm F)]

Specific_heat_ratio 1.4000

block	name	imax	jmax	kmax	num_node	nperiod	RPM
1	fadm_inlet	25	33	2	1650	360	0
2	fadm_gg	25	81	2	4050	360	0
3	chbr_gg	41	73	2	5986	360	0
4	chbr_iarc_a	25	13	2	650	360	0
5	chbr_iarc_w	33	13	2	858	360	0

6	gut_inlet	45	81	2	7290	360	0
7	gut_marc_c	65	13	2	1690	360	0
8	gut_marc_h	25	17	2	850	360	0
9	gut_parc_c	37	13	2	962	360	0
10	gut_parc_h	25	13	2	650	360	0
11	gut_chbr	77	49	2	7546	360	0
12	chbr_ctw	25	57	2	2850	360	0
13	chbr_cylp	73	49	2	7154	360	0
14	chbr_bend	57	57	2	6498	360	0

total number of nodes: 48684

velocity components on surface (ft/sec)

surface	mfVr	mfVz	mfVm	mfVt	mfWt	mfV_
inlet	0.000	138.763	138.763	517.851	517.851	536.120
lrd_2	6.253	80.530	76.120	359.543	359.543	367.922
bturn	0.256	73.849	73.862	182.701	182.701	197.176
r3	43.121	2.858	43.234	117.385	117.385	125.474
outlet	32.271	-0.128	32.271	84.216	84.216	90.329

velocity angles (deg)

surface	mfAtan(Vt/Vr)	alpha_tr	mfAtan(Vt/Vz)	alpha_tz	mfAtan(Vt/Vm)	alpha_tc
inlet		74.999	74.999			
lrd_2		97.141	77.375			
bturn		67.914	67.991			
r3	70.297	69.829				
outlet	69.381	69.034				

Mach number

surface	V_Mach	VrMach	VzMach	VmMach	VtMach
inlet	0.4662	0.0000	0.1207	0.1207	0.4503
lrd_2	0.2794	0.0033	0.0319	0.0395	0.2756
bturn	0.1639	0.0002	0.0611	0.0611	0.1520
r3	0.1006	0.0310	0.0020	0.0310	0.0952
outlet	0.0731	0.0247	-0.0001	0.0247	0.0686

fmrd_gut_bend_a_614_mt_ys_clen_cyl.run

static variables

surface	tarea	tMassFlow	Pressure	mfTemp	Density	del mfEntropy
	in2	lbm/sec	psia	F	lbm/ft3	mBtu/(lbm F) (e-3)
inlet	0.906	-0.1249	29.865	90.00	0.1465	0.0000
lrd_2	3.120	-0.1160	29.720	96.05	0.1435	2.4684
bturn	1.615	-0.1131	29.676	106.10	0.1414	7.3718
r3	3.142	0.1121	29.912	108.49	0.1419	7.8508
outlet	3.927	-0.1120	30.000	109.24	0.1421	7.9657

total variables

surface	mfTotalPress	mfTotalTemp	vfTotalPressDyn	mfKineticEnergy	mfKineticEnergy_t
	psia	F	psia	ft2/s2	ft2/s2
inlet	34.662	113.88	34.408	143712.148	134084.572
lrd_2	32.125	107.37	32.074	68092.195	65085.845
bturn	30.291	109.40	30.286	19847.658	17060.551
r3	30.156	109.81	30.155	7955.441	6936.364
outlet	30.127	109.93	30.127	4137.671	3585.786

massflowParameter inlet -0.1038 frac -0.69268

integral separator efficiency

inlet	lrd_2	kinetic_t	0.48541
inlet	bturn	kinetic_t	0.12724

diffuser coefficients

		pressure	efficiency_h	enthalpy_isentropic	enthalpy
inlet	r3	0.00972	0.01325	0.01026	0.77396
bturn	r3	0.38286	0.53636	0.38757	0.72259
inlet	outlet	0.02817	0.03687	0.02970	0.80551
bturn	outlet	0.52681	0.56018	0.53274	0.95101

backflow_radial_parameter r3 0.00005

bac

Appendix C
Market Study

Research and Development of an Integral Separator for a Centrifugal Gas Processing Facility

Market Research Report

Prepared for
Energent

April 26, 2005

Prepared by

Jenny C. Servo, Ph.D.
Theresa Kingston

DAWNBEAKER ®
2117 Buffalo Road, Suite 193
Rochester, NY 14624
(585)594-0025

Table of Contents

Introduction

The purpose of this ***Market Research Report*** is to provide relevant information that will assist **Energent** in determining the best strategy for commercialization of the **centrifugal gas processing facility (CENGAS)** technology. This is a preliminary assessment and is intended to both compliment and augment information that you have regarding the commercial potential for the DOE funded technology.

1.0 Market Pull

1.1. Market need

A recent compilation of natural gas reserves indicates that there are 302 trillion cf for North America and 4,947 trillion cf for the World. 60% of the World's reserves are classified as *stranded* or *remote* in subsea and offshore reserves that are difficult to access due to high cost and complexity of processing equipment required to lower the dewpoint, separate liquids and compress the gas for transportation to a point of use. Natural gas must be compressed at high pressure before it can be transported by pipeline. The transport of compressed gas by ship has been so far rejected for economic and safety reasons. For pipeline transport, the transport specifications are aimed at preventing the formation of a liquid phase, the clogging of the line by hydrates, and excessive corrosion. To put this in perspective, in the Gorgon Project, a subsea development planned off the coast of Australia, the presence of both water and CO2 producing carbonic acid, requires expensive “duplex” alloy piping for corrosion resistance which will add $3/4 to $1B to the project.

Mature gas processing technologies have been developed to remove moisture for conventional applications (glycol dehydration, amine sweetening, lean oil absorption, solid bed adsorption and the use of turbocompressors for dewpoint control and natural gas liquids removal). However, these processes have features that limit their application in subsea and remote resources. Specifically, the available equipment has a large footprint, volume, and weight: large energy consumption; complex control and batch requirements; reliability and maintainability requirements for turbocompressors. A typical adsorption plant for 745,000 lb/h of gas, may require a space of 460 sq ft for major components, weigh 190 tonnes and require 15 MMB/h of energy for regeneration. With industry estimated costs for standard platforms of 100,000 per tonne, minimizing the weight and footprint of processing equipment is highly desirable.

Improvements in size, weight, reliability, and cost are vital for utilization of future gas resources and must be capable of subsea and unmanned operation. The goal is to produce a compact unit that would simultaneously reduce the dewpoint and separate and remove the liquids generated. (Integral Separator)

Energent is developing a centrifugal gas processing facility (CENGAS) that utilizes high separation and purification forces achieved by centrifugal forces in the flow to achieve

higher throughput and more compact equipment. One of the components of the CENGAS facility is the ***Integral Separator*** which is the subject of this Phase II proposal. The Integral Separator is a compact gas-liquid separator which divides all of the centrifugal forces and re-compression energy from the flow swirl created by the two-phase expansion.

For the subsea application, end-users are looking to decrease the cost of the transmission pipes from subsea wells by removal of water prior to transmission which means that they could use less expensive pipes. Specifically, "the presence of both water and CO2, producing carbonic acid, requires expensive "duplex" alloy piping for corrosion resistance. Subsea removal of water and liquids and compression would result in a cost savings of $3/4 to $1B by enabling the use of carbon steel piping instead of the more expensive duplex piping. A reduction of capital cost (CAPEX) of this magnitude would result in a substantial reduction in the gas production cost and would accelerate the development of that resource. Also of importance are the reduction in footprint and weight, ability to separate and remove the liquids generated at the subsea level

1.2. SBIR Project and Expected Outcomes

The Integral Separator is one of three components of the CENGAS facility. Its functions are to (1) lower the temperature of the gas stream by near isentropic expansion in order to condense out natural gas liquids and water, (2) Separation of the liquids from the gas using a moving liquid separation surface driven by the flow swirl, and (3) re-compression of the separated gas using the flow swirl and a radial diffuser to provide a high pressure for transport in a pipeline. Methanol or another hydrate inhibitor can be injected in the Integral separator nozzles to enable expansion to sub-freezing temperatures without hydrate formation.

The process begins with the well flow, “inlet”. The flow is throttled to the desired inlet pressure through valve “VLV-100”. Water is mixed, “MIX-100” to ensure that the gas is saturated with water vapor. The flow is cooled or heated by an exchanger, “E-100”, to set the required inlet temperature. The free liquids are separated at the higher inlet temperature in “Separator 1” to minimize the amount of hydrate inhibitor that must be injected to prevent hydrate formation at the lower expansion temperature.

The saturated gas stream flows to the Integral Separator mixer, “MIX-102”, where the seed liquid “Added Liquid” is injected. The mixture is expanded in the two-phase nozzle, “Nozzle”. The nozzle is modeled with an expander module in HYSYS where the input efficiency is the value calculated with the nozzle code.

The value proposition for energy companies involved with offshore and subsea extraction of natural gas is that they could drastically reduce the costs of a project (potentially by up to a billion dollars), if they could remotely and automatically extract the water from the wet gas at the subsurface level. This ability would enable the energy company to use a less expensive piping to transport that natural gas as the concern for the corrosive effect of water in the wet gas would be minimized.

1.3. Impact

Until there are cost effective, alternative forms of energy the US will continue to be dependent upon natural gas and oil. A recent compilation of natural gas reserves give 302 trillion cf for North America and 4,947 trillion cf for the World. Of these, 60% are considered remote or "stranded". Use of techniques and products such as those proposed by Energent will result in economically making these remote or stranded assets available.

2.0 Industry Trends

Before examining the potential opportunity for Energent's integral separator in subsea applications, an overview will be provided of the natural gas industry with special emphasis placed on offshore reserves and associated processing of natural gas. As this industry is global, information will be included that reflects the composition of this industry but with special emphasis placed on the US.

2.1 Structure of the industry

The top publicly integrated oil and gas companies with valuation caps exceeding $100 billion are referred to as the *"super majors"* and include The Royal Dutch/Shell Group and the Exxon/Mobil Group. Globally, the top private companies are Saudi Aramco of Saudia Arabia and PDVSA of Venezuela. US major integrated oil and gas companies include Amerada Hess Corporation, Occidental Petroleum, and Conoco Phillips.[9]

Company	Earnings 2004
Amerada Hess Corporation	$14,311 (In Millions)
Anadarko Petroleum Corporation	$1.6 billion
Apache Corporation	$1.7 billion
BP p.l.c. (only U.S. operations included)	
Burlington Resources, Inc.	
Chesapeake Energy Corporation	$2,709 Million
ChevronTexaco Corporation	$13.3 billion
ConocoPhillips Inc.,	
Devon Energy Corporation	$2.2 billion
Dominion Resources, Inc.	$1.249 billion
EOG Resources, Inc.	$614.0 million
Equitable Resources Inc.	$108.1 million
Exxon Mobil Corporation	$25,330 million
Kerr McGee Corporation	$404.0 million
Lyondell Chemical Company	$5,968 million
Marathon Oil Corporation	$1.261 billion
Occidental Petroleum Corporation	$2.491 billion
Premcor Inc.	$165.2 million
Royal Dutch/Shell Group (only U.S. operations included)	$18.5 billion
Sunoco, Inc.	
Tesoro Petroleum Corporation	
Unocal Corporation	$1.21 billion
Valero Energy Corporation	$1.21 billion
Williams Companies, Inc.	$1.21 billion
XTO Energy, Inc.	$1,947,601 million

[9] Kerr-McGee Corp (NYSE:KMG)

Within the US, independent gas producers are responsible for over 82% of overall domestic natural gas production. Furthermore, 90% of the wells in the US are drilled by independent producers and produce 82% of the nation's natural gas. Moreover, they play a major role in Federal Offshore activities, accounting for nearly 80% of the Gulf of Mexico's shallow water leases, and 50% of deepwater leases. [10]

Independent Producers At-a-Glance...

Number of Independents.....5,000
Avg. Number of Employees.....12
Avg. Age of Business.....23 years
Percent of U.S. Wells Drilled.....90%
Operating on Federal Onshore Land.....49%
Operating Internationally.....11.6%

Total Independents' Percent of U.S. Natural Gas Production.....82%
Total Independents' Percent of U.S. Oil Production.....68%

Public vs. Private Independents: Publicly traded independents account for 23% of oil and 32% of natural gas production. Private independents account for 45% of oil and 50% gas production. (source: DOE).

Offshore: Independents hold 80% of the Gulf of Mexico shallow water leases and 50% of deepwater leases. At the last four lease sales, independents had the majority of high lease bids.

The number and type of entities involved with the natural gas industry is depicted below. [11]As mentioned at the outset the part of this process of greatest interest is "Processing". The specific challenge to be explored is referred to as subsea processing as a means of creating pipeline quality dry natural gas.

Producers	Over 8,000 in the U.S. ranging from integrated producers to small one-person operations.
Processing	In the U.S. there are over 580 natural gas processing plants.
Pipelines	There are an estimated 160 pipeline companies in the U.S. Together, they operate over 285,000 miles of pipe. Of this, nearly 180,000 miles consists of interstate pipelines.
Storage	In the U.S. there are 114 natural gas storage operators, which have control over 415 underground storage facilities. The facilities maintain storage capacity of 3,923 Bcf of natural gas and deliver a daily average of 78Bcf per day.
Marketing	In 2,000, there were 260 companies engaged in the marketing of natural gas. Nearly 80% of al the natural gas supplied that year passed through the hands of these natural gas marketers.
Local Distribution Companies	In the U.S. there are over 1,200 natural gas distribution companies, with ownership of over 833,000 miles of distributed pipe.

[10] 2005 Oil and Natural Gas Issues Briefing Book. The Independent Petroleum Association of America. 2005 http://www.ipaa.org/info/2005BriefingBook.pdf
[11] Natural Gas. www.naturalgas.org/business/industry.asp0

Natural gas processing involves the treatment of raw gas in order to meet *sales quality gas specifications.* "Natural gas, as produced from underground formations, is a mixture of methane and other gases, which can include natural gas liquids (NGLs), water vapour, inert gases, CO2, and H2S. For the raw gas to be moved onto a gas transmission system, it must be processed to meet the sales quality specifications of the transmission system. In general, the water vapour, CO2 and H2S must be removed as well as some of th NGLs such that the sales quality is composed mainly of methane and small amount of NGLs."[12] Raw gas is collected from producing wells through a pipeline network or gathering system which moves the gas to a gas processing plant.

2.2. US legislation

Federal, Interstate, and Inter-Government agreements have a profound effect on the development of natural resources. This is clearly evident in testimony such as that made on April 19, 2005 before the Senate Committee on Energy and Natural Resources by Charles Davidson on behalf of the Independent Petroleum Association of America and other organizations. Mr. Davidson indicated that the United States was the only developed country in the world with a blanket moratoria that made the coastal areas off limits to energy development starting in 1981. Mr. Davidson asked that in formulating the policies for the future that the advances made in offshore energy activity be considered. He highlighted a number of advances: (1) the ability to more readily find resources using 3-D seismic and visualization technologies, (2) a decrease in the number of wells need in both exploration and development of those resources due to advances in drilling – specifically directional, horizontal, extended reach, and multi-lateral drilling, (3) decreases in the need for surface facilities due to advances in subsea facilities – specifically subsea tiebacks to central manifolds, which cover 20-30 miles and allow producers to make use of a single production platform such as the Ticonderoga, (4) decreases in the visibility of operations also effected by subsea operations, and (5) care and compatibility with the environment.

Davidson maintains that the more we explore the more convinced we are that there is more natural gas available in locations that are currently under the moratoria.[13] The IPAA maintains that 2/3 of known reserves in the US are still untapped.

[12] Overview http://ww.lorngl.com/operations/

[13] Statement of Charles Davidson, Chairman, President and CEO, Noble Energy Inc. Before the Senate Committee on Energy and Natural Resources, April 19, 2005.

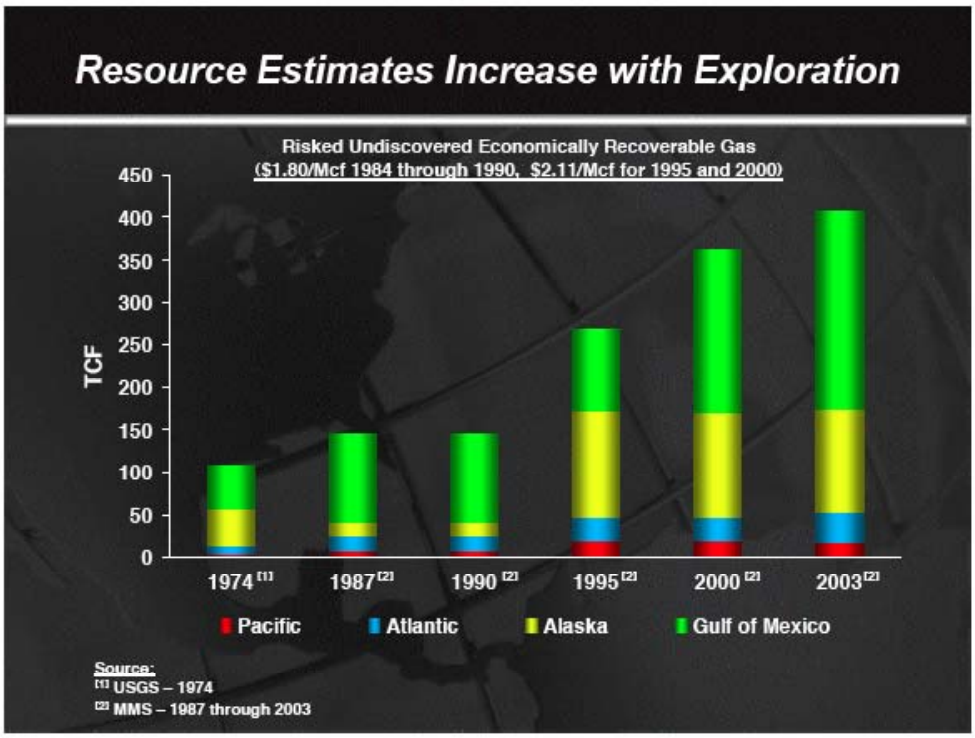

Lee Fuller in his testimony on behalf of the Independent Petroleum Association of America before the Committee on Energy and Commerce on February 16, 2005 indicated that the ability to develop these national resources is dependent upon access to federal lands, both onshore and offshore. Currently, access is constrained by a myriad of leasing and permitting restrictions. [14] He maintained that given the significant resources on the Outer Continental Shelf lands currently off limits by congressional and Executive Branch moratoria to exploration, development and production of natural gas and crude oil, Congress should put in place a process to being lifting of moratoria and allow states to share in revenues generated by federal lease bonuses and royalties in proportion to the amount of leasing and production that occurs off their coasts. In addition, the Administration's budget proposal for FY'06 eliminates all federal funding of oil and natural gas technology and regulatory evaluation programs. Fuller maintained the importance of continuing oil and gas R&D programs.

2.3. The Federal Energy Regulatory Commission (FERC)

Although FERC does not directly regulate gas producers, its regulatory activities do indirectly affect gas producers. [15] FERC regulates interstate and intrastate gas pipelines

[14] Testimony of Lee Fuller on behalf of the Independent Petroleum Association of American before the Committee on Energy and Commerce on February 16, 2005.
[15] White Paper: FERC Regulation of Gas Transmission Lines: Implications for Gas Quality Variances. September 30, 1998

and must assure that all shippers (producers) must have access to the same services, specifications, and rates. The implication is that a pipeline company may not relax its standards to one customer, without relaxing them for all. Gas pipeline companies can grant variances to their requirements for pipeline gas quality (for example, more or less condensate). However, FERC regulations requires that if such variances are granted to one of a pipeline company's customers, it must be granted to all others to avoid potential liability.

2.4 World's natural gas reserves

Proven natural gas reserves are steadily increasing. According to data reported in the *Oil & Gas Journal* in 2004 worldwide reserve estimates were 6,076 trillion cubic feet.[16] According to the Energy Information Administration (EIA) the developing world accounted for virtually all the increase in proved reserves. Almost three-quarters of the world's natural gas reserves are located in the Middle East and Eastern Europe and the Former Soviet Union (EE/FSU) with Russia, Iran, and Qatar combined accounting for about 58% of the total. [17]

Figure 39. World Natural Gas Reserves by Region as of January 1, 2004

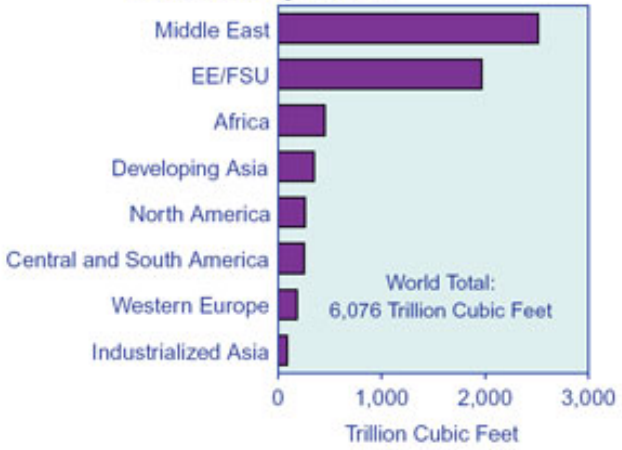

In 2003, the greatest regional increase (23%) in upstream gas development came from Sub-Sahara Africa. There was also a 13.8% increase in natural gas production in the

[16] International Energy Outlook 2004. EIA
[17] The following figure is taken from the preceding report

Middle East and 6% increase from Latin America.[18] The following figure shows Gas Development Projects by Region[19].

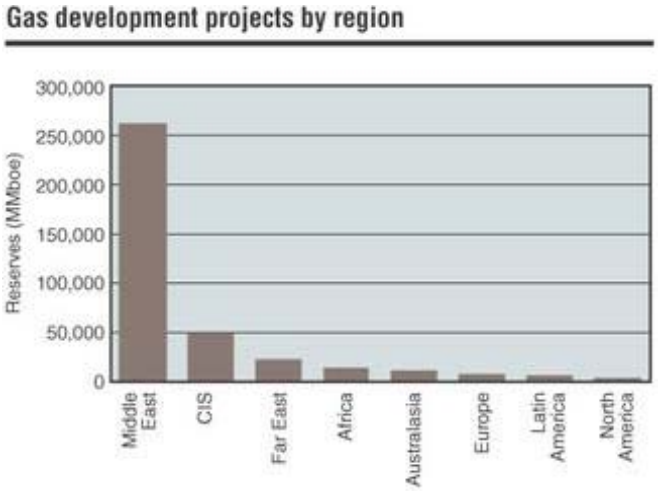

2.5 North America

The United States holds 3.1% of the world's natural gas reserves. Presently North America produces approximately as much natural gas as it consumes. The North American gas market is tightly integrated with Canada supplying the bulk of US imports and the US supplying imports to Mexico. Total natural gas imports are projected to supply 21% of total US natural gas consumption in 2010 and 23% in 2025, compared with recent historical levels of 15%. It is expected that as our consumption grows, that the US will import more Liquid Natural Gas (LNG). In fact it is anticipated that all imported natural gas in the future will be LNG. To that end more LNG plants and receiving terminals are being built.

2.6 Offshore and Subsea

US production saw a slight decline, but there has been a steady increase in deep water projects off the Gulf of Mexico.[20]

[18] Growth in Gas Projects to Dominate Upstream Development. http://www.gasnet.com.br/artigos/artigos_view2.asp?cod=598

[19] CIS stands for commonwealth of Independent States and includes Armenia, Azerbaija, Belarus, Kazakhstan, Kyrgyzstan, republic of Moldova, Russian Federation, Tajikistan, Turkmenistan, Ukraine, Uzbekistan

[20] Figure taken from Davidson's presentation to Congress. Statement of Charles Davidson, Chairman, President and CEO, Noble Energy Inc. Before the Senate Committee on Energy and Natural Resources, April 19, 2005.

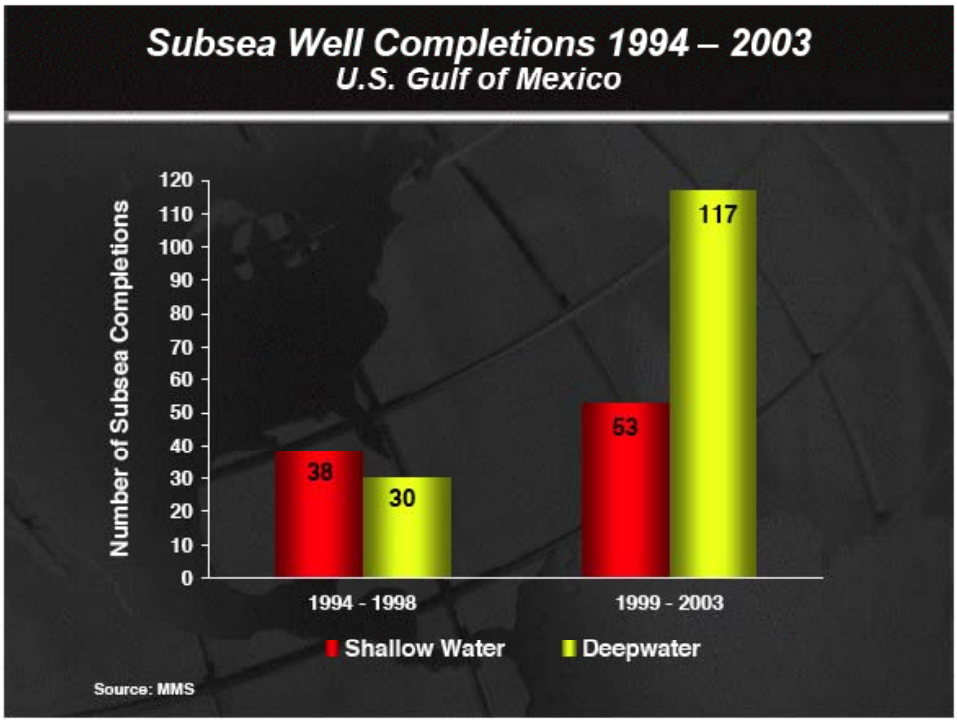

According to this report "While the field sizes of the Middle East dominate the reserve picture, the CIS has the largest number of potential gas developments…including the phase III of Karachaganak in Kazakhstan, Shtokmanovskoye in the deepwater offshore Russia, and the combined development of the Sakhalin Island projects. …Major offshore developments in Indonesia, including Natuna in the longer term and Tangguh in the more near term should attract significant investment from current operations during the next several years. Development of several giant projects onshore China (Kela 2 and Tazhong 10 and the development of major deepwater gas developments in Australia (Sunrise and Gorgon) will contribute significantly to global production during the next three to five years."[21]

Garrison et al predictions regarding offshore development projects is represented in the following figure. They conclude that the vast majority of reserves associated with near term development projects is found in the shallow-shelf waters around the globe, primarily due to the massive resource of the North field/South Pars complex.

[21] http://www.gasnet.com.br/artigos/artigos_view2.asp?cod=598

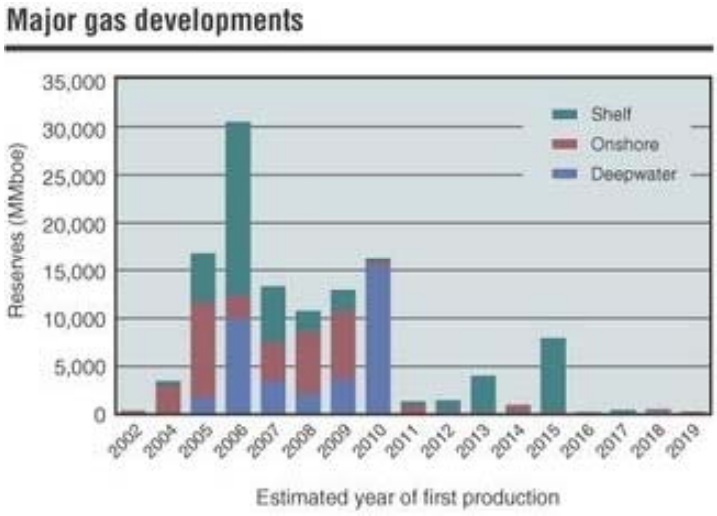

3.0 The Market

The preceding discussion of industry trends was intended to provide the context for a discussion of the market opportunity for Energent's integral separator. As indicated at the outset, the integral separator would be used subsea to remove liquids close to the wellhead. By so doing one decreases the corrosiveness of the wet gas and consequently, less expensive subsea piping could then be used to safely transport the gas to shore for further processing. Before exploring this issue in detail, an overview of subsea developments will be presented.

Often referred to as Subsea completions this technology has been enabling in early production from deepwater, remote, and marginal fields. Approximately 1,200 susbsea wells have been completed in various configurations including single-satellite wells; subsea trees on steel-template structures with production manifolds; and clustered well systems. The most active areas for subsea tree installations has been the North Sea were 40% of the worlds subsea installations have been made. Other prominent regions include waters off the coast of Norway and Brasil.[22]

In a 2002 article entitled *Shifting to the Seabed*, the history of subsea processing was provided.[23] Processing hydrocarbons at the seabed rather than on offshore platforms makes sense, especially when the wells are further offshore in deeper water. Bringing large volumes of water and sand to the surface presents the problem of having to dispose of the produced water and extracted sand. The earliest experiment with subsea processing occurred in 1970 when bp conducted a trial at Zakum field, in Abu Dhabi. Other trials are noted in the following table.

[22] Subsea completions http://www.spe.org/spe/jsp/basic/0,,1104_1714_1004123,00.html
[23] Shifting to the Seabed, Frontiers, August 2002.

Year	Experiment and site
1970	Bp trial in Zakum field , Abu Dhabi
1989	British Offshore Engineering Technology (BOET) separator trial in Argyll field, North Sea
2000	Norsk Hydro's Troll Pilot for separation and water injection in the Troll C field, Norway
2001	Petrobas operational test offshore Brazil of a gas-liquid separator known as Vasps – vertical annular separation and pumping system – an idea originating in bp in the 1980's

Bp has remained interested in the potential of subsea processing and has proposed the following requirements:

- The system will operate for 20 years without intervention
- A size that can be handled practically – a specific goal is to be able to lower a payload of 250t in water depths of 3000m or greater by 2005
- Rather than components, a subsea tool kit is required. A typical tool kit would co ntain gravity separators, cyclones for degassing and deoiling, water injection pumps, a power supply, and a range of monitoring and control devices.

In order to develop an integrated solution, in 2002 bp teamed with ChevronTexaco and two of the world's subsea equipment designers, ABB and Kvaerner to create the subsea processing collaboration (SPC). The primary goal of the collaboration was to identify technology gaps that must be addressed in order for subsea processing to become economically viable. Some Points of Contact relative to this initiative are provided in Appendix A. An example of a project that combines subsea components is the "compact subsea separation combined with efficient sand management" a project being undertaken by FMC Kongsberg Subsea, CDS Separation Technology, and Statoil.[24]

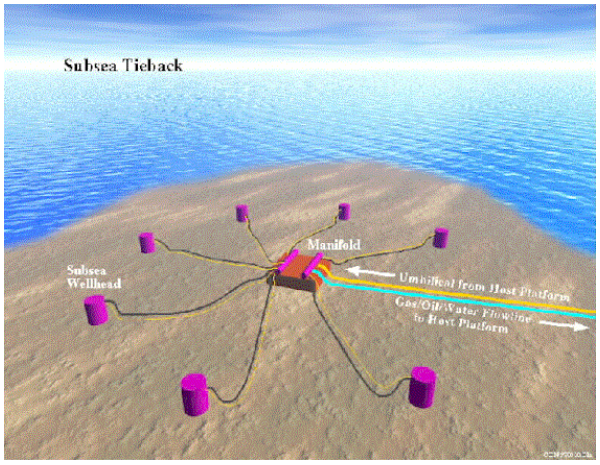

[24] Demo 2000: From R&D to the market

In the subsea market, the most frequent scenario discussed are tie backs and subsea trees. A tieback is an offshore field developed with one or more wells completed on the seafloor, using subsea. The wells are connected by flowlines and umbilicals - the pathways for electrical and hydraulic signals - to a production facility in another area. A subscription database called ***subseazone.com*** provides a listing globally of all existing and subsea oil, oil & gas, and gas/condensate offshore projects by region (Included as separate appendices). In addition, one can purchase a market research report for approximately $3,600 (converted from pounds)[25] from Infield entitled "*Global Perspectives – Subsea market Update – 2004-2008*". According to the synopsis of the 180 page report "2,121 subsea wells are forecast to be installed in the period 2004/08. This represents a 71% growth from the period 1999/03, where 1,242 wells were installed. Overall, the market forecast expenditure is set to rise from a total of $18.6bn during the period 1999/03 to $31.3bn during 2004/08."

The DeepStar project, an R&D consortium operated by Texaco and involving 21 operating companies and 40 supplier organizations are looking to use subsea wells in the Gulf of Mexico (GOM). [26], [27] Echoing the earlier comments made by bp, the spokesperson for Deepstar indicates that we want standard interfaces between vendor components that will allow us to prebuild subsea trees.[28] The focus of DeepStar however appears to be strictly an oil application.

According to Bergman and Landrum, other factors that effect the ability to increase the effectiveness of deepwater hydrocarbon development is the natural gas infrastructure. The authors indicate that if a mature gas infrastructure is not in place and the natural gas is to be marketed, the options are limited to liquefaction of the gas or conversion of the gas to a more readily transportable liquid. Although most near term development is likely to occur via tiebacks, to become independent of the infrastructure, the envision a scenario where from the "subsea manifolds, subsea pumps would move liquids to submerged offloading buoys. Oil and gas would be taken on board the shuttles where the gas would be converted to a more easily transportable liquid… A control buoy would be the only permanent structure on the sea." This vision is represented by the following figure.[29]

[25] http://www.infield.com/shop/product.asp?cookiecheck=yes&P_ID=122
[26] http://otrc.tamu.edu/Pages/subsys.htm
[27] http://otrc.tamu.edu/Pages/subseawell.htm
[28] http://www.spe.org/spe/jsp/basic/0,,1104_1714_1004123,00.html
[29] http://www.worldenergy.org/wec-geis/publications/default/tech_papers/17th_congress/2_1_12.asp

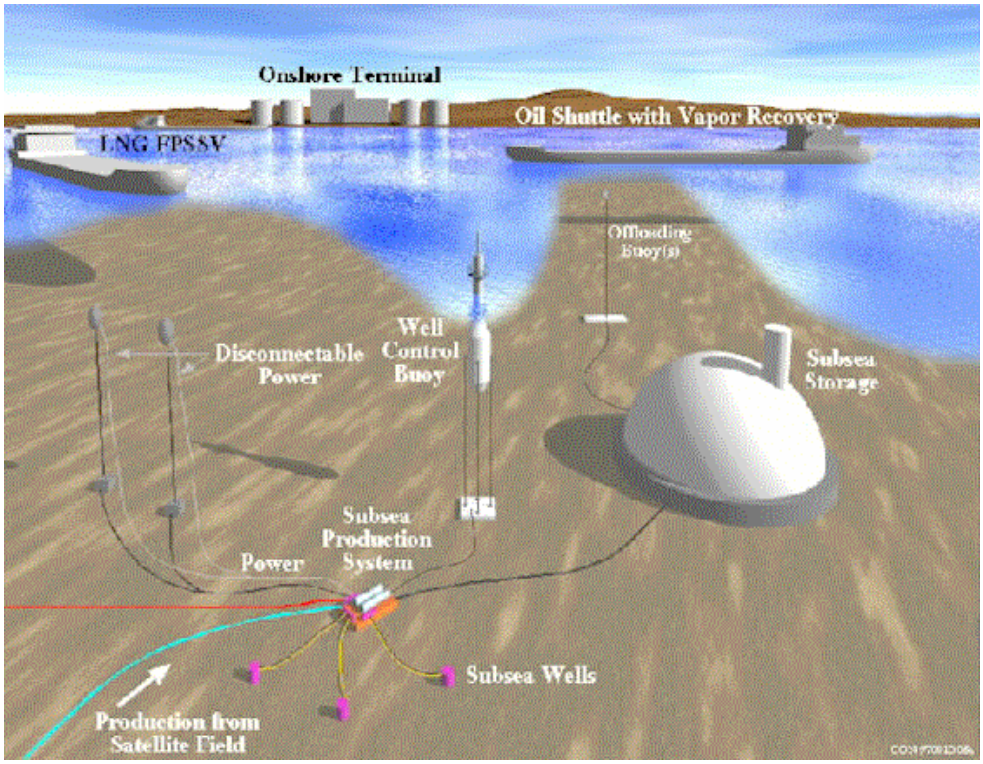

4.0 Competition

In reviewing the literature on subsea separation of natural gas, a number of organizations and/or projects recur including The Troll Pilot, Cameron, and FMC.

4.1. The Troll Pilot is a subsea separator system that separates gas, water, oil, and sand. The system has gone through extensive qualification testing including a full-scale subsea test and is now available for installation.[30] Although the system uses man robust, off-the-shelf components, it also has a new component that is patented[31] – an inlet section that removes gas before the well stream enters the separator and routes the gas through a bypass line. "This is designed with the inlet cyclone positioned partly above the separator vessel. In this location it can easily be sized for a very high gas flowrate compared to a similar inlet cyclone positioned inside the vessel which is the usual case. This fees almost the entire separator volume for oil-watersolids separation. It is a novel concept that allows the separator volume to be reduced by approximately 50% compared to state-of-the-art designs with equal flowrate capacities and separation performance. This is a very important improvement as it is critical to design subsea separators that fall within the lifting weight capacities of intervention ships."[32]

[30] Design and Performance – Testing of a New Solution for Subsea Separation, August 16, 2004
[31] It does not appear that the technology is patented in the US, but in Norway
[32] Ibid, page 2

Qualification work on the project was extensive and funded by Statoil ASA and the Norwegian Demo 2000 programme. The large scale test system had the following characteristics

- Gas capacity of 3000 Am3/hr at a maximum density of 50 kg/m3. equivalent to 160 MMSCFD natural gas at 60 barg
- Total liquid capacity of 800 m3/h, equivalent to 120,000 BPD, and the ability to circulate both oil and water at 0 to 800 m3/h
- The ability to use a high molecular weight gas to represent high-pressure gas at a relatively low operating pressure.

4.2. FMC Technologies

FMC is a $2.8 B publicly traded company on the New York Stock Exchange. It is a global leader providing mission-critical technology solutions for the energy, food processing and air transportation industries. FMC Technologies designs, manufactures and services technologically sophisticated systems and products for its customers through its FMC Energy Systems, FMC FoodTech and FMC Airport Systems businesses. The company employs over 9,000 people and has 32 manufacturing facilities.

Subsea Systems represented 37% of the company's consolidated earnings in 2004. "*The development of our integrated subsea systems usually includes initial engineering design studies, subsea trees, control systems, manifolds, seabed template systems, flowline connection and tie-in systems, installation and workover tools, and subsea wellheads. In order to provide these systems and services, we utilize highly-developed system and detail engineering, project management and global procurement, manufacturing, assembly and testing capabilities. Further, we provide service technicians for installation assistance and field support for commissioning, intervention and maintenance of our subsea systems throughout the life of the oilfield. Additionally, we provide tools such as our LWI (light well intervention) system for certain well workover and intervention tasks.* "[33]

With respect to separation systems in 2003, FMC took 55% ownership in CDS Engineering, the Netherlands company mentioned earlier that collaborated on the Troll project. FMC has committed to purchase the remaining 45% in 2009. CDS' separation technology modifies conventional separation technologies by moving the flow in a spiral, spinning motion.

FMC installed its first subsea tree in 1967 and has a prodigious history of subsea installations. In the past three days they have announced contracts for subsea installations in the Perseus-over-Goodwyn Project, Offshore Western Australia; the Agbami Project, offshore Nigeria, and a new project for Petrobas.

[33] 10-K 3/14/05

4.3. Cooper Cameron

Cooper Cameron (CAM-NYSE), another publicly traded company, is a leading supplier of surface and subsea pressure control equipment for rigs and production equipment. Revenues in 2004 exceeded $2B. It competes head-to-head with FMC in the subsea market. In 2004 the company made 3 acquisitions including Petreco International, a supplier of oil and gas separators for $90 M, Unicel, a supplier of oil separation equipment, and Precision Case Parts (PRC) a valve business. The company has a number of larges subsea projects pending primarily in Nigeria, and Angola.

Appendix A

Points of Contact

Name	Organization	Contact Info	Notes
David Brookes	**bp**	Director, Deepwater Technology Program BrookeDA@bp.com	
Brian Oswald	**bp**		
David Walker		Deepwater Technology Advisor to bp	

Norsk patenttidende — Nye pate

(51) **Klasse :** B01D
(21) **Søknadsnr :** 20040472
(22) **Inng.dag :** 2004.02.03
(30) **Prioritet :** 2003.02.04, NL, 1022581
(24) **Løpedag** 2004.02.03
(71) **Søker**
CDS Engineering
Business Park IJsseloord 2, Delta 101
ARNHEIM, 6825MN
Nederland
(74) **Fullmektig**
Oslo Patentkontor AS
Postboks 7007 Majorstua
OSLO, 0306
Norge
(72) **Oppfinner**
David Stanbridge
Rembrandtlaan
ARNHEIM, 6814JM
Nederland
(54) **Benevnelse**
Syklonseparator og fremgangsmåte for separasjon av en blanding.

Appendix D
Reduced Data from CEESI Tests

Date	Run No.	gas flow	liquid flow	inlet p	vortex p	outlet p	inlet t	vortex t
5/23/2006	1	4.53	0	506.6	402.5	409.2	88.9	82
methanol	2	4.53	0.0189	510.86	402.8	408.6	89.5	83.1
	2a	4.55	0.012	510.8	402.9	408.87	89.6	83.1
	3	4.52	0	492.3	394.2	399.4	53.4	54.23
	4	4.31	0	460	362.8	368.8	49.13	45.35
	5	4.34	0	459.6	362.4	367.7	49.16	45.09
	6	4.28	0.02185	463.4	362.7	367.06	49.4	44
	7	3.7	0.02325	447.55	366.8	370.37	49.07	44.05
	8	2.82	0.0332	416.18	376.5	377.9	47.63	46.10
	9	4.21	0	458.1	363.3	368.2	50.8	46.1
	10	4.23	0.01823333	458.6	362.4	367.2	51.07	46.3
	11	4.22	0.0433	459.03	361.7	366.5	51.2	46.5
	12	3.9	0.046	443.9	365.57	369.417	50.61	47.23
	13	2.98	0.0448	419.95	372.8	374.9	49.86	48.4
	14	2.20	0.0453	402.29	377.76	383.25	48.87	49.3
	15	1.86	0.0438	395	380.43	380.74	48.07	50.115
	16	4.12	0.04485	456.2	360.76	365.4	51	47.23
	17	2.48	0	266.4	211.096	214.25	48.9	46.68
decane	18	2.47	0.0172	268.9	211.55	214.28	49.1	46.9
	19	2.39	0.02825	269.88	212.02	214.64	49.54	47.6
	20	2.43	0.03865	269.85	211.7	214.3	49.19	47.46
	21	2.14		195.6	127.7	131.23	48.76	46.91
	22	2.14	0.0303	198.97	127.72	131.01	49.16	46.34
	23	2.14	0.0206	198.4	127.4	131.4	49.1	46.1
6/2/2006	1	7.64	0	750.1	610.1	626.5	49.9	
	2	7.47	0	747.9	608.1	624.5	50.2	
	3	7.59	0	757.4	614.6	630.7	50.2	
decane	4	7.58	0.02	750.1	610.8	627.3	51.4	
	5	7.60	0.085	750.7	609.0	625.4	51.7	
	6	7.66	0.049	750.3	608.2	624.6	51.9	
	7	7.59	0.089	722.1	615.8	628.2	51.2	
	8							
	9	3.1	0.036	658.1	637.9	640.0	48.1	
	1	5.07	0	519.6	423.1	434.7	50.6	
	2	5.14	0	519.3	423.0	434.7	50.9	
	3	5.11	0	522.0	428.6	440.0	50.5	
	4	5.07	0.019	523.3	426.3	437.6	51.5	
	5	5.07	0.035	523.5	425.8	436.7	51.1	
	6	5.07	0.048	524.1	425.6	436.6	51.5	
	7	4.38	0.037	502.5	431.7	439.7	50.7	
	8	1.86	0.036	456.5	446.6	447.8	47.3	
	9	5.06	0.019	522.2	425.6	436.7	5.06	
	1	2.38	0	249.9	203.2	208.9	48.9	

	2	2.35	0	250.4	203.5	209.1	48.8	
	3	2.35	0	251.9	206.2	211.8	48.8	
	4	2.37	0.018	253.5	205.1	210.2	48.7	
	5	2.3	0.035	254.2	205.2	210.3	49.3	
	6	2.34	0.051	254.5	204.9	210.0	48.7	
	7	2.08	0.036	244.7	207.4	211.4	48.2	
	8	0.78	0.035	220.0	215.4	216.0	46.5	
6/26/2006	23	8.8	0	873.6	695.1	727.8	76.9	65
	24	8.8	0	873.6	695.4	727.3	77	65
	25	8.8	0	873.4	695.4	726.9	76.9	65
	26	8.8	0	873.7	696	727	76.8	64.9
	27	8.8	0	874.3	697.2	728	76.8	65
	28	8.8	0	875	700	730	76.9	65.1
	29	8.8	0	878.6	705	734	77	65.4
	30	8.8	0	884	716	745	77	65.9
6/27/2006	1	9.11	0	876.5	713.8	730.4	56.4	44
	2	9.2	0	877.1	714.6	730.9	56.6	44.4
	3	9.18	0.018	877.1	713.2	729.5	57.1	
	4	9.1	0.019	876.6	712.7	725.2	57	
	5	9.1	0.018	875.1	711.6	728.1	57.7	
	6	9.15	0.018	874.4	709.1	728.3	57.1	
	7	9.15	0.018	873.7	711.2	727.8	57.2	
	8	9.06	0.018	873.7	711.4	727.7	57.3	
	9	9.15	0.018	873	709.5	723.9	57.7	
	10	9.19	0.017	872.9	710.9	727.6	57.3	
	11	9.1	0.035	873.5	710.9	727.8	57.8	
	12	9.08	0.035	873.6	711.2	728.2	57.7	
	13	9.16	0.036	873.1	711.2	728.1	57.9	
	14	9.14	0.035	872.7	711.1	727.6	57.6	
	15	9.24	0.034	849.5	726	733.2	57.2	
6/27/2006	1	9.1	0	871.8	714.1	732.5	58.8	46.8
	2	9.1	0.05	874	713.8	731.8	59.3	
	3	9.1	0.048	873.8	713.6	731.3	59.6	
	4	9.1	0.049	847.3	724.9	731.9	58.6	

outlet t	pressure rise	L1	t1	L2	t2	mc1	mc2
	6.7						
82.8	5.8	9	81.65			0.005148	
82.76	5.97	8	84.5			0.004422	
	5.2						
42.9	6						
42.9	5.3						
43.05	4.36	8	59.98667	10	59.98667	0.006229	0.007786
44.23	3.57	8	57.14333	9.666667	57.14333	0.006539	0.007901
45.96	1.4	8	46.21667	12	46.21667	0.008085	0.012127
45.0	4.9						
45.4	4.8	8	79.87	6	47.36	0.004678	0.005917
45.61	4.8	8	70.14333	6	17.41333	0.005327	0.016093
46.34	3.847	8	64.79333	6	16.20667	0.005767	0.017291
48.04	2.1	8	40.14667	6	12.05667	0.009307	0.023243
48.73	5.49	8	31.18333	6	11.82667	0.011982	0.023695
49.34	0.31	8	29.68667	6	11.61333	0.012586	0.02413
45.76	4.64	8	63.87	6	16.995	0.00585	0.016489
45.99	3.154						
46.25	2.73	8	42.86667	6	23.20333	0.007277	0.010083
46.8	2.62	8	34.83333	6	23.21	0.008955	0.01008
46.65	2.6	8	34.74667	6	13.89	0.008977	0.016843
45.04	3.53						
45.73	3.29	8	33.66667	6	21.7	0.009265	0.010781
	4	8	31.89	6	31.89	0.009782	0.007336
	16.4	0		0			
	16.4	0		0			
	16.1	0		0			
	16.5	8	39.29333	6	108.57	0.007939	0.002155
	16.4	8	23.97	6	39.28667	0.013014	0.005955
	16.4	8	15.48667	6	29.66	0.020142	0.007888
	12.4	8	24.01333	6	49.07	0.01299	0.004768
	2.1	8	24.40333	6	10.14333	0.012783	0.023065
	11.6	0		0			
	11.7	0		0			
	11.4	0		0			
	11.3	8	46.07667	6	49.03	0.00677	0.004772
	10.9	8	19.92	6	25.71	0.01566	0.0091
	11	8	14.92333	6	19.68333	0.020903	0.011886
	8	8	20.912	6	18.74333	0.014917	0.012482
	1.2	8	26.18	6	8.453333	0.011915	0.027676
	11.1						
	5.7	0		0			

	5.6	0		0			
	5.6	0		0			
	5.1	8	55.33333	6	19.52667	0.005637	0.011981
	5.1	8	20.94333	6	11.16	0.014894	0.020964
	5.1	8	12.48	6	8.433333	0.024995	0.027741
	4.0	8	21.13	6	10.31	0.014763	0.022692
	0.6	8	12.47	6	17.67333	0.025015	0.013238
68.2	32.7						
68.2	31.9						
68.2	31.5						
68	31.0						
68	30.8						
68	30.0						
68.5	29.0						
68.8	29.0						
47.2	16.6						
47.5	16.3						
47.9	16.3	8	136.9	10	140	0.002279	0.002785
47.7	12.5	8	82.2	10	74.95	0.003795	0.005202
48.5	16.5	8	80	8	158.5	0.003899	0.001968
48	19.2	8	89.2	8	160.6	0.003497	0.001942
48	16.6	8	71.51	8	164.54	0.004362	0.001896
48.3	16.3	8	64.83	8	172.67	0.004812	0.001807
48.6	14.4	8	85.925	8	151.59	0.00363	0.002058
48.3	16.7	8	85.045	8	155.75	0.003668	0.002003
48.8	16.9	8	34.825	8	73.15	0.008957	0.004264
48.7	17.0	8	31.61	8	81.35	0.009868	0.003835
49.1	16.9	8	28.62	8	84.23	0.010899	0.003703
48.8	16.5	8	26.33	8	86.43	0.011847	0.003609
50.1	7.2	8	83.815	8	71.65	0.003722	0.004354
50.2	18.4						
50.7	18.0	8	16.355	8	58.745	0.019073	0.00531
51.1	17.7	8	22.145	8	48.99	0.014086	0.006367
52.2	7.0	8	15.01			0.020782	

effc1	effc1,2	effp	mg/ml
		0.064	0
0.272	0.272	0.054	0.004172
0.368	0.368	0.055	0.002637
0.000		0.053	0
0.000		0.062	0
0.000		0.055	0
0.285	0.641	0.043	0.005105
0.281	0.621	0.044	0.006284
0.244	0.609	0.035	0.011773
0.000		0.052	0
0.257	0.581	0.050	0.00431
0.123	0.495	0.049	0.010261
0.125	0.501	0.049	0.011795
0.208	0.727	0.045	0.015034
0.265	0.788	0.224	0.020591
0.287	0.838	0.021	0.023548
0.130	0.498	0.049	0.010886
0.000	0.000	0.057	0
0.423	1.009	0.048	0.006964
0.317	0.674	0.045	0.01182
0.232	0.668	0.045	0.015905
		0.052	0
0.306	0.662	0.046	0.014159
0.475	0.831	0.056	0.009626
		0.117	0
		0.117	0
		0.113	0
0.397	0.505	0.118	0.002639
0.153	0.223	0.116	0.011184
0.411	0.572	0.115	0.006397
0.146	0.200	0.117	0.011726
0.355	0.996	0.104	0.011613
		0.120	0
		0.121	0
		0.122	0
0.356	0.607	0.116	0.003748
0.447	0.707	0.112	0.006903
0.435	0.683	0.112	0.009467
0.403	0.741	0.113	0.008447
0.331	1.100	0.121	0.019355
0.000	0.000	0.115	0.003755
		0.122	0

		0.119	0
		0.123	0
0.313	0.979	0.105	0.007595
0.426	1.025	0.104	0.015217
0.490	1.034	0.103	0.021795
0.410	1.040	0.107	0.017308
0.715	1.093	0.130	0.044872
		0.183	0
		0.179	0
		0.177	0
		0.174	0
		0.174	0
		0.171	0
		0.167	0
		0.173	0
		0.102	0
		0.100	0
0.127	0.281	0.099	0.001961
0.200	0.474	0.076	0.002088
0.217	0.326	0.101	0.001978
0.194	0.302	0.116	0.001967
0.242	0.348	0.102	0.001967
0.267	0.368	0.100	0.001987
0.202	0.316	0.088	0.001967
0.216	0.334	0.103	0.00185
0.256	0.378	0.104	0.003846
0.282	0.392	0.105	0.003855
0.303	0.406	0.104	0.00393
0.338	0.442	0.102	0.003829
0.109	0.238	0.058	0.00368
		0.117	0
0.381	0.488	0.112	0.005495
0.293	0.426	0.110	0.005275
0.424		0.057	0.005385

Appendix E
CEESI Test Data

Energent Dew Point Controller Tests -- May and June 2006

Test Num ber:		40	40	40
Data Point:		1	2	3
Date of Test:		6/27/2006	6/27/2006	6/27/2006
Barometric Pressure (psia):		12.188	12.188	12.188
Ambient Temperature (deg F):		75.46	76.67	76.58
START Time of Test Point:		10:18:08	10:21:11	10:36:59
STOP Time of Test Point:		10:20:08	10:23:17	10:51:21
DRY SECTION -- TURBINE METER				
Turbine Meter Density	lb/cu ft	3.3495	3.3504	3.3556
Turbine Meter Pressure	psia	901.59	902.16	901.70
Standard Deviation of Pressure	%	0.01	0.01	0.05
Turbine Meter Temperature	deg. F	74.43	74.57	73.88
Standard Deviation of Temperature	%	0.12	0.07	0.32
Turbine Meter Frequency	Hz	82.107	82.105	81.811
Standard Deviation of Frequency	%	0.88	0.85	0.83
Turbine Meter Viscosity	lb/sec-in	7.1351E-07	7.1369E-07	7.1329E-07
Turbine Meter Reynolds Number (Bore)		2.9941E+06	2.9941E+06	2.9898E+06
Turbine Meter Factor	pulses/cu ft	28.451	28.451	28.451
Turbine Meter Mass Flow	lb/hr	34798.5	34807.4	34736.9
By-Pass Velocity Measured by Ultrasonic	ft/sec	0.000	0.000	0.000
By-Pass Mass Flow Measured by Ultrasonic	lb/sec	0.0	0.0	0.0
Mass Flow to Dew Point Controller	**lb/sec**	9.6662	9.6687	9.6491
LIQUID INJECTION --- Stoddard Solvent				
Liquid Mass Flow (Injection)	lb/sec	0.0000	0.0000	0.0177
Standard Deviation of Injection Mass Flow	%			13.44
Liquid Density,	lb/cu f	48.540	48.538	48.645
LIQUID LOAD Liquid Injection (lb/s) / Turbine (lb/s)		0.00000	0.00000	0.00184
DEW POINT CONTROLLER				
Natural Gas Density	lb/cu ft	3.4913	3.4897	3.4851
Inlet Pressure	psia	888.72	889.31	888.88
Standard Deviation of Pressure	%	0.01	0.01	0.05
Inlet Temperature	deg. F	56.38	56.75	56.97
Standard Deviation of Temperature	%	0.16	0.13	0.45
Exit Pressure	psia	742.40	743.05	741.02
Standard Deviation of Pressure	%	0.02	0.01	0.05
Exit Temperature	deg. F	47.16	47.46	47.68
Standard Deviation of Temperature	%	0.18	0.14	0.48
Differential Pressure across Controller	P10 - P15	146.31	146.27	147.86
Differential Pressure across Controller	(by dP cell)	144.76	144.71	146.31

Housing Pressure	psia	P1	711.94	712.88	713.36
Standard Deviation of Pressure	%		0.02	0.02	0.17
Housing Temperature	deg. F	T1	44.06	44.39	55.75
Standard Deviation of Temperature	%		0.17	0.18	13.43
Secondary Collector Pressure	psia	P12	725.85	726.72	724.82
Standard Deviation of Pressure	%		0.02	0.01	0.05
Main Outlet Pressure	psia	P13	749.82	750.96	750.62
Standard Deviation of Pressure	%		0.01	0.01	0.06
Recovered Liquid Pressure	psia	P14	711.82	712.71	714.82
Standard Deviation of Pressure	%		0.02	0.02	0.42
Valve Positions					
Valve Downstream of Energent	% open		100%	65%	65%
Valve Downstream of Venturi (by-pass)	% open		0%	0%	0%

ENGLISH UNITS

40	40	40	40	40	40	40
4	5	6	7	8	9	10
6/27/2006	6/27/2006	6/27/2006	6/27/2006	6/27/2006	6/27/2006	6/27/2006
12.188	12.188	12.188	12.188	12.188	12.188	12.188
77.41	78.69	78.46	78.84	78.66	78.17	79.81
10:52:18	11:02:11	11:11:00	11:19:19	11:25:32	11:35:09	11:41:26
10:56:04	11:07:46	11:14:47	11:21:56	11:28:41	11:38:44	11:45:59
3.3571	3.3454	3.3464	3.3416	3.3440	3.3410	3.3386
900.69	900.19	899.34	898.73	898.38	897.70	897.71
0.03	0.01	0.02	0.01	0.01	0.01	0.01
73.32	74.24	73.79	74.01	73.63	73.65	73.88
0.18	0.42	0.23	0.10	0.10	0.21	0.15
82.009	82.102	81.755	81.988	81.749	82.029	81.955
0.68	0.81	0.88	1.04	0.78	0.85	0.88
7.1283E-07	7.1313E-07	7.1276E-07	7.1273E-07	7.1249E-07	7.1236E-07	7.1246E-07
3.0002E+06	2.9919E+06	2.9817E+06	2.9860E+06	2.9804E+06	2.9885E+06	2.9832E+06
28.451	28.451	28.451	28.451	28.451	28.451	28.451
34836.2	34754.3	34618.1	34666.3	34589.9	34677.1	34620.8
0.000	0.000	0.000	0.000	0.000	0.000	0.000
0.0	0.0	0.0	0.0	0.0	0.0	0.0
9.6767	9.6540	9.6161	9.6295	9.6083	9.6325	9.6169
0.0176	0.0170	0.0169	0.0173	0.0167	0.0181	0.0169
13.83	13.67	14.41	14.60	13.99	12.14	13.51
48.617	48.600	48.580	48.589	48.549	48.575	48.529
0.00182	0.00177	0.00176	0.00179	0.00174	0.00188	0.00176
3.4797	3.4728	3.4727	3.4681	3.4662	3.4625	3.4624
887.92	887.38	886.59	886.01	885.71	885.08	884.99
0.03	0.01	0.02	0.01	0.01	0.02	0.01
57.05	57.44	57.13	57.30	57.34	57.40	57.38
0.33	0.40	0.13	0.43	0.02	0.28	0.09
740.40	740.44	740.44	739.98	739.99	739.99	739.89
0.01	0.02	0.01	0.01	0.00	0.02	0.01
47.80	48.25	48.03	48.11	48.27	48.39	48.35
0.32	0.35	0.15	0.47	0.03	0.31	0.12
147.51	146.94	146.16	146.03	145.72	145.09	145.10
145.95	145.39	144.63	144.53	144.13	143.52	143.64

714.62	715.17	715.06	717.34	721.09	714.35	713.14
0.04	0.02	0.01	0.02	0.01	0.02	0.01
58.51	56.18	56.79	53.41	52.35	54.74	55.13
0.48	0.15	0.41	0.29	0.05	0.70	0.08
724.30	723.94	721.17	723.53	723.51	721.43	723.01
0.01	0.01	0.02	0.01	0.01	0.02	0.01
749.61	748.77	748.85	747.89	747.18	747.05	747.08
0.06	0.02	0.01	0.02	0.01	0.01	0.01
718.57	721.73	720.97	730.19	745.21	721.51	718.06
0.05	0.07	0.02	0.04	0.01	0.03	0.03
65%	65%	65%	65%	65%	65%	65%
0%	0%	0%	0%	0%	0%	0%

40	40	40	40	40	40
11	12	13	14	15	16
6/27/2006	6/27/2006	6/27/2006	6/27/2006	6/27/2006	6/27/2006
12.188	12.188	12.188	12.188	12.188	12.188
78.25	70.96	77.61	78.28	78.10	77.82
11:51:46	11:57:31	12:03:17	12:07:13	12:18:00	12:27:53
11:56:34	11:59:42	12:06:21	12:10:11	12:22:37	12:31:14
3.3359	3.3314	3.3350	3.3305	3.2371	2.9166
898.44	898.38	897.81	897.34	873.05	788.99
0.01	0.01	0.02	0.02	0.01	0.02
74.45	74.86	74.27	74.51	73.52	69.74
0.18	0.22	0.08	0.09	0.14	0.25
81.99	82.10	81.99	82.16	86.21	102.09
0.90	0.74	0.90	0.92	0.57	0.39
7.1287E-07	7.1303E-07	7.1265E-07	7.1267E-07	7.0728E-07	6.8950E-07
2.9806E+06	2.9797E+06	2.9804E+06	2.9825E+06	3.0652E+06	3.3551E+06
28.451	28.451	28.451	28.451	28.450	28.448
34609.5	34607.3	34597.5	34622.0	35313.4	37681.7
0.000	0.000	0.000	0.000	4.097	29.419
0.0	0.0	0.0	0.0	1.2	7.6
9.6137	9.6131	9.6104	9.6172	8.6379	2.8889
0.0341	0.0338	0.0338	0.0342	0.0362	0.0340
4.56	5.43	4.96	4.92	4.27	4.94
48.514	48.507	48.508	48.492	48.489	48.450
0.00355	0.00352	0.00352	0.00355	0.00420	0.01178
3.4604	3.4582	3.4574	3.4568	3.3575	3.0652
885.68	885.57	885.01	884.65	861.80	783.82
0.01	0.01	0.02	0.02	0.01	0.01
57.82	57.98	57.82	57.73	57.27	51.29
0.34	0.44	0.37	0.31	0.37	0.04
740.15	740.40	740.16	739.88	745.57	768.45
0.01	0.01	0.01	0.02	0.03	0.02
48.82	48.97	48.92	48.81	50.20	51.70
0.28	0.37	0.37	0.26	0.30	0.12
145.52	145.18	144.85	144.76	116.23	15.36
144.20	143.86	143.49	143.36	114.82	14.58

713.35	714.32	717.04	719.86	729.14	766.89
0.13	0.02	0.16	0.01	0.03	0.02
55.15	54.64	52.72	51.60	53.04	59.05
0.72	0.16	0.49	0.29	0.31	0.65
723.20	723.48	723.23	723.04	732.30	767.11
0.02	0.01	0.01	0.01	0.03	0.02
747.00	746.87	746.13	745.44	749.50	769.21
0.02	0.01	0.03	0.02	0.02	0.02
718.79	721.56	732.14	743.54	747.99	769.07
0.41	0.06	0.65	0.02	0.03	0.02
65%	65%	65%	65%	65%	65%
0%	0%	0%	0%	25%	50%

Energent Dew Point Controller Tests -- May and June 2006

Test Num ber:		41	41	41
Data Point:		1	2	3
Date of Test:		6/27/2006	6/27/2006	6/27/2006
Barometric Pressure (psia):		12.168	12.168	12.168
Ambient Temperature (deg F):		81.60	82.76	81.86
START Time of Test Point:		13:20:16	13:26:51	13:35:48
STOP Time of Test Point:		13:22:43	13:29:45	13:37:58
DRY SECTION -- TURBINE METER				
Turbine Meter Density	lb/cu ft	3.2989	3.3040	3.3015
Turbine Meter Pressure	psia	896.64	898.89	898.67
Standard Deviation of Pressure	%	0.01	0.01	0.01
Turbine Meter Temperature	deg. F	76.94	77.38	77.53
Standard Deviation of Temperature	%	0.13	0.06	0.06
Turbine Meter Frequency	Hz	82.267	82.371	82.446
Standard Deviation of Frequency	%	0.87	0.86	0.97
Turbine Meter Viscosity	lb/sec-in	7.1362E-07	7.1429E-07	7.1432E-07
Turbine Meter Reynolds Number (Bore)		2.9541E+06	2.9597E+06	2.9600E+06
Turbine Meter Factor	pulses/cu ft	28.451	28.451	28.451
Turbine Meter Mass Flow	lb/hr	34339.0	34436.0	34441.5
By-Pass Velocity Measured by Ultrasonic	ft/sec	0.000	0.000	0.000
By-Pass Mass Flow Measured by Ultrasonic	lb/sec	0.000	0.000	0.000
Mass Flow to Dew Point Controller	**lb/sec**	9.5386	9.5656	9.5671
LIQUID INJECTION --- Stoddard Solvent				
Liquid Mass Flow (Injection)	lb/sec	0.0000	0.0488	0.0477
Standard Deviation of Injection Mass Flow	%		2.15	2.44
Liquid Density,	lb/cu f	48.110	48.205	48.224
LIQUID LOAD Liquid Injection (lb/s) / Turbine (lb/s)		0.00000	0.00510	0.00499
DEW POINT CONTROLLER				
Natural Gas Density	lb/cu ft	3.4350	3.4403	3.4377
Inlet Pressure	psia	883.98	886.19	885.99
Standard Deviation of Pressure	%	0.01	0.01	0.01
Inlet Temperature	deg. F	58.97	59.38	59.53
Standard Deviation of Temperature	%	0.14	0.18	0.22
Exit Pressure	psia	744.65	743.82	743.50
Standard Deviation of Pressure	%	0.01	0.01	0.01
Exit Temperature	deg. F	50.26	50.79	51.01
Standard Deviation of Temperature	%	0.15	0.23	0.19
Differential Pressure across Controller	P10 - P15	139.33	142.36	142.49
Differential Pressure across Controller	(by dP cell)	137.88	140.89	141.00

Housing Pressure	psia	P1	710.94	722.21	714.32
Standard Deviation of Pressure	%		0.02	0.01	0.11
Housing Temperature	deg. F	T1	46.85	54.42	57.19
Standard Deviation of Temperature	%		0.16	0.45	0.31
Secondary Collector Pressure	psia	P12	726.00	725.91	725.86
Standard Deviation of Pressure	%		0.01	0.01	0.01
Main Outlet Pressure	psia	P13	748.40	747.13	748.13
Standard Deviation of Pressure	%		0.02	0.01	0.02
Recovered Liquid Pressure	psia	P14	726.77	745.11	717.77
Standard Deviation of Pressure	%		0.20	0.03	0.33
Valve Positions					
Valve Downstream of Energent	% open		65%	65%	65%
Valve Downstream of Venturi (by-pass)	% open		0%	0%	0%

ENGLISH UNITS

41
4
6/27/2006
12.168
82.92
13:42:43
13:44:48

3.1957
870.37
0.01
76.20
0.24
87.025
0.41
7.0794E-07
3.0516E+06
28.451
35190.3

4.964
1.401

8.3740

0.0498
2.38

48.213

0.00595

3.3283
859.52
0.00
58.60
0.10

750.22
0.01
52.21
0.08

109.31
107.97

734.04
0.02
55.59
0.20

737.20
0.01

753.23
0.01

751.60
0.02

65%
25%

Energent Dew Point Controller Tests -- May and June 2006

Test Num ber:		42	42	42
Data Point:		1	2	3
Date of Test:		6/28/2006	6/28/2006	6/28/2006
Barometric Pressure (psia):		12.148	12.148	12.148
Ambient Temperature (deg F):		57.59	58.12	57.35
START Time of Test Point:		14:35:12	14:38:16	14:42:13
STOP Time of Test Point:		14:37:19	14:40:13	14:44:13
DRY SECTION -- TURBINE METER				
Turbine Meter Density	lb/cu ft	3.2661	3.2699	3.2789
Turbine Meter Pressure	psia	904.93	903.93	902.88
Standard Deviation of Pressure	%	0.03	0.02	0.03
Turbine Meter Temperature	deg. F	84.82	84.00	82.62
Standard Deviation of Temperature	%	0.26	0.27	0.21
Turbine Meter Frequency	Hz	80.758	80.589	80.579
Standard Deviation of Frequency	%	0.84	0.98	0.79
Turbine Meter Viscosity	lb/sec-in	7.1926E-07	7.1862E-07	7.1769E-07
Turbine Meter Reynolds Number (Bore)		2.8486E+06	2.8484E+06	2.8597E+06
Turbine Meter Factor	pulses/cu ft	28.452	28.452	28.452
Turbine Meter Mass Flow	lb/hr	33373.5	33342.3	33430.2
By-Pass Velocity Measured by Ultrasonic	ft/sec	0.000	0.000	0.000
By-Pass Mass Flow Measured by Ultrasonic	lb/sec	0.000	0.000	0.000
Mass Flow to Dew Point Controller	**lb/sec**	9.2704	9.2617	9.2862
LIQUID INJECTION --- Stoddard Solvent				
Liquid Mass Flow (Injection)	lb/sec	0.0000	0.0000	0.0000
Standard Deviation of Injection Mass Flow	%			
Liquid Density,	lb/cu f	48.426	48.464	48.486
LIQUID LOAD Liquid Injection (lb/s) / Turbine (lb/s)		0.00000	0.00000	0.00000
DEW POINT CONTROLLER				
Natural Gas Density	lb/cu ft	3.2951	3.2920	3.2912
Inlet Pressure	psia	893.37	892.36	891.21
Standard Deviation of Pressure	%	0.03	0.03	0.03
Inlet Temperature	deg. F	76.95	76.82	76.42
Standard Deviation of Temperature	%	0.02	0.06	0.09
Exit Pressure	psia	742.57	740.87	739.75
Standard Deviation of Pressure	%	0.06	0.04	0.04
Exit Temperature	deg. F	68.08	67.85	67.43
Standard Deviation of Temperature	%	0.06	0.09	0.12
Differential Pressure across Controller	P10 - P15	150.79	151.49	151.45
Differential Pressure across Controller	(by dP cell)	148.91	149.70	149.66

Housing Pressure	psia	P1	718.74	717.06	715.79
Standard Deviation of Pressure	%		0.07	0.06	0.03
Housing Temperature	deg. F	T1	64.64	64.44	64.02
Standard Deviation of Temperature	%		0.04	0.09	0.08
Secondary Collector Pressure	psia	P12	728.68	726.88	725.82
Standard Deviation of Pressure	%		0.06	0.05	0.03
Main Outlet Pressure	psia	P13	752.78	751.20	750.11
Standard Deviation of Pressure	%		0.06	0.04	0.03
Recovered Liquid Pressure	psia	P14	715.40	711.80	708.93
Standard Deviation of Pressure	%		0.12	0.08	0.04
Valve Positions					
Valve Downstream of Energent	% open		100%	85%	75%
Valve Downstream of Venturi (by-pass)	% open		0%	0%	0%

ENGLISH UNITS

42	42	42	42	42
4	5	6	7	8
6/28/2006	6/28/2006	6/28/2006	6/28/2006	6/28/2006
12.148	12.148	12.148	12.148	12.148
56.74	56.30	56.24	56.16	56.32
14:45:11	14:48:14	14:52:11	14:55:14	14:59:15
14:47:11	14:50:14	14:54:11	14:57:14	15:01:15
3.2858	3.2870	3.2885	3.2947	3.3043
902.94	903.37	904.30	905.22	907.32
0.01	0.01	0.01	0.01	0.00
81.94	82.00	82.24	82.00	81.91
0.13	0.09	0.09	0.00	0.08
80.373	80.323	80.172	80.077	79.798
0.82	0.82	0.92	0.71	0.83
7.1735E-07	7.1747E-07	7.1779E-07	7.1786E-07	7.1825E-07
2.8597E+06	2.8585E+06	2.8531E+06	2.8548E+06	2.8516E+06
28.452	28.452	28.452	28.452	28.452
33415.1	33406.1	33358.3	33381.3	33362.1
0.000	0.000	0.000	0.000	0.000
0.000	0.000	0.000	0.000	0.000
9.2820	9.2795	9.2662	9.2726	9.2672
0.0000	0.0000	0.0000	0.0000	0.0000
48.470	48.445	48.415	48.395	48.380
0.00000	0.00000	0.00000	0.00000	0.00000
3.2943	3.2986	3.3026	3.3059	3.3152
891.26	891.74	892.72	893.68	895.85
0.01	0.01	0.01	0.01	0.01
76.13	75.90	75.92	76.00	75.98
0.06	0.04	0.03	0.02	0.02
740.23	741.00	742.33	743.62	746.69
0.04	0.02	0.02	0.01	0.01
67.11	66.85	66.83	66.92	66.97
0.11	0.07	0.02	0.02	0.03
151.02	150.74	150.39	150.06	149.16
149.35	149.02	148.66	148.33	147.39

716.29	717.05	718.51	720.21	723.80
0.03	0.02	0.02	0.02	0.01
63.77	63.52	63.55	63.67	63.78
0.11	0.07	0.02	0.02	0.01
726.26	727.14	728.62	730.15	733.50
0.03	0.02	0.01	0.01	0.01
750.59	751.41	752.85	754.21	757.57
0.02	0.02	0.02	0.01	0.01
707.77	707.21	707.15	707.22	707.28
0.02	0.01	0.00	0.01	0.01
70%	65%	60%	55%	50%
0%	0%	0%	0%	0%

Energent Dew Point Controller Tests -- May and June 2006

Test Num ber:		43	43	43
Data Point:		1	2	3
Date of Test:		6/29/2006	6/29/2006	6/29/2006
Barometric Pressure (psia):		12.175	12.175	12.175
Ambient Temperature (deg F):		79.71	80.39	78.14
START Time of Test Point:		10:03:41	10:16:07	10:41:30
STOP Time of Test Point:		10:05:42	10:31:01	10:42:54
DRY SECTION -- TURBINE METER				
Turbine Meter Density	lb/cu ft	3.3582	3.3622	3.3978
Turbine Meter Pressure	psia	942.87	948.22	935.58
Standard Deviation of Pressure	%	0.03	0.10	0.04
Turbine Meter Temperature	deg. F	92.50	94.31	85.50
Standard Deviation of Temperature	%	0.22	0.75	0.00
Turbine Meter Frequency	Hz	81.916	81.472	80.204
Standard Deviation of Frequency	%	0.79	0.89	1.08
Turbine Meter Viscosity	lb/sec-in	7.3161E-07	7.3385E-07	7.2608E-07
Turbine Meter Reynolds Number (Bore)		2.9208E+06	2.8996E+06	2.9155E+06
Turbine Meter Factor	pulses/cu ft	28.452	28.452	28.452
Turbine Meter Mass Flow	lb/hr	34807.0	34660.2	34481.3
By-Pass Velocity Measured by Ultrasonic	ft/sec	0.000	0.000	0.000
By-Pass Mass Flow Measured by Ultrasonic	lb/sec	0.000	0.000	0.000
Mass Flow to Dew Point Controller	**lb/sec**	9.6686	9.6278	9.5782
LIQUID INJECTION --- Stoddard Solvent				
Liquid Mass Flow (Injection)	lb/sec	0.0000	0.0316	0.0000
Standard Deviation of Injection Mass Flow	%		5.44	
Liquid Density,	lb/cu f	48.397	48.483	48.413
LIQUID LOAD Liquid Injection (lb/s) / Turbine (lb/s)		0.00000	0.00329	0.00000
DEW POINT CONTROLLER				
Natural Gas Density	lb/cu ft	3.3325	3.3303	3.4427
Inlet Pressure	psia	P 931.32	936.66	924.87
Standard Deviation of Pressure	%	0.03	0.10	0.04
Inlet Temperature	deg. F	T1 90.33	92.80	76.82
Standard Deviation of Temperature	%	0.16	0.77	0.16
Exit Pressure	psia	P 768.11	773.12	771.45
Standard Deviation of Pressure	%	0.03	0.13	0.04
Exit Temperature	deg. F	T1 80.70	83.41	68.43
Standard Deviation of Temperature	%	0.19	0.90	0.10
Differential Pressure across Controller	P10 - P15	163.21	163.54	153.42
Differential Pressure across Controller	(by dP cell)	161.28	161.69	151.55

Housing Pressure	psia	P1	754.59	759.67	757.90
Standard Deviation of Pressure	%		0.04	0.13	0.04
Housing Temperature	deg. F	T1	80.58	83.78	74.91
Standard Deviation of Temperature	%		0.25	0.87	0.38
Secondary Collector Pressure	psia	P12	754.48	759.73	758.59
Standard Deviation of Pressure	%		0.03	0.13	0.04
Main Outlet Pressure	psia	P13	779.16	783.58	781.71
Standard Deviation of Pressure	%		0.04	0.13	0.03
Recovered Liquid Pressure	psia	P14	777.73	782.04	780.34
Standard Deviation of Pressure	%		0.03	0.13	0.03
Valve Positions					
Valve Downstream of Energent	% open		100%	100%	100%
Valve Downstream of Venturi (by-pass)	% open		0%	0%	0%

ENGLISH UNITS

	43
	4
	6/29/2006
	12.175
	82.16
	10:45:58
	10:51:32
	3.3895
	935.57
	0.03
	86.31
	0.24
	80.591
	0.79
	7.2652E-07
	2.9206E+06
	28.452
	34563.3
	0.000
	0.000
	9.6009
	0.0323
	5.31
	48.438
	0.00337
	3.4346
	924.91
	0.03
	77.60
	0.17
	767.62
	0.09
	68.71
	0.10
	157.29
	155.41

754.86
0.10
72.22
0.33

755.04
0.10

777.86
0.09

776.34
0.08

100%
0%

Energent Dew Point Controller Tests -- May and June 2006

Test Num ber:		44	44	44
Data Point:		1	2	3
Date of Test:		6/29/2006	6/29/2006	6/29/2006
Barometric Pressure (psia):		12.175	12.175	12.175
Ambient Temperature (deg F):		81.20	82.07	72.51
START Time of Test Point:		11:03:43	11:10:04	11:29:03
STOP Time of Test Point:		11:05:08	11:26:57	11:34:19
DRY SECTION -- TURBINE METER				
Turbine Meter Density	lb/cu ft	3.3243	3.3213	3.3213
Turbine Meter Pressure	psia	915.40	910.99	907.54
Standard Deviation of Pressure	%	0.03	0.17	0.03
Turbine Meter Temperature	deg. F	83.56	82.02	80.57
Standard Deviation of Temperature	%	0.11	0.79	0.34
Turbine Meter Frequency	Hz	81.640	82.145	82.259
Standard Deviation of Frequency	%	0.92	0.85	0.86
Turbine Meter Viscosity	lb/sec-in	7.2079E-07	7.1907E-07	7.1762E-07
Turbine Meter Reynolds Number (Bore)		2.9248E+06	2.9473E+06	2.9573E+06
Turbine Meter Factor	pulses/cu ft	28.452	28.451	28.451
Turbine Meter Mass Flow	lb/hr	34339.7	34521.5	34568.7
By-Pass Velocity Measured by Ultrasonic	ft/sec	0.000	0.000	0.000
By-Pass Mass Flow Measured by Ultrasonic	lb/sec	0.000	0.000	0.000
Mass Flow to Dew Point Controller	**lb/sec**	9.5388	9.5893	9.6024
LIQUID INJECTION --- Stoddard Solvent				
Liquid Mass Flow (Injection)	lb/sec	0.0000	0.0200	0.0197
Standard Deviation of Injection Mass Flow	%		9.94	10.57
Liquid Density,	lb/cu f	48.363	48.397	48.385
LIQUID LOAD Liquid Injection (lb/s) / Turbine (lb/s)		0.00000	0.00208	0.00205
DEW POINT CONTROLLER				
Natural Gas Density	lb/cu ft	3.5117	3.5015	3.4888
Inlet Pressure	psia	902.82	898.38	895.06
Standard Deviation of Pressure	%	0.03	0.16	0.03
Inlet Temperature	deg. F	60.99	60.13	59.91
Standard Deviation of Temperature	%	0.11	0.22	0.06
Exit Pressure	psia	751.92	743.90	739.59
Standard Deviation of Pressure	%	0.05	0.28	0.06
Exit Temperature	deg. F	52.27	50.89	50.49
Standard Deviation of Temperature	%	0.20	0.51	0.10
Differential Pressure across Controller	P10 - P15	150.89	154.48	155.47
Differential Pressure across Controller	(by dP cell)	149.13	152.79	153.73

Housing Pressure	psia	P1	739.35	722.98	726.73
Standard Deviation of Pressure	%		0.05	0.35	0.06
Housing Temperature	deg. F	T1	58.39	61.82	56.39
Standard Deviation of Temperature	%		0.09	8.36	1.39
Secondary Collector Pressure	psia	P12	739.75	727.08	726.94
Standard Deviation of Pressure	%		0.05	0.22	0.06
Main Outlet Pressure	psia	P13	761.43	754.70	749.36
Standard Deviation of Pressure	%		0.05	0.27	0.05
Recovered Liquid Pressure	psia	P14	760.24	724.42	747.98
Standard Deviation of Pressure	%		0.05	0.40	0.06
Valve Positions					
Valve Downstream of Energent	% open		100%	100%	100%
Valve Downstream of Venturi (by-pass)	% open		0%	0%	0%

ENGLISH UNITS

44	44	44	44	44	44	44
4	5	6	7	8	9	10
6/29/2006	6/29/2006	6/29/2006	6/29/2006	6/29/2006	6/29/2006	6/29/2006
12.175	12.175	12.175	12.175	12.175	12.175	12.175
83.31	82.28	76.98	81.43	83.49	84.13	83.90
11:35:00	11:48:27	12:01:53	12:07:06	12:14:35	12:19:48	12:25:55
11:42:07	11:53:38	12:05:41	12:10:14	12:17:41	12:24:51	12:27:58
3.3421	3.1104	2.9862	2.9831	3.1064	3.3273	3.3150
913.48	850.09	814.44	814.35	848.48	905.29	905.61
0.05	0.04	0.01	0.01	0.01	0.03	0.01
80.98	77.57	74.87	75.18	77.28	79.03	80.40
0.22	0.93	0.15	0.13	0.29	0.47	0.11
81.384	92.058	98.452	98.410	91.864	81.853	82.292
0.89	0.42	0.39	0.49	0.39	0.80	0.90
7.1907E-07	7.0455E-07	6.9643E-07	6.9655E-07	7.0410E-07	7.1640E-07	7.1714E-07
2.9383E+06	3.1572E+06	3.2796E+06	3.2742E+06	3.1485E+06	2.9531E+06	2.9549E+06
28.452	28.450	28.449	28.449	28.450	28.451	28.451
34415.4	36233.1	37203.9	37148.9	36109.6	34461.3	34517.6
0.000	10.299	19.577	19.624	10.364	0.000	0.000
0.000	2.829	5.163	5.170	2.843	0.000	0.000
9.5598	7.2355	5.1711	5.1489	7.1870	9.5726	9.5882
0.0190	0.0161	0.0203	0.0324	0.0324	0.0346	0.0492
10.62	12.71	9.83	4.71	4.87	4.20	2.47
48.367	48.328	48.294	48.301	48.296	48.281	48.278
0.00199	0.00223	0.00392	0.00630	0.00451	0.00362	0.00513
3.5143	3.2701	3.1468	3.1476	3.2695	3.4840	3.4798
901.28	840.90	807.62	807.49	839.33	893.06	893.33
0.02	0.04	0.02	0.01	0.01	0.04	0.01
60.17	57.42	54.76	54.63	56.80	59.54	60.02
0.18	0.20	0.27	0.30	0.08	0.18	0.16
750.19	752.04	761.11	760.92	751.25	737.08	735.95
0.02	0.02	0.01	0.01	0.01	0.07	0.01
51.02	52.32	52.62	52.49	51.73	50.13	50.52
0.20	0.19	0.20	0.21	0.09	0.14	0.16
151.09	88.86	46.51	46.58	88.08	155.98	157.38
149.31	87.38	45.37	45.53	86.68	154.03	155.45

737.71	744.84	757.42	757.20	744.48	724.66	723.54
0.03	0.02	0.01	0.01	0.02	0.07	0.01
55.90	57.32	59.83	58.88	56.63	54.73	54.55
0.35	0.17	0.18	0.32	0.24	0.52	0.28
738.02	745.07	757.37	757.17	744.61	724.79	723.66
0.03	0.02	0.01	0.01	0.01	0.08	0.01
759.90	757.64	763.72	763.44	756.92	747.11	746.11
0.02	0.02	0.01	0.01	0.01	0.06	0.01
758.49	756.94	763.49	763.10	756.06	745.59	744.47
0.02	0.02	0.01	0.01	0.02	0.07	0.02
50%	100%	100%	100%	100%	100%	100%
0%	30%	45%	45%	30%	0%	0%

44	44	44
11	12	13
6/29/2006	6/29/2006	6/29/2006
12.175	12.175	12.175
84.06	83.43	80.14
12:29:17	12:32:45	12:37:21
12:32:29	12:34:37	12:42:53
3.3194	3.3470	3.3377
906.41	913.06	911.30
0.07	0.04	0.01
80.29	80.31	80.51
0.24	0.28	0.34
82.16	80.86	81.57
1.01	1.07	0.73
7.1725E-07	7.1865E-07	7.1838E-07
2.9538E+06	2.9252E+06	2.9439E+06
28.451	28.452	28.451
34509.3	34241.9	34447.7
0.000	0.000	0.000
0.000	0.000	0.000
9.5859	9.5116	9.5688
0.0741	0.0695	0.0205
0.99	0.80	9.21
48.271	48.272	48.256
0.00773	0.00730	0.00215
3.4788	3.5093	3.5021
893.91	901.02	899.18
0.01	0.03	0.01
60.32	60.50	60.39
0.06	0.07	0.27
735.41	748.19	747.46
0.01	0.02	0.02
50.92	51.44	51.18
0.07	0.08	0.26
158.50	152.83	151.72
156.62	151.04	149.91

723.10	736.22	728.26
0.02	0.02	0.04
54.59	54.77	59.36
0.12	0.25	1.05
723.11	736.31	734.94
0.02	0.03	0.05
745.57	758.00	758.07
0.02	0.02	0.01
743.64	756.20	731.94
0.02	0.03	0.11
100%	50%	50%
0%	0%	0%

Energent Dew Point Controller Tests -- May and June 2006

Test Num ber:		45	45	45
Data Point:		1	2	3
Date of Test:		6/29/2006	6/29/2006	6/29/2006
Barometric Pressure (psia):		12.163	12.163	12.163
Ambient Temperature (deg F):		59.19	59.90	61.16
START Time of Test Point:		13:37:05	13:42:06	13:51:23
STOP Time of Test Point:		13:38:59	13:44:00	13:55:02
DRY SECTION -- TURBINE METER				
Turbine Meter Density	lb/cu ft	#NAME?	#NAME?	#NAME?
Turbine Meter Pressure	psia	729.46	730.04	735.53
Standard Deviation of Pressure	%	0.02	0.01	0.02
Turbine Meter Temperature	deg. F	75.31	76.38	77.03
Standard Deviation of Temperature	%	0.28	0.08	0.42
Turbine Meter Frequency	Hz	80.730	81.079	80.254
Standard Deviation of Frequency	%	0.90	0.78	0.75
Turbine Meter Viscosity	lb/sec-in	6.8128E-07	6.8187E-07	6.8311E-07
Turbine Meter Reynolds Number (Bore)		#NAME?	#NAME?	#NAME?
Turbine Meter Factor	pulses/cu ft	#NAME?	#NAME?	#NAME?
Turbine Meter Mass Flow	lb/hr	#NAME?	#NAME?	#NAME?
By-Pass Velocity Measured by Ultrasonic	ft/sec	0.000	0.000	0.000
By-Pass Mass Flow Measured by Ultrasonic	lb/sec	0.000	0.000	0.000
Mass Flow to Dew Point Controller	lb/sec	#NAME?	#NAME?	#NAME?
LIQUID INJECTION --- Stoddard Solvent				
Liquid Mass Flow (Injection)	lb/sec	0.0000	0.0209	0.0158
Standard Deviation of Injection Mass Flow	%		9.82	15.86
Liquid Density,	lb/cu f	47.875	47.945	47.968
LIQUID LOAD Liquid Injection (lb/s) / Turbine (lb/s)		#NAME?	#NAME?	#NAME?
DEW POINT CONTROLLER				
Natural Gas Density	lb/cu ft	#NAME?	#NAME?	#NAME?
Inlet Pressure	psia P	720.00	720.52	726.22
Standard Deviation of Pressure	%	0.02	0.01	0.02
Inlet Temperature	deg. F T1	57.07	57.16	57.61
Standard Deviation of Temperature	%	0.05	0.06	0.06
Exit Pressure	psia P	598.82	597.14	605.92
Standard Deviation of Pressure	%	0.03	0.03	0.02
Exit Temperature	deg. F T1	49.50	49.58	50.22
Standard Deviation of Temperature	%	0.03	0.04	0.07
Differential Pressure across Controller	P10 - P15	121.18	123.37	120.31
Differential Pressure across Controller	(by dP cell)	119.92	122.10	118.85

Housing Pressure	psia	P1	584.02	581.80	590.25
Standard Deviation of Pressure	%		0.04	0.04	0.03
Housing Temperature	deg. F	T11	68.63	69.02	69.55
Standard Deviation of Temperature	%		0.46	0.56	0.53
Secondary Collector Pressure	psia	P12	589.30	586.35	596.57
Standard Deviation of Pressure	%		0.04	0.03	0.03
Main Outlet Pressure	psia	P13	606.73	605.87	614.49
Standard Deviation of Pressure	%		0.03	0.03	0.02
Recovered Liquid Pressure	psia	P14	587.11	583.43	591.10
Standard Deviation of Pressure	%		0.04	0.04	0.04
Valve Positions					
Valve Downstream of Energent	% open		100%	100%	50%
Valve Downstream of Venturi (by-pass)	% open		0%	0%	0%

ENGLISH UNITS

45	45	45	45	45	45	45
4	5	6	7	8	9	10
6/29/2006	6/29/2006	6/29/2006	6/29/2006	6/29/2006	6/29/2006	6/29/2006
12.163	12.163	12.163	12.163	12.163	12.163	12.163
62.79	69.85	80.24	80.06	79.60	84.07	84.53
13:59:39	14:03:41	14:07:13	14:10:45	14:14:04	14:20:13	14:23:20
14:02:02	14:05:59	14:08:37	14:12:34	14:15:33	14:22:06	14:25:28
#NAME?	#NAME?	#NAME?	#NAME?	#NAME?	#NAME?	#NAME?
729.47	729.61	730.09	731.10	739.87	684.89	685.40
0.03	0.01	0.00	0.04	0.01	0.01	0.00
77.10	77.74	77.98	77.59	76.71	77.60	76.53
0.23	0.10	0.06	0.34	0.03	0.10	0.29
81.607	81.865	81.983	81.199	78.891	91.893	91.260
0.81	0.72	0.94	1.07	0.62	0.28	0.33
6.8210E-07	6.8242E-07	6.8262E-07	6.8261E-07	6.8372E-07	6.7486E-07	6.7445E-07
#NAME?	#NAME?	#NAME?	#NAME?	#NAME?	#NAME?	#NAME?
#NAME?	#NAME?	#NAME?	#NAME?	#NAME?	#NAME?	#NAME?
#NAME?	#NAME?	#NAME?	#NAME?	#NAME?	#NAME?	#NAME?
0.000	0.000	0.000	0.000	0.000	10.042	10.043
0.000	0.000	0.000	0.000	0.000	#NAME?	#NAME?
#NAME?	#NAME?	#NAME?	#NAME?	#NAME?	#NAME?	#NAME?
0.0227	0.0316	0.0464	0.0745	0.0715	0.0236	0.0354
8.62	6.06	2.31	1.28	0.59	8.50	4.60
47.952	47.941	47.922	47.930	47.927	47.899	47.869
#NAME?	#NAME?	#NAME?	#NAME?	#NAME?	#NAME?	#NAME?
#NAME?	#NAME?	#NAME?	#NAME?	#NAME?	#NAME?	#NAME?
719.74	719.91	720.40	721.69	730.27	677.52	678.20
0.02	0.01	0.01	0.13	0.15	0.03	0.01
57.60	57.81	58.05	58.14	57.96	56.03	56.23
0.15	0.02	0.09	0.05	0.13	0.06	0.03
595.02	595.02	594.95	596.21	608.57	604.85	605.56
0.00	0.00	0.01	0.82	0.81	0.04	0.01
50.01	50.22	50.48	50.74	50.99	51.94	52.31
0.16	0.03	0.09	0.06	0.19	0.12	0.05
124.72	124.89	125.45	125.48	121.71	72.68	72.64
123.50	123.78	124.33	124.25	120.41	71.56	71.46

585.48	585.39	585.31	586.70	599.37	599.38	600.26
0.02	0.02	0.01	0.87	0.84	0.05	0.02
58.23	56.51	56.23	55.74	55.41	57.53	58.59
0.43	0.48	0.08	0.37	0.53	0.52	0.12
585.47	585.35	585.31	586.65	599.15	599.60	600.42
0.01	0.01	0.01	0.90	0.88	0.05	0.02
602.98	602.91	602.68	603.71	615.97	609.59	610.19
0.01	0.01	0.02	0.75	0.73	0.04	0.01
602.05	601.84	601.40	602.01	614.54	609.01	609.54
0.02	0.02	0.03	0.74	0.71	0.05	0.02
100%	100%	100%	100%	50%	100%	100%
0%	0%	0%	0%	0%	35%	35%

45	45	45	45	45	45	45
11	12	13	14	15	16	17
6/29/2006	6/29/2006	6/29/2006	6/29/2006	6/29/2006	6/29/2006	6/29/2006
12.163	12.163	12.163	12.163	12.163	12.163	12.163
85.76	84.82	86.03	85.31	73.14	82.78	86.83
14:26:17	14:31:14	14:34:46	14:37:58	14:40:07	14:45:47	14:51:20
14:28:01	14:33:17	14:36:39	14:39:22	14:42:25	14:49:00	14:55:00
#NAME?	#NAME?	#NAME?	#NAME?	#NAME?	#NAME?	#NAME?
685.58	660.63	660.91	661.21	663.54	745.30	768.09
0.01	0.02	0.01	0.01	0.33	1.00	0.01
76.11	76.01	75.53	75.44	75.29	77.05	79.54
0.05	0.19	0.20	0.07	0.16	0.72	0.48
91.19	97.24	96.88	96.87	95.05	77.63	74.16
0.41	0.54	0.33	0.37	4.72	2.40	0.93
6.7429E-07	6.7024E-07	6.7006E-07	6.7007E-07	6.7037E-07	6.8483E-07	6.9006E-07
#NAME?	#NAME?	#NAME?	#NAME?	#NAME?	#NAME?	#NAME?
#NAME?	#NAME?	#NAME?	#NAME?	#NAME?	#NAME?	#NAME?
#NAME?	#NAME?	#NAME?	#NAME?	#NAME?	#NAME?	#NAME?
10.046	17.637	17.646	17.670	18.080	0.000	0.000
#NAME?	#NAME?	#NAME?	#NAME?	#NAME?	0.000	0.000
#NAME?	#NAME?	#NAME?	#NAME?	#NAME?	#NAME?	#NAME?
0.0483	0.0190	0.0330	0.0505	0.0482	0.0236	0.0196
2.22	10.84	5.11	2.25	3.38	16.29	10.55
47.839	47.857	47.853	47.839	47.891	47.854	47.830
#NAME?	#NAME?	#NAME?	#NAME?	#NAME?	#NAME?	#NAME?
#NAME?	#NAME?	#NAME?	#NAME?	#NAME?	#NAME?	#NAME?
678.37	654.85	655.21	655.54	676.06	732.34	759.90
0.03	0.01	0.01	0.01	4.10	0.03	0.01
56.17	54.37	54.19	54.08	54.78	57.76	58.18
0.09	0.03	0.04	0.07	2.39	0.04	0.18
605.56	611.69	611.84	611.84	616.07	616.30	658.38
0.01	0.02	0.01	0.01	0.23	0.03	0.02
52.38	52.51	52.47	52.52	52.33	50.78	52.10
0.07	0.03	0.06	0.06	0.87	0.06	0.18
72.81	43.16	43.37	43.70	59.99	116.04	101.51
71.63	42.37	42.56	42.86	59.20	114.80	100.18

600.09	608.31	608.54	608.56	611.50	607.38	650.40
0.02	0.02	0.01	0.00	0.46	0.03	0.01
58.18	59.70	59.53	59.50	59.72	57.20	57.77
0.27	0.25	0.10	0.24	1.14	0.39	0.38
600.31	608.57	608.75	608.74	611.64	607.34	650.44
0.01	0.02	0.01	0.00	0.47	0.03	0.01
609.94	614.08	614.20	613.96	619.40	623.49	664.78
0.01	0.02	0.02	0.01	0.35	0.03	0.02
609.21	613.95	613.90	613.67	618.95	622.54	664.02
0.02	0.02	0.01	0.02	0.33	0.03	0.02
100%	100%	100%	100%	50%	40%	30%
35%	55%	55%	55%	55%	0%	0%

45
18
6/29/2006
12.163
69.06
15:04:05
15:06:08

#NAME?
770.28
0.01
80.24
0.08
74.10
0.70
6.9080E-07
#NAME?
#NAME?
#NAME?

0.000
0.000

#NAME?

0.0784
0.38

47.789

#NAME?

#NAME?
762.14
0.01
58.82
0.04

658.09
0.02
53.07
0.03

104.04
102.65

650.02
0.02
57.59
0.23

650.09
0.02

664.15
0.02

662.80
0.04

30%
0%

Energent Dew Point Controller Tests -- May and June 2006

Test Num ber:		46	46	46
Data Point:		1	2	3
Date of Test:		6/30/2006	6/30/2006	6/30/2006
Barometric Pressure (psia):		12.156	12.156	12.156
Ambient Temperature (deg F):		78.05	77.21	79.20
START Time of Test Point:		9:24:36	9:32:01	9:36:05
STOP Time of Test Point:		9:26:24	9:33:57	9:37:59
DRY SECTION -- TURBINE METER				
Turbine Meter Density	lb/cu ft	1.8703	1.8715	1.8670
Turbine Meter Pressure	psia	530.00	530.58	530.03
Standard Deviation of Pressure	%	0.01	0.02	0.01
Turbine Meter Temperature	deg. F	71.22	71.43	71.94
Standard Deviation of Temperature	%	0.15	0.06	0.11
Turbine Meter Frequency	Hz	79.881	79.932	79.784
Standard Deviation of Frequency	%	1.07	0.87	1.00
Turbine Meter Viscosity	lb/sec-in	6.4924E-07	6.4940E-07	6.4954E-07
Turbine Meter Reynolds Number (Bore)		1.7866E+06	1.7884E+06	1.7804E+06
Turbine Meter Factor	pulses/cu ft	28.466	28.466	28.466
Turbine Meter Mass Flow	lb/hr	18894.1	18918.2	18837.3
By-Pass Velocity Measured by Ultrasonic	ft/sec	0.000	0.000	0.000
By-Pass Mass Flow Measured by Ultrasonic	lb/sec	0.000	0.000	0.000
Mass Flow to Dew Point Controller	**lb/sec**	5.2484	5.2550	5.2326
LIQUID INJECTION --- Stoddard Solvent				
Liquid Mass Flow (Injection)	lb/sec	0.0000	0.0187	0.0188
Standard Deviation of Injection Mass Flow	%		11.35	12.21
Liquid Density,	lb/cu f	48.268	48.373	48.392
LIQUID LOAD Liquid Injection (lb/s) / Turbine (lb/s)		0.00000	0.00355	0.00360
DEW POINT CONTROLLER				
Natural Gas Density	lb/cu ft	1.9297	1.9318	1.9295
Inlet Pressure	psia	P 523.16	523.68	523.15
Standard Deviation of Pressure	%	0.01	0.03	0.01
Inlet Temperature	deg. F	T1 53.90	53.90	53.92
Standard Deviation of Temperature	%	0.01	0.04	0.05
Exit Pressure	psia	P 436.62	434.68	434.06
Standard Deviation of Pressure	%	0.03	0.04	0.02
Exit Temperature	deg. F	T1 48.78	48.52	48.42
Standard Deviation of Temperature	%	0.05	0.08	0.04
Differential Pressure across Controller	P10 - P15	86.53	89.00	89.08
Differential Pressure across Controller	(by dP cell)	86.26	88.77	88.85

Housing Pressure	psia	P1	430.08	424.04	423.37
Standard Deviation of Pressure	%		0.03	0.04	0.02
Housing Temperature	deg. F	T1	59.13	60.63	61.65
Standard Deviation of Temperature	%		0.35	0.18	0.20
Secondary Collector Pressure	psia	P12	429.91	427.79	427.16
Standard Deviation of Pressure	%		0.02	0.03	0.02
Main Outlet Pressure	psia	P13	441.69	440.65	440.01
Standard Deviation of Pressure	%		0.04	0.03	0.02
Recovered Liquid Pressure	psia	P14	441.12	425.08	424.47
Standard Deviation of Pressure	%		0.03	0.05	0.05
Valve Positions					
Valve Downstream of Energent	% open		100%	100%	100%
Valve Downstream of Venturi (by-pass)	% open		0%	0%	0%

ENGLISH UNITS

46	46	46	46	46	46	46
4	5	6	7	8	9	10
6/30/2006	6/30/2006	6/30/2006	6/30/2006	6/30/2006	6/30/2006	6/30/2006
12.156	12.156	12.156	12.156	12.156	12.156	12.156
78.26	80.67	79.40	79.67	82.06	83.03	82.73
9:39:03	9:44:40	9:48:37	9:53:05	9:57:41	10:01:04	10:03:47
9:41:47	9:47:03	9:51:02	9:55:08	9:59:46	10:02:38	10:05:02
1.8662	1.8741	1.8888	1.9332	1.8604	1.8603	1.8628
529.81	532.66	536.44	547.75	529.42	530.00	530.78
0.01	0.01	0.03	0.01	0.03	0.00	0.01
71.93	72.57	72.53	72.35	72.84	73.33	73.43
0.16	0.17	0.20	0.09	0.22	0.13	0.06
80.147	79.528	78.679	75.797	80.737	80.672	80.557
0.79	0.86	0.87	0.78	0.82	0.80	0.77
6.4951E-07	6.5016E-07	6.5064E-07	6.5208E-07	6.4985E-07	6.5013E-07	6.5028E-07
1.7878E+06	1.7798E+06	1.7733E+06	1.7446E+06	1.7945E+06	1.7922E+06	1.7916E+06
28.466	28.466	28.467	28.467	28.466	28.466	28.466
18915.0	18848.4	18793.4	18530.8	18995.2	18979.1	18977.5
0.000	0.000	0.000	0.000	0.000	0.000	0.000
0.000	0.000	0.000	0.000	0.000	0.000	0.000
5.2542	5.2357	5.2204	5.1474	5.2765	5.2720	5.2715
0.0194	0.0181	0.0180	0.0157	0.0340	0.0511	0.0733
12.24	12.68	12.25	15.66	5.39	1.88	0.54
48.386	48.379	48.373	48.380	48.380	48.381	48.378
0.00369	0.00345	0.00345	0.00305	0.00645	0.00969	0.01390
1.9279	1.9398	1.9562	2.0028	1.9262	1.9283	1.9309
522.88	525.80	529.91	541.34	522.49	523.16	523.92
0.02	0.01	0.03	0.01	0.03	0.01	0.01
54.01	54.02	54.09	54.13	54.03	54.16	54.26
0.01	0.04	0.01	0.04	0.06	0.04	0.04
433.66	438.15	444.63	462.72	432.02	431.77	431.61
0.02	0.01	0.02	0.02	0.01	0.02	0.00
48.53	48.61	48.80	49.28	48.47	48.62	48.73
0.03	0.03	0.03	0.06	0.14	0.04	0.02
89.21	87.64	85.28	78.62	90.46	91.39	92.31
89.03	87.39	84.74	78.43	90.23	91.05	92.11

427.11	431.75	438.57	456.83	425.43	425.26	425.17
0.03	0.01	0.03	0.01	0.01	0.01	0.03
57.45	56.06	55.61	55.86	54.92	54.68	54.66
0.77	0.31	0.10	0.07	0.19	0.13	0.08
426.80	431.50	438.33	456.73	425.19	425.01	425.01
0.03	0.02	0.02	0.01	0.00	0.01	0.01
439.03	443.57	449.99	467.45	437.23	436.91	436.68
0.03	0.02	0.03	0.01	0.01	0.02	0.03
438.24	442.76	449.27	466.89	436.33	435.85	435.44
0.03	0.02	0.02	0.02	0.02	0.03	0.04
100%	50%	40%	30%	100%	100%	100%
0%	0%	0%	0%	0%	0%	0%

46	46	46	46	46
11	12	13	14	15
6/30/2006	6/30/2006	6/30/2006	6/30/2006	6/30/2006
12.156	12.156	12.156	12.156	12.156
82.59	84.16	84.64	86.09	86.16
10:07:16	10:14:11	10:19:03	10:25:07	10:28:44
10:09:10	10:16:15	10:20:33	10:27:45	10:30:53
1.8745	1.7333	1.7359	1.6605	1.6637
533.82	496.52	497.00	477.35	477.95
0.01	0.01	0.00	0.02	0.01
73.41	73.23	73.05	73.35	73.10
0.11	0.08	0.07	0.10	0.13
79.83	90.80	90.60	97.14	96.99
0.76	0.53	0.47	0.43	0.44
6.5068E-07	6.4580E-07	6.4579E-07	6.4350E-07	6.4347E-07
1.7856E+06	1.8923E+06	1.8910E+06	1.9463E+06	1.9473E+06
28.466	28.464	28.464	28.464	28.464
18925.4	19905.8	19891.5	20400.8	20410.0
0.000	9.917	9.955	18.512	18.603
0.000	1.518	1.526	2.715	2.734
5.2571	4.0112	3.9992	2.9520	2.9359
0.0743	0.0243	0.0343	0.0207	0.0352
0.70	8.96	4.24	11.23	4.18
48.383	48.355	48.318	48.306	48.302
0.01414	0.00606	0.00857	0.00703	0.01198
1.9426	1.8051	1.8070	1.7390	1.7414
526.99	491.26	491.71	473.32	473.89
0.01	0.01	0.01	0.03	0.01
54.40	52.93	52.90	51.61	51.57
0.04	0.07	0.03	0.07	0.05
436.66	439.18	439.33	444.42	444.61
0.01	0.02	0.01	0.02	0.02
49.02	50.16	50.20	50.83	50.94
0.05	0.06	0.05	0.05	0.08
90.32	52.08	52.37	28.90	29.27
90.19	51.96	52.25	28.81	29.23

430.34	435.25	435.35	442.30	442.55
0.02	0.03	0.01	0.03	0.02
55.17	57.38	58.11	61.18	61.98
0.32	0.20	0.09	0.23	0.15
430.19	435.38	435.50	442.36	442.66
0.01	0.02	0.01	0.02	0.01
441.58	442.06	442.01	445.72	445.86
0.02	0.02	0.02	0.03	0.02
440.31	441.66	441.53	445.76	445.80
0.05	0.03	0.01	0.02	0.02
50%	100%	100%	100%	100%
0%	30%	30%	40%	40%

Energent Dew Point Controller Tests -- May and June 2006

Test Num ber:		47	47	47
Data Point:		1	2	3
Date of Test:		6/30/2006	6/30/2006	6/30/2006
Barometric Pressure (psia):		12.145	12.145	12.145
Ambient Temperature (deg F):		86.84	85.19	86.65
START Time of Test Point:		10:55:04	11:00:20	11:04:24
STOP Time of Test Point:		10:56:13	11:01:30	11:05:59
DRY SECTION -- TURBINE METER				
Turbine Meter Density	lb/cu ft	0.8791	0.8889	0.8895
Turbine Meter Pressure	psia	260.36	262.89	263.13
Standard Deviation of Pressure	%	0.02	0.01	0.02
Turbine Meter Temperature	deg. F	72.70	72.29	72.35
Standard Deviation of Temperature	%	0.00	0.11	0.07
Turbine Meter Frequency	Hz	82.094	80.459	80.394
Standard Deviation of Frequency	%	0.62	0.85	0.98
Turbine Meter Viscosity	lb/sec-in	6.2181E-07	6.2183E-07	6.2187E-07
Turbine Meter Reynolds Number (Bore)		9.0026E+05	8.9204E+05	8.9195E+05
Turbine Meter Factor	pulses/cu ft	28.494	28.494	28.494
Turbine Meter Mass Flow	lb/hr	9118.3	9035.4	9035.1
By-Pass Velocity Measured by Ultrasonic	ft/sec	0.000	0.000	0.000
By-Pass Mass Flow Measured by Ultrasonic	lb/sec	0.000	0.000	0.000
Mass Flow to Dew Point Controller	**lb/sec**	2.5329	2.5098	2.5098
LIQUID INJECTION --- Stoddard Solvent				
Liquid Mass Flow (Injection)	lb/sec	0.0000	0.0174	0.0157
Standard Deviation of Injection Mass Flow	%		13.75	15.92
Liquid Density,	lb/cu f	48.016	48.083	48.114
LIQUID LOAD Liquid Injection (lb/s) / Turbine (lb/s)		0.00000	0.00693	0.00627
DEW POINT CONTROLLER				
Natural Gas Density	lb/cu ft	0.9117	0.9213	0.9213
Inlet Pressure	psia	256.99	259.54	259.79
Standard Deviation of Pressure	%	0.02	0.01	0.01
Inlet Temperature	deg. F	50.40	50.34	50.76
Standard Deviation of Temperature	%	0.05	0.07	0.11
Exit Pressure	psia	214.43	214.15	214.33
Standard Deviation of Pressure	%	0.03	0.01	0.03
Exit Temperature	deg. F	48.73	48.71	48.95
Standard Deviation of Temperature	%	0.01	0.07	0.03
Differential Pressure across Controller	P10 - P15	42.56	45.38	45.45
Differential Pressure across Controller	(by dP cell)	42.50	45.39	45.43

Housing Pressure	psia	P1	211.09	209.06	209.33
Standard Deviation of Pressure	%		0.02	0.02	0.02
Housing Temperature	deg. F	T1	67.28	47.33	46.87
Standard Deviation of Temperature	%		0.04	0.49	0.10
Secondary Collector Pressure	psia	P12	211.11	210.93	211.21
Standard Deviation of Pressure	%		0.02	0.01	0.04
Main Outlet Pressure	psia	P13	216.90	217.12	217.36
Standard Deviation of Pressure	%		0.02	0.02	0.03
Recovered Liquid Pressure	psia	P14	216.96	209.39	209.53
Standard Deviation of Pressure	%		0.02	0.01	0.02
Valve Positions					
Valve Downstream of Energent	% open		100%	100%	100%
Valve Downstream of Venturi (by-pass)	% open		0%	0%	0%

ENGLISH UNITS

47	47	47	47	47	47	47
4	5	6	7	8	9	10
6/30/2006	6/30/2006	6/30/2006	6/30/2006	6/30/2006	6/30/2006	6/30/2006
12.145	12.145	12.145	12.145	12.145	12.145	12.145
86.46	87.32	88.06	86.68	85.89	86.40	86.26
11:07:18	11:10:35	11:16:01	11:19:53	11:22:57	11:26:05	11:29:03
11:09:21	11:13:08	11:18:24	11:21:22	11:24:36	11:27:59	11:30:27
0.8892	0.8936	0.9020	0.9165	0.8929	0.8940	0.8962
263.09	264.59	267.26	271.37	264.59	264.99	265.50
0.02	0.04	0.02	0.05	0.05	0.02	0.00
72.48	72.94	73.47	73.43	73.27	73.47	73.24
0.06	0.16	0.10	0.06	0.10	0.06	0.07
80.427	79.791	78.941	76.489	79.926	79.386	79.023
0.80	0.93	0.68	0.77	0.78	0.84	0.95
6.2193E-07	6.2224E-07	6.2267E-07	6.2298E-07	6.2238E-07	6.2250E-07	6.2244E-07
8.9186E+05	8.8876E+05	8.8690E+05	8.7280E+05	8.8939E+05	8.8423E+05	8.8247E+05
28.494	28.494	28.495	28.495	28.494	28.495	28.495
9034.9	9008.1	8995.5	8856.9	9016.5	8965.9	8947.3
0.000	0.000	0.000	0.000	0.000	0.000	0.000
0.000	0.000	0.000	0.000	0.000	0.000	0.000
2.5097	2.5022	2.4988	2.4602	2.5046	2.4905	2.4853
0.0156	0.0155	0.0208	0.0192	0.0356	0.0536	0.0734
15.91	15.47	10.97	12.13	4.68	1.95	0.79
48.110	48.112	48.096	48.097	48.093	48.098	48.112
0.00623	0.00620	0.00831	0.00781	0.01420	0.02154	0.02952
0.9215	0.9272	0.9365	0.9533	0.9266	0.9282	0.9310
259.71	261.18	263.90	268.23	261.21	261.61	262.22
0.01	0.03	0.01	0.03	0.02	0.01	0.01
50.55	50.43	50.86	50.60	50.78	50.74	50.52
0.16	0.10	0.18	0.08	0.28	0.11	0.15
214.47	216.84	220.62	227.27	214.67	214.49	214.23
0.03	0.07	0.02	0.03	0.01	0.03	0.03
48.95	48.85	49.49	49.45	49.08	49.46	49.43
0.11	0.08	0.14	0.10	0.26	0.05	0.05
45.24	44.33	43.28	40.96	46.54	47.12	48.00
45.27	44.46	43.45	41.04	46.50	47.21	47.93

211.29	213.75	217.56	224.47	211.86	211.83	211.73
0.02	0.02	0.01	0.01	0.02	0.04	0.02
68.41	66.56	65.77	64.89	63.88	63.67	63.17
1.13	0.21	0.34	0.15	0.26	0.65	0.47
211.35	213.71	217.51	224.41	211.80	211.78	211.78
0.02	0.02	0.01	0.00	0.01	0.02	0.02
216.70	218.96	222.59	229.17	216.97	216.74	216.58
0.01	0.01	0.03	0.03	0.04	0.03	0.04
216.61	218.86	222.44	229.08	216.63	216.28	215.93
0.03	0.02	0.02	0.02	0.03	0.03	0.07
100%	50%	40%	30%	100%	100%	100%
0%	0%	0%	0%	0%	0%	0%

47	47	47	47	47
11	12	13	14	15
6/30/2006	6/30/2006	6/30/2006	6/30/2006	6/30/2006
12.145	12.145	12.145	12.145	12.145
87.62	87.34	85.87	84.95	84.66
11:34:24	11:39:01	11:45:17	11:48:34	11:51:17
11:37:02	11:40:15	11:47:25	11:49:58	11:53:16
0.8364	0.8375	0.7912	0.7918	0.7911
248.54	249.10	235.45	235.51	235.20
0.02	0.00	0.02	0.01	0.00
73.34	73.81	72.97	72.74	72.51
0.14	0.14	0.10	0.07	0.11
88.66	88.55	97.03	96.91	97.02
0.37	0.39	0.37	0.42	0.40
6.2119E-07	6.2144E-07	6.2008E-07	6.1999E-07	6.1986E-07
9.2597E+05	9.2564E+05	9.6046E+05	9.6012E+05	9.6059E+05
28.493	28.493	28.491	28.491	28.491
9369.5	9369.9	9701.0	9696.1	9698.9
8.819	8.857	20.604	20.721	20.551
0.651	0.655	1.440	1.449	1.436
1.9512	1.9476	1.2549	1.2443	1.2582
0.0196	0.0347	0.0217	0.0339	0.0186
12.77	4.83	10.66	5.05	11.80
48.072	48.064	48.062	48.068	48.097
0.01007	0.01781	0.01728	0.02728	0.01480
0.8714	0.8724	0.8284	0.8289	0.8285
245.96	246.20	233.72	233.85	233.57
0.01	0.20	0.01	0.01	0.02
50.04	49.97	48.74	48.74	48.44
0.18	0.18	0.47	0.20	0.11
218.35	218.33	221.41	221.42	221.43
0.03	0.07	0.01	0.01	0.01
50.31	50.41	50.95	50.94	50.49
0.13	0.21	0.20	0.08	0.04
27.61	27.87	12.31	12.43	12.14
27.78	28.05	12.33	12.53	12.19

216.26	216.33	220.49	220.52	220.54
0.03	0.04	0.03	0.02	0.02
66.32	65.22	67.29	66.08	65.93
0.18	0.18	0.55	0.16	0.23
216.28	216.34	220.60	220.60	220.60
0.00	0.05	0.00	0.00	0.00
219.33	219.38	221.82	221.78	221.82
0.03	0.13	0.01	0.03	0.02
219.37	219.41	221.97	221.85	221.97
0.01	0.16	0.01	0.03	0.01
100%	100%	100%	100%	100%
30%	30%	40%	40%	40%